PHYTOCHEMICAL AND BIOLOGICAL INVESTIGATION OF *LATHYRUS LINIFOLIUS* AS A POSSIBLE TREATMENT IN DIABESITY

A thesis presented by

Abdullah Rzgallah R Alzahrani

in fulfilment of the requirement for the degree of

Doctor of Philosophy

2019

Strathclyde Institute of Pharmacy and Biomedical Sciences

University of Strathclyde

This thesis is the result of the author's original research. It has been composed by the author and has not been previously submitted for examination which has led to the award of a degree.

Signed:

Date:

ACKNOWLEDGEMENTS

First and foremost, I would like to express my grateful thanks to Allah for blessing me and giving me the strength to complete my PhD study.

My deepest thanks go to my parents, Sheikh Rzgallah Alzahrani and Sheikha Alwah Alzahrani for their unconditional love, support and prayers during my study. My thanks extend to all of my brothers and sisters and in particular to Dr. Mohammed Alzahrani, for their support during my study.

Indeed, I would not be at this stage without the support of my wife Malak Alzahrani. I thank her for her support, patience and encouragement during my PhD study. I cannot forget my little baby boy Rezgallah, who was born during the final stages of my studies. He was a gift from Allah and his morning smiles were powerful doses of love which provided me with strength during the day to write up my thesis and his evening smiles were potent stress relievers.

Furthermore, I would like to take this opportunity to express my thanks to my supervisor Dr. Valerie Ferro for her encouragement, support, wisdom and guidance which helped me to complete my studies. Dr. Val believed in me and was always there for me when I needed her support or advice and I am highly honoured to be under her supervision.

My thanks extend to Prof. Alexander Gray and Prof. John Igoli for their help and support with the phytochemical analysis, to Mrs Louise Young and Grainne Abbott for their help in the biological assays, to Dr. Rothwelle Tate for supervising the molecular biology part of my thesis and to Dr. Ayman Gebril for helping in animal dissection. I also thank Mr Mark Goff for supplying me with the required plant materials used in the study.

I thank the government of Kingdom of Saudi Arabia, represented by Umm Al-Qura University, for funding my PhD study. I would also like to express my sincere thanks to Prof. Saeed Alghamdi, for his support and encouragement throughout my PhD study.

Finally, I thank all of my colleagues in the laboratory for their support, help and cooperation during my PhD study.

PUBLICATIONS

Alzahrani, A.R., Woods, N., Rothwelle, T., Sliwowska, J.H., Ferro, V.A. (In preparation). Kisspeptin - a peptide linking metabolism and reproduction: From bench to clinic. *Metabolism*.

Obeid, M.A., Al Qaraghuli, M.M., Alsaadi, M., Alzahrani, A.R., Niwasabutra, K. and Ferro, V.A., 2017. Delivering natural products and biotherapeutics to improve drug efficacy. *Therapeutic delivery*, 8(11), pp.947-956.

Al Qaraghuli, M.M., Alzahrani, A.R., Niwasabutra, K., Obeid, M.A. and Ferro, V.A., 2017. Where traditional drug discovery meets modern technology in the quest for new drugs. *Annals of pharmacology and pharmaceutics*, 2(11), pp.1-5.

Alzahrani, A., Abbott, G., Young, L.C., Igoli, J., Gray, A.I. and Ferro, V.A., 2016. Phytochemical and biological investigation of *Calliandra surinamensis* as a potential treatment for diabetes. *Planta Medica*, 82(S 01), S1-385.

POSTER COMMUNICATION

Phytochemical and biological investigation of *Calliandra surinamensis* as a potential treatment for diabetes. 9th Joint Natural Products Conference. July 2016, Copenhagen, Denmark

TABLE OF CONTENTS

LIST OF FIGURES

Chapter 1, General introduction

Chapter 2, Phytochemical analysis of tubers and extracts of *L. linifolius*

Chapter 3, Investigation of the potential anti-diabetic activity of *L. linifolius*

Chapter 4, The potential anti-oxidant and anti-inflammatory activity of *L. linifolius*

Chapter 5, RNA Sequencing of Pancreatic Tissues

Chapter 6, Animal Study on Obese Zucker Rats

LIST OF TABLES

Chapter 1, General introduction

Chapter 2, Phytochemical analysis of tubers and extracts of *L. linifolius*

LIST OF APPENDICES

LIST OF ABBREVIATIONS

1D NMR	One-dimensional NMR
2D NMR	Two-dimensional NMR
2DG	2-deoxyglucose
2DG6P	2-deoxyglucose-6-phosphate
2-H PG	2-hour plasma glucose
6PDG	6-phosphodeoxygluconate
ACETONE-D_6	Deuterated acetone
AD	Alzheimer's disease
ADIPOQ	Adiponectin gene
AMPK	Adenosine monophosphate-activated protein kinase
B2M	Beta-2-microglobulin
BA	Betulinic acid
BED	Binge eating disorder
BG	Blood glucose
BMI	Body mass index
BPB	*Betula platyphylla* bark
BSA	Bovine serum albumin
BVM	Bevirimat
BW	Body weight
CACO2	Human colorectal adenocarcinoma cells
CASP1	Caspase-1
CAT	Catalase
CC	Column chromatography
CCL20	C-C Chemokine ligand 20
CD40	CD40 molecule gene
CD40LG	CD40 ligand gene
$CDCL_3$	Deuterated chloroform
CDNA	Complementary DNA
CG	*Citrus grandis*

COA	Coenzyme A
COSY	Correlation Spectroscopy
CRO	C-reactive protein
CRT	*Cyperus rotundus* tubers
CT	Cycle threshold
CV	Cardiovascular
CVDS	Cardiovascular diseases
CYP450	Cytochromes P450
D	Doublet
DCF	2', 7'–dichlorofluorescein
DCFDA	2',7'–dichlorofluorescein diacetate
Dd	Doublet of doublet
DEGS	Differentially expressed genes
DGE	Delayed gastric emptying
DH2O	Deionised water
DIFMUP	6,8-difluoro-4-methylumbelliferyl phosphate
DM	Diabetes mellitus
DMH	1,2-dimethylhydrazine
DMSO	Dimethyl sulfoxide
DMSO-D_6	Deuterated DMSO
DNASES	Deoxyribonucleases
DPPH	2,2-Diphenyl-1-picrylhydrazyl
DPPH●	DPPH free radical
DPPIV	Dipeptidyl peptidase IV
DSDNA	Double-stranded DNA
DTT	Dithiothreitol
EA	Ethyl acetate
ECG	Electrocardiographic
EDTA	Ethylene-diamine-tetraacetic acid
EGCG	Epigallocatechin gallate
ERK	Extracellular signal–regulated kinase
FBS	Foetal bovine Serum
FC	Flash chromatography
FFA	Free fatty acid
FI	Food intake
FPG	Fasting plasma glucose
FTP	Green tea polyphenols
G6PDH	Glucose-6-phosphate dehydrogenase
GD	*Gynura divaricata* (L.) DC
GDM	Gestational diabetes mellitus
GIP	Glucose dependent insulinortopic polypeptide
GIT	Gastrointestinal tract
GK	Goto-Kakizaki
GLC	Gas liquid chromatography
GLP-1	Glucagon-like peptide 1
GLUT1	Glucose transporter 1
GLUT4	Glucose transporter 4
GLY-PRO	Gly-pro-7-amido-4-methylcoumarin hydrobromide

GO	Gene ontology
GSH	Reduced glutathione
GSIS	Glucose-stimulated insulin secretion
GSR	Glutathione reductase
GSSG	Oxidised glutathione
GST	Glutathione S-transferase
H_2O_2	hydrogen peroxide
HAECS	Human aortic endothelial cells
HAS	Hibiscus anthocyanins
HBA1C	Hemoglobin A1c
HBSS	Hanks' Balanced Salt Solution
HDL	High-density lipoprotein
HEPES	4-(2-hydroxyethyl)-1-piperazineethanesulfonic acid
HEPG2	Human hepatic cells
Hex	Hexane
HFHS	High-fat, high-sucrose diet
HG	High glucose
HIS	High isovlavone soy
HIT-T15	Hamster pancreatic β-cells
HMBC	Heteronuclear Multiple Bond Coherence
HPLC	High performance liquid chromatography
HPRT1	Hypoxanthine phosphoribosyltransferase 1
HRV	Human rhinovirus
HSA	Human serum albumin
HSQC	Heteronuclear Single Quantum Coherence
HTS	High throughput screening
HUVEC	Human umbilical vein endothelial cells
Hz	Hertz
IC_{50}	The half maximal inhibitory concentration
ICAM-1	Intracellular adhesion molecule-1
ICE	Interleukin-1 converting enzyme
IDF	International Diabetes Federation
IDT	Integrated DNA Technologies
IGF	Insulin growth factor
IκB	Inhibitor of kappa B
IKK	IκB kinase
IL1B	Interleukin 1 beta gene
IL1B	Interleukin 1 beta
INS-1	Rat pancreatic β-cells
IP	Intraperitoneal
IRS-1	Insulin receptor substrate 1
IV	Intravenous
J	Coupling constant
JNK	c-jun N-terminal kinase
kD	Kilodaltons
KEGG	Kyoto Encyclopedia of Genes and Genomes
Ki	Inhibitory constant
KRG	Korean red ginseng

LDL	Low-density lipoprotein
LEP	Leptin gene
LL	*Lathyrus linifolius*
LLL EA	Ethyl acetate extract of LL leaves
LLL HEX	Hexane extract of LL leaves
LLL MEOH	Methanol extract of LL leaves
LLT EA	Ethyl acetate extract of LL tubers
LLT HEX	Hexane extract of LL tubers
LLT MEOH	Methanol extract of LL tubers
LPL	Lipoprotein lipase
LPS	Lipopolysaccharide
M	Multiplets value
MAPK	Mitogen activated protein kinase
MCA	Melt curve analysis
MCP-1	Monocyte chemoattractant protein 1
MDA-MB-231	Human breast cancer cells
MEK	Raf/mitogen extracellular kinase
MENA	Middle East and North Africa
MeOH	Methanol
METh	Methanolic extract of *Tournefortia hartwegiana*
MG	Miglitol
MI	Myocardial infarction
MIP-1B	Macrophage inflammatory protein 1β
MIS	Maturation inhibitors
mRNA	Messenger Ribonucleic Acid
MULT	Multiplets
NADPH	Nicotinamide adenine dinucleotide phosphate
NCDS	Non-communicable diseases
NCTC cells	Human skin cell line
NEAA	Non-essential amino acids
NGS	Next generation sequencing
NGSP	National Glycohemoglobin Standardization Program
NMR	Nuclear Magnetic Resonance
NO	Nitric oxide
NOESY	Nuclear Overhauster Effect Spectroscopy
NOX	NADPH oxidase
NPCS	Nucleus pulposus cells
NTC	Non-template control
OD	Optical density
OGTT	Oral glucose tolerance test
OZR	Obese Zucker rats
Panc-1	pancreatic cancer proliferating cell nuclear antigen 1 cells
PC	Paper chromatography
PCR	Polymerase Chain Reaction
PDX-1	Pancreatic and duodenal homeobox 1
PGE_2	Prostaglandin E2
PKB	Protein kinase B
PL	Pancreatic lipase

PP	Purple Perilla
PPAR-Γ	Peroxisome proliferator-activated receptor gamma
PPM	Parts per million
PTP 1B	Protein tyrosine phosphatase 1B
PTY-2	*Pueraria tuberosa* tubers
PYY	Peptide YY
RA	Rheumatoid arthritis
RIN	RNA Integrity Number
RM	Repeated metformin
RNA	Ribonucleic Acid
RNA-SEQ	RNA sequencing
RNASES	Ribonucleases
ROS	Reactive oxygen species
RPM	Rotation per minute
RQI	RNA quality indicator
RT	Reverse Transcriptase
RT-	Without Reverse Transcriptase
RT-QPCR	Real time quantitative PCR
S	Singlet
S/C	Subcutaneous
SD	Sprague Dawley
SEC	Size-Exclusion Chromatography
SGLT2	Sodium-glucose cotransporter
SIRT-1	Sertuin-1
SM	Single metformin
SOCS3	Cytokine signalling 3
SOD	Superoxide dismutase
SSDNA	Single-stranded DNA
STZ	Streptozotocin
T1DM	Type I diabetes mellitus
T2DM	Type II diabetes mellitus
TBP	TATA box binding protein
T-BUOOH	Tert-butyl hydroperoxide
TCA CYCLE	Tricarboxylic acid cycle
TFMS	Bis(4-Trifluoromethylsulfonamidophenyl)-1,4-diisopropylbenzine
TGF-B	Transforming growth factor beta
TLC	Thin layer chromatography
T_M	Melting temperature
TNF-α	Tumor necrosis factor-alpha
TNFRSF19	TNF receptor superfamily member 19 gene
TR+	With Reverse Transcriptase
U937	Human monocyte cell line
VAS	Visual analogue scales
VCAM-1	Vascular cell adhesion molecule-1
VLC	Vacuum liquid chromatography
WI	Water intake
ZDF	Diabetic Zucker rats

B-TC6	Mouse pancreatic β-cells

MATERIALS AND REAGENTS

MATERIAL/REAGENT	SUPPLIER
0.2µM FILTER	Sigma Aldrich, UK
20-ML GLASS VIAL	VWR, UK
4-METHYL UMBELLIFERYL OLEATE	Sigma Aldrich, UK
4-NITROPHENYL A-D-MALTOHEXASIDE	Sigma Aldrich, UK
4-NITROPHENYL-A-D-GLUCOPYRANOSIDE	Sigma Aldrich, UK
5X DNA LOADING BUFFER	Bioline, UK
6,8-DIFLUORO-4-METHYLUMBELLIFERYL PHOSPHATE (DIFMUP)	Invitrogen Ltd, UK
6MM CONE BALL	Retsch, UK
75CM^2 CELL CULTURE FLASKS	Sigma Aldrich, UK
96-WELL CELL CULTURE PLATES	Sigma Aldrich, UK
96-WELL HALF AREA PLATE (BLACK)	Grenier Bio-One, UK
96-WELL HALF AREA PLATE (CLEAR)	Grenier Bio-One, UK
ABI STEPONE PLUS SYSTEM	Applied Biosystems, UK
ACARBOSE	Sigma Aldrich, UK
ACETONE-D$_6$	Sigma Aldrich, UK
ACETONITRILE	Sigma Aldrich, UK
AGAROSE (MOLECULAR GRADE)	Bioline, UK
ALAMARBLUE™ CELL VIABILITY REAGENT	Invitrogen, UK
ANTI-BUMPING GRANULES	BDH, UK
BEAD MILL (MM301)	Retsch, UK
BIS(4-TRIFLUOROMETHYLSULFONAMIDOPHENYL)-1,4-DIISOPROPYLBENZINE (TFMS)	Sigma Aldrich, UK
BOVINE SERUM ALBUMIN	Sigma Aldrich, UK
CDCL$_3$	Sigma Aldrich, UK

CELLOSOLVE	Sigma Aldrich, UK
CELLULOSE EXTRACTION THIMBLES (SINGLE THICKNESS)	VWR, UK
DIPEPTIDYL PEPTIDASE IV (DPPIV)	Sigma Aldrich, UK
DITHIOREITOL	Sigma Aldrich, UK
DMEM	Invitrogen, UK
DMSO	Sigma Aldrich, UK
DMSO-D_6	Sigma Aldrich, UK
DPPH	Sigma Aldrich, UK
ETHANOL	Sigma Aldrich, UK
ETHYL ACETATE (HPLC GRADE)	Sigma Aldrich, UK
ETHYLENE-DIAMINE-TETRA-ACETIC ACID (EDTA)	Sigma Aldrich, UK
EXPERION DNA 12K ANALYSIS KIT	Bio-Rad, UK
EXPERION™ RNA STDSENS ANALYSIS KIT	Bio-Rad, UK
FARLEY'S RUSKS	H.J. Heinz Foods UK Ltd., UK
FOETAL BOVINE SERUM	Biosera, UK
GEL RED (STOCK IS 10,000X)	Biotium, UK
GLUCOSE UPTAKE-GLO™ KIT	Promega, UK
GLY-PRO-7-AMIDO-4-METHYLCOUMARIN HYDROBROMIDE	Sigma Aldrich, UK
HBSS	Thermo Fisher, UK
HEPES	Sigma Aldrich, UK
HEXANE (HPLC GRADE)	Fisher Chemicals
HYPERLADDER™50BP, 50BP TO 2000BP	Bioline, UK
ILLUSTRA GFX PCR DNA AND BAND PURIFICATION KIT	GE Healthcare, UK
INGENSUS UV IMAGING SYSTEM	Syngene, UK
L-GLUTAMINE	Life Technologies, UK
LIPOPOLYSACCHARIDE (LPS) (L2630)	Sigma Aldrich, UK
M199 MEDIUM	Sigma Aldrich, UK
METHANOL (HPLC GRADE)	VWR, UK

MICROAMP® FAST OPTICAL 96-WELL REACTION PLATES	Thermo Fisher Scientific, UK
MICROSCOPE	Olympus, Japan
NANODROP™ SPECTROPHOTOMETER (2000C)	Thermo Fisher Scientific, UK
NEW BORN CALF SERUM	Invitrogen, UK
NMR TUBES (5 X 178 MM)	VWR, UK
NON-ESSENTIAL AMINO ACIDS	Life Technologies, UK
ORLISTAT	Sigma Aldrich, UK
P32/98	Enzo, UK
PANCREATIC LIPASE (TYPE II FROM PORCINE PANCREAS)	Sigma Aldrich, UK
PARAFFIN WAX	Sigma Aldrich, UK
PENICILLAN/STREPTOMYCIN	Life Technologies, UK
P-NITROPHENYL-A-D-GLUCOPYRANOSIDE	Sigma Aldrich, UK
POLYSINE MICROSCOPE SLIDES	Thermo Scientific, UK
PORCINE PANCREAS α-AMYLASE	Sigma Aldrich, UK
POWERUP™ SYBR™ GREEN MASTER MIX	Applied Biosystems, UK
PRIMUS96 PCR MACHINE	MWG Biotech, UK
PROTEIN TYROSINE PHOSTPHATASE	Sigma Aldrich, UK
QIAZOL LYSIS REAGENT	Qiagen, UK
RNEASY MIDI KIT	Quiagen, UK
SODIUM ACETATE	Sigma Aldrich, UK
SODIUM CHLORIDE	Sigma Aldrich, UK
SODIUM PHOSPHATE DIBASIC HEPTAHYDRATE	Sigma Aldrich, UK
SODIUM PHOSPHATE MONOBASIC DEHYDRATE	Sigma Aldrich, UK
SODIUM PYRUVATE	Thermo Fisher, UK
TERT-BUTYL HYDROPEROXIDE (T-BUOOH)	Sigma Aldrich, UK
TETRO cDNA SYNTHESIS KIT	Bioline, UK
TLC GRADE SILICA [SILICA GEL 60H]	Merck, UK

TRIPLE EXPRESS	Life Technologies, UK
TRIS-BORIC ACID-ETHYLENEDIAMINETETRAACETIC ACID (TBE)	Gibco, UK
TRIS-HCL	Sigma Aldrich, UK
YEAST α-GLUCOSIDASE	Sigma Aldrich, UK

ABSTRACT

Diabetes is a world-wide issue which can affect people at any age. It is ranked as one of the top 10 diseases responsible for death worldwide. According to the International Diabetes Federation, 424.9 million people worldwide were estimated to have diabetes in 2017 (90% with type 2 diabetes) and this number is projected to reach 629 million patients by 2045. The current treatments for managing diabetes are linked with a number of side effects including severe hypoglycaemia, permanent neurological deficit, stomach-ache, headache, lactic acidosis, liver damage, dizziness and death in some cases. Therefore, there is a need for improved anti-diabetic drugs with fewer side effects to enhance patient compliance and to control blood glucose levels more tightly. Natural products and plants in particular, offer an alternative to synthetic drugs. *Lathyrus linifolius* is a plant whose tubers have historically been used as an appetite suppressant during medieval times in times when food was scarce. Due to the close link between appetite suppressants and the treatment of diabetes/obesity, the plant's leaves and tubers were examined for their potential anti-diabetic and anti-obesity activity.

This project aimed to: 1) produce *Lathyrus linifolius* extracts using Soxhlet apparatus extraction from which bioactive compounds could be isolated by column chromatography and characterised by nuclear magnetic resonance (NMR); 2) assess the anti-diabetic and anti-obesity activity of the extracts and compounds; 3) investigate the anti-inflammatory and anti-oxidant activity of the extracts and compounds in *in vitro* assays; 4) identify the effects of the tuber treatment on the gene expression of appropriate diabesity components in normal rat pancreatic tissues obtained from a previous study in which rats were fed with tubers; and 5) re-assess *Lathyrus linifolius* effects on obese Zucker rats and monitor the effects on body weight, food intake, water intake and blood glucose levels.

1) Four compounds were isolated for the first time from the ethyl acetate extract of the tubers; these were betulinic acid, lupeol, stigmasterol and β-sitosterol. The isolated compounds are known for their beneficial effects on hyperglycaemia and obesity to some extent. Betulinic acid was the major component in the tubers and leaves.

2) In biological assays, the ethyl acetate extract and betulinic acid from the tubers were potent α-glucosidase inhibitors ($P<0.05$) with IC_{50} of 9.5 µg/ml and 5.5 µM, respectively. Moreover, the leaf ethyl acetate and methanol extracts were also strong inhibitors of α-glucosidase ($P<0.05$) with IC_{50} of 0.58 µg/ml and 4.3 µg/ml, respectively. In an anti-obesity assay, based on pancreatic lipase, the ethyl acetate tuber extract at 30 µg/ml and betulinic acid at 30 µM showed 50% enzyme inhibition ($P<0.05$); and the hexane extract from the leaves showed 30% inhibition. In HepG2 cells, leaf hexane extract showed a significant increase in glucose uptake which was comparable to that of insulin. These findings showed promising results for the plant to be used as an anti-diabetic and anti-obesity agent. Inflammation and oxidative stress are implicated in diabesity and determined the subsequent investigation.

3) Moreover, all the plant extracts and isolated compounds at 30 µg/ml or 30 µM showed a greater than 70% protection ($P<0.05$) in L929 cells (mouse fibroblasts commonly used for anti-inflammatory studies) from the cytotoxic effects of tumour necrosis factor alpha (10 µM). This was followed by investigating the ability of *Lathyrus linifolius* to inhibit nuclear factor kappa-light-chain-enhancer of activated B cells (NF-ƙB) in the NCTC cell line (human skin cells transfected with a NF-ƙB luciferase reporter vector, used in anti-inflammatory studies). Betulinic acid, ethyl acetate extract of the tubers, hexane and ethyl acetate extracts of the leaves inhibited NF-ƙB which gave a NF-ƙB % inhibition of 70, 40, 30 and 30, respectively. A betulinic acid inhibition curve was performed and found to inhibit NF-ƙB expression with an IC_{50} of 22.8 µM. Oxidative stress was then investigated following the positive findings in the anti-inflammatory assays. *Lathyrus linifolius* extracts and isolated compounds were not reactive oxygen species-generators and significantly ($P<0.05$) protected cells from reactive oxygen species generated by tert-butyl hydroperoxide in SH-SY5Y (neuronal), HepG2 (hepatic) and Panc1 (pancreatic) cells, except lupeol in HepG2 cells. In HepG2 cells, glutathione levels were significantly ($P<0.05$) increased by ethyl acetate extract of the tubers which confirmed the potential anti-oxidant activity of *Lathyrus linifolius*.

4) It was considered pertinent to carry out a retrospective investigation into any gene changes using RNA-Sequencing and real-time quantitative polymerase chain reaction (RT-qPCR) on RNA isolated from rat pancreatic tissues in a feeding study with *Lathyrus linifolius* tubers carried out by Woods (2017). It was found that the adiponectin gene (*Adipoq*) was highly up-regulated ($P<0.05$) whereas genes that contribute to pancreatic β-cells damage for example *Il1β* and *Tnfrsf19* were down-regulated ($P<0.05$).

5) Then, the biological effects of *Lathyrus linifolius* on an animal model for diabesity were followed up. Dried, powdered *Lathyrus linifolius* tubers (100-200 mg/kg BW) were dissolved in deionised water, mixed with Farley's rusks and given to obese Zucker rats daily for 16 days. However, the results showed that there were no effects on the body weight, food intake, water intake or blood glucose of Zucker rats and this may have occurred due to the low *Lathyrus linifolius* dosage used and the short duration of the study. It was decided not to carry out any further investigation (such as RNA- Sequencing) after this as there was no significant difference in results between the obese Zucker rats and normal rats as observed in the previous feed study.

These findings suggest that compounds from *Lathyrus linifolius* could possibly be used as anti-diabetic and anti-obesity agents in the future, based on the positive results obtained from the *in vitro* and *ex vivo* assays in this study. This study should be followed by assessing the effects of *Lathyrus linifolius* on body weight, food intake, water intake and blood glucose in humans.

Chapter 1

1. General introduction

1.1. Introduction

Diabetes mellitus (DM) can be defined as a chronic disease which is characterised by high levels of blood glucose (BG) or hyperglycaemia (Punthakee *et al.*, 2018). Individuals with diabetes are not capable of producing any or sufficient levels of insulin or cannot utilise insulin efficiently (IDF, 2017). Insulin is a hormone which is produced by the pancreas gland in the body and it plays a fundamental role in transporting glucose molecules from the bloodstream into cells of the body in order to produce energy (Rodbard, 2016). Hyperglycemia occurs when there is a lack of insulin or inability of cells to respond to insulin levels. This increase in bloodstream glucose levels is a hallmark of diabetes (Ogurtsova *et al.*, 2017). Uncontrolled diabetes is a life-threatening condition because it can result in damage to various body organs and causes other complications such as cardiovascular diseases (CVDs), neuropathy, nephropathy and retinopathy (which can cause blindness) (Konstantinos *et al.*, 2018). However, well controlled diabetes can delay or even prevent diabetes complications.

1.1.1. Prevalence of diabetes

Diabetes is a world-wide issue which can affect people of all ages (Gillespie, 2001). Diabetes is ranked one of the top 10 diseases responsible for death, along with the three major non-communicable diseases (NCDs): CVDs, cancer and respiratory conditions (Ogurtsova *et al.*, 2017). Diabetes is responsible for 80% of all pre-mature deaths. NCDs were responsible for 39.5 million out of the 56.4 million world-wide deaths in 2015 (Roth *et al.*, 2018). One of the major challenges with diabetes is that 30-80% of diabetic people are undiagnosed. Thus, lifestyle changes, early detection and better therapeutic treatments are required to improve diabetes management.

According to the International Diabetes Federation (IDF), 424.9 million people worldwide were estimated to have diabetes in 2017 (90% with type 2 diabetes, T2DM) and this number is the highest so far as shown in Figure 1.1 (Chatterjee *et al.*, 2017).

Diabetes alone was responsible for the deaths of approximately 4 million people in 2017 (IDF, 2017). Diabetes prevalence is projected to increase by 48% and reach 629 million patients in 2045. The IDF Diabetes Atlas depends heavily on the quality and availability of data sources for its diabetes estimates. Diabetes estimates are calculated for 221 countries and territories which are then grouped together to produce estimates for regions and the world. Countries without data sources have their diabetes figures projected based on similar countries with data sources. Data sources for the IDF Diabetes Atlas come from peer-reviewed articles and national health surveys which includes WHO STEP surveys. Other sources include Health Ministries and informal communication within the IDF network. Any sources of data released before 1990 are excluded and are not used to generate diabetes estimates.

Diabetes almost equally affects males and females (Figure 1.2). Three-hundred and twenty-seven million diabetics are under the age of 64 and 98 million patients are over 65 years (Figure 1.3.). There are seven IDF regions: Africa, Europe, Middle East and North Africa, South and Central America, South-East Asia and Western Pacific. The number of people with diabetes in 2017 and projected number of diabetics for each IDF region is summarised in Table 1.1. The increase in the number of people with diabetes has led to increased expenditure on healthcare and reached USD 727 billion in 2017, which is three times more than what was spent in 2006 (Figure 1.4).

The top five countries in terms of numbers of patients with diabetes are China, India, the United States, Brazil and Mexico (IDF, 2017). However, these countries do not have the highest prevalence of diabetes due to their large populations. Approximately 39 million people have diabetes in the MENA (Middle East and North Africa) region, of which 18% are in Saudi Arabia; the highest prevalence in this region (Ogurtsova *et al.*, 2017). By comparing Saudi Arabia with the UK, the prevalence percentage of diabetes in adults (20-79 years) is 17% in Saudi Arabia which is more than three times that of the UK (5.4%) (IDF, 2017).

Diabetes classification and diagnosis are complex and the three main types are type I (T1DM), T2DM and gestational diabetes (GDM).

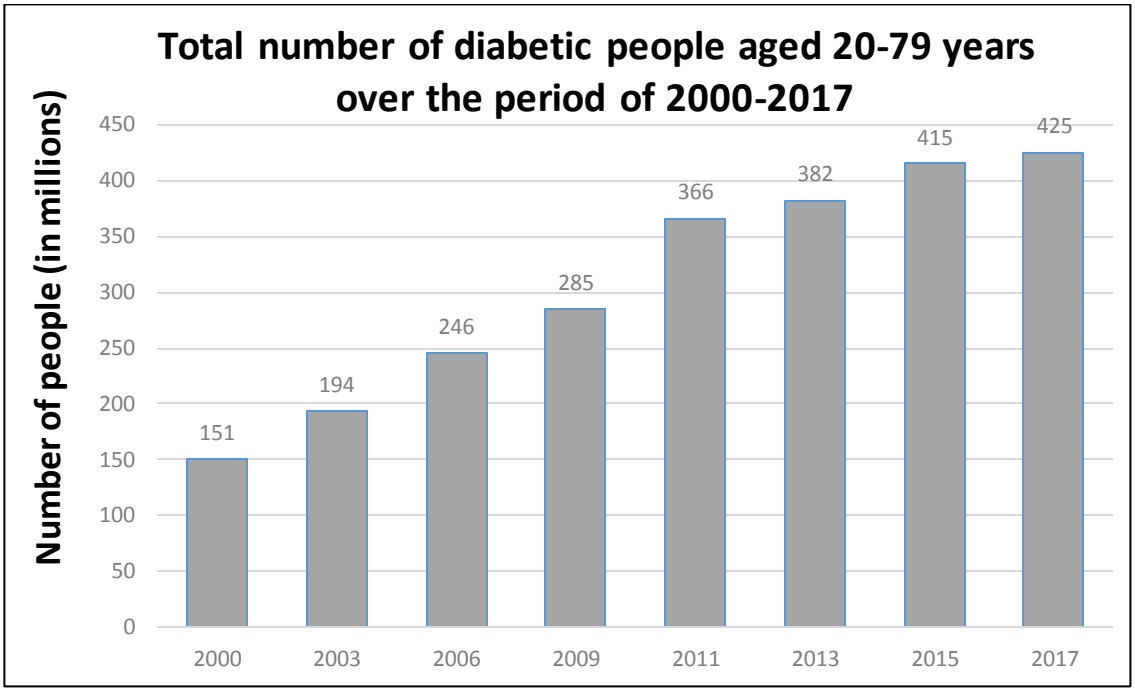

Figure 1. 1: The trend in the number of people with diabetes between 2000 and 2017. Diabetes has increased over the years and affected 425 million people world-wide in 2017 (IDF, 2017).

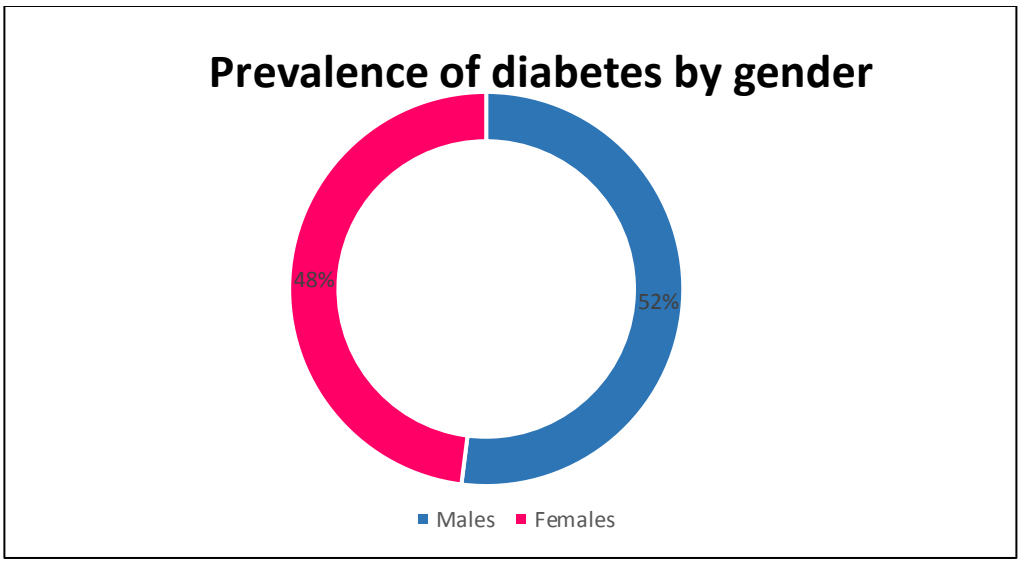

Figure 1. 2: The world-wide distribution of diabetes among both males and females aged 20-79 years (IDF, 2017).

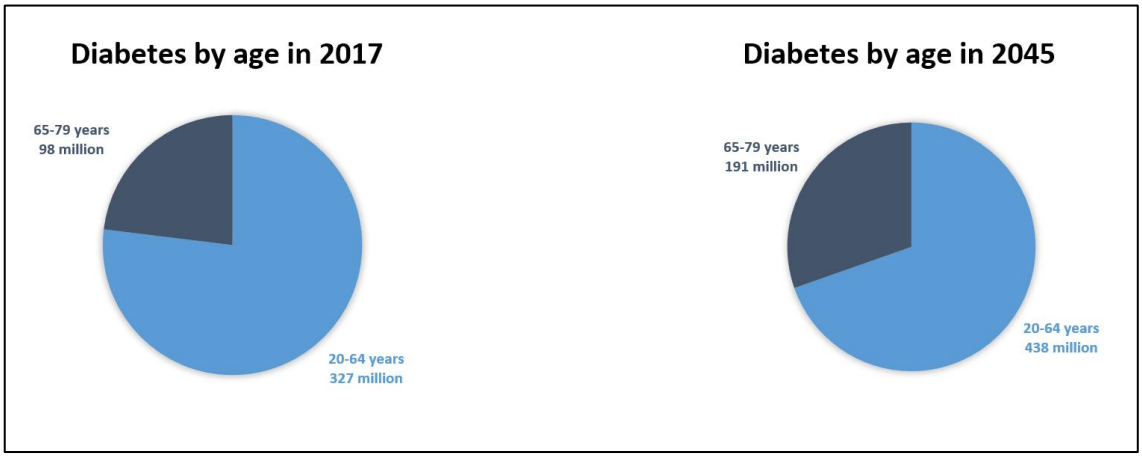

Figure 1. 3: The world-wide distribution of diabetes by age in 2017 and the projected increase in 2045 (IDF, 2017).

Table 1. 1: The number of diabetic patients per IDF region in 2017 and projected data for 2045 (IDF, 2017; Ogurtsova *et al.*, 2017).

IDF region	**No. of diabetic patients (millions) in 2017**	**Projected no. of diabetic patients (millions) in 2045**	**Projected percentage increase**
Africa	16	41	156
Europe	58	67	16
Middle East and North Africa	39	82	110
North America and Caribbean	46	62	35
South and Central America	26	42	62
South-East Asia	82	151	84
Western Pacific	159	183	15
World	**425**	**629**	**48**

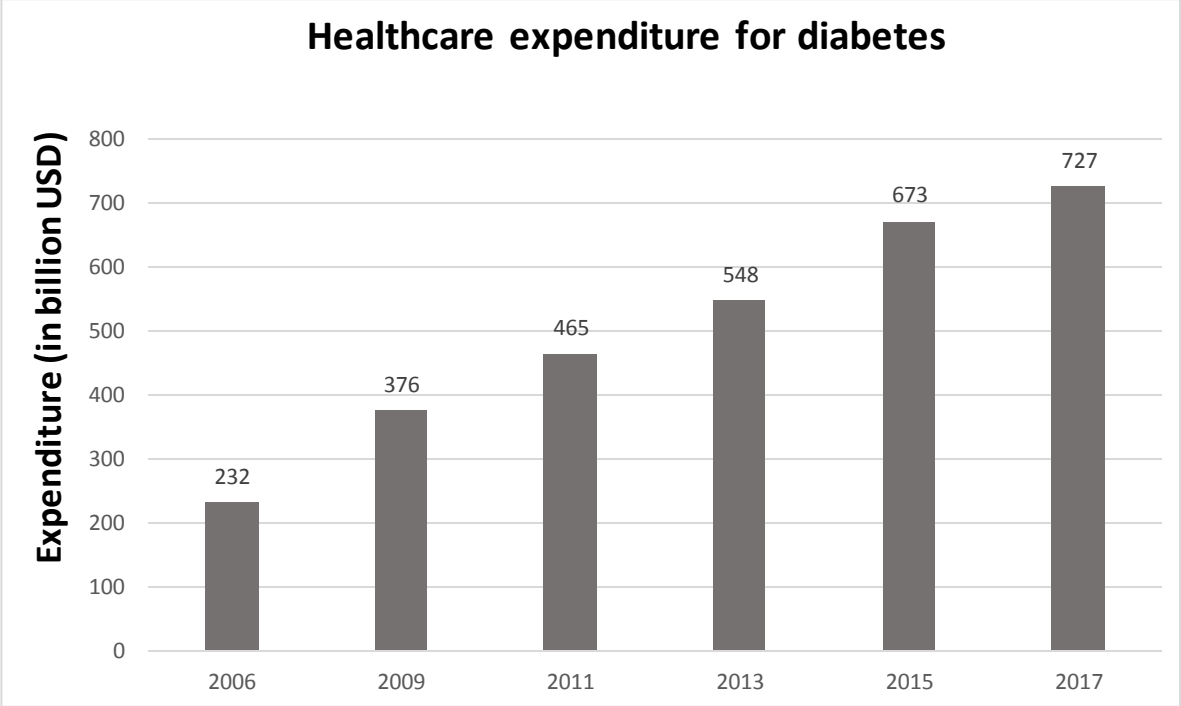

Figure 1. 4: Diabetic patients' expenditure on healthcare between 2006 and 2017 world-wide (IDF, 2017).

1.2. Types of diabetes

Diabetes can be characterised into the following categories:

I. T1DM: This type develops when β-cells in the pancreas are destroyed by the immune system resulting in no insulin being secreted. T1DM can occur at any age although it is more frequently seen in children in their mid-teens. The current therapy is to provide insulin which is delivered by injections or pumps. T1DM accounts for approximately 5% of all diabetes (Chauhan *et al.*, 2010). Currently there are no established and effective ways to prevent its occurrence (Jacobsen *et al.*, 2019)

II. T2DM: This is also known as non-insulin-dependent diabetes mellitus. The onset of T2DM is usually later than T1DM. It is the most common form of diabetes and accounts for 90%-95% of all diabetes (Chatterjee *et al.*, 2017). T2DM is usually initiated when cells in the muscles, liver and fat tissues do not utilise insulin properly; this is known as insulin resistance. This will increase the need for intracellular insulin to lower the levels of glucose inside

them. As a consequence, β-cells in the pancreas gradually lose their ability to produce insulin in sufficient amounts. There are a number of risk factors associated with developing T2DM; including age, obesity, family history of diabetes and/or gestational diabetes, race/ethnicity, physical inactivity and impaired glucose metabolism (Kahn *et al.*, 2006).

III. GDM: This is characterised by glucose intolerance which usually occurs in the second or third trimester of pregnancy (Ryckman *et al.*, 2015). Treatment is required to protect both mother and infant and this usually involves changing diet, increasing physical activity and insulin (Koivusalo *et al.*, 2016). Approximately 10% of women with GDM continue to have high levels of BG and this usually progresses to T2DM. The risk factors for developing GDM are similar to those for T2DM. Infants whose mothers had GDM are at a high risk of developing obesity and diabetes (mainly T2DM) at some point in their lives (Damm *et al.*, 2016).

Other types of diabetes:

I. Type III diabetes: This is regarded as a neuroendocrine disease in which T2DM develops and progresses to Alzheimer's disease (AD). T2DM and AD patients share similar β-amyloid deposits in the pancreas and the brain (Mittal *et al.*, 2016; Steen *et al.*, 2005; De la Monte and Wands, 2008).

II. Type 3c diabetes: This is less common than T1DM and T2DM, known as pancreatogenic diabetes (Hardt *et al.*, 2008). It is a secondary diabetes caused as a result of a disease of exocrine pancreas. The most common exocrine pancreatic disease is chronic pancreatitis (Ewald *et al.*, 2012). This condition develops when the pancreas becomes inflamed or some part of it is removed and this leads to no insulin being produced by the pancreas (Hart *et al.*, 2016). Therefore, this type of diabetes requires urgent insulin therapy.

1.3. Pathogenesis and pathophysiology of T1DM and T2DM

1.3.1. Pathogenesis of T1DM

T1DM is an autoimmune disease that occurs as a result of the destruction of the pancreatic β-cells which are responsible for secreting insulin. The clinical features of the disease occur when the destruction of the β-cells reaches the end stage. There are seven features explained by Al Homsi and Lukic (1992) which categorise T1DM as an autoimmune disease. These are:

A. The infiltrated islets of the pancreas show the presence of some immune system cells.
B. The disease shows an association with class II (immune response) genes of the major histocompatibility complex (MHCII).
C. The presence of specific autoantibodies.
D. Changes to the cells responsible for regulating the immune system, T cells and specifically, CD4+.
E. The production of some interleukins (IL) by the monokines and T helper (TH1) cells.
F. The disease responds well to immune therapy.
G. Other organs are seen to be affected by autoimmune diseases in people suffering from T1DM or in their family members.

1.3.2. Pathophysiology of T1DM

When the β-cells are destroyed, the pancreatic α-cells become abnormal, resulting in the secretion of high levels of glucagon (Briant *et al.*, 2016). In normal conditions, glucagon levels are suppressed when hyperglycaemia presents. However, in T1DM, this does not occur. As a consequence, some metabolic disruptions occur. The most common metabolic defect is ketoacidosis in the absence of insulin (DeFronzo *et al.*, 2015a). A number of biochemical abnormalities are seen in tissues as a consequence of insulin deficiency. Levels of free fatty acids in the plasma become abnormal due to unregulated lipolysis; hence, glucose metabolism is affected and suppressed in skeletal muscles and other peripheral tissues (Ozougwu *et al.*, 2013). The expression of the genes responsible for the expression of mainly glucokinase in liver and GLUT4 family

transporters in adipocytes, which are responsible for controlling the response of tissues to levels of insulin is decreased (Raju and Raju, 2010). The two main consequences of T1DM are glucose metabolism impairment and lipid metabolism abnormalities (Faerch *et al.*, 2009), which are discussed in the following paragraphs.

A. Glucose metabolism impairment

Glucose production is increased by the liver in T1DM (Yki-Järvinen, 2010). Initially, glycogen stores are mobilised in such a way as to initiate the gluconeogenesis process which leads to glucose production (Hatting *et al.*, 2018). Non-hepatic tissues are also affected by insulin deficiency and this is seen more in skeletal muscles and adipose tissues, within which insulin is essential for the uptake of glucose (D'Adamo and Caprio, 2011). This leads to the glucose transporter protein moving towards the plasma membrane of these tissues. The reduction of glucose uptake by the peripheral tissue is faced by a decrease in glucose metabolism. Insulin regulates the levels of glucokinase which is responsible for targeting insulin inside tissues (Ozougwu *et al.*, 2013). Therefore, in T1DM, the phosphorylation of glucose is decreased and this leads to high levels of glucose in the blood. Both the increase of gluconeogenesis in the liver and reduced glucose metabolism in peripheral tissues leads to an increase in BG levels (Hatting *et al.*, 2018). The kidney is able to absorb glucose in normal conditions, however in situations where glucose levels are high, it might be passed into the urine as glucosuria (Lytvyn *et al.*, 2014). As the kidney loses the ability to absorb glucose, water and electrolytes are also lost. Hence, thirst mechanisms are initiated to compensate, leading to polydipsia. Glucosuria and tissue catabolism cause a negative calorie balance which increases food intake and appetite leading to polyphagia (Adinortey, 2017).

B. Lipid metabolism abnormalities

Insulin plays a major role in storing energy following meals in the form of glycogen in hepatocytes and skeletal muscles (Nikoulina *et al.*, 2000). With the help of insulin, hepatocytes are also responsible for the synthesis and storage of triglycerides in adipocytes. The triglycerides are rapidly mobilised when insulin is not present; hence, high levels of free fatty acids are found in plasma (Ginsberg *et al.*, 2005). Apart from

the brain, the free fatty acids (FFA) are taken up by many tissues to form energy. In the mitochondria, levels of malonyl Coenzyme A (CoA) decrease and levels of Acyl-CoA rise in the absence of insulin (Ozougwu *et al.*, 2013). Fatty acids are oxidised to acetyl CoA in the mitochondria and further oxidation to acetyl CoA takes place in the tricarboxylic acid cycle (TCA cycle) (Cronan and Laporte, 2005). In contrast, in the hepatocytes, acetyl CoA is not oxidised by the TCA cycle, but is instead metabolised to form ketone bodies such as acetoacetate and β-hydroxybutyrate (Fukao *et al.*, 2004). The generated ketone bodies are used to produce energy in the heart, brain and skeletal muscles (Magistretti and Allaman, 2013). In T1DM, high levels of free fatty acids and ketone bodies lead to a reduction in glucose utilisation. Hence, hyperglycaemia occurs. Excessive production of ketone bodies leads to a condition called ketoacidosis (Weinstock *et al.*, 2013). One of the metabolites of acetoacetate is acetone which can be exhaled by the lungs. Therefore, a distinctive smell is emitted from the mouth of a person who has ketoacidosis (Blaikie *et al.*, 2014). Lipoprotein lipase (LPL) is an enzyme which acts on plasma triglycerides; it uses insulin to function (Morigny *et al.*, 2016). Therefore, where there is insulin deficiency, hypertriglycerides are produced.

1.3.3. Pathogenesis of T2DM

In T2DM, glucose plasma concentration is not well controlled within the acceptable range and this is believed to be a result of two pathological defects (Ozougwu *et al.*, 2013). One is the disruption of the pancreatic β-cells which leads to less insulin being produced and the other is the impairment of insulin's action on tissues due to insulin resistance mechanisms (DeFronzo *et al.*, 2015a). Environmental factors can contribute to the pathogenesis of T2DM as described below:

1.3.4. Environmental factors in T2DM

Ageing, physical inactivity, alcohol consumption and obesity, among others are risk factors of developing T2DM (Chatterjee *et al.*, 2017; DeFronzo *et al.*, 2015b). Obesity usually occurs due to physical inactivity which in turns leads to reduced muscle mass and therefore, insulin resistance is induced in many obese patients. Diet is a major component that is implicated in obesity (Kahn *et al.*, 2006). The enlargement of adipose tissues as a result of sedentary lifestyle and unbalanced eating patterns is a

cause of obesity and also of T2DM (Sáinz *et al.*, 2015). There is a 4-5-fold increased risk of developing T2DM in individuals with mild obesity or whose body mass index (BMI) is above 25 (Ozougwu *et al.*, 2013). Obesity is a major environmental factor causing diabetes and it can be prevented or managed in many cases (Lecube *et al.*, 2017). Glycation is the process of glucose auto-oxidation and changes to the polyol pathway (López-Díez *et al.*, 2016). Hence, glycation generates free radicals and increases oxidative stress. Free radicals can also be generated by macrophages and T killer cells are believed to be damaging to pancreatic β-cells (Gerber and Rutter, 2017).

1.4. Diabesity

Diabetes which is associated with obesity is now termed diabesity or obesity-dependent diabetes (Farag and Gaballa, 2010). Obesity is a worldwide problem which is characterised by excess adipose tissue in the body which leads to other health complications (Pappachan *et al.*, 2018). These include T2DM and CVDs such as hypertension. The BMI is the parameter used to class people as overweight or obese and it is calculated using the body weight and height of individuals as shown in the formula below (Velazquez and Apovian, 2018).

$$BMI = \frac{\text{Body weight (Kg)}}{\text{Squared Height (m)}}$$

Overweight individuals have a BMI of ≥ 25 kg/m^2 and obese people have BMI of ≥ 30 kg/m^2, more details are in Table 1.2 (WHO, 2019).

Table 1.2: Use of BMI for the classification of adults who are underweight, overweight and obese.

Classification	BMI (kg/m^2)
Under weight	< 18.5
Ideal body weight	18.5-24.9
Overweight	≥ 25
Pre-obese	25-29.9

Obese	≥ 30
Obese class I	30-34.9
Obese class II	35-39.9
Obese class III	≥ 40

1.4.1. Prevalence of Obesity

Obesity is a world-wide issue and in 2016 there were more than 650 million people globally who were considered obese, while 1.9 billion adults were considered overweight (WHO, 2018). Obesity can affect all people irrespective of their gender and age.

1.4.2. Causes of obesity

Unhealthy eating practices and poor weight control can be seen among adults with risks of eating disorders and obesity (Kessler *et al.*, 2013). Thus, the identification of eating disorders at an early stage is a key factor in preventing the development of obesity.

Binge eating disorder (BED): This is the most common eating disorder among adults and it impacts on an individual's emotional and physical health (Ivezaj *et al.*, 2016). BED is a condition in which people eat large quantities of food in a very short period of time on a regular basis in a process called binging and this is linked to severe obesity (Schag *et al.*, 2013). People with BED have been found to develop an overweight state at an earlier age in comparison to people who do not have BED (McCuen-Wurst *et al.*, 2018). Binging episodes are associated with foods high in sugar, fats, high salts and low amounts of vitamins and minerals. BED patients often develop depression as they are unhappy about their binging habits (Gluck *et al.*, 2001). Patients with BED are susceptible of developing T2DM, CVDs, gallbladder disease and hyperlipidaemia (Allison *et al.*, 2007). Patients with BED often have a lower quality of life and face difficulties in their societies (Gluck *et al.*, 2001).

1.5. Inflammation in diabesity

Obesity progressing to insulin resistance and eventually to T2DM is poorly understood but is implicated in the failure of pancreatic β-cells to secrete insulin to overcome insulin resistance. This results in chronic hyperglycaemia (Saltiel and Olefsky, 2017). Obese and T2DM patients have elevated levels of white blood cells and plasma levels of coagulation factors such as fibrinogen and plasminogen activator inhibitor 1 (PAI-1), acute-phase proteins (C-reactive protein (CRP)) and serum amyloid A (SAA), pro-inflammatory cytokines such as tumor necrosis factor alpha (TNFα), interleukin (IL)-1β and IL6 and chemokines (Duncan *et al.*, 2003; Esser *et al.*, 2014). These inflammatory mediators were found to improve and reduce in patients following lifestyle changes which cause weight loss (Belalcazar *et al.*, 2013; Bruun *et al.*, 2006; Bastard *et al.*, 2000). Levels of these pro-inflammatory mediators are directly proportional to the degree of insulin resistance. There are several studies that have identified the possibility of using inflammatory mediators as predictors for T2DM due to the positive relationship between them (Duncan *et al.*, 2003; Esser *et al.*, 2014). Clinical and experimental data has shown that adipose tissue, pancreas, liver and skeletal muscle are the sites of inflammation where diabesity is present (Esser *et al.*, 2014). Diabetic patients as well as diabetic animal models showed that such tissues were infiltrated by macrophages (Tate *et al.*, 2016; Kohlgruber and Lynch, 2015). Macrophages are cells capable of producing pro-inflammatory cytokines such as TNFα, IL1β and IL6 (Wang *et al.*, 2018a). These cytokines act in an autocrine and a paracrine manner to interfere peripherally with insulin signaling and to promote insulin resistance by activating c-JUN N-terminal kinase (JNK) and nuclear factor-kappa B (NF-κB) pathways that are found in tissues of obese and T2DM patients. They also play a central role in promoting inflammation in tissues (Shimobayashi *et al.*, 2018; Chen *et al.*, 2015).

1.6. Current management for diabetes

The aim of diabetes management is to achieve adequate control of plasma glucose in the target range without causing hypoglycaemia (Raveendran *et al.*, 2018). According to SIGN guidelines (2010) on managing diabetes, lifestyle management must be

considered as the first-line treatment (Raveendran *et al.*, 2018). All types of diabetes are improved by changing adverse lifestyle factors. Smoking cessation, increased physical activity, weight loss and a healthy diet are of benefit in preventing CVDs. If diabetes is not well controlled then pharmacological treatment is crucial (BNF, 2019).

1.6.1. Pharmacological treatment

1.6.1.1. T1DM management

As the β-cells of the pancreas do not produce insulin in T1DM, the only treatment available is to administer insulin by injections, pumps or syringes (BNF, 2019). Insulin can be obtained from three sources: bovine, porcine and human. Insulin products are also classed as rapid-, short-, intermediate- and long-acting insulin (Table 1.3) (BNF, 2019).

Table 1. 3: Insulin types used in the management of T1DM.

Class	Name	Onset	Peak (hours)	Duration (hours)
Rapid-acting insulin	Insulin glulisine	10-20 min	1	3
	Insulin lispro	15 min	1-1.5	2-5
	Insulin aspart	10-20 min	1-3	3-5
Short-acting insulin	Insulin regular	30-60 min	2-5	6-8
Intermediate-acting insulin	Insulin isophane	1-1.5 h	6-12	15-24

Long-acting insulin	Insulin glargine	1 h	N/A	24
	Insulin detemir	3-4 h	6-8	24

1.6.1.2. T2DM management

The first-line of treatment for patients diagnosed with T2DM is lifestyle management which involves changes in diet and increased physical activity. These measures are usually sufficient to bring blood glucose levels to normal (Raveendran *et al.*, 2018; Chauhan *et al.*, 2010). However, if hyperglycaemia is still not well controlled by changes in lifestyle, then pharmacological treatments are necessary (Raveendran *et al.*, 2018). These work mainly through three modes of action: stimulating the pancreatic β-cells to produce more insulin, reducing the body's demand for insulin or decreasing the rate of gluconeogenesis in the liver (Bösenberg and van Zyl, 2008). Current drugs used for the management of T2DM and their mechanisms of actions are detailed in Table 1.4.

Insulin can also be administered to people with T2DM only if agents in Table 1.4 do not control BG levels. It can be used in combination with other anti-diabetic agents (BNF, 2019). There are a number of side effects associated with the above pharmacological treatments. Hence, herbal medicines are considered to be a good alternative.

Table 1. 4: Pharmacological treatment for T2DM (Chaudhury *et al.*, 2017; Davies *et al.*, 2018; Pappachan *et al.*, 2018; Raveendran *et al.*, 2018; Van De Laar *et al.*, 2005; Baron, 1998).

Anti-diabetic class	Representative drugs	Mode of Action	Duration of action	% HbA1C reduction	Hypoglycaemia risk	Effects on body weight (BW)	Cardiovascular (CV) benefits/risks
Biguanides	metformin	Work by inhibiting gluconeogenesis in the liver and enhances glucose uptake by tissues	5 hours	1-2	None	Slight reduction in BW	Decrease Myocardial infarction (MI) by almost 40%, and coronary heart associated deaths by 50%.
Sulfonylureas	Glimepiride Glyburide Glypizide Gliclazide	Their action relies on stimulating the β-cells to produce more insulin, sulfonylureas are only of benefit if there are some functioning pancreatic β-cells		1-2	High	Increase BW	Increased CV risks, mainly because of hypoglycaemic effects.
α-glucosidase inhibitors	Acarbose Miglitol	They slow down the rate of carbohydrate digestion and postpone the absorption of glucose. They inhibit α-glucosidase which is the enzyme responsible for the		0.5-1	Moderate	No effects	Decrease coronary heart associated deaths

		break-down of carbohydrates					
Thiazolidinediones	Pioglitazone Rosiglitazone	They reduce BG by making the cells of the body more sensitive to insulin		0.5-1.4	Moderate	Increase BW	Cause cardiac failure
Sodium-glucose cotransporter (SGLT2) inhibitor	Canagliflozin Dapagliflozin Empagliflozin	Decrease plasma glucose by increasing renal excretion of glucose (glucosuria). Block 90% of glucose reabsorption in renal proximal convoluted tubule			low		Decrease CV risks
Glucagon-like peptide 1 (GLP-1) receptor agonists	Liraglutide Exenatide Dulaglutide	Enhance the pancreatic β-cells to produce more insulin by activation of GLP-1 receptor. They delay gastric emptying, decrease glucagon and increase feeling of satiety	24 hours 4-6 hours 7 days	0.5-1.5	None	Decrease BW	Decrease CV risks
Dipeptidyl peptidase IV (DPPIV) inhibitors	Sitagliptin Saxagliptin Vidagliptin Linagliptin Alogliptin	Inhibit DPPIV activity, and therefore prolong the action of GLP		0.5-0.8	low		Decrease CV risks

1.7. Issues with conventional blood glucose-lowering agents

Current treatment for managing diabetes is linked with a number of side effects as shown in Table 1.5. These include severe hypoglycaemia, permanent neurological deficit, stomachache, headache, lactic acidosis, liver damage, dizziness and death in some cases.

Table 1. 5: Summary of the side effects associated with current anti-diabetic drugs (Prabhakar and Doble, 2011; Chaudhury *et al.*, 2017)

Anti-diabetic drug/ class	Target at molecular level	Target site/ tissues	Side effect
Insulin	Insulin receptors	Liver, skeletal muscles, and fat tissues	Hypoglycemia, weight gain, and allergies to injections
Sulphonylureas	Sulphonylureas receptor, K^+ ATP channel	β-cells of the pancreas	Hypoglycemia and weight gain
Biguanides	Target is still unclear	Liver and muscle tissues	Lactic acidosis and gastrointestinal tract (GIT) discomfort. May cause anaemia and neuropathy in elderly
α-glucosidase inhibitors	α-glucosidase enzyme	Intestine	GIT discomfort
Thiazolidinedione	peroxisome proliferator-activated receptor gamma (PPAR-γ)	Liver,muscle, and fat tissues	Weight gain, anaemia and oedema
GLP-1 agonists	GLP-1 receptors	A-cells of the pancreas and L-cells of the intestinal mucosa	Hypoglycemia, pancreatitis, nausea and diarrhea

DPP IV inhibitors	DPP IV enzyme	Intestine	Pancreatitis, nausea and headache

Therefore, there is a need for better anti-diabetic drugs with fewer side effects to enhance patient compliance and to control BG levels more tightly. Natural products and plants in particular offer an alternative to synthetic drugs.

1.8. Natural products and diabetes

Over the centuries, plants have been used to treat various diseases including diabetes, CVDs and cancer (Middleton *et al.*, 2000). Diabetes management in the absence of any side effects remains a challenge in drug discovery (Kameswararao *et al.*, 2003). There are a number of natural products recommended for use in diabetes management, including *Agaricus blazei*, *Panax quinquefolius*, *Lagerstroemia speciose*, and *Cinnamomum aromaticum*. Plants are used therapeutically world-wide because of their effectiveness, fewer side effects and they are also considered to be cheaper than synthetic drugs. Approximately 800 plants have been used to manage diabetes and only 50% of them were experimentally shown to possess anti-diabetic activity (Prabhakar and Doble, 2011). However, only 109 plants are reported to have a clear mechanism of action (Prabhakar and Doble, 2011). The main active compound classes are thought to be alkaloids, flavonoids, tannins, terpenoids, polysaccharides, steroids, carbohydrates, chalcones and phenolic acids (Prabhakar and Doble, 2008). Plants can alter carbohydrate metabolism by various means. These include protecting pancreatic β-cells from damage, restoring β-cell function, enhancement of insulin release, increase glucose uptake by cells and can also have anti-oxidant activities (Prabhakar and Doble, 2011). Table 1.6 provides a list of synthetic diabetic drugs and traditional plants used for managing diabetes, their mode of action and target tissues. The market for herbal medicine is increasing and the scientific evidence of plant compound efficacy is also increasing. However, the regulation of such a market is still not well controlled and therefore the use of plants needs to be evaluated in more detail (Ernst, 2000). Hence, such plants need their efficacy, safety and side effects to be outlined. Table 1.7 shows recent clinical trials and their status to investigate anti-diabetic and

anti-obesity activity of plant extracts.

Table 1. 6: List of synthetic diabetic drugs and traditional plants used for managing diabetes and their mode of action and target tissues (Prabhakar and Doble, 2011)

Group/ Class	Targeted tissue/ mechanisms of action	Synthetic drug	Medicinal plant
Hypoglycaemia inducers	Enhancing insulin release in the pancreas	Sulphonylurea, miglitinides	*Lagerstroemia speciose, Momordica charantia, Trigonella foenum-graecum, Gymnema sylvestre.*
Inhibition of carbohydrate absorption	Reduce glucose absorbance in the intestine	Acarbose	*Phaseolus vulgaris, Plantago ovata, T. foenum-graecum.*
Insulin sensitisers	Reduce glucose absorbance in the liver, and increase glucose uptake in adipose tissues and skeletal muscles	Metformin, thiazolidinedione	*Panax quinquefolius, Lagerstroemia speciose, Cinnamomum aromaticum*
Others	----------	Exenatide, pramlintide, saxagliptin, sitagliptin	*Salvia hispanica, Stevia rebaudiana*

Table 1. 7: Clinical trials on medicinal plants for diabetes and obesity management.

Study	Status	Conditions	Interventions	Results	ID
Yerba Mate (*Ilex paraguariensis* A.St.-Hil.): Assessment of Cardiovascular Health (YMCH-2015)	C	Cardiovascular disease and Diabetes Mellitus	Yerba Mate Extract	None	NCT02789722
Effect of Pomegranate Extract Intake on Body Composition and Blood Pressure	U	Cardiovascular disease, Diabetes Mellitus and obesity	Dietary Supplement: Pomegranate extract	None	NCT02017132
Efficacy Study of IZN-6D4 Gel for the Treatment of Diabetic Foot Ulcers	C	Diabetic foot ulcer	IZN-6D4 Gel	None	NCT01427569
Evaluation of Fenugreek Seed Extract In Type- 2 Diabetes: An Add-On Study	C	Diabetes Mellitus	Dietary Supplement: *Trigonella foenum-graecum* extract	None	NCT02700477
Bauhinia Forficata in Diabetic Patients	C	Diabetes Mellitus	*Bauhinia forficata*	None	NCT02760017
Effect of Yoghurts Enriched With XXS (Mixture of Natural Polyphenolic Compounds and Plant Extracts) on the	C	Obesity and overweight	Dietary Supplement: yoghurts enriched with XXS	None	NCT02810041

Evolution of Weight in Overweight Subjects (VITALIM Senior)					
Ginger Capsules for the Chronic Treatment of Obesity	U	Obesity	Dietary Supplement: Dry extract of ginger	None	NCT02742194
Safety and Efficacy Study of Tarragon on Insulin Action in Humans (5011)	C	Obesity	Dietary Supplement: An alcoholic extract of *Artemisia dracunculus* L.	None	NCT01057576

C=completed, U=unknown

1.8.1. *Lathyrus* L

Lathyrus L. is a genus that belong to the tribe of Fabeae, a subdivision of the Fabaceae family (Allaby, 2012). There are around 380 species in the Fabeae tribe which evolved in the eastern Mediterranean in the period of middle Miocene (14 million years ago) (Jacovo *et al.*, 2019). Species of the Fabeae are distributed in Eurasia, tropical Africa and the Americas. *Lathyrus* genus consists of approximately 160 species which are distributed in the Northern Hemisphere, temperate regions (Asmussen and Liston, 1998; Kupicha, 1983). They are found in Asia, Europe, North America, South America and tropical East Africa; the number of species in each region is shown in Figure 1.5. The Eastern Mediterranean is considered the main centre for *Lathyrus* diversity with smaller centres in the Americas (Gurung and Pang, 2011; Kupicha, 1983).

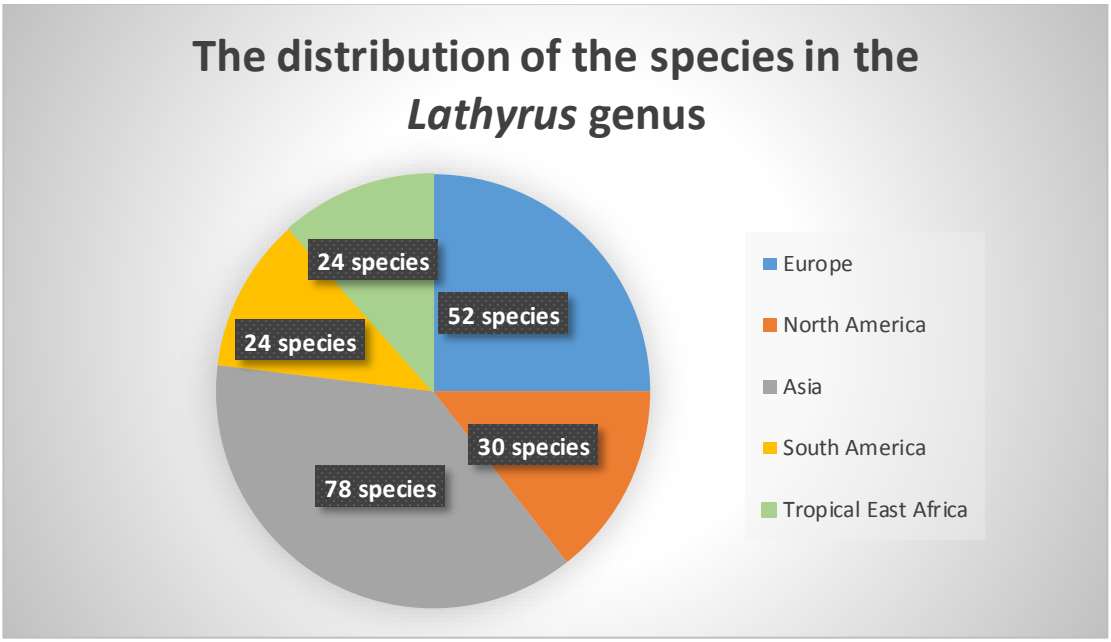

Figure 1. 5: The distribution of *Lathyrus* genus in various parts of the world.

The habitats of *Lathyrus* species is very diverse. They can be found in open pastures, fields, slopes woods, marshes, seashores, forest margins, meadows, sand dunes and roadsides (Asmussen and Liston, 1998). Both annual and perennial species are found in the genus, with a climbing or sprawling habit using simple or branched tendrils (Asmussen and Liston, 1998). *Lathyrus* species possess bee-pollinated papilionoid flowers with various colours (yellow, orange, red, purple, violet, blue or white)

(Asmussen and Liston, 1998; Kenicer *et al.*, 2005). These species can be productive in low nutrient soils due to their ability for biological N fixation (BNF) and some of the species have roots which help with stability in arid environments and this feature is relevant to *Lathyrus linifolius* (Reichard) Bässler (Jacovo *et al.*, 2019).

1.8.1.1. *Lathyrus linifolius*

L. linifolius (LL) (Table 1.8) is cultivated for both aesthetic purposes and aromatic flowers and therefore it is considered as a horticultural species (Jacovo *et al.*, 2019). LL plays an important role in semi-natural and ecological interactions by attracting oligophagous butterflies and moths such *as Leucoptera lathyrifoliella form orobi, Phyllonorycter nigrescentella, Grapholita jungiella, Grapholita lunulana* and *Zygaena lonicerae*. Some of these butterflies became extinct as a consequence of LL loss from such habitats (Nilsson *et al.*, 2008). LL is found in both grazed and ungrazed semi-natural grass lands with low altitudes (20-350 m above sea level) (Jacovo *et al.*, 2019). It grows in low nutrient soils with a pH of 4-7 (Grime *et al.*, 2014). LL is believed to be present on approximately 60% of the European territories including throughout the United Kingdom but does not grow in North Europe where the climate is extremely cold (Grime *et al.*, 2014).

Table 1. 8: Characteristics and classification of LL.

Plant Name	*L. linifolius*
Family	Fabaceae
Tribe	Fabeae
Genus	Lathyrus
Species	*Lathyrus linifolius* (Reichard) Bässler
Synonyms	*Lathyrus tuberosus, Lathyrus montanus* Bernh, *Lathyrus linifolius var. montanus* (Bernh.) Bässler, *Lathyrus macrorrhizus* Wimm, *Orobus tuberosus* L., *Lathyrus linifolius var. montanus* (Bernh.) Baessler, *Orobus linifolius* Reichard (NBN-Atlas, 2019)

Common names	Heath Pea, Bitter Vetch, Bitter Vetchling, liquor-knots, liquory-knots and liquorice vetch.
Growing form	Perennial plant
Height	15-30 cm
Flower	Purple-bluish colour
Flowering time	May-June
Leaves	Alternate, stalked, stipulate. Blade pinnate, 2–4-pairs, lacking tendrils. Leaflets elliptic–lanceolate–linear, blunt, with entire margins. Stipules large.
Fruit	Brown-blackish in colour and produces 6-10 seeds per pod.

1.8.1.1.1. Historical use of LL

Historical uses of LL have been addressed in a number of records, but most specifically from the Scottish Highlands in the 17th century. During Medieval times, the tubers of LL were consumed as food by people for several reasons. They were used to overcome inebriation symptoms, relieve chest diseases and to relieve flatulence. Tubers were also used as flavouring agents (Jacovo *et al.*, 2019). They were sliced and immersed in hot water or neutral alcohol which was then used to give a liquorice-like taste in beverages; hence, liquor-knots, liquory-knots and liquorice vetch are other common names for the tubers of LL. Thirdly, tubers were fermented for the production of beers with a neutral spirit flavour. The more general use of the tubers was believed to be as an appetite suppressant because they prevent the feelings of hunger (Jacovo *et al.*, 2019). An appetite could be suppressed for weeks and in some cases even up to a month following the consumption of the tubers of LL.

1.8.1.1.2. Scientific research on LL

1.8.1.1.2.1. Leaves of LL

At the time of writing this report, there was only one article regarding the leaves of LL which was published in 1939. Charaux was the first person to isolate oroboside from the leaves of LL (Charaux and Rabate, 1939). Oroboside has been identified in other plants including fruits of *Cudrania tricuspidata* (Jo *et al.*, 2017; Song *et al.*, 2017), fruits of *Fructus Sophorae* (Yang *et al.*, 2019b), peels of *Pyrus ussuriensis* Maxim (Qiu *et al.*, 2018), leaves of *Lagerstroemia speciose* (Choi *et al.*, 2010) and leaves of *Eclipta prostrata* (Chung *et al.*, 2017).

Oroboside, orobol 7-O-glucoside, is a derivative of orobol (Figure 1.6). A study by Choi *et al.* showed that oroboside had antiviral activities with a broad spectrum against human rhinovirus (HRV) species (Choi *et al.*, 2010). Orobol is a rare isoflavone which has several biological activities. To start with, recent research by Yang *et al.* showed that orobol (20 µM) inhibited the adipocyte differentiation in 3T3-L1 preadipocytes (Yang *et al.*, 2019a). Secondly, orobol was found to enhance the sensitivity of human ovarian carcinoma to cisplatin (Isonishi *et al.*, 2003). Furthermore, isolated orobol from *Eclipta prostrata* was evaluated for its anti-inflammatory activity against lipopolysaccharide (LPS)-induced nitric oxide (NO), prostaglandin E2 (PGE_2) and TNFα release in RAW264.7 cells. The findings showed that orobol inhibited NO and PGE_2 with IC_{50} values of 5 µM and 50 µM, respectively but that the compound was inactive against TNFα (Tewtrakul *et al.*, 2011). Lastly, orobol was found to be an anti-oxidant. Qiu *et al.* showed that orobol scavenges reactive oxygen species (ROS) in a DPPH assay and had an IC_{50} value of 29 µg/ml (Qiu *et al.*, 2018).

A: Oroboside

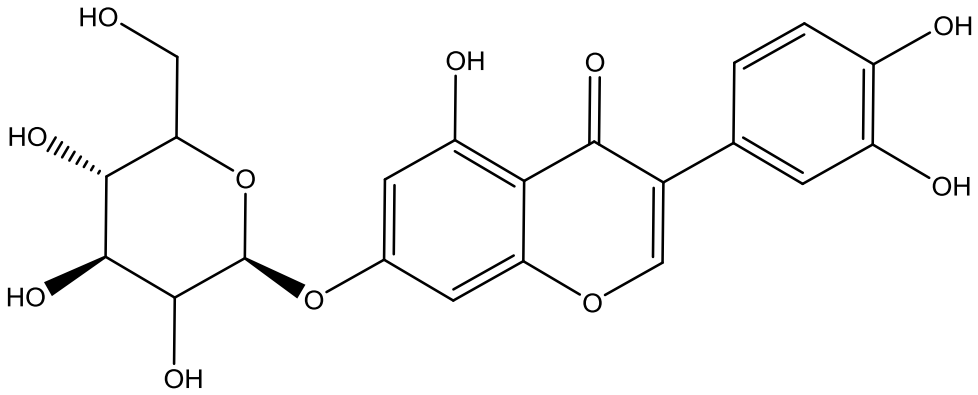

B: Orobol

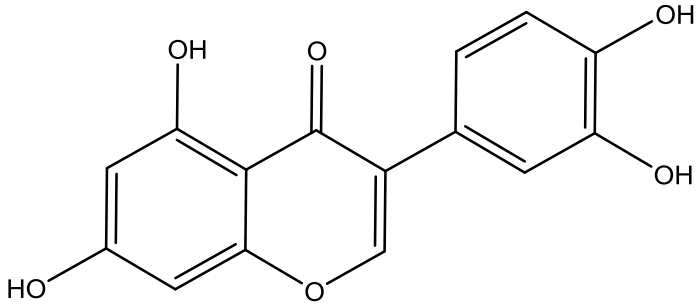

Figure 1. 6: Chemical structures of Oroboside (A) and orobol (B).

1.8.1.1.2.2. Flowers of LL

Three anthocyanins, delphinidin, petunidin and malvidin, were identified in the flowers of LL by Pecket when studying the flower colour variation among the *Lathyrus* species (Pecket, 1960). Anthocyanins are hydrophilic flavonoid compounds which impart colour to plants' flowers and fruits (Glover and Martin, 2012). Anthocyanins are known to possess a broad spectrum of biological activities. Firstly, anthocyanins were found to be potent inhibitors of NO which indicates that such compounds have anti-inflammatory activities (Wang and Mazza, 2002). In addition, anthocyanins are potent anti-oxidant agents. A study by Wang *et al.* looked at the antioxidant activity of *Hibiscus* anthocyanins (HAs) (Wang *et al.*, 2000). HAs were found to significantly

decrease levels of lactate dehydrogenase and malondialdehyde induced by tert-butyl hydroperoxide (t-BuOOH). The study also showed that oral administration of HAs *in vivo* decreased oxidative liver damage caused by t-BuOOH. Moreover, hepatotoxicity following exposure to carbon tetrachloride is significantly lowered in rats treated with anthocyanins from petals of *H. rosasinensis* (Obi *et al.*, 1998).

1.8.1.1.2.3. Tubers of LL

A private limited company called Heath Pea Ltd. was established in 2006 and it advertised a new slimming aid, which was based on the tubers of LL. However, this company was dissolved from the Companies House register in September 2017 and unfortunately, there was no publication from the company regarding the activity of LL tubers (LLT). A recent PhD study by Woods investigated the activity of LLT using various *in vitro* and *in vivo* tests (Woods, 2017). An ethyl acetate extract of LLT (LLT EA) was found to be a strong inhibitor for α-glucosidase, an enzyme implicated in diabetes which suggested that it has therapeutic potential for diabetes. However, the compound responsible for this activity was not isolated and tested. Therefore, there was still a need to fractionate and isolate compounds from LLT EA extract and test against α-glucosidase. LL tubers were also dissolved in water and given to rats by oral gavage. Their body weight (BW), water intake (WI) and food intake (FI) were monitored. All of the monitored parameters were comparable to the control and this might be as a result of the low LL tuber dose and/ or the incorrect route of administration (oral gavage) used in the research.

Obesity is linked to diabetes and particularly to T2DM. Hence, the current research aims to investigate the potential anti-diabetic and anti-obesity activities of LL tubers and leaves and isolate compounds responsible for their activity. This aim will be achieved by looking at various research aspects which are discussed and explained in Chapters 2-6. A summary of the chapters in the thesis is shown in Figure 1.7. Briefly, Chapter 2 looks at the collection of plant materials and phytochemistry methods used to isolate and identify compounds present in the tubers and leaves of LL and the isolates and extracts that were used in subsequent chapters. The anti-diabetic activity is assessed in Chapter 3 using various enzymatic assays and glucose uptake assays in

cells. Chapter 4 investigates the anti-oxidant and anti-inflammatory properties of LL extracts and isolated compounds, while in Chapter 5, RNA sequencing (RNA-Seq) was carried out on pancreatic tissues of normal Sprague Dawley (SD) male rats treated with LL tubers by Woods (2017) to provide a comprehensive picture of the genes and pathways affected by LL tubers. An *in vivo* experiment was carried out on obese male and female Zucker rats and the animals were monitored in terms of their BW, FI, WI and BG levels as detailed in Chapter 6. Lastly, the main findings and concluding remarks are summarised in Chapter 7.

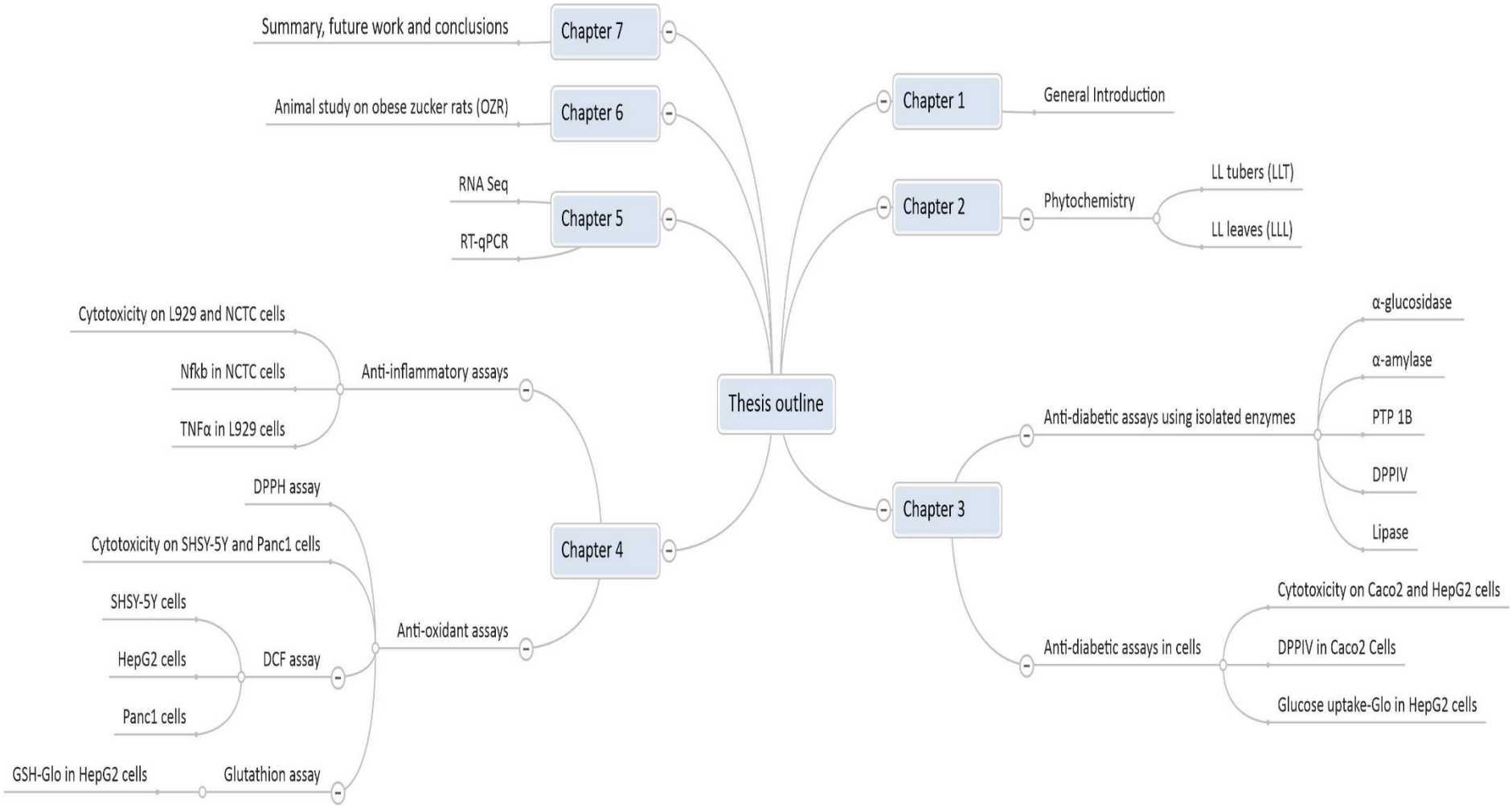

Figure 1. 7: Diagram outlining the main research aspects of each chapter in the current research.

Chapter 2

2. Phytochemical analysis of tubers and extracts of *L. linifolius*

2.1. Introduction

Natural products play a fundamental role in the area of drug discovery. In today's medicine, more than 50% of the drugs on the market are derived from natural products (Clark, 1996). A number of drugs are considered to be hallmarks of today's pharmaceutical care and originate from natural products. These include morphine, digoxin, vincristine, vitamin A, theophylline, quinine, penicillin G, doxorubicin, cyclosporine and taxols (Cheuka *et al.*, 2017). Natural products and plants have been used as sources for therapeutics for centuries. It is documented that Ancient Egyptians practiced medicine since 2900 BC. The Egyptian pharmaceutical practice was first recorded in "Ebers Papyrus" which is believed to date back to 1500 BC (Newman and Cragg, 2007). More than 700 active drugs were described in the Papyrus and most of these drugs were from plants. The Papyrus provided details of various drug formulations including gargles, tablets, snuffs, ointments and infusions where water, milk, honey and beer were the vehicles used to deliver the drugs (Newman and Cragg, 2007). The use of plants as crude samples is not commonly used these days. Instead, isolation and purification of the active constituents are the preferred methods in today's pharmaceutical care (Cheuka *et al.*, 2017). Thirteen new approved natural products derived agents were approved between 2005 and 2007, indicating that natural products are valuable sources in today's medicine (Butler, 2008). Isolated natural products have shown broad therapeutic spectra, as anti-bacterial, anti-cancer and anti-diabetics (Cheuka *et al.*, 2017). Approximately 50% of the natural products have a low log p value, hence they get absorbed easily and this complies with "Lipinski's Role of five" for orally available drugs (Ganesan, 2008).

Phytochemistry is a branch of chemistry which deals with the life of plants and the compounds produced by them (Singh, 2011). The use of plants as anti-diabetic agents is applied in two preferred forms. The first is to create a mixture which contains various plant active ingredients or extracts. These extracts can be obtained by dissolving plant materials in solvents with different polarities in order to produce different extracts

(Sasidharan *et al.*, 2011). The other preferred form is the isolation of the active pure compounds from plants (Rasoanaivo *et al.*, 2011). This second form is superior to the first, as the dose can be given precisely.

The main active plant classes with hypoglycaemic activity are alkaloids, flavonoids, tannins, terpenoids, chalcones and phenolic acids (Prabhakar and Doble, 2011, Raut *et al.*, 2016).

2.1.1. Alkaloids

Alkaloids are nitrogen-containing compounds with naturally occurring amines that possess a broad spectrum of pharmacological actions (Raut *et al.*, 2016). In 1819, the alkaloid name was first described by a German chemist Carl Friedrich Wilhelm (Aniszewski, 2007). The name "alkaloid" comes from two words "alkali" and "loid" which combined have the meaning of "alkali like". This means that such compounds are alkaline (basic) (Aniszewski, 2007). Berberine (Figure 2.1) is a well-known alkaloid that possesses anti-hyperglycaemic effects. It is isolated from various plants including *Tinospora cordifolia* (Mittal and Sharma, 2017), *Berberis aquifolium* (Cicero and Baggioni, 2016), *B. aristata* (Semwal *et al.*, 2018), *B. vulgaris* (Imenshahidi and Hosseinzadeh, 2016) and *Coptis chinensis* (Lee *et al.*, 2018). *Catharanthus roseus* was reported to have alkaloids such as catharanthine, vindoline and vindolinine (Figure 2.1) which all have hypoglycaemic effects (Pan *et al.*, 2016).

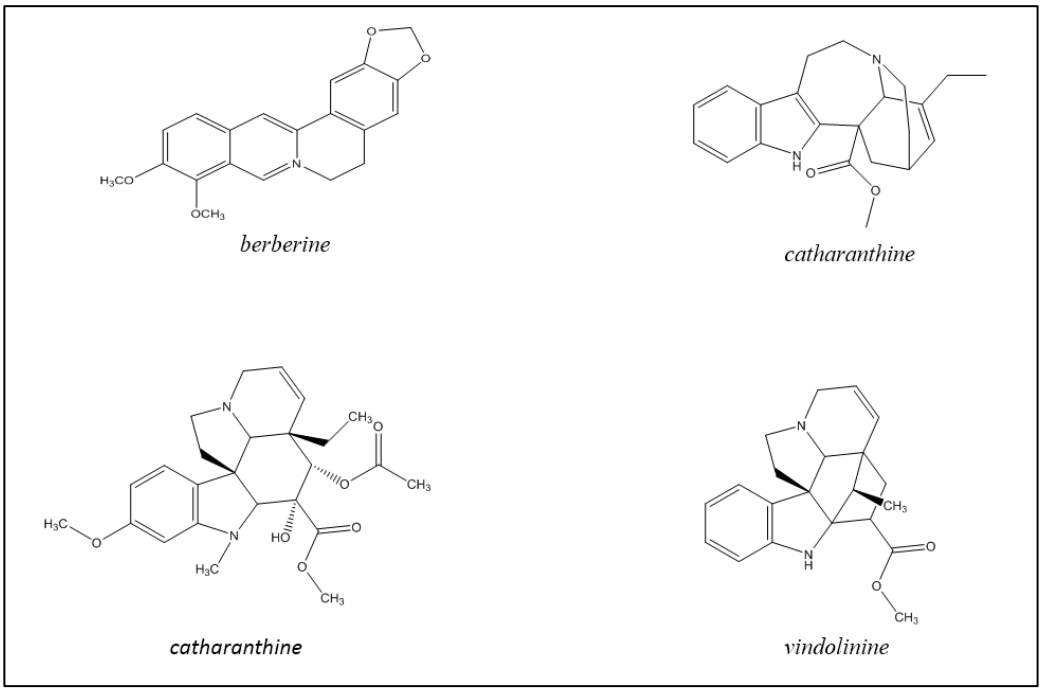

Figure 2. 1: Chemical structure of alkaloids with hypoglycemic effects.

2.1.2. Flavonoids

Flavonoids are a group of many bioactive chemicals with different chemical structures and features (Panche *et al.*, 2016). They exist in fruits, vegetables, herbs and other plant foods. There are at least 6000 phenolic compounds listed in the flavonoids class. These compounds have 15 carbon atoms with two aromatic rings and a heterocyclic ring (Figure 2.2) (Heller and Forkmann, 2017). Flavonoids are acceptably classed into 6 sub-classes: flavonols, flavones, flavanones, flavan-3-ols, isoflavones and anthocyanidins (Panche *et al.*, 2016).

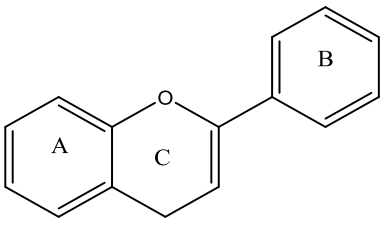

Figure 2. 2: Generic structure of a flavonoid. A & B are aromatic rings and C is a six-membered heterocyclic ring.

It is believed that some flavonoids exhibit hypoglycaemic effects by enhancing glucose and oxidative metabolic pathways (Li *et al.*, 2016). Quercetin (Figure 2.3) is found to elevate glucokinase activity in the liver which enhances insulin release from the pancreas (Berroukeche *et al.*, 2019). Other flavonoids such as hesperidin and naringin (Figure 2.3) are found to decrease BG levels in diabetic mice when administered at a dose of 0.2 g/kg (Hii and Howell, 1985).

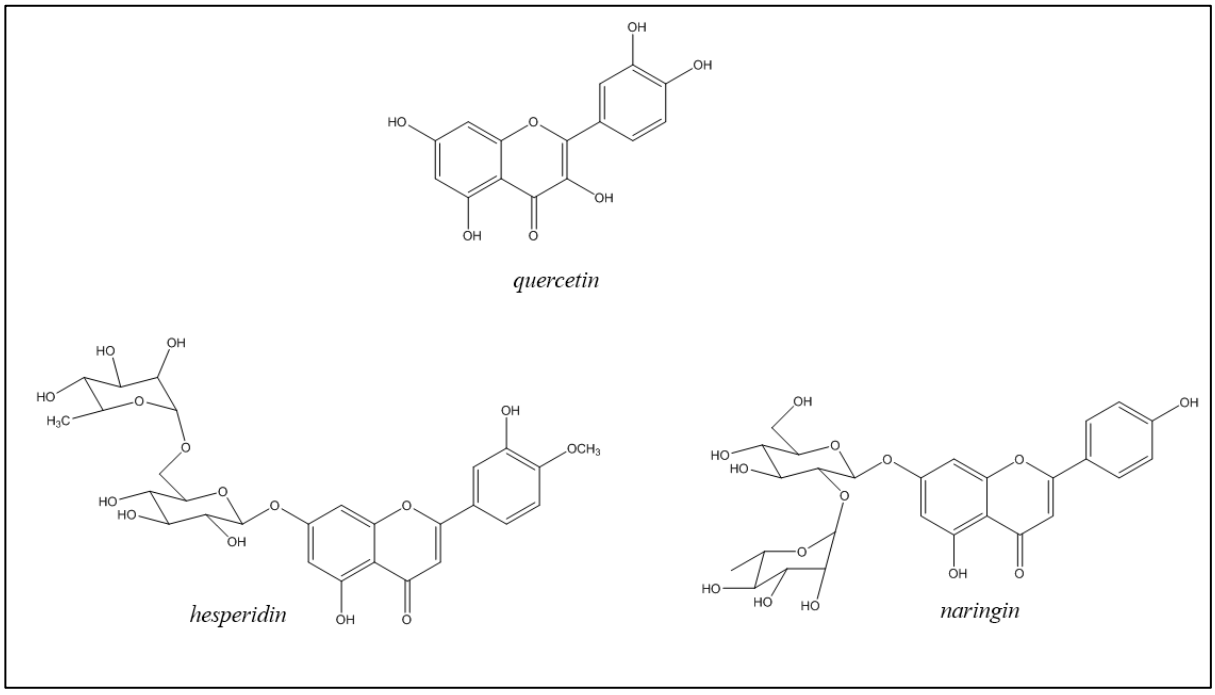

Figure 2. 3: Chemical structure of flavonoids with hypoglycemic effects.

2.1.3. Tannins

Tannins are also classed as plant polyphenols and they can be found in all parts of higher plants such as bark, seeds, roots, leaves and fruits (Hassanpour *et al.*, 2011). They are called "tannins" because such chemicals have astringent and tanning features (Raut *et al.*, 2016). Tannins are important defense mechanisms for plants which protect against bacteria, insects and animal herbivory. Tannins are large compounds with molecular weights ranging from 500 to 30,000 Da and they also possess strong anti-oxidant activities (Serrano *et al.*, 2009). Gallotannins and ellagitannins are the most common type of tannins which can undergo hydrolysis (Niemetz and Gross, 2005).

Some gallotannins (Figure 2.4) are found to possess anti-diabetic activity by acting on the insulin pathways; they phosphorylate the insulin receptor and insulin receptor substrate 1, and increase mRNA expression of GLUT4 and PI3-kinase (Kanaujia *et al.*, 2010). Ellagitannins have been found to competitively inhibit α-glucosidase enzyme in a dose-dependent manner (McDougall *et al.*, 2005).

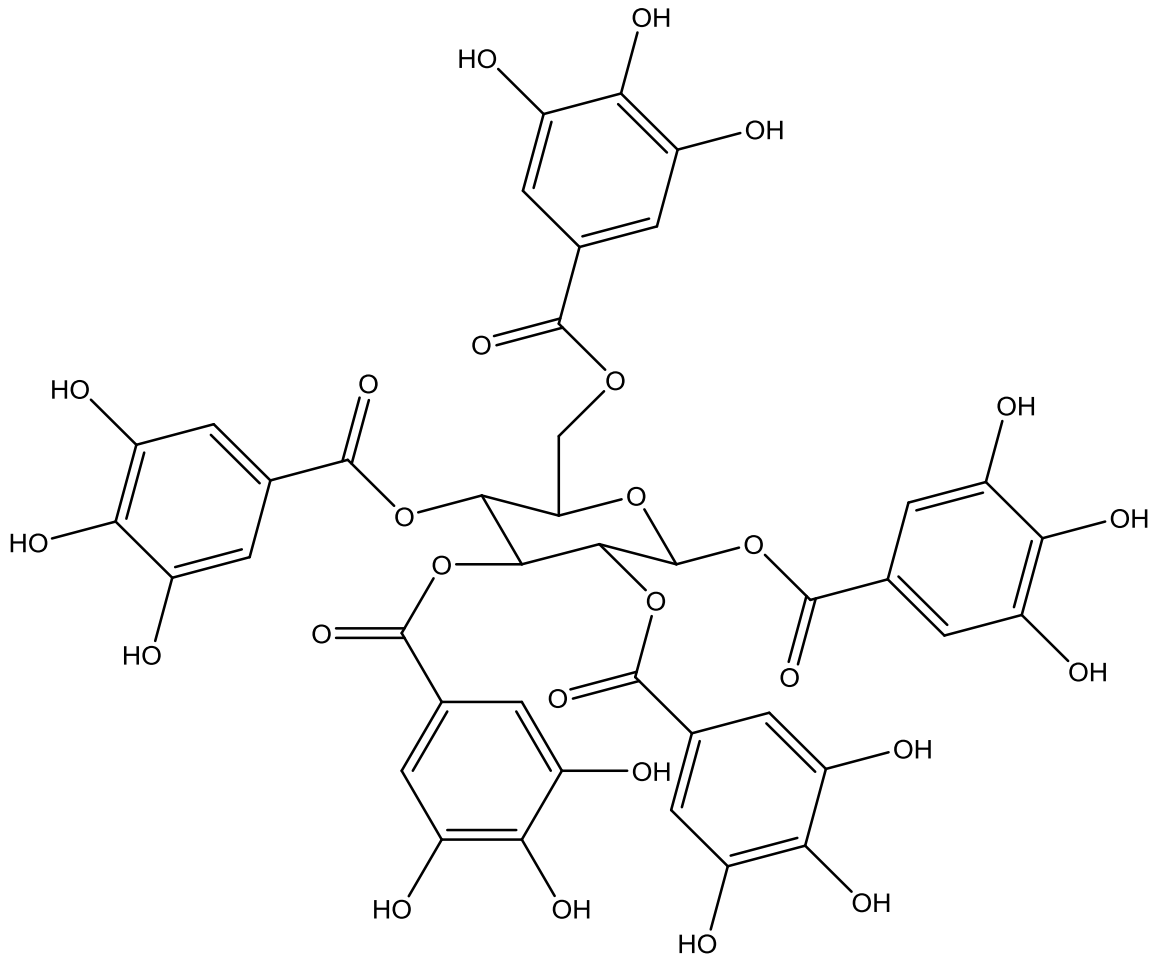

Figure 2. 4: General structure of gallotanins.

2.1.4. Terpenes and Terpenoids

Terpenes and terpenoids are plant constituents that possess similar chemical structures and differ in some functional groups (Zwenger and Basu, 2008). Terpenoids are terpenes that have been modified by oxidative mechanisms, methyl group removal and

by rearranging the isoprene carbon skeleton (Wagner and Elmadfa, 2003). Pentacyclic triterpenes are produced by plants and are responsible for many biological activities. These compounds are classed into oleanane-type triterpenes, ursane-type triterpenes and lupane-type triterpenes (Laszczyk, 2009). Ursolic acid and oleanolic acid (Figure 2.5) are pentacyclic triterpenes that have been reported to inhibit the activity of protein tyrosine phosphatase 1B (PTP 1B) (Na *et al.*, 2006; Zhang *et al.*, 2008). PTP 1B is a negative regulator for insulin release; therefore, deactivating this enzyme is a potential target for managing diabetes and enhancing insulin release (Zhang and Lee, 2003). Ursolic acid also stimulates insulin receptors to be phosphorylated and this enhances glucose uptake (Zhang *et al.*, 2006).

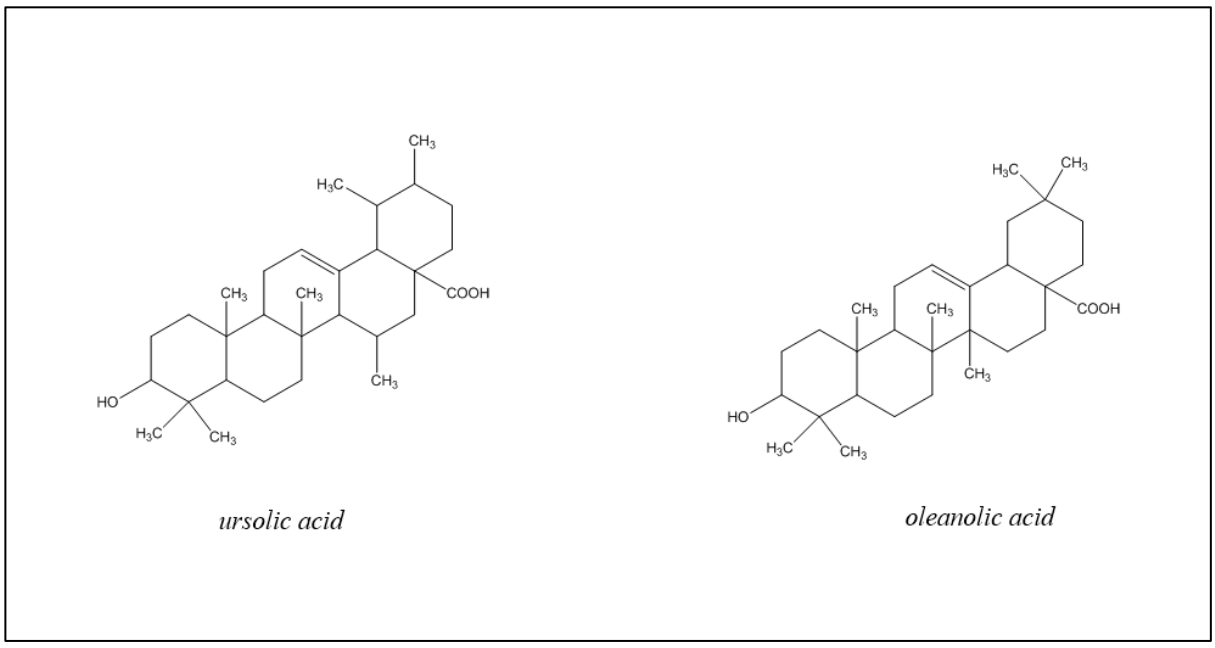

Figure 2. 5: Chemical structure of pentacyclic triterpenes with hypoglycemic effects.

2.1.5. Chalcones

Chalcones are a group of phytoconstituents that are α, β- unsaturated ketones with two aromatic rings (Sahu *et al.*, 2012). They have various biological activities including anti-diabetic properties (Enoki *et al.*, 2007). The compound 2-hydroxy-40'-

methoxychalcone (Figure 2.6) is a chalcone with predicted anti-diabetic activity from the fact that it possesses anti-atherosclerotic activity (Hsieh *et al.*, 2012). It stimulates peroxisome proliferator-activated receptor gamma (PPAR-γ) mRNA and protein expression in muscle cells (Hsieh *et al.*, 2012).

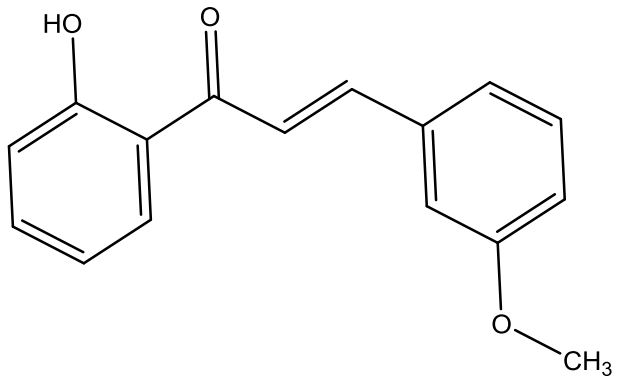

Figure 2. 6: Chemical structure of 2-hydroxy-40'-methoxychalcone.

2.1.6. Phenolic acids

Phenolic acids are non-flavonoid polyphenolic compounds that are found in many fruits and vegetables (Rentzsch *et al.*, 2009). These compounds are derived from benzoic and cinnamic acids (Pandey and Rizvi, 2009). Phenolic acids are known as potent anti-oxidant compounds (Sroka and Cisowski, 2003). They also have anti-diabetic activity e.g. ferulic acid (Figure 2.7) has been reported to be a hypoglycaemic agent (Jung *et al.*, 2007). Moreover, such compounds increase the activity of glucokinases and glycogen production in the liver and therefore regulate BG in the body (Vinayagam *et al.*, 2016). Adiponectin, a positive regulator of BG, was found to be significantly increased by hydrangeic acid (Figure 2.7) (Zhang *et al.*, 2009). Cinnamic acid (Figure 2.7) is also a hypoglycaemic agent that has been found to enhance insulin release and activate insulin-mediated glucose transport (Hafizur *et al.*, 2015).

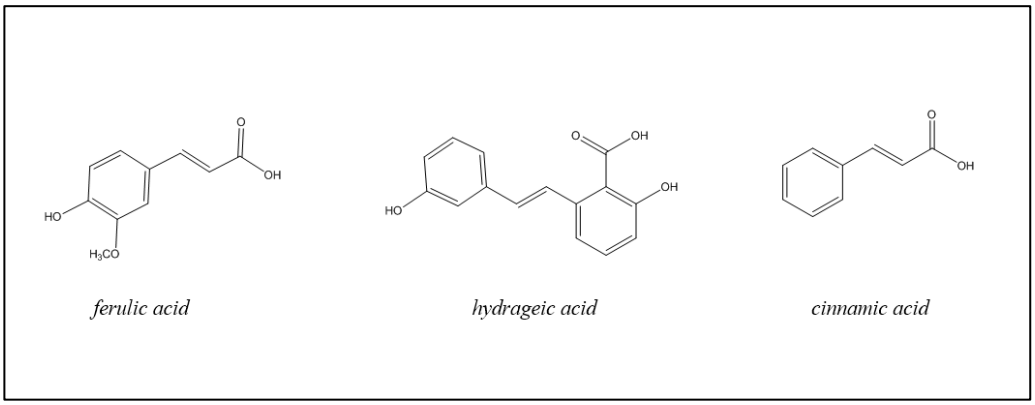

Figure 2. 7: Chemical structure of phenolic acids with anti-diabetic activity.

2.1.7. Plant collection and extraction

Plants can produce various compounds at different concentrations, depending on the season and the stresses that surround the plants (Figueiredo *et al.*, 2008). Therefore, it is sometimes challenging to get the same activity from the plants that have been collected in different seasons. Once the plant materials (e.g. leaves, roots, and tubers) are collected, they are dried and then ground using a pestle and mortar or a grinder to produce fine powder materials. This process is called homogenisation.

2.1.8. Plant extraction

Following the homogenisation step, the powder is exposed to various solvents with different polarities (Azmir *et al.*, 2013). Some classic examples of solvents used in phytochemistry are shown in Table 2.1.

Table 2. 1: Solvents used to yield extracts from plants.

Polarity	Name	Chemical structure
Non-polar	Hexane, Hex	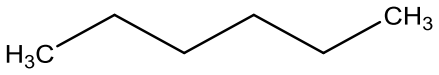
Semi-polar	Ethyl acetate, EA	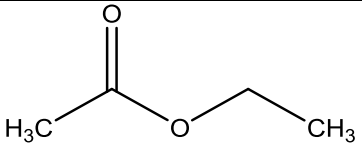
Polar	Methanol, MeOH	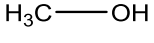

Maceration and Soxhlet apparatus extraction are the two most common methods of extracting plant materials (Azmir *et al.*, 2013). Maceration is the process in which plant extracts are yielded by soaking the plant materials in a solvent (Jones and Kinghorn, 2006). Soxhlet extraction involves soaking the plant in a solvent at a high temperature and allows for continued extraction (Ncube *et al.*, 2008; Azmir *et al.*, 2013). Following the extraction process, extracts are dried and prepared for the separation step.

2.1.9. Methods of separation

Plant extracts contain mixtures of several compounds and therefore separation techniques are required to isolate and purify the compounds present in them. These techniques include the following (Li *et al.*, 1998; Harborne, 1998; Romanik *et al.*, 2007): Paper chromatography (PC), Thin layer chromatography (TLC), High performance liquid chromatography (HPLC), Column chromatography (CC), Gas liquid chromatography (GLC) and Electrophoresis.

These separation methods assist in separating compounds based on the compounds' molecular weight, charge and the way in which they interact with the stationary phase (Romanik *et al.*, 2007). TLC and CC are discussed in more depth below as they were the separation methods used in this project.

2.1.9.1. Thin Layer Chromatography (TLC)

TLC is an easy and simple form of chromatography which is fundamental for separating compounds in mixtures (Stahl and Mangold, 1975). TLC is helpful in decision making when it comes to choosing mobile phases for other separation methods such as CC, flash chromatography (FC) and vacuum liquid chromatography (VLC). TLC separation is achieved by applying a spot of samples (which have already been dissolved in a suitable solvent) by capillary tube above the bottom edge (1cm) of a TLC-grade silica gel-coated sheet (Marston, 2011). A mixture of suitable solvents is then added to the TLC tank as a mobile phase and is allowed to settle down for a few minutes. The TLC plate that is already spotted is inserted inside the TLC tank. The

mobile phase is allowed to move until it reaches 1cm from the top of the TLC plate. The TLC plate will then be removed and the solvent front is marked with a pencil and the plate will be air-dried. The TLC plate can be visualised under UV light (λ 254nm and 366nm) after being visually examined in daylight. Then, anisaldehyde-H_2SO_4 spray can be used to spray the plate (5ml sulphuric acid, 85ml MeOH, 10ml glacial acetic acid and 0.5ml anisaldehyde) and the plate is heated for one minute at 110 °C. The distance travelled by each spot (sample) is then divided by the total distance travelled by the mobile phase to give Rf values for the samples. Rf values aid in pooling similar samples together, which are then dried before being analysed by ,for example, nuclear magnetic resonance (NMR).

2.1.9.2. Size-Exclusion Chromatography (SEC)

Size-Exclusion Chromatography (SEC) is also called gel filtration chromatography or molecular sieve chromatography (Hong *et al.*, 2012). As its name suggests, SEC achieves the separation of compounds in terms of their molecular weight. SEC was here performed by adding a slurry of 35g of Sephadex LH-20 to a 20.5cm height and 1.5cm diameter glass column. This separation method is preferred for polar extracts and in particular MeOH extracts. The extract can be dissolved in a small amount of MeOH and applied to the top of the glass column. The extract's elution might be achieved by using a suitable solvent such as 100% MeOH and samples/fractions are collected for example every 3 ml in 10 ml glass vials.

2.1.9.3. Column Chromatography (CC)

This type of chromatography is used to isolate and fractionate both polar and non-polar compounds from mixtures (Hostettmann and Marston, 2001). Compounds move down the column at different rates and therefore, CC separates compounds based on differential adsorption to the adsorbent to yield fractions and pure compounds. This technique is commonly applied to plant mixtures because of several reasons. To start with, CC has a variety of column sizes allowing the procedure to be carried out on both small and large scale materials (from milligrams to kilograms). Secondly, CC is a simple and inexpensive technique which allows for the disposal of the stationary

phase; thus, cross-contamination is prevented. CC is performed using the gravity or vacuum to move solvents.

2.1.10. Spectroscopic techniques

2.1.10.1. Nuclear Magnetic Resonance (NMR)

NMR is a method used to perform structural elucidation for compounds in crude extracts, fractions and pure samples. NMR is advantageous because it is highly reliable and robust, as well as being a non-destructive tool (Gray *et al.*, 2012). NMR is capable of identifying the types and numbers of atoms present per sample (Jackman and Sternhell, 2013). NMR uses radio-frequency to cause nuclei excitation. Common atoms detected by NMR include hydrogen (^{1}H) and carbon (^{13}C). Atoms' chemical shifts are expressed either as in delta (δ) scale or parts per million (ppm), and this information is shown in the Proton (^{1}H) and Carbon (^{13}C) spectra. The peak area in NMR spectra is called the integral, which is an approximate representation of the number of atoms per signal. Coupling constant *J* is the multiplets value (m) that provide information on the nuclei number that is coupled to the atom.

Proton (^{1}H) and Carbon (^{13}C) NMR are known as one-dimensional NMR (1D NMR) techniques which are still used these days. However, for advanced structural elucidation, two-dimensional NMR (2D NMR) techniques are employed. 2D NMR includes Correlation Spectroscopy (COSY) which analyses the proton splitting patterns to find out the number of protons on the adjacent carbon atom. COSY techniques look at ^{1}H-^{1}H connectivity where the proton spectra are plotted on two axes to create cross peaks around the diagonal of the square graph. The second 2D NMR is Nuclear Overhauster Effect Spectroscopy (NOESY). This technique looks at signals created by protons which are close to each other in space and do not have to be bonded. The third type is Heteronuclear Multiple Bond Coherence (HMBC) which determines the connectivity between carbon atoms and their hydrogen atoms. Lastly, Heteronuclear Single Quantum Coherence (HSQC) detects heteronuclear correlations over longer ranges of up to 4 bonds.

2.2. Aims and Objectives

This chapter aims to isolate and analyse the phytochemical constituents of leaves and tubers of LL; this will be achieved by:

1. Collecting and drying plant materials and grinding them into powder form.
2. Performing Soxhlet extraction on the ground plant materials.
3. Analysing the extracts using NMR.
4. Performing CC on the EA extract of the tubers (LLT EA) to isolate compounds; this extract showed positive anti-diabetic activity in previous research, but responsible compounds for the activity were not isolated.
5. Structural elucidation of the isolates using ^{1}H and ^{13}C NMR techniques.

2.3. Materials and methods

2.3.1. Plant collection

Tubers and leaves of LL (Figures 2.8 and 2.9) were collected from Reading in England by Mark Goff, founder of Bitter Vetch Company, in September 2016. The leaves and tubers of LL were grown using seeds that were originally obtained from Soutra Aisle. Soutra Aisle was the largest hospital in Scotland during medieval times where inhabitants of the hospital consumed LL tubers to fight hunger and thirst. Plant identity was confirmed by Dr. Kenicer (Royal Botanic Gardens Edinburgh) who, studied the *Lathyrus* genus during his PhD and Dr Brian Moffat who was the excavation leader at Soutra Aisle. The plant materials were air-dried to minimise degradation of materials and to prevent mould contamination.

Figure 2. 8: LL tubers used in this project.

Figure 2. 9: LL leaves used in this project.

2.3.2. Plant grinding and powdering

Dried LL tubers and leaves were ground in a grinder to produce powders for easier extraction with the Soxhlet apparatus.

2.3.3. Plant Extractions

Compounds were extracted from LL tubers and leaves using a Soxhlet apparatus. Three solvents were used to extract most of the chemicals from the plant – these were Hex, EA and MeOH. The fine powder was placed in a cellulose extraction thimble and extractions carried out using each solvent, run for 6 hours per day over four days. Extraction flasks contained anti-bumping granules to prevent solvents from bumping as they heated. A rotary evaporator was used to concentrate the extracts by evaporating the solvents at 40°C under reduced pressure. Extracts were placed in pre-weighed glass

beakers which were accurately labelled and left to completely dry under the fume hood. Following complete solvent evaporation, the crude extracts were weighed and the percentage yield was calculated using the following formula:

$$\%\ Yield = \frac{\text{Weight of crude extract (g)}}{\text{Weight of plant material used (g)}}\ X\ 100$$

2.3.4. NMR samples

Twenty mg of each crude extract was dissolved in suitable deuterated NMR solvents (CDCl3, acetone-d_6 and DMSO- d6) and then 600µl of the solution was placed into an NMR tube (5 x 178 mm) to a depth of 4cm. NMR spectra were processed using MestReNova software 8.1.2 (Mestrelab Research, A Coruña, Spain). Structures of identified compounds were then drawn using ChemDraw Professional software, Version 17.1.0.105 (19) (PerkinElmer, Yokohama, Japan).

2.3.5. CC

CC was applied to separate compounds present in the ethyl acetate extract of the tubers (LLT EA). These crude extracts showed activities against α-glucosidase. Therefore, it was decided to find out the compound that was responsible for the activity and test it in various biological assays.

CC was prepared using an open glass column (55 x 3 cm) that was packed with 50g of silica gel 60 saturated with 100% Hex solvent. Two g of tuber EA extract was dissolved in the lowest amount of Hex and then pre-adsorbed in silica gel 60 and left to dry in the fume hood. Then, the pre-adsorbed extract was added to the top of the column and followed by inserting a cotton plug to prevent disturbance of the loaded material by the elution solvent system. The elution of samples was started by adding 100% Hex, and then the gradient elution was continued. The polarity was increased by 5% each time (300 ml of each solvent system) using EA until it reached 100% EA. The last solvent system was 5% (v/v) MeOH in EA – higher MeOH percentages can

dissolve the silica gel. Samples/fractions were collected every 15ml in a 20ml glass vial.

2.4. Results

2.4.1. Extraction using Soxhlet apparatus

The percentage yields of the extracts from tubers and leaves of LL are shown in Tables 2.2 and 2.3. Leaves and tubers produced similar yields, MeOH extracts being the highest, followed by EA and then Hex.

Table 2. 2: % yield of LL tubers from Soxhlet extraction.

Solvent system	Powder used (g)	Crude extract (g)	% Yield
EA	528	4	0.8
Hex	528	2	0.4
MeOH	528	10	1.9

Table 2. 3: % yield of LL leaves from Soxhlet extraction.

Solvent system	Powder used (g)	Crude extract (g)	% Yield
EA	420	4	1
Hex	420	1	0.2
MeOH	420	8	2

2.4.2. Characteristics of crude samples by NMR

The characteristics of crude extracts were obtained by analysing the NMR spectra (Figures 2.10- 2.15). A summary of the main compounds in each extract is given in Table 2.4.

Table 2. 4: Main class/ compounds present in the extracts of tubers and leaves of LL.

Part of LL	**Solvent (Extract Name)**		
Tubers	**Hexane (LLT Hex)**	**Ethyl acetate (LLT EA)**	**Methanol (LLT MeOH)**
Constituents	Mixture of unsaturated fatty acids, fatty compounds and betulinic acid (BA)	Mainly BA	Mixture of sugars and possibly some oligosaccharides
Leaves	**Hexane (LLL Hex)**	**Ethyl acetate (LLL EA)**	**Methanol (LLL MeOH)**
Constituents	Mixture of unsaturated fats and fatty compounds	Mainly fatty acids and glycerides	Mixture of sugars and possibly some oligosaccharides.

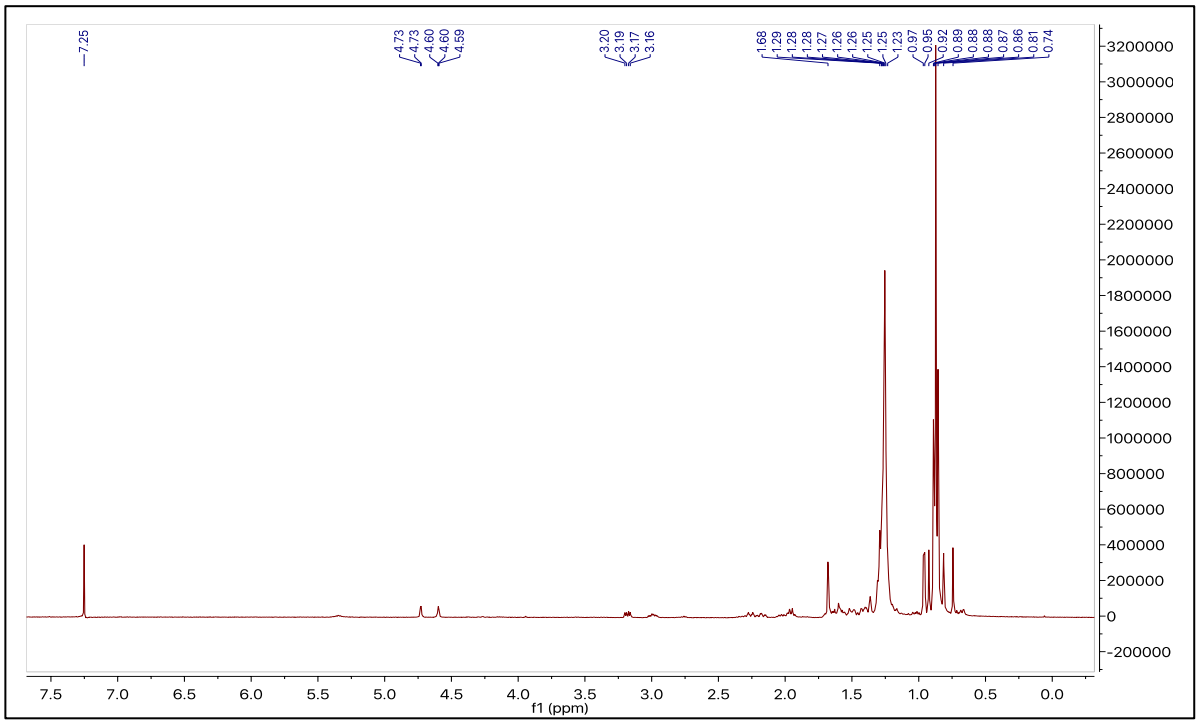

Figure 2. 10: ^{1}H (400 MHz) NMR spectrum of LLT Hex extract in $CDCl_3$

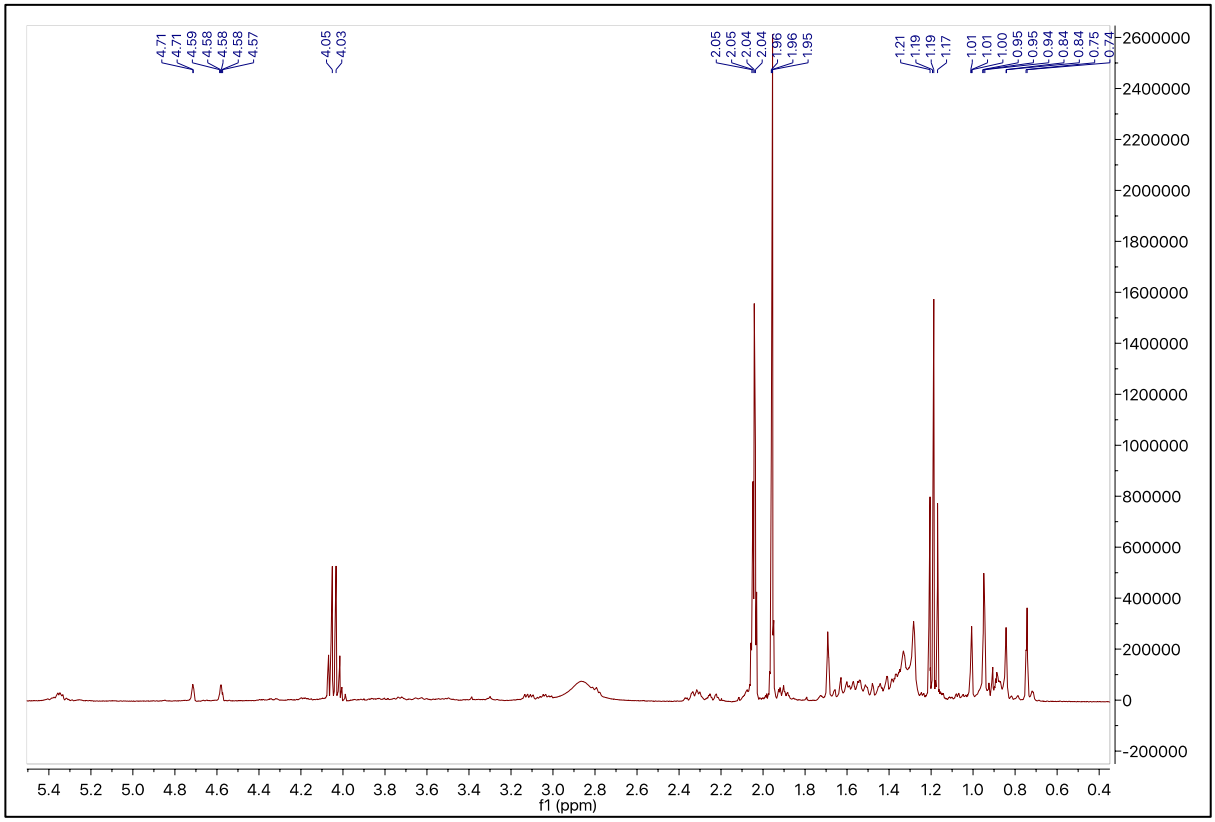

Figure 2. 11: ^{1}H (400 MHz) NMR spectrum of LLT EA extract in Acetone-D_6

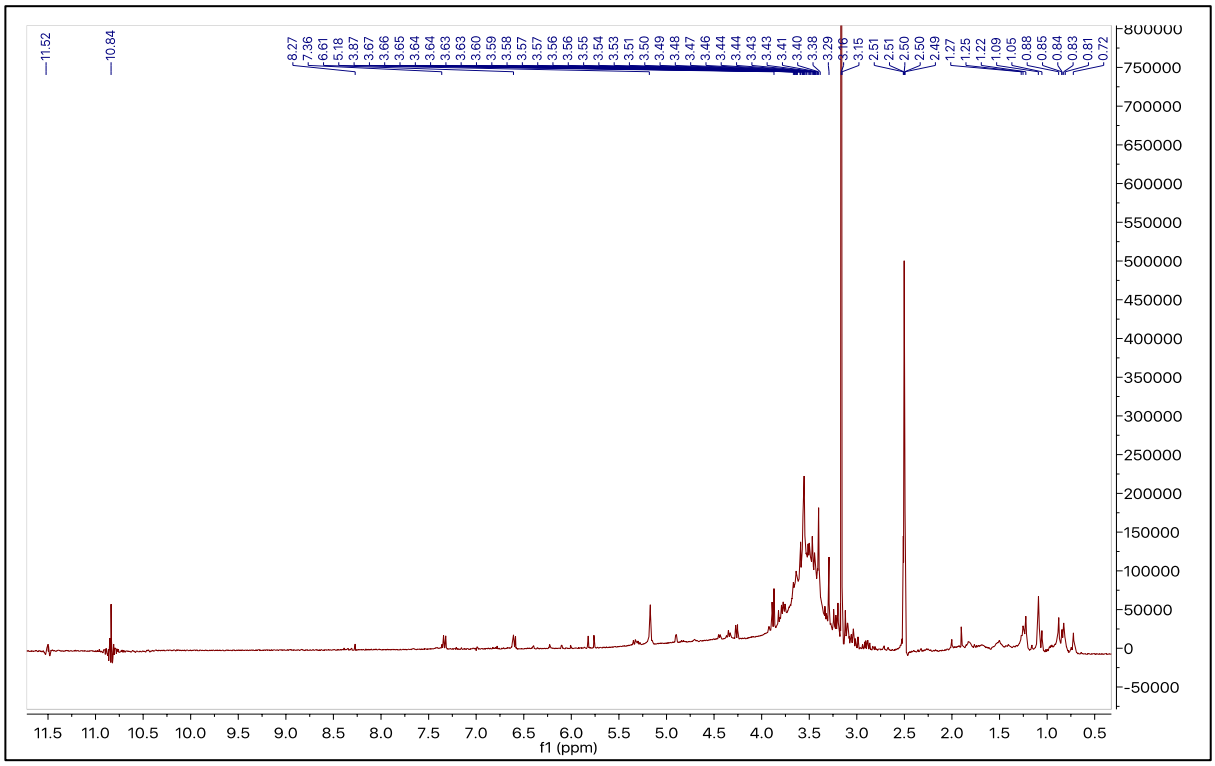

Figure 2. 12 ^{1}H (400 MHz) NMR spectrum of LLT MeOH extract in DMSO-d6.

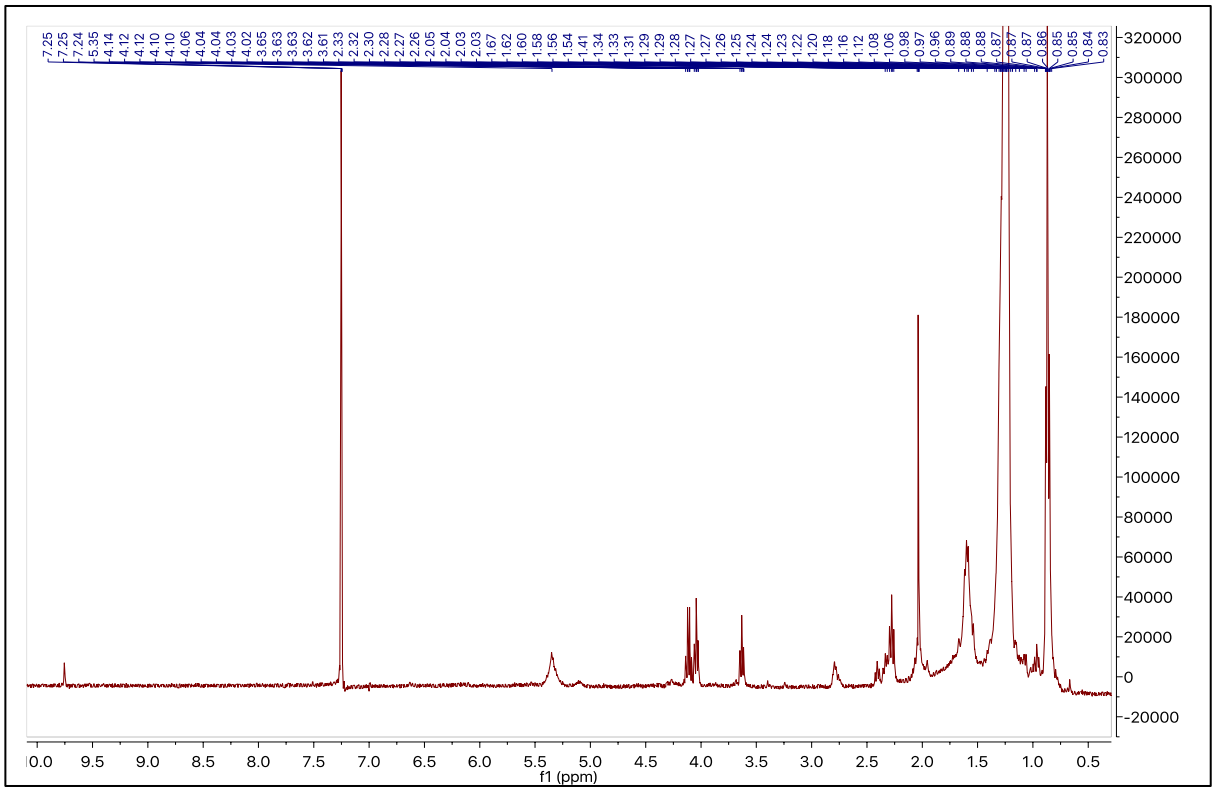

Figure 2. 13: ^{1}H (400 MHz) NMR spectrum of LLL Hex extract in $CDCl_3$

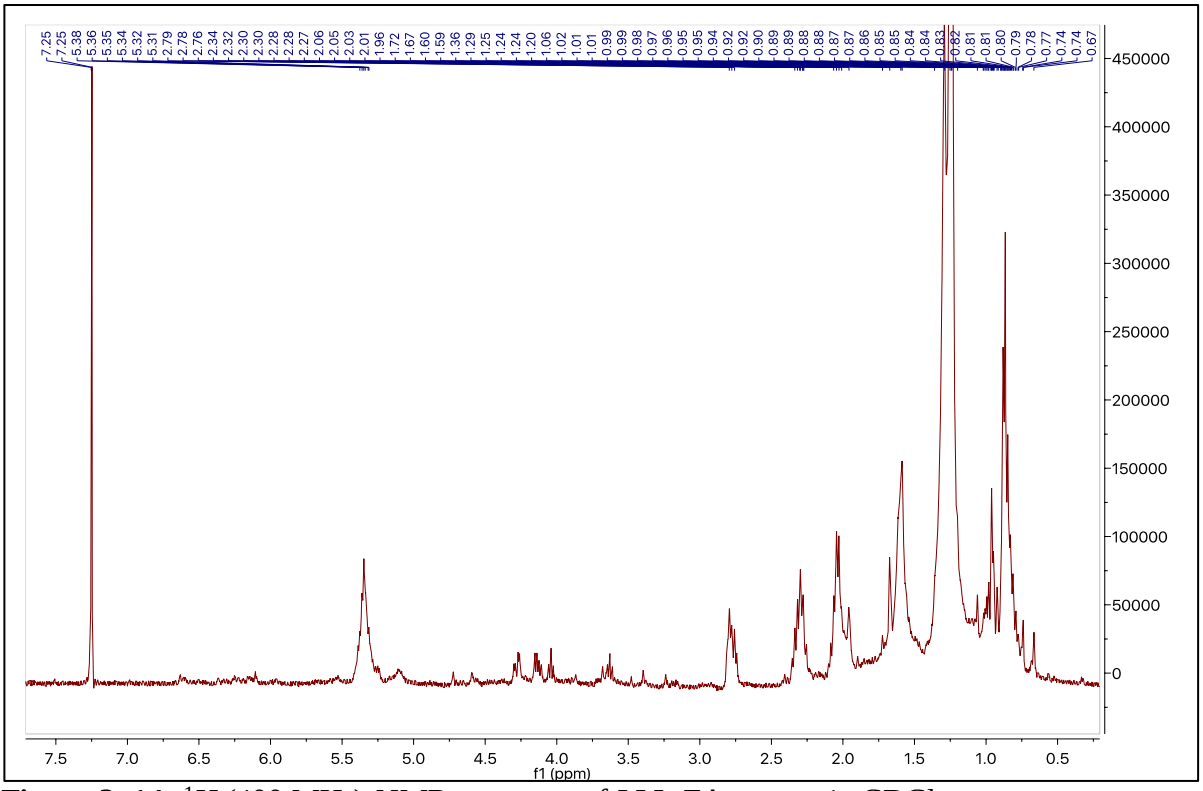

Figure 2. 14: ^{1}H (400 MHz) NMR spectrum of LLL EA extract in $CDCl_3$.

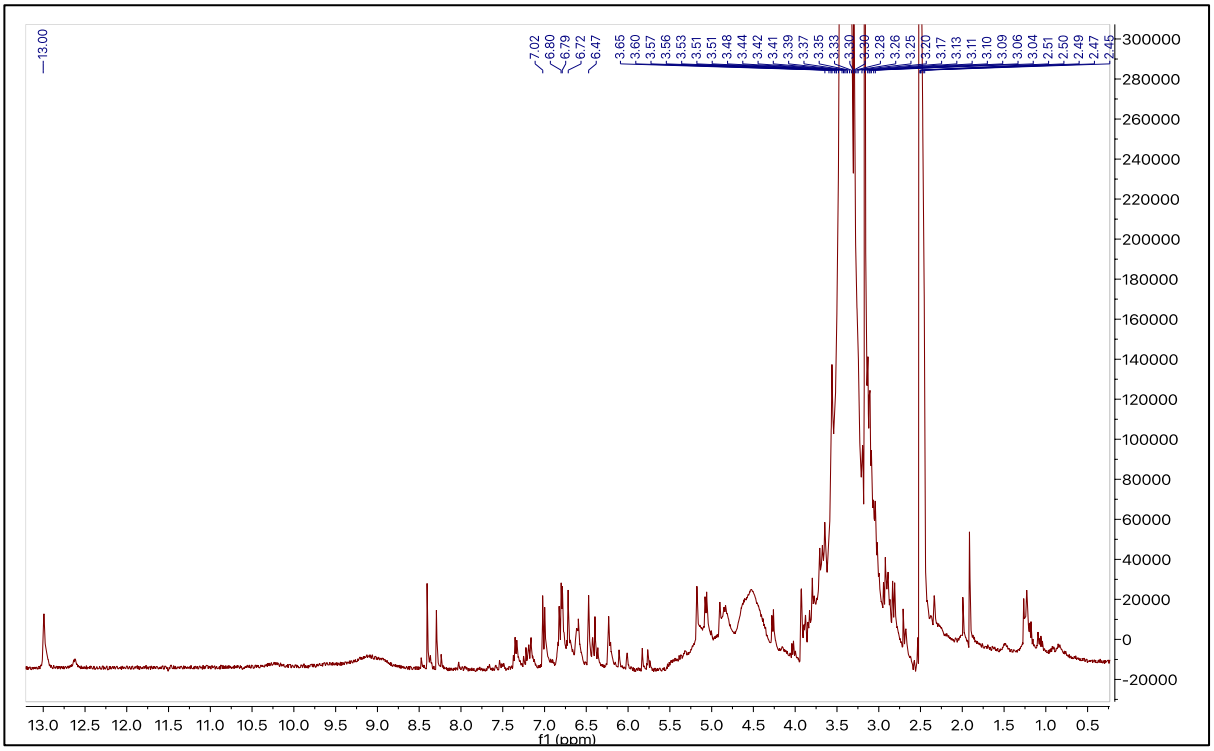

Figure 2. 15: ^{1}H (400 MHz) NMR spectrum of LLL MeOH extract in DMSO-D_6.

2.4.3. CC of LLT EA extract.

Four compounds were isolated from LLT EA extract as detailed below:

2.4.3.1. Characterisation of fractions 12-16 as BA

The compound (Figure 2.16) showed a purple coloured spot on the TLC plate after spraying with anisaldehyde-sulphuric acid reagent and heating. The ^{1}H NMR spectrum (Figure 2.17) showed the presence of two methylene protons (H-29) at δ_H ppm 4.74 and 4.61, a methyl (H-30) attached to a double bonded carbon at 1.69 and five other methyl protons between 0.76-0.98 ppm. Further, the spectrum showed other signals at 3.19 (dd, *J* = 11.4, 4.8 Hz, H-3) and 3.00 (td, *J* = 10.8, 4.8 Hz, H-19). The ^{13}C NMR (Figure 2.18) showed a total of 30 carbon atoms including six methyl signals, one oxygen bearing carbon, one methylene, one quaternary double bonded carbon and one carboxylic acid carbon signal. The compound was therefore identified as BA by comparing the data in Table 2.5 with those reported in the literature (Prakash and Prakash, 2012; Igoli and Gray, 2008).

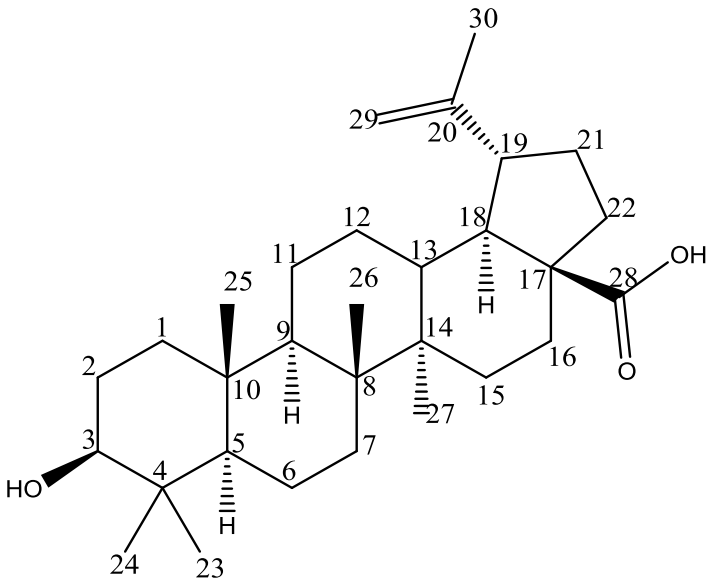

Betulinic acid

Figure 2. 16: Chemical structure of the isolated BA from LLT EA extract.

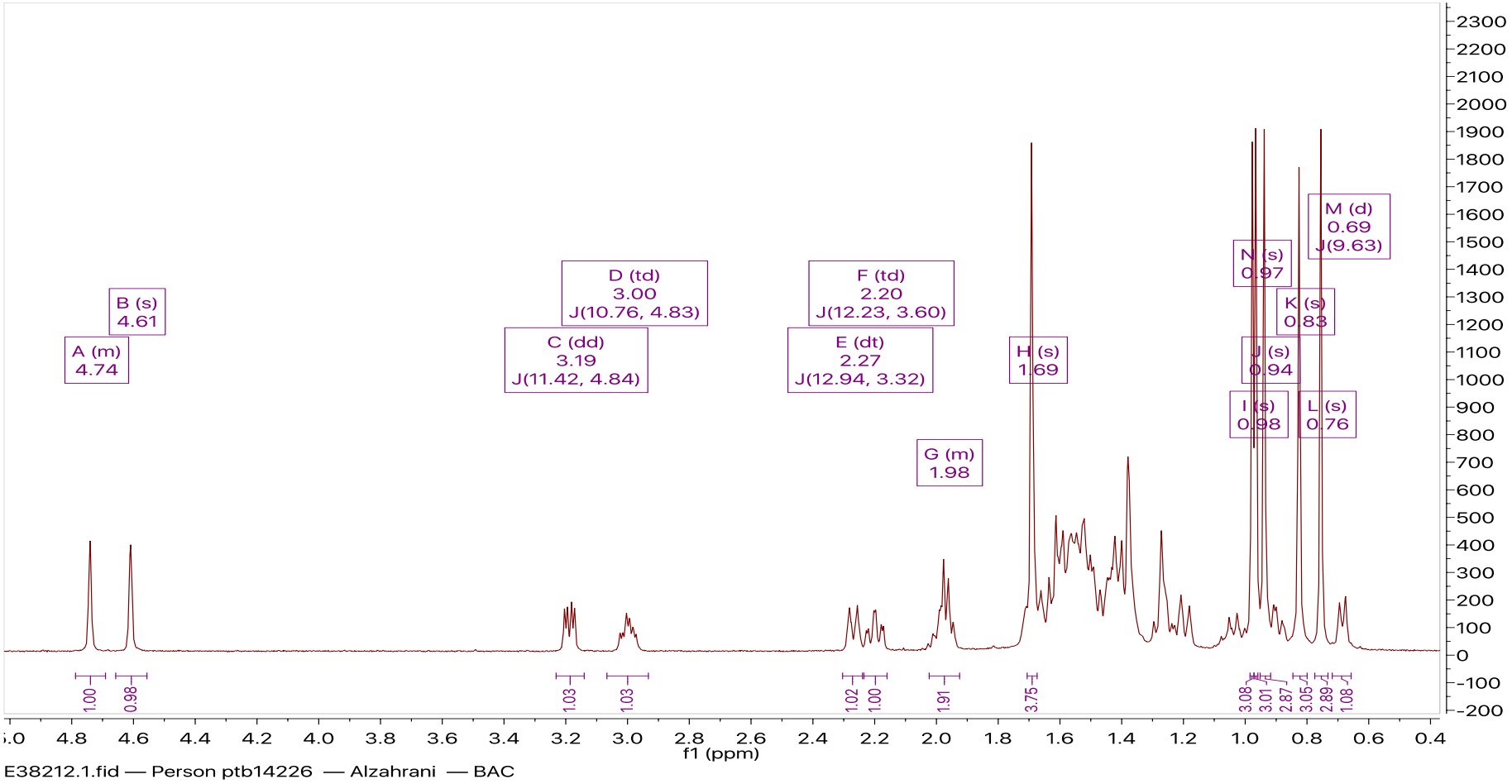

Figure 2. 17: ^{1}H NMR spectrum (400 MHz) of BA in $CDCl_3$.

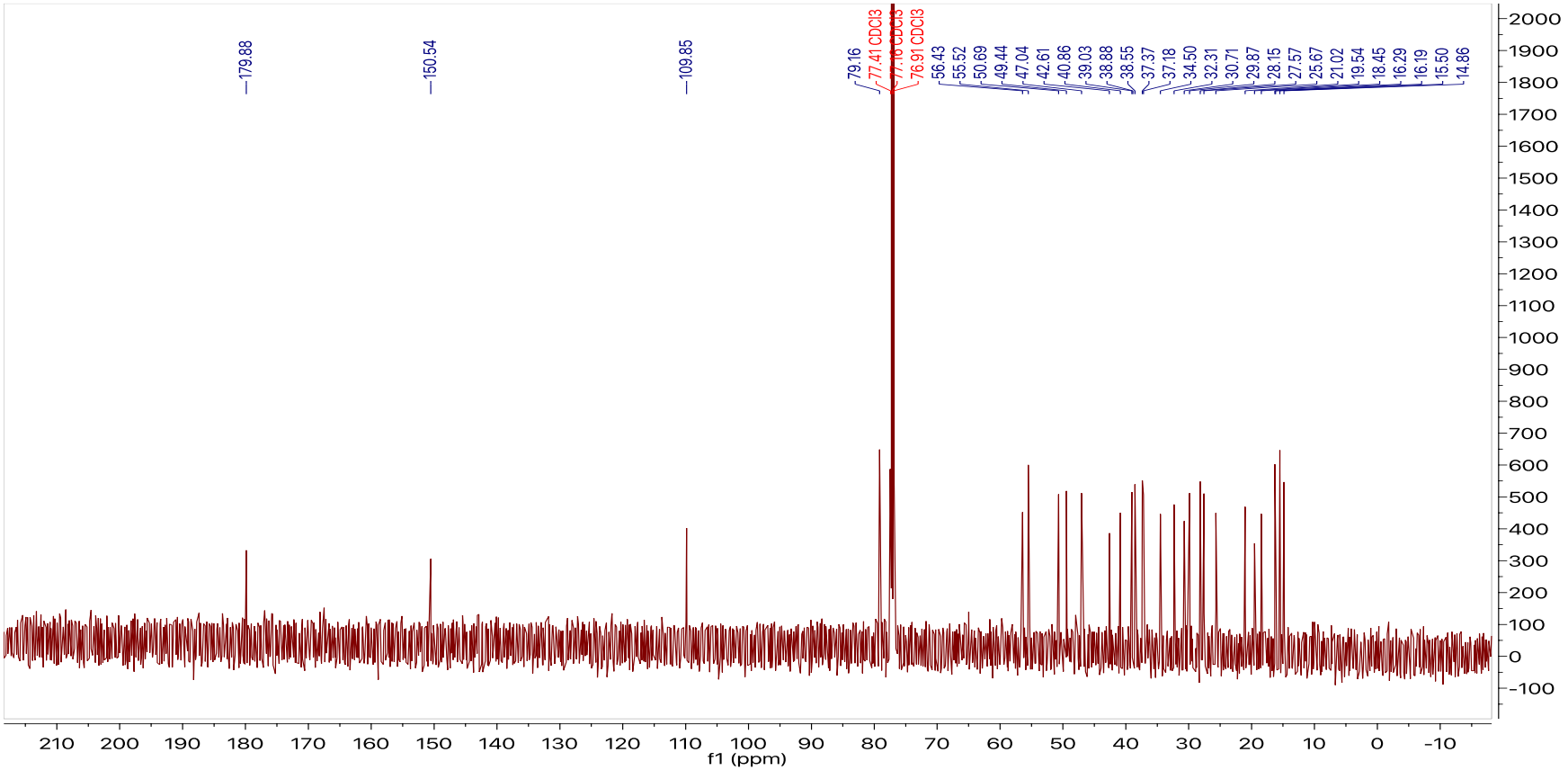

Figure 2. 18: ^{13}C NMR NMR spectrum (400 MHz) of BA in $CDCl_3$.

Table 2. 5: ^{1}H and ^{13}C NMR (400 MHz, $CDCl_3$,) data obtained for BA.

Position	Carbon δ ppm (MULT)	Proton δ ppm (MULT, J (Hz))
1	38.7 (CH_2)	*
2	27.4 (CH_2)	*
3	79.2 (CH)	3.19 (dd, *J* = 11.4, 4.8)
4	38.9 (C)	-
5	55.4 (CH)	0.69 (d, *J* = 9.6)
6	18.3 (CH_2)	*
7	34.3 (CH_2)	*
8	40.7 (C)	-
9	50.5 (CH)	*
10	37.2 (C)	-
11	20.9 (CH_2)	*
12	25.5 (CH_2)	*
13	38.4 (CH)	*
14	42.5 (C)	-
15	30.6 (CH_2)	*
16	32.2 (CH_2)	2.27 (dt, *J* = 12.9, 3.3)
17	56.3 (C)	-
18	46.9 (CH)	*
19	49.3 (CH)	3.00 (td, *J* = 10.8, 4.8)
20	150.5 (C)	-
21	29.7 (CH_2)	2.20 (td, *J* = 12.2, 3.6)
22	37.0 (CH_2)	*

23	28.0 (CH_3)	0.98 (s)
24	15.4 (CH_3)	0.76 (s)
25	16.0 (CH_3)	0.83 (s)
26	16.1 (CH_3)	0.94 (s)
27	14.7 (CH_3)	0.97 (s)
28	179.9 (C)	-
29	109.9 (CH_2)	4.74 (m), 4.61(s)
30	19.4 (CH_3)	1.69 (s)

* Overlapped signals

2.4.3.2. Characterisation of Fractions 20-22 as Lupeol

The compound in fractions 20-22 gave a purple spot characteristic of a terpenoid when sprayed with anisaldehyde-sulphuric acid reagent and heated. The ^{1}H NMR spectrum (Figure 2.20) showed the presence of two methylene protons (H-29) at δ ppm 4.71 (d, J = 2.5 Hz), 4.59 (t, J = 2.0 Hz), a methyl attached to a double bond at 1.71 (H-30) and six other methyl groups between 0.77-1.04 ppm. Proton H-3 and H-19 were observed at 3.22 (dd, J = 11.4, 4.9 Hz) and 2.39 (m), respectively. The ^{13}C NMR (Figure 21) showed a total of 30 carbon atoms made up of seven methyl carbons, one oxygen bearing carbon, one methylene carbon and one quaternary carbon attached to the methylene. No carbonyl carbon(s) were observed (confirmed by the absence of a carbonyl carbon in its ^{13}C NMR spectrum). The compound was identified as lupeol (Figure 2.21) and data in Table 2.6 was compared with those in the literature (Prakash and Prakash, 2012, Igoli and Gray, 2008). Lupeol showed a strong similarity to BA with little chemical shift differences except at C-28 which in BA was at 179.9 (COOH) but 17.9 (CH_3) in lupeol.

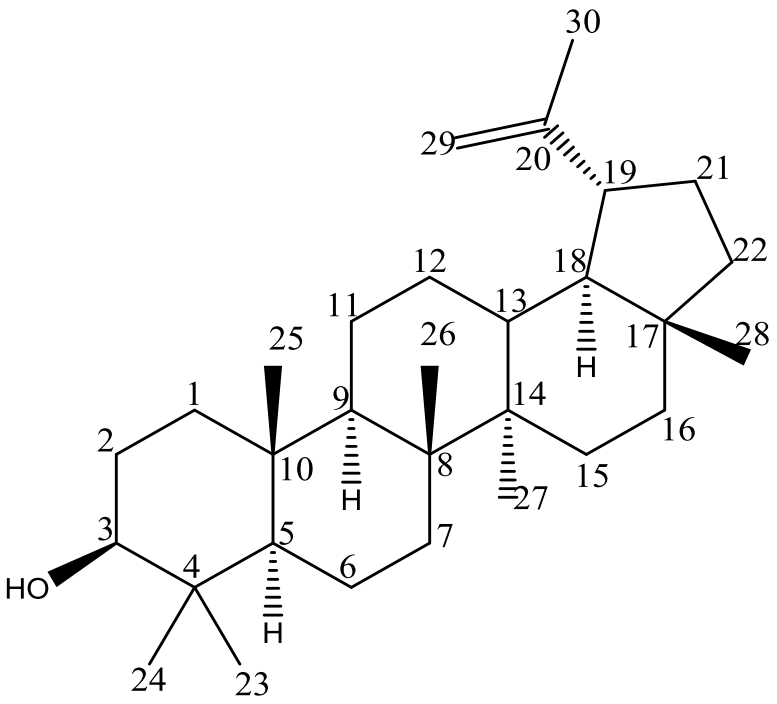

Lupeol

Figure 2. 19: Chemical structure of the isolated lupeol from LL EA extract.

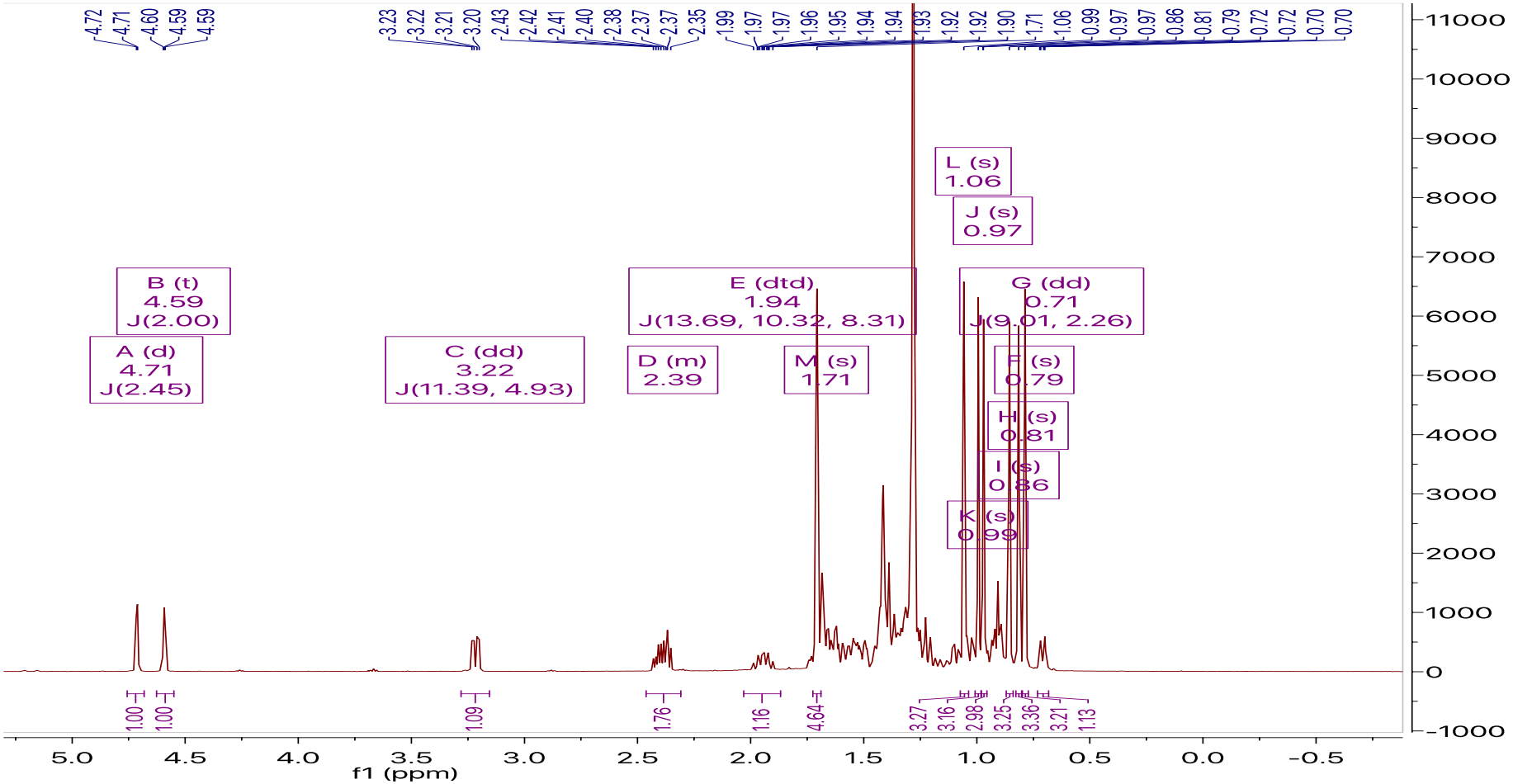

Figure 2. 20: ^{1}H NMR spectrum (400 MHz) of lupeol in $CDCl_3$.

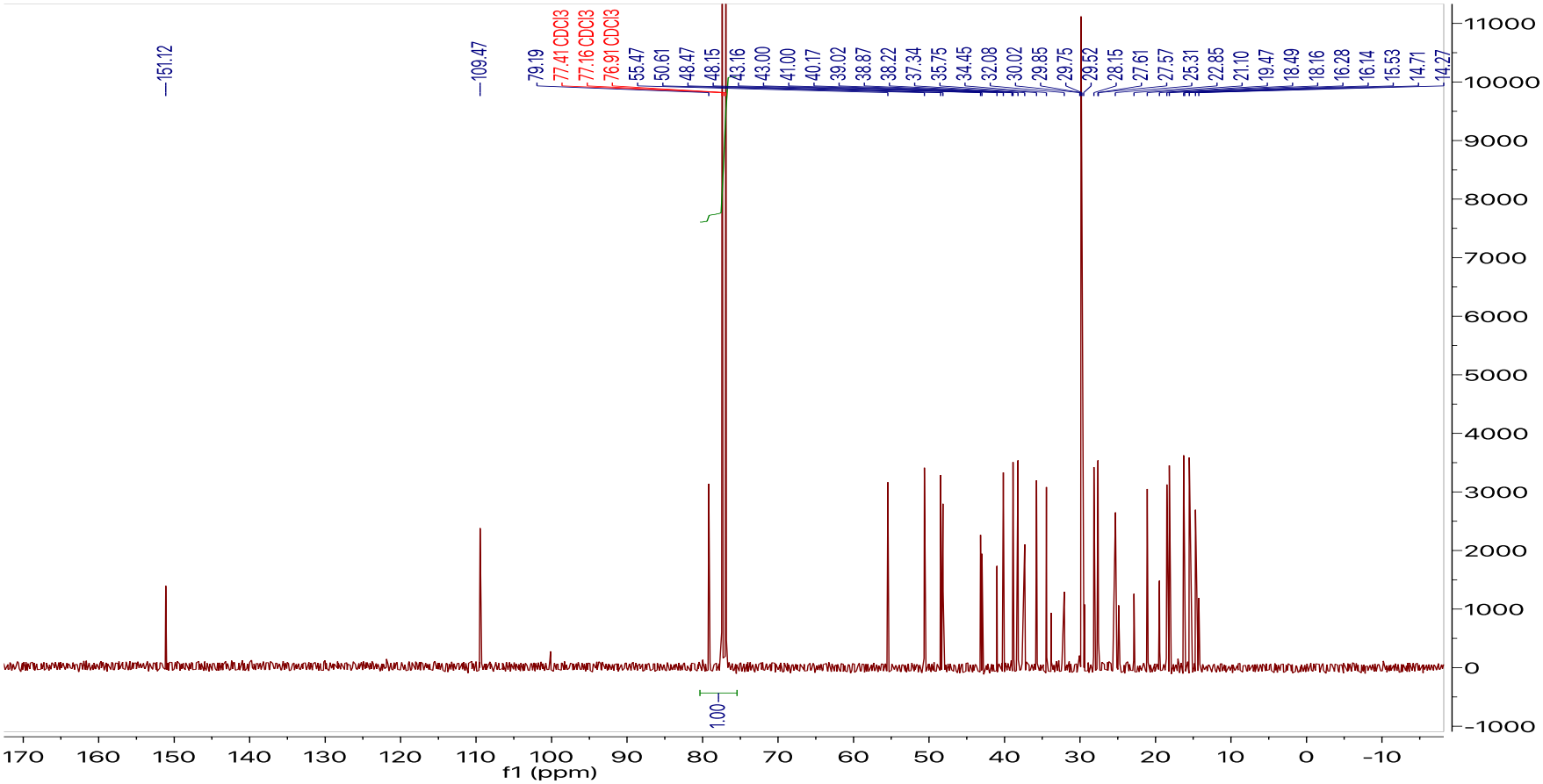

Figure 2. 21: ^{13}C NMR NMR spectrum (400 MHz) of lupeol in $CDCl_3$.

Table 2. 6: ^{1}H and ^{13}C NMR (400 MHz, $CDCl_3$,) data obtained for lupeol.

Position	**Carbon δ ppm (MULT)**	**Proton δ ppm (MULT, J (Hz))**
	Carbon (δ ppm)	Proton (δ ppm)
1	38.8 (CH_2)	*
2	27.4 (CH_2)	*
3	78.9 (CH)	3.22 (dd, *J* = 11.4, 4.9)
4	38.6 (C)	-
5	55.2 (CH)	0.71 (dd, *J* = 9.0, 2.3)
6	18.2 (CH_2)	*
7	34.2 (CH_2)	*
8	40.8 (C)	-
9	50.4 (CH)	*
10	37.1 (C)	-
11	20.9 (CH_2)	*
12	25.1 (CH_2)	*
13	38.0 (CH)	*
14	42.8 (C)	-
15	27.4 (CH_2)	*
16	35.5 (CH_2)	1.94 (dtd, *J* = 13.7, 10.3, 8.3)

17	42.9 (C)	-
18	48.2 (CH)	*
19	47.9 (CH)	2.39 (m)
20	150.9 (C)	-
21	29.8 (CH_2)	1.98 (m)
22	39.9 (CH_2)	*
23	27.9 (CH_3)	0.97 (s)
24	15.3 (CH_3)	0.79 (s)
25	16.0 (CH_3)	0.86 (s)
26	15.9 (CH_3)	1.06 (s)
27	14.5 (CH_3)	0.99 (s)
28	17.9 (CH_3)	0.81 (s)
29	109.2 (CH_2)	4.71 (d, J = 2.5), 4.59 (t, J = 2.0)
30	19.2 (CH_3)	1.71 (s)

* Overlapped signals.

2.4.3.3. Characterisation of Fractions 8-10 as β-Sitosterol and Stigmasterol

The compounds in fractions 8-10 (Figure 2.22) also gave a purple colour characteristic of a phytosterol when sprayed with anisaldehyde-sulphuric acid reagent and heating. The ^{1}H NMR spectrum (Figure 2.23) showed the presence of three olefinic protons at δppm 5.38 (d, 2H, *J* = 5.1 Hz, H-6 for sitosterol and stigmasterol) and 5.18 (dd, 1H, *J* = 15.2, 8.7 Hz, H-22a for stigmasterol) and 5.04 (dd, 1H, *J* = 15.2, 8.6 Hz, H-22b for stigmasterol) as they integrated in the ratio 2:1:1. The oxymethine proton H-3 was at 3.54 (td, *J* = 11.2, 5.4). The spectrum also showed a set of tertiary methyl groups between 0.69-1.58 ppm. Their ^{13}C NMR spectrum (Figure 2.24) showed the expected number of carbons with some overlapping signals. It showed an oxygen bearing carbon at δ_C 71.8 ppm and four olefinic carbon signals at 121.7 (CH), 129.3 (CH), 139.3 (C) and 140.8 (C). Their spectra were observed to be identical to those published in the literature for sitosterol and stigmasterol (Chaturvedula and Prakash, 2012; Habib *et al.*, 2007).

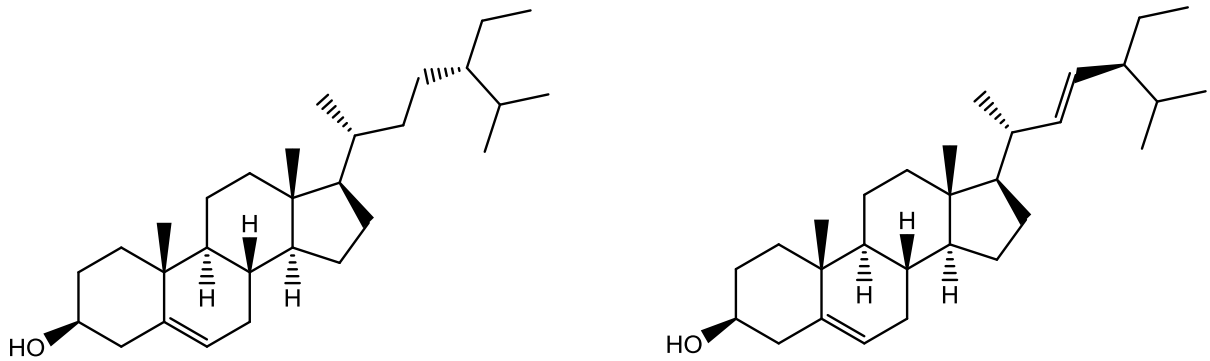

Figure 2. 22: Chemical structures of the isolated β-sitosterol and stigmasterol from LLT EA extract.

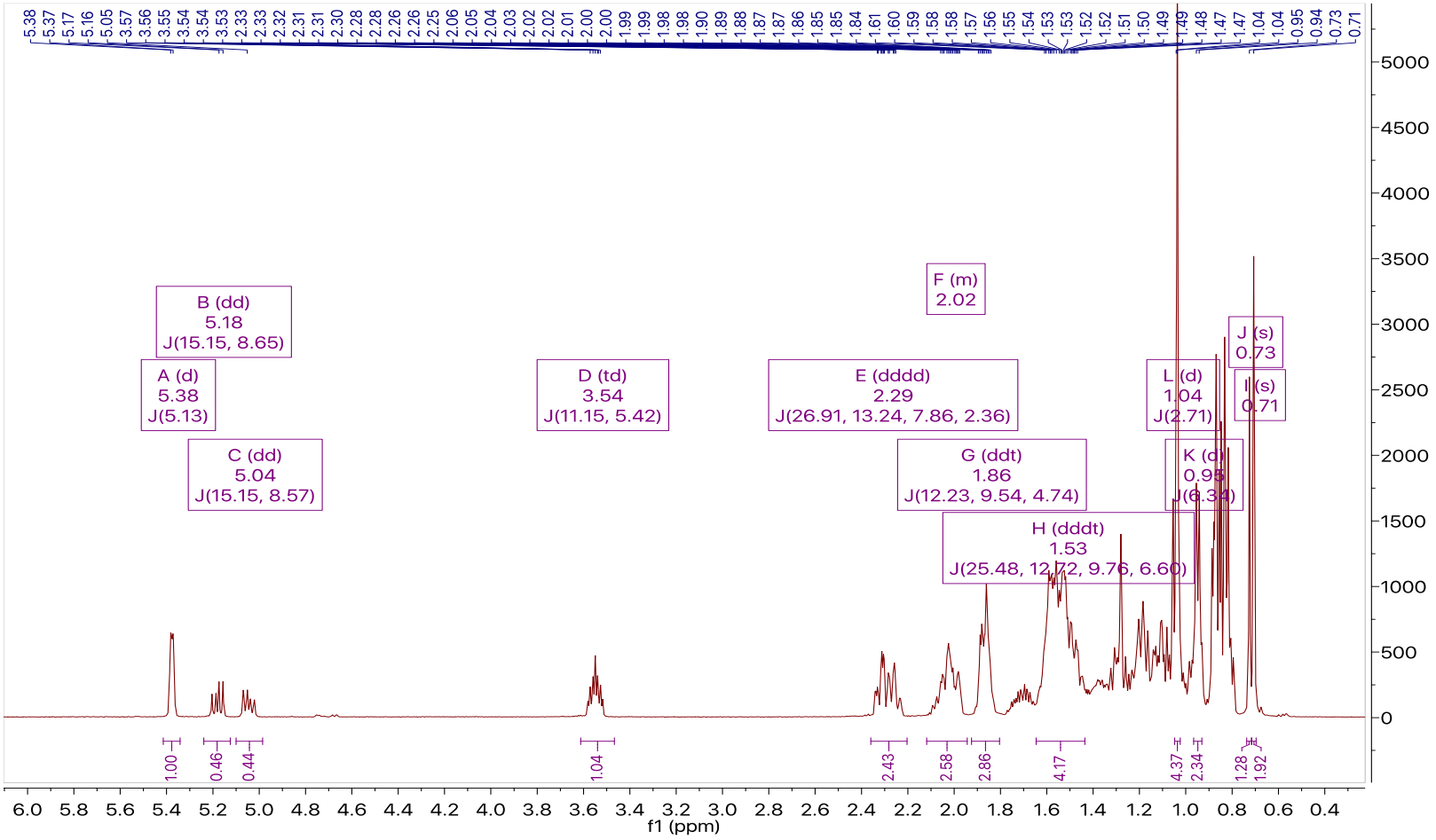

Figure 2. 23: ^{1}H NMR spectrum (400 MHz) of β-sitosterol and stigmasterol in $CDCl_3$.

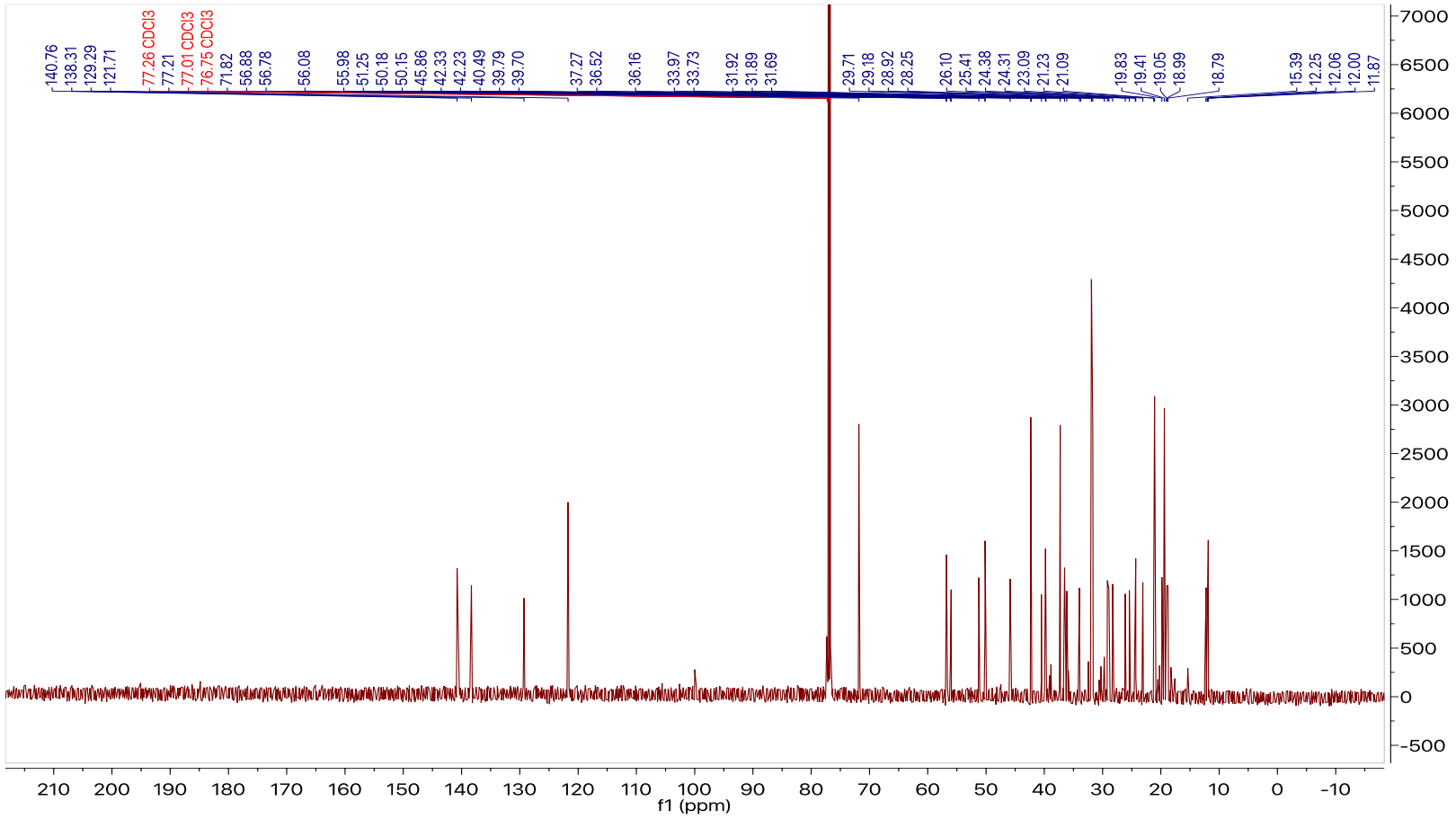

Figure 2. 24: ^{13}C NMR NMR spectrum (400 MHz) of β-sitosterol and stigmasterol in $CDCl_3$.

2.4.4. Summary of the phytochemical process carried out on *L. linifolius*

The extraction process from leaves and tubers of LL as well as the isolation of compounds are summarised in Figure 2. 25.

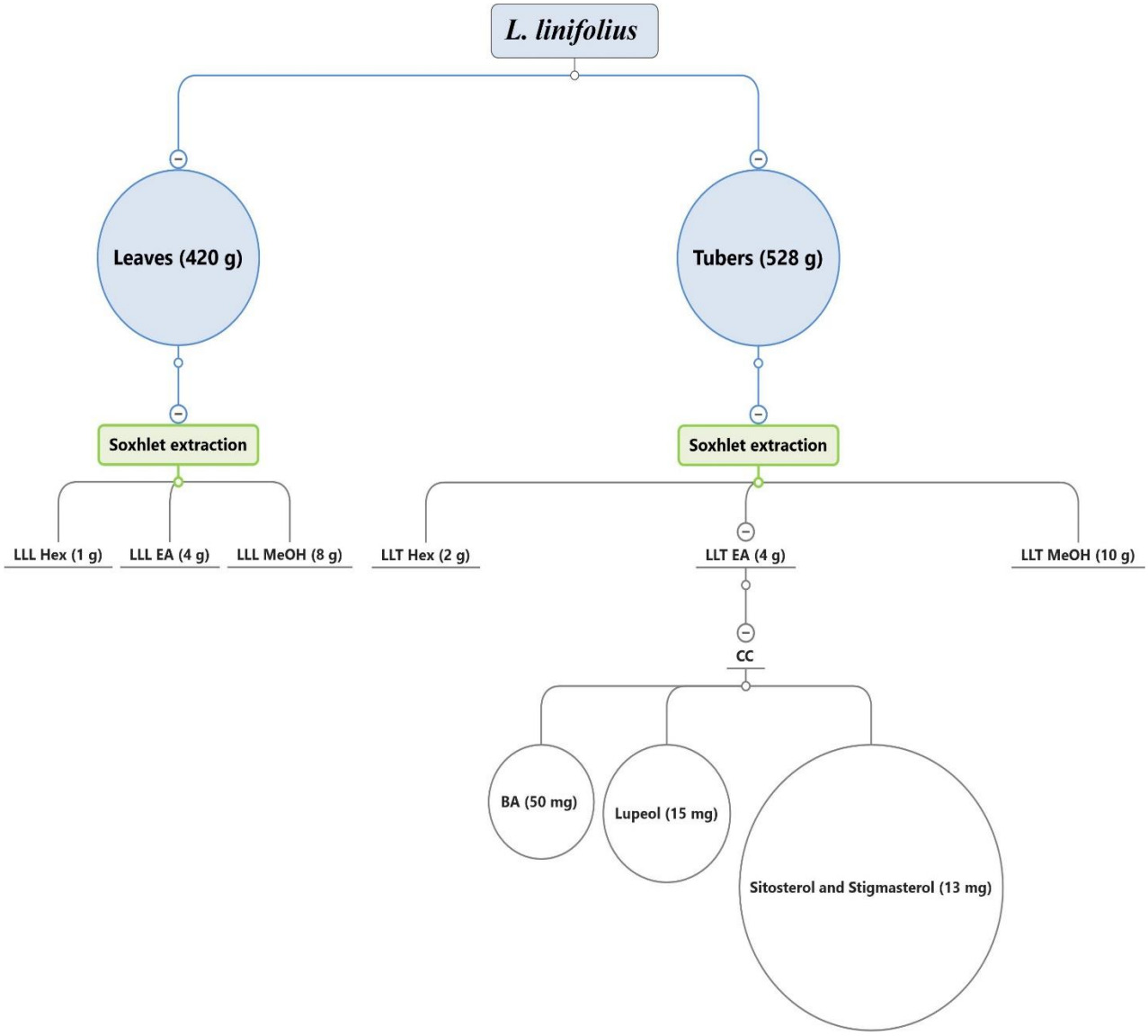

Figure 2. 25: Schematic diagram showing the extraction and isolation processes carried out on *L. linifolius*.

2.5. Discussion and Conclusions

Tubers and leaves of LL were ground into a powder before being extracted by Soxhlet extraction. Traditionally, LL tubers were eaten as a whole and there was no known historical use for the LL leaves. For the first time, this study was used to examine both. In order to extract as many bioactive compounds as possible, continuous Soxhlet extraction using three solvents with increasing polarity was considered the ideal extraction method. However, Soxhlet extraction involves continuous extraction with high temperatures and therefore volatile and heat-sensitive compounds are lost or degraded with this extraction method (Luque de Castro and Priego-Capote, 2010). The extraction process began with Hex, followed by EA and finished with MeOH. NMR spectra for Hex extracts showed the presence of unsaturated fatty acids and fatty compounds and these types of compounds were expected due to Hex being a non-polar solvent. EA extracts showed the presence of terpenes, whereas MeOH extracts contained sugars and possibly some oligosaccharides which are polar compounds and are expected to be present in MeOH extracts (Bimakr *et al.*, 2011).

Due to the time limitation in this project, CC was carried out on LLT EA extract only in order to isolate bioactive compounds. LLT EA showed a strong inhibition of α-glucosidase, a negative regulator in diabetes shown in the study carried out by Woods (2017). However, the compounds responsible for this activity were not isolated or identified. Hence, there is a need for identifying the inhibitors of α-glucosidase in the LLT EA extract. CC on LLT EA extract yielded the extraction and the isolation of four compounds from LL for the first time; these are BA, lupeol and a mixture of β-sitosterol and stigmasterol.

BA was the major component in the LLT EA extract and was isolated in large quantities (50 mg, yield 1.3%). This was the first time that BA has been isolated from the tubers of LL. Woods (2017) showed that BA was present in the LLT Hex extract by examining the NMR spectra for the crude extract. This is consistent with the finding of this study as BA was also identified to be present in both LLT Hex and LLT EA extracts. BA is a pentacyclic lupane-type triterpene which is found in abundance in the Plant Kingdom (Cichewicz and Kouzi, 2004; Yogeeswari and Sriram, 2005). BA was

first isolated in 1948 from the bark of *Platanus acerifolia*, London plane tree (Ding, 2012). It is estimated that 2.5% of BA is found in the outer bark of many trees (Yogeeswari and Sriram, 2005). The presence and isolation of BA from various plants has been reported in many publications. To illustrate this with some examples, BA was isolated from twigs of *Coussarea paniculata* (Prakash Chaturvedula *et al.*, 2003), legume of *Caesalpinia paraguariensis* (Argentinean plant) (Woldemichael *et al.*, 2003), roots of *Anemone raddeana* (Yamashita *et al.*, 2002), bark of *Zizyphus joazeiro* (Schuhly *et al.*, 1999), root bark of *Ipomea pescaprae* (Krogh *et al.*, 1999) and leaves of *Syzygium claviforum* (Fujioka *et al.*, 1994). LLT EA extract is a good source of BA when compared with other plants known for the BA production, Table 2.7 shows the % yields of BA isolated from LLT EA and other plants from the literature.

Table 2. 7: Comparisons of BA % yields from LL and other plants from the literature.

Plant	% Yield	Reference
Tubers of *Lathyrus linifolius*	1.3	
Twigs of *Coussarea paniculata*	0.2	(Prakash Chaturvedula *et al.*, 2003)
Leaves of *Eucalyptus camaldulensis*	0.2	(Begum *et al.*, 2002)
Leaves of *Strychnos vanprukii*	0.01	(Chien *et al.*, 2004)
Stem bark of *Dichapetalum gelonioides*	0.32	(Fang *et al.*, 2006)
Leaves of *Nerium oleander*	0.05	(Fu *et al.*, 2005)

BA has a broad spectrum of reported biological activities including anti-HIV, anti-malarial, anti-oxidant, anti-bacterial, anti-depression, anthelmintic and anti-hyperglycaemia activities (Fujioka *et al.*, 1994; Patlolla and Rao, 2012; Bori *et al.*, 2012). Firstly, BA has anti-HIV activity; it inhibits the replication of HIV-1 (Fujioka

et al., 1994). Moreover, BA derivatives have been shown to inhibit HIV-1 entry to cells, HIV-protease and HIV-reverse transcriptase (Xu *et al.*, 1996; Bori *et al.*, 2012). Bevirimat (BVM), a BA derivative, was found to be effective against HIV-1. BVM belongs to a class of drugs called maturation inhibitors (MIs). This drug was approved for clinical trials before it failed in the study as 50% of the patients were resistant to the treatment (Neyret *et al.*, 2019). Secondly, BA has anti-cancer activities. It was found to suppress tumour growth in a number of cancer cells including prostate cancer, hepatic cancer, colorectal cancer, breast cancer, pancreatic cancer and leukaemia (Patlolla and Rao, 2012; Hussein-Al-Ali, 2014). BA is currently in phase I/II clinical trials for the treatment of dysplastic nevi treatment, a condition that can progress and transform into melanoma (ClinicalTrials.gov, 2019). Thirdly, *in vitro* and *in vivo* studies showed that BA possesses anti-inflammatory activities when administered at high concentrations. Its anti-inflammatory activity is believed to be caused by its inhibitory effects on non-neurogenic pathways (Del Carmen Recio *et al.*, 1995; Huguet *et al.*, 2000). Fourthly, pentacyclic triterpenes including BA possess anti-diabetic activities (Ding *et al.*, 2018). BA was found to lower BG levels in diabetic mice by the regulation of insulin signalling pathways and the inhibition of α-glucosidase (Vinayagam *et al.*, 2017; Ding *et al.*, 2018).

The second isolated compound from LLT EA was lupeol (15 mg, yield 0.39%) and this was the first time that lupeol has been isolated from LL. In the study by Woods (2017) lupeol was not identified in the extracts and this was again mainly because the extracts were not subjected to CC by Woods (2017). Lupeol consists of 5 membered rings in which four are six-membered rings and one is a five-membered ring (Corrêa *et al.*, 2009). Like BA, lupeol is a pentacyclic triterpene compound that belongs to the lupane group (Rao *et al.*, 2017; Wang *et al.*, 2018b). Lupeol is widely distributed in the Plant Kingdom and is found in some fruit and vegetables (Guo *et al.*, 2018; Beserra *et al.*, 2018). Sources of lupeol include carrot roots, mango pulp, melon seeds, cucumber and soybean (Gallo and Sarachine, 2009; Duke, 2017). Lupeol has been isolated from a number of plants including leaves of *Quercus obtusata* (Sánchez-Burgos *et al.*, 2015), leaves of *Walsura trifoliate* (Rao *et al.*, 2017), stems of *Betula alnoides* (Chaniad *et al.*, 2019) and bark of *Hymenocardia acida* (Igoli and Gray,

2008). Unlike BA, LL does not seem to be a good source for lupeol because, as shown in Table 2.8, there are several plants known to yield higher lupeol when compared with LL.

Table 2. 8: Comparisons of lupeol % yields from LL and other plants from the literature.

Plant	% Yield	Reference
Tubers of *Lathyrus linifolius*	0.39	
Stem bark of *Crataeva religiosa*	0.33	(Bani *et al.*, 2006)
Barks of *Sorbus commixta*	2.30	(Na *et al.*, 2009)
Leaves of *Pimenta. racemosa*	0.10	(Fernández *et al.*, 2001)
Bark of *B. ceiba*	13	(You *et al.*, 2003)
Stem bark of *Crataeva nurvala*	0.60	(Shirwaikar *et al.*, 2004)
Stem bark of *Allanblackia monticola*	0.15	(Nguemfo *et al.*, 2009)
Bark of *Bowdichia virgiloides*	1.3	(Cordero *et al.*, 2004)
Root bark of *Euclea undulata*	7.14	(Deutschländer *et al.*, 2011)

Lupeol possesses a number of biological activities including anti-inflammatory, anti-oxidant, hepatoprotective, anti-arthritis, anti-TB, anti-HIV and anti-diabetic activities (Guo *et al.*, 2018; Lee *et al.*, 2007; Han and Bakovic, 2015). A study by Guo *et al.* (2018) looked at the effects of lupeol in inhibiting apoptosis that is initiated by high glucose (HG) levels in rabbit nucleus pulposus cells (NPCs). The HG plus lupeol group showed a significant decrease in apoptotic rate and ROS level when compared with the HG only group (Guo *et al.*, 2018). Moreover, lupeol exhibited anti-oxidant

activity by scavenging ROS and inducing the activity of catalase (CAT) and superoxide dismutase (SOD) (Lee *et al.*, 2007; Han and Bakovic, 2015). It is also known that lupeol has potential anti-cancer activities. A study by Liu *et al.* showed that lupeol significantly inhibited the proliferation of human pancreatic cancer proliferating cell nuclear antigen-1 (Panc-1) cells and the effect was dose-dependent (Liu *et al.*, 2015). Lupeol induced apoptosis in Panc-1 cells and this was believed to be achieved by cell cycle arrest at GO/G1 phase and upregulating p21 and p27 genes and downregulating cyclin D1. Sunitha *et al.* (2001) demonstrated the hepatoprotective effects of lupeol against cadmium-induced toxicity in rats (Sunitha *et al.*, 2001). The study showed that daily oral administration of lupeol (150 mg/kg) for three days prior to injecting cadmium chloride improved the levels of anti-oxidants and anti-oxidising enzymes as well as malonaldehyde levels when compared to control rats that received cadmium chloride only.

A mixture of β-sitosterol and stigmasterol (13 mg, yield 0.34%) was isolated from LLT EA extract for the first time and these compounds were not identified in the study by Woods (2017). This was again mainly because the extracts were not subjected to CC by Woods (2017). β-sitosterol and stigmasterol belong to a class of phytochemicals called phytosterols and they are found in various medicinal plants. These two phytosterols have generally been considered safe and no undesirable side effects were associated with them (Saeidnia *et al.*, 2014). Stigmasterol was first isolated in 1906 from the seeds of Calabar (Adolf Wind Form, 1907). Sources of stigmasterol include *Emilia sonchifolia* (Gao *et al.*, 1993), *Eclipta prostrate* (Han *et al.*, 1998), *Croton sublyratus* (De-Eknamkul and Potduang, 2003), *Gypsophila oldhamiana* (Yang *et al.*, 1999) and *Desmodium styracifolium* (Li *et al.*, 2007). Whereas, sources of β-sitosterol include *Rubus suavissimus* (Chaturvedula and Prakash, 2012), *Solanum surattense* (Gupta *et al.*, 2011), *Asclepias curassavica* (Baskar *et al.*, 2010), *Nyctanthes arbortristis* (Nirmal *et al.*, 2012), *Momordica charantia* (Sen *et al.*, 2012) and *Odontonema strictum* (Pierre and Moses, 2015). β-sitosterol and stigmasterol are always in the form of a mixture and it is challenging to separate them. The only difference between the two compounds is the presence of C22=C23 double bond in Stigmasterol and C22- C23 single bond in β-sitosterol (Pierre and Moses, 2015;

Kamboj and Saluja, 2011a). LL is not a rich source for β-sitosterol and stigmasterol when comparing the % yields with other plants as shown in Table 2.9.

Table 2. 9: Comparisons of β-sitosterol and stigmasterol % yields from LL and other plants from the literature.

Plant	β-sitosterol (% Yield)	Stigmasterol (% Yield)	Reference
Tubers of *Lathyrus linifolius*	0.17	0.17	
Aerial parts of *Ageratum conyzoides*	0.89	0.89	(Kamboj and Saluja, 2011b)
Leaves of *Rubus suavissimus*	6.67	4.33	(Chaturvedula and Prakash, 2012)
Leaves of *Odontonema strictum*	0.16	0.16	(Pierre and Moses, 2015)
Fruits of *Solanum xanthocarpum*	0.083	0.09	(Khanam and Sultana, 2012)
Aerial parts of *Aristolochia indica*	1.4	-------	(Karan *et al.*, 2012)
Leaves of *Asclepias curassavica*	9.25	-------	(Baskar *et al.*, 2010)
Aerial parts of *Bacopa monnieri*	-------	0.06	(Ghosh *et al.*, 2011)

Plant phytosterols have been investigated in clinical trials and mainly for their anti-hypercholesteremia effects as detailed in Table 2.10. Stigmasterol has a broad range of pharmacological actions including anti-osteoarthritis, anti-hypercholesteraemic, anti-tumour, anti-hyperglycaemia, anti-oxidant, anti-inflammatory and anti-mutagenic activities (Gabay *et al.*, 2010; Gao *et al.*, 2008; Batta *et al.*, 2006; Jamaluddin *et al.*, 1994). To start with, Gabay *et al.* investigated the anti-osteoarthritis activity of

stigmasterol using new-born mouse chondrocytes and human osteoarthritis chondrocytes (Gabay *et al.*, 2010). The chondrocytes were incubated for 18 hours with or without interleukin 1 beta (IL1β) before incubation with stigmasterol for two days. Incubation with IL1β for 18 hours increased the expression of genes involved in cartilage turnover and stigmasterol was found to reduce the expression of such genes. Another activity of stigmasterol is anti-hypercholesterolemia. Batta *et al.* found that stigmasterol competes with cholesterol for intestinal absorption of cholesterol and therefore lowers cholesterol plasma levels (Batta *et al.*, 2006). Thirdly, a study carried out by Gao *et al.* revealed potential anti-tumour activity of stigmasterol in A549 cells, the compound inhibited the lyase activity of the DNA polymerase β and potentiated the activity of bleomycin, a known anti-cancer drug (Gao *et al.*, 2008). Anti-hyperglycaemia is another biological effect of stigmasterol, Jamaluddin *et al.* showed that oral administration of a chloroform extract of *Parkia speciosa* at 100 mg/kg BW to alloxan-induced diabetic rats resulted in decreasing levels of BG (Jamaluddin *et al.*, 1994). The extract was identified as a mixture containing β-sitosterol (66%) and stigmasterol (34%). Following the separation of the two compounds, the anti-hyperglycaemic activity was lost and therefore it was concluded that the activity is achieved by a synergistic effect. If the study by Jamaluddin *et al.* (1994) was to be repeated using LLT EA extract and assuming the anti-diabetic effect of the extract is due to β-sitosterol and stigmasterol, this extract would need to be administered at approximately 29 g/kg BW in order to provide 100 mg/kg BW of the mixture of β-sitosterol and stigmasterol. This is a very high dosage to be applied in practice and therefore the anti-diabetic activity of the LL plant is unlikely to occur from the mixture of β-sitosterol and stigmasterol.

Table 2. 10: Clinical trials on plant-derived phytosterols.

Study	Status	Conditions	Interventions	Results	ID
Phytosterol Supplementation and Cardiovascular Risk	C	Hypercholesteremia	Phytosterol	None	NCT00153738
Plant Sterols and Plant Stanols and Liver Inflammation	R	Non-Alcoholic Fatty Liver Disease	Plant sterol-enriched margarine	None	NCT03627819
Effect of the Consumption of a Fermented Dairy Product Enriched With Plant Sterols	C	Mild Hypercholesterolemic Subjects	Low-fat dairy fermented product (drinkable) enriched with plant sterols-esters (1,6g /day equivalent as free sterols)	None	NCT01521156
Effect of the Consumption of a Fermented Milk Enriched With Plant Sterols (France)	C	Mildly Hypercholesterolemic Subjects	Low fat fermented dairy product enriched with plant sterol esters (0,8 g equivalent as free sterols)	None	NCT01574469
Genetic Basis for Heterogeneity in Response of Plasma Lipids to Plant Sterols	C	Hyperlipidemia	Dietary Supplement: Plant sterol	None	NCT01131832
Effect of the Consumption of a Fermented Milk Enriched With Plant Sterols (Italy)	C	Mildly Hypercholesterolemic Subjects	Plain low-fat dairy fermented product (drinkable) enriched with plant sterols-esters (1,6g /day equivalent as free sterols).	None	NCT01574482
Pilot Study in the Cholesterol Absorption Reduction After Consumption of Low-fat, Drinkable Fermented Milk	C	Mildly Hypercholesterolemic Subjects	Low fat drinkable fermented dairy product enriched with 1.6g of plant sterol (as free equivalent) per unit	None	NCT01571869

Enriched With Plant Sterols					
Effects of Fermented Milk Product Enriched With Plant Sterols and Policosanols in Mild Hypercholesterolaemic Adults)	C	Mildly Hypercholesterolemic Subjects	1-Low fat drinkable fermented dairy product enriched with 1.6g of plant sterol (as free equivalent) + 10 mg of policosanols per unit 2-Low fat drinkable fermented dairy product enriched with 1.6g of plant sterol (as free equivalent) + 20 mg of policosanols per unit	None	NCT01571882

C=completed, R=Recruiting

Similarly to stigmasterol, β-sitosterol has various reported therapeutic pharmacological actions including anti-hypercholestrolemic, anti-tumour, anti-hyperglycaemia, anti-oxidant, anti-inflammatory, anti-mutagenic and neuroprotective activities (Awad *et al.*, 2000; Wang *et al.*, 2015; Baskar *et al.*, 2012; Gupta *et al.*, 2011). Firstly, Prieto *et al.* showed that β-sitosterol has anti-inflammatory activities; it inhibited the expression of vascular adhesion and intracellular adhesion molecule 1 in TNFα-stimulated human aortic endothelial cells (HAECs) when administered at doses of 0.1 to 200 μM (Prieto *et al.*, 2006). The compound was also found to inhibit NFκB phosphorylation and therefore it possesses anti-inflammatory activity. Moreover, β-sitosterol has anti-tumour activity and this was demonstrated by Awad *et al.* (2000) who found that when the compound was administered to human breast cancer cells (MDA-MB-231) it was found to induce apoptosis and suppressed tumour growth (Awad *et al.*, 2000). β-sitosterol possesses hypocholesterolemic activity as it decreases levels of cholesterol and triglycerides in animal models (Wang *et al.*, 2015). Another area where β-sitosterol is effective is acting as an anti-oxidising compound. β-sitosterol was found to improve levels of anti-oxidants and anti-oxidising enzymes in 1,2-dimethylhydrazine (DMH)-induced colon carcinogenesis (Baskar *et al.*, 2012). Moreover, it was also found to protect pancreatic tissues by enhancing anti-oxidant levels (Radika *et al.*, 2013). β-sitosterol is also considered to be anti-diabetic because it enhances insulin levels and reduces levels of glucose, nitric oxide (NO) and HbA1c in STZ-induced diabetic rats when administered at 10, 15 and 20 mg/kg BW (Gupta *et al.*, 2011). However, it is challenging to apply this to a LLT EA extract due to the fact that the % yield of β-sitosterol (0.17%) was low and this would require administration of the extract at high doses (6-12 g/kg BW).

In conclusion, LL is a new source of BA, lupeol, β-sitosterol and stigmasterol which were isolated for the first time from the EA extract of the tubers. These isolated compounds are known to possess various biological activities and include anti-hyperglycaemia effects. Therefore, the anti-diabetic activity of leaves and tuber extracts, as well as the isolated compounds will be investigated in depth in Chapter 3. Future work should consider fractionation of the extracts of LL leaves and isolate bioactive compounds.

Chapter 3

3. Investigation of the potential anti-diabetic activity of *L. linifolius*

3.1. Introduction

For centuries, natural products from medicinal plants and herbs have been used for the management of diabetes. These days, a number of plants such as *Allium sativum, Aloe ferox Mill, Vinca major* L. and *Cannabis sativa* L are being heavily investigated for their anti-diabetic potential (Odeyemi and Bradley, 2018). Plants containing peptides, soluble fibres, and phenolics have been found to have some anti-diabetic effects (Lacroix and Li-Chan, 2014). Historically, LL tubers were consumed in medieval times which allowed people to survive without food for weeks or even a month. The appetite suppressant activity of LL tubers was studied by (Woods, 2017) and there was some evidence supporting this belief. As there is a clear link between obesity and T2DM (Nguyen *et al.*, 2011), LL tubers and leaves were chosen for anti-diabetic investigation. Tubers were selected due to the fact that they were traditionally eaten, whereas the leaves were selected for the first time as this part of the plant is renewable, unlike the tubers. Some of the means by which anti-diabetic agents achieve therapeutic effects are through enzyme inhibition and glucose uptake enhancement, as described below.

3.1.1. α-amylase and α-glucosidase

Two enzymes, α-amylase and α-glucosidase, play important roles in regulating BG levels. The two enzymes are carbohydrate hydrolysing enzymes, α-amylase (from saliva and pancreas) degrades starch and polysaccharides to smaller oligosaccharides such as maltose. Oligosaccharides can be metabolised further by intestinal α-glucosidase to form absorbable monosaccharides such as glucose which enter the blood stream (Figure 3.1) (Da Costa Mousinho *et al.*, 2013; Bothon *et al.*, 2013). Therefore, high activities of α-amylase and α-glucosidase result in hyperglycaemic effects, which can damage pancreatic β-cells and impair glucose uptake by tissues (Jyothi *et al.*, 2012; Joshi *et al.*, 2015). Therefore, an assay that measures the inhibition

of these enzymes can be a good approach to determining the anti-diabetic activity of chemicals (Da Costa Mousinho *et al.*, 2013; Narkhede *et al.*, 2011).

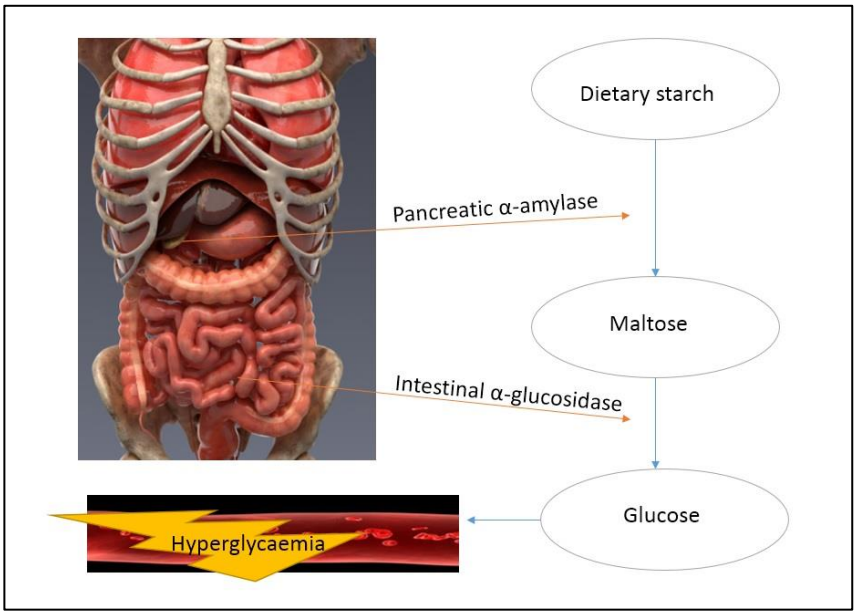

Figure 3. 1: Pathway of carbohydrate metabolisms by α-amylase and α-glucosidase.

In the UK, acarbose (Figure 3.2) is the only α-amylase and α-glucosidase inhibitor available to manage T2DM. Acarbose is a natural product obtained by the fermentation of *Actinoplanes* sp. (Schwientek *et al.*, 2012; Schaffert *et al.*, 2019). It reversibly binds to the enzymes and prevents break down of carbohydrates to small molecules. Acarbose reduces HbA1c by 0.6-1% (Weng *et al.*, 2015). As a result of this inhibition, carbohydrates arrive at the large bowel and get digested by bowel microbes and this causes flatulence, bloating and diarrhea (Figueiredo-González *et al.*, 2016). In practice, these side effects are minimised by starting acarbose at low doses (50mg) and then titrated up every two weeks (Gu *et al.*, 2015).

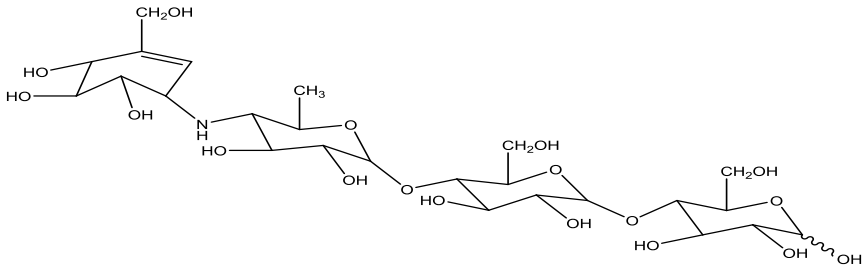

Figure 3. 2: Acarbose chemical structure.

There are a number of plants that showed activity against α-glucosidase enzyme. To start with, a study by Chen *et al.* showed that leaf and stem extracts of *Ampelopsis grossedentata* inhibited α-glucosidase (Chen *et al.*, 2016). The activity was as a result of a compound called 40-O-(2-N,N-hydroxy ethyl-toluene-4-sulfonyl)-ethyl myricetin which gave an IC_{50} of 9.3 μM against α-glucosidase; this compound was administered orally to normal and streptozotocin (STZ)-induced diabetic mice at a dose of 50mg/kg and resulted in decreased postprandial BG. Moreover, this compound reduced the fasting BG of STZ-induced diabetic mice. Rengasamy *et al.* showed that *Ecklonia maxima* extracts inhibited α-glucosidase and the active compounds were dibenzo [1,4] dioxine-2,4,7,9-tetraol and hexahydroxyphenoxydibenzo [1,4] dioxine (eckol) (Rengasamy *et al.*, 2013). Other plants with inhibitory effects on α-glucosidase include leaf extracts of *Garcinia bancana* Miq, *Garcinia daedalanthera* Pierre, *Garcinia kydia* Roxb, *Garcinia hombroniana*, and *Garcinia rigida* (Mahayasih *et al.*, 2017). Several plants have been reported to be potent inhibitors of α-amylase. These include *Bryophyllum pinnatum* (Ojo *et al.*, 2018), Teucrium species (Dastjerdi *et al.*, 2015), and *Myrcia salicifolia* (Figueiredo-González *et al.*, 2016).

3.1.2. Dipeptidyl peptidase IV *(*DPPIV)

Normally, following the consumption of a meal, L and K cells in the intestine secrete the incretin hormones GLP-1 and glucose dependent insulinortopic polypeptide (GIP), respectively (Pais *et al.*, 2016). GLP-1 and GIP play an important role in glucose homeostasis by enhancing the secretion of insulin and inhibiting glucagon secretion (Pais *et al.*, 2016). People with T2DM have an impaired incretin response to meals. Hence, the development of new drugs that improve the incretin response to meals is crucial for managing diabetes. Agents which improve the response of incretin include agonists for the GLP-1 receptor (incretin-mimetics) and other inhibitors of DPPIV. DPPIV deactivates GLP-1 and GIP and other peptides like GLP-2 and peptide YY (PYY); hence, drugs inhibiting DPPIV could play a major role in managing diabetes (Figure 3.3) (Olivares *et al.*, 2018). There are a number of studies using mice that have shown DPPIV null mice to have improved glucose tolerance as well as a resistance to developing obesity, despite a high fat diet being consumed by the mice (Conarello *et al.*, 2003; Dobrian *et al.*, 2010). Other studies showed the benefits of DPPIV inhibition

in regulating blood pressure and therefore reducing the risk of developing CVD (Zhang *et al.*, 2019). Current DPPIV inhibitors used in practice include sitagliptin, saxagliptin, vidagliptin, and linagliptin (Figure 3.4).

There are several plants with anti-diabetic activity that are inhibitors of DPPIV such as *Lagerstroemia speciose*, *Nigella sativa*, *Swietenia macrophylla* King, *Hedera nepalensis*, and *Fagonia cretica* (Elya *et al.*, 2015, Saleem *et al.*, 2014). A study by Semaan *et al.* showed that a flavonoids fraction extracted from *Allophylus cominia*, a plant traditionally used in Cuba to treat T2DM, inhibited DPPIV with an inhibitory constant (Ki) of 2.6 µg/ml (Semaan *et al.*, 2017). The plant was also found to be active against α-amylase, α-glucosidase, and PTP 1B enzymatic assays. Incretin agonists can be used as therapy in T2DM, as they prolong the action of GLP-1 and GIP. Srivastava *et al.* showed that the administration of an aqueous extract of *Pueraria tuberosa* tubers (PTY-2), a known DPPIV inhibitor, to rats with STZ-induced diabetes resulted in improved blood glucose levels (Srivastava *et al.*, 2018). PTY-2 treatment given to diabetic rats showed increased levels of GLP-1 and GIP in plasma. Moreover, PTY-2 significantly increased pancreatic expression GLP-1R, GIP-R, Bcl2, and insulin.

Incretin mimetics and DPPIV inhibitors do not cause hypoglycaemia, which is a common side effect of other anti-diabetic agents. However, incretin mimetics are not preferred due to their very short half-life (2 min) as they are rapidly degraded and inactivated by DPPIV (Sharma *et al.*, 2018). Hence, DPPIV inhibitors are favoured over incretin mimetics. However, there are a number of side effects that might develop when DPPIV is inhibited. These include pancreatitis, angioedema and other infective disorders (Suman *et al.*, 2016). DPPIV is also seen to be expressed in inflammatory cells, thus it is believed that DPPIV inhibitors can also be beneficial to treat inflammatory diseases such as rheumatoid arthritis (RA) (Waumans *et al.*, 2015).

3.1.3. Protein tyrosine phosphatase 1B enzyme (PTP 1B)

PTP 1B is a negative regulator of the insulin signalling pathway (Figure 3.5). The first step in glucose uptake by cells through GLUT4 is phosphorylation of the insulin and insulin substrate receptors within the cells, a mechanism deactivated by a PTP 1B diet

(Krishnan *et al.*, 2018). This deactivation of the phosphorylation step leads to a reduction in the glucose uptake by cells (Obanda and Cefalu, 2013). Hence, PTP 1B inhibitors can prolong the phosphorylation process and enhance glucose uptake by cells. PTP 1B also negatively regulates the leptin receptor pathway (Figure 3.5). In previous studies, PTP 1B knockout mice demonstrated an improved glycaemic control and greater resistance to weight gain on a high fat diet (Tsou *et al.*, 2014). Hence, the identification of novel PTP 1B inhibitors is an objective of this project.

A number of plants used traditionally for managing diabetes were found to inhibit PTP 1B. A study by Tiong *et al.* showed that *Catharanthus roseus* (L.) G. Don leaves extract, which is used to traditionally manage diabetes in India, South Africa, Malaysia, and China, inhibited PTP 1B activity (Tiong *et al.*, 2013). The active alkaloids in this plant were vindolidine, indolicine and vindolinine with IC_{50} of 18.2 µM, 11.6 µM, and 14.1 µM, respectively. Moreover, Kim and Kim showed that an aqueous extract of Korean red ginseng (KRG), *Panax ginseng*, was given to 5 week old Goto-Kakizaki (GK) male rats at daily doses of 0.2 g/kg for 5 weeks until the age of 12 weeks (Kim and Kim, 2012). The study revealed that treatment with KRG showed a significant decrease in blood glucose in comparison with the control group; adipose and skeletal muscles showed a down-regulation of PTP 1B. Moreover, the pancreas showed a significant insulin up-regulation in the treated group.

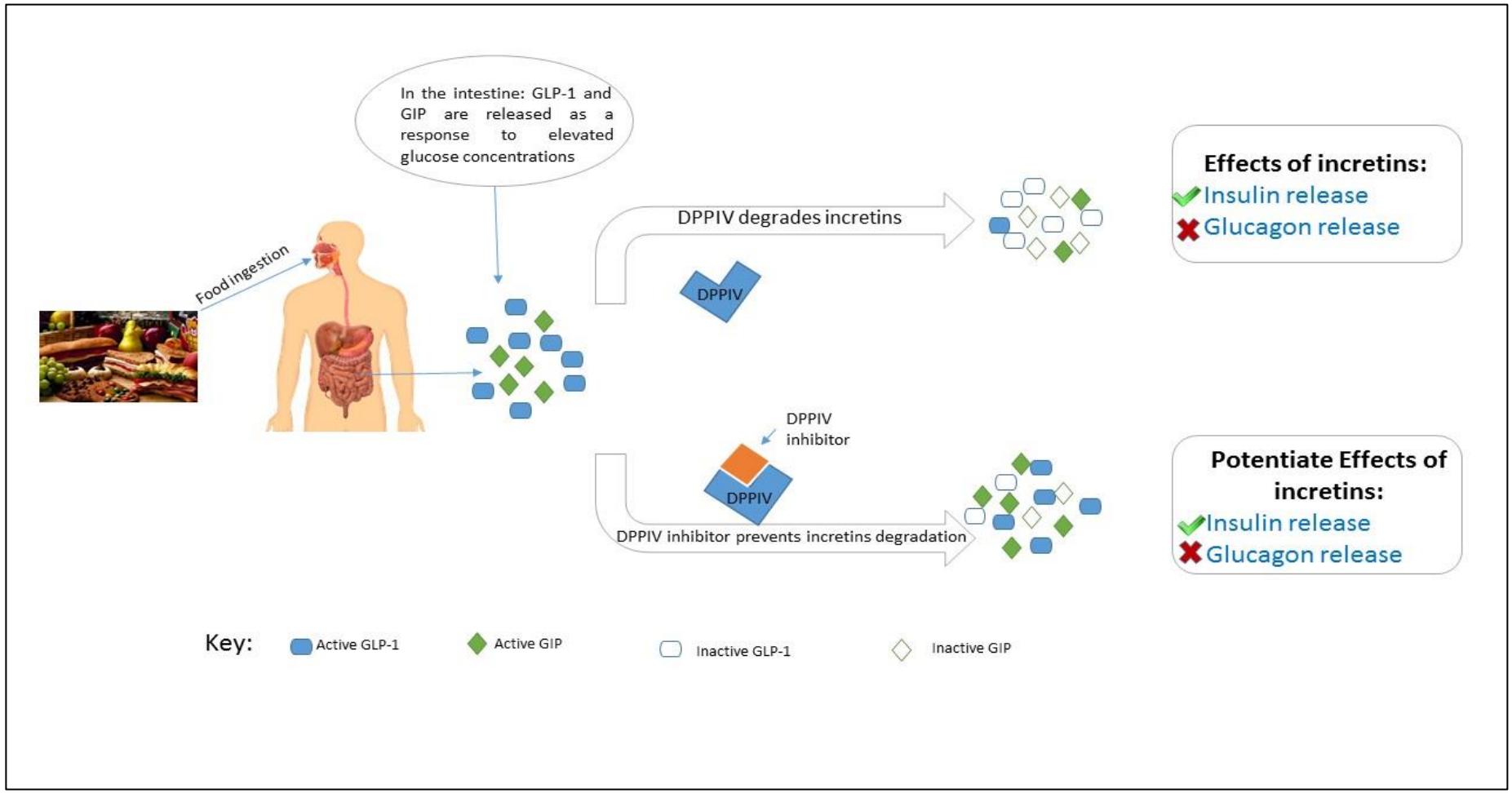

Figure 3. 3: Regulation of insulin release by incretins and their inhibitor, DPPIV.

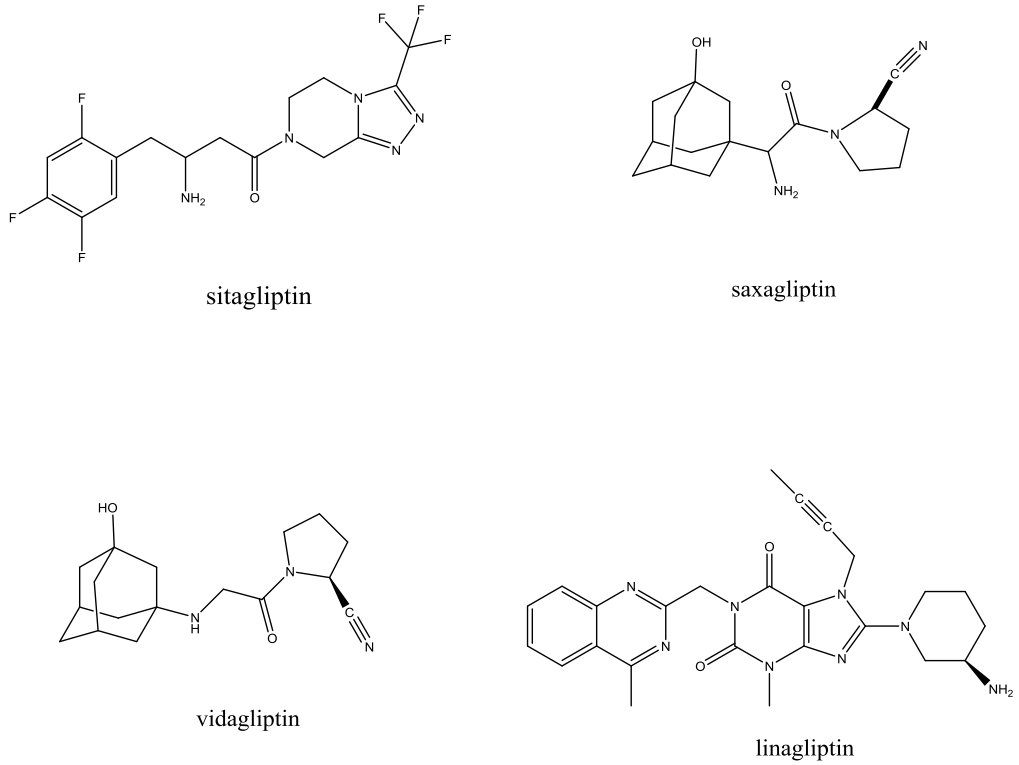

Figure 3. 4: Chemical structures of DPPIV inhibitors used in the clinic for managing T2DM.

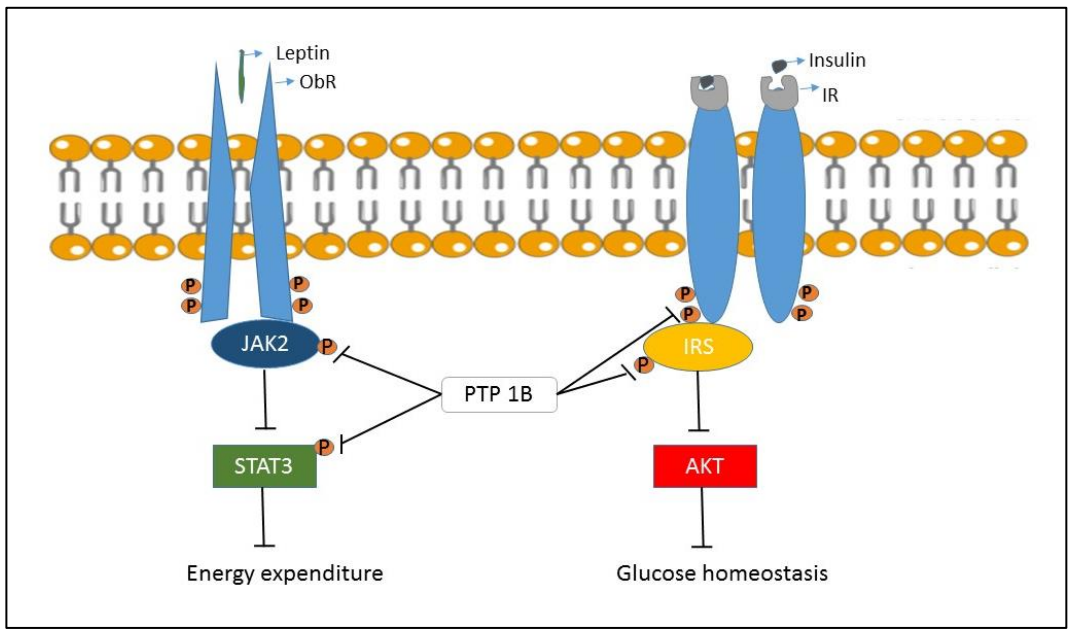

Figure 3. 5: The physiological signaling pathways involving PTP 1B (Sun *et al.*, 2016).

3.1.4. Pancreatic Lipase

Pancreatic lipase (PL) is a fundamental enzyme in fat absorption and digestion. PL is responsible for the cleavage of approximately 70% of dietary fats including triglycerides and phospholipids (Figure 3.6), which contribute to obesity (Glisan *et al.*, 2017). Finding inhibitors of PL is beneficial in obesity as less fats will be absorbed. Currently, Orlistat (Figure 3.7), derivative of the natural product lipstatin, is the only licenced PL inhibitor in the UK (Jeong *et al.*, 2014; Booth *et al.*, 2015).

PL inhibition by a number of plants was investigated previously in a number of studies. A study by Sellami *et al.* showed that aqueous extracts of *Cinnamomum verum* bark (cinnamon) and *Mentha aquatica* leaves (mint) resulted in 92% and 87% PL inhibition, respectively (Sellami *et al.*, 2017). On the other hand, these two plants showed no activity against PL when extracted with EA or Hex. In addition, Julnaryn *et al.*, (2012) investigated effects of a number of edible plants against PL, aqueous extracts of *Morus alba* (mulberry) and *Ginkgo biloba* (ginkgo) inhibited the enzyme with IC_{50} of 10 µg/ml and 50 µg/ml respectively (Julnaryn *et al.*, 2012). A study by Kiage‐Mokua *et al.* showed that ethanolic extracts of *Tabebuia impetiginosa*, *Arctium lappa L.*, *Calendula officinalis*, *Helianthus annuus*, *Linum usitatissimum and L. propolis*, inhibited PL *in vitro* (Kiage‐Mokua *et al.*, 2012). In a follow-up study, these plants were assessed *in vivo* for their ability to inhibit PL. Plant extracts were administered orally to rats with a high fat diet. Extract of bark of *Tabebuia impetiginosa* showed significant reduction in postprandial plasma triglycerides.

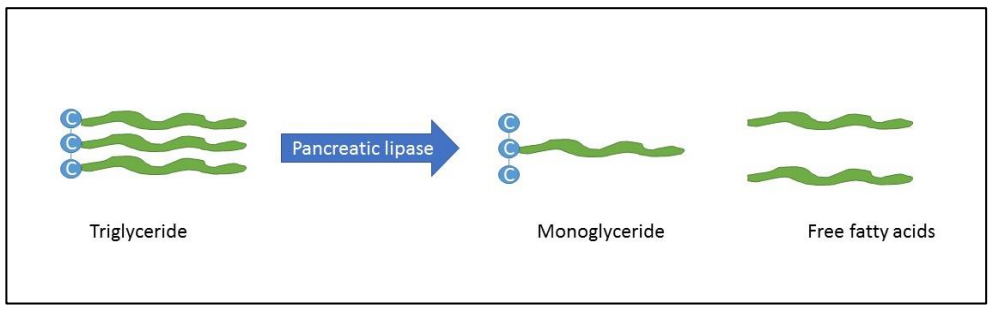

Figure 3. 6: Conversion of triglycerides to monoglycerides and free fatty acids by PL.

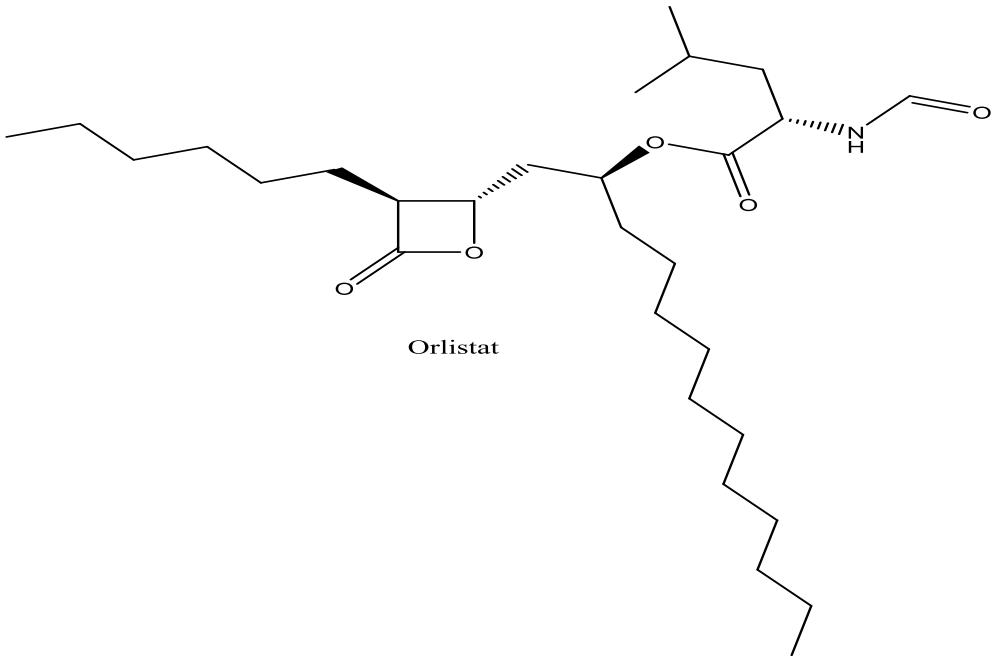

Figure 3. 7: Chemical structure of orlistat, a PL inhibitor.

3.1.5. Cell viability

Cell viability is assessed by various methods; these include integrity of plasma membrane, ability to synthesise DNA, total DNA activity, ATP presence, enzyme activity, and more commonly cellular reducing conditions (Eilenberger *et al.*, 2018). alamarBlue™ (Figure 3.8) is a reagent that is used in this study to ensure that the tested samples are non-cytotoxic to the cells, before commencing screening or in order to evaluate non-toxic concentrations to carry out assays. It takes advantage of the cells' ability to reduce resazurin (indicator of cell metabolic activity). Viable cells maintain a reducing environment in the cytosol of the cell. The active compound in alamarBlue™ is resazurin, which is a safe cell permeable agent that is blue-coloured and non-fluorescent (Präbst *et al.*, 2017). Once resazurin is inside the cells, healthy cells are capable of reducing it to resorufin. Resorufin is a highly fluorescent red-coloured compound. Therefore, viable cells will simultaneously reduce resazurin to resorufin, resulting in high fluorescence being generated. On the other hand, non-viable cells are unable to carry out the conversion of resazurin to resorufin and therefore will be coloured blue and show no fluorescence (Eilenberger *et al.*, 2018).

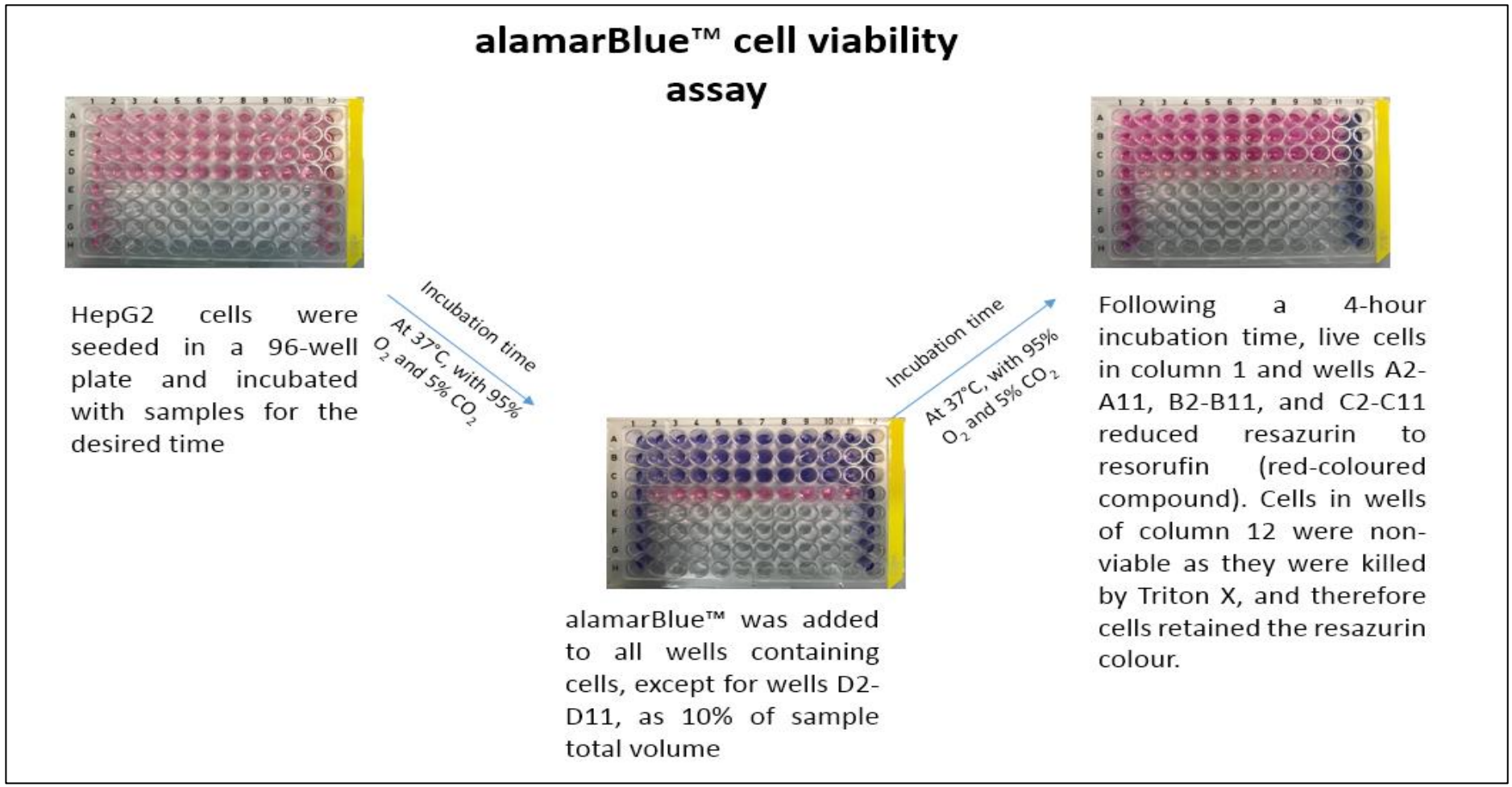

Figure 3. 8: alamarBlue™ cell viability assay work template.

3.1.6. Glucose uptake in HepG2 cells

In this research, glucose uptake in the HepG2 cell line was investigated using the Promega Glucose Uptake-Glo™ kit (Figure 3.9) following treatment with extracts of LL tubers and leaves. This assay is superior to other assays as it is a non-radioactive bioluminescence assay that is capable of determining the glucose concentration in viable mammalian cells (Choromanska *et al.*, 2018). The assay is sensitive to detecting 2-deoxyglucose-6-phosphate (2DG6P). In normal conditions, when 2-deoxyglucose (2DG) is administered into cells, 2DG will be transported across the cell membrane and then phosphorylated (as glucose, G6P). G6P is further modified by cell enzymes; however, these enzymes are not able to modify 2DG6P. Hence, 2DG6P accumulates inside the cells. Following this accumulation (10 min), a stop buffer, which is highly acidic, is added to stop the 2DG uptake by initiating cell lysis and stop any NADPH activity in the cells. Then, a very basic solution (neutralisation buffer) is added to bring the acidic environment to a neutral state. The final step is the addition of a detection reagent which contains the following components: glucose-6-phosphate dehydrogenase (G6PDH), NADP+, reductase, luciferase reagent and reductase substrate. G6PDH converts 2DG6P to 6-phosphodeoxygluconate (6PDG) by oxidation and continuously reduces $NADP^+$ to NADPH. The enzyme reductase converts reductase substrate to luciferin by using NADPH. Then, luciferase uses luciferin to generate luminescence signals that are directly proportional to the 2DG6P concentrations in cells.

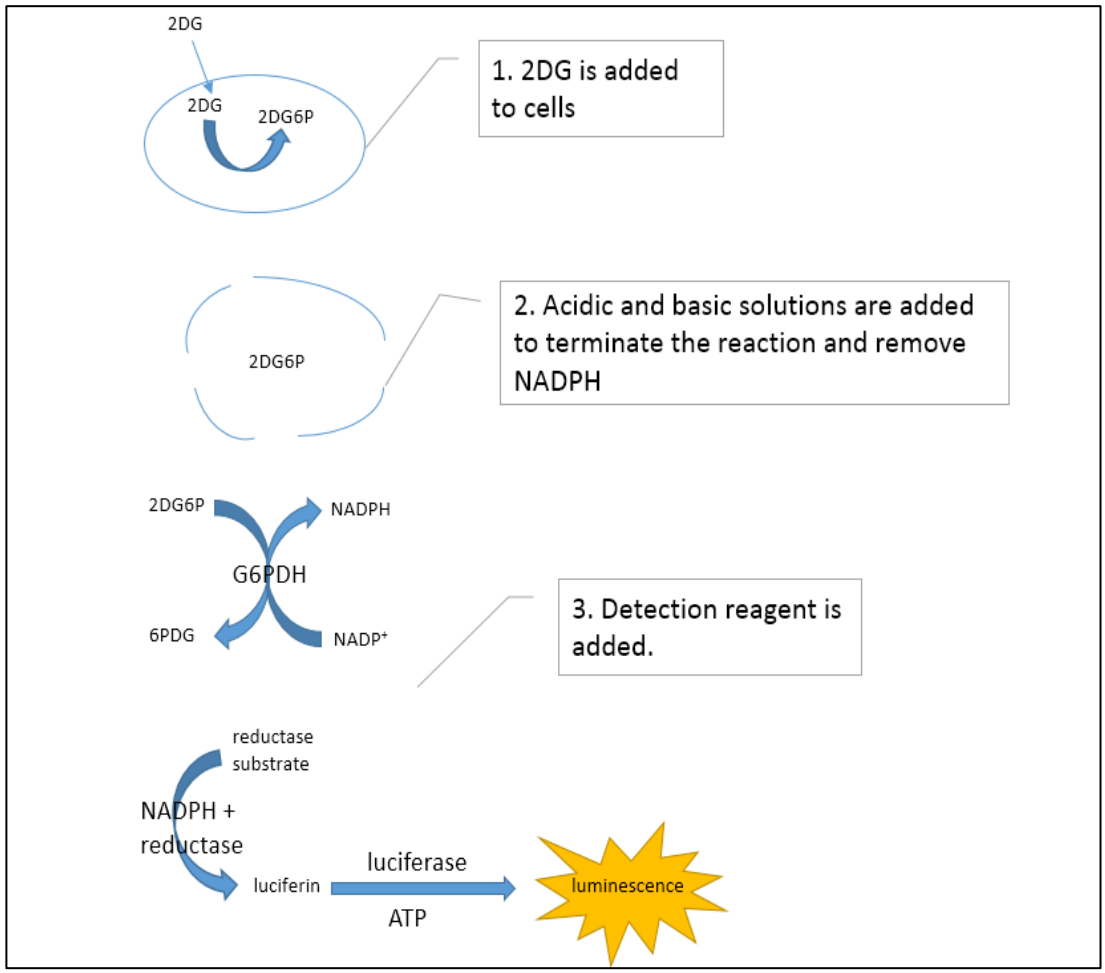

Figure 3.9: Glucose Uptake-Glo™ assay used to determine glucose levels in cell lines.

3.2. Aims and Objectives

This chapter aims to evaluate the anti-diabetic potential of LL extracts and isolated compounds. The specific aims were:

1. To test the inhibitory activity of LL extracts and isolated compounds against the following isolated enzymatic assays, commonly used to assess anti-diabesity activity in *in vitro* studies.
    - α-glucosidase
    - α-amylase
    - PTP 1B
    - DPPIV

- PL

2. To test the cytotoxic effects of the extracts of LL tubers and leaves and the isolated compounds on Caco2 and HepG2 cells before performing anti-diabetic assays on them to ensure that tested samples are non-cytotoxic to the cells.
3. To test the inhibitory activity of LL extracts and isolated compounds against cell-expressed DPPIV in Caco2 cells.
4. To study the effects of LL extracts and isolated compounds on glucose uptake by HepG2 cells, cells known to possess glucose transporters.

3.3. Materials and methods

3.3.1. Enzyme inhibition assays

3.3.1.1. Sample preparation

Samples (10 mg/ml or 10 mM) were diluted using an assay buffer to yield a concentration of 30 µg/ml for extracts and 30 µM for isolated compounds. Samples were tested at several concentrations in which 30µg/ml or 30µM was the highest tested concentration.

3.3.1.2. General protocol for the enzyme inhibition assays

Ten µl of extracts, isolated compounds or a reference standard was added to wells of a 96-well half-area plate. Then 20 µl of enzyme was added to the wells and the plate was shaken for 1 min on a plate shaker. The plate was incubated at 37°C for 10 minutes for α-glucosidase, 30 min for α-amylase, PTP 1B and DPPIV and 15 min for PL. Ten µl of substrate was added to all wells and the plate was incubated at 37°C for another 10 min for α-glucosidase, 30 min for α-amylase and DPPIV and 25 min for pancreatic lipase. Optical density 450nm for α-glucosidase and α-amylase or fluorescence at 355nm/460nm (Excitation/Emission) for PTP 1B, PL and DPPIV was read on a Wallac Victor plate reader.

3.3.1.3. α-glucosidase inhibition assay

The α-glucosidase inhibition assay was carried out with some modifications to the method described by Kwon *et al.* (2008). The assay buffer was prepared by mixing 24.5ml of 0.2M sodium phosphate dibasic heptahydrate with 25.5ml of 0.2M sodium phosphate monobasic dehydrate before being topped-up to 100 ml using distilled water and calibrated to pH 6.8. A stock concentration of yeast α-glucosidase was prepared in distilled water as 75 units/ml and stored at -20°C. The final enzyme concentration used in the assay was 0.2 units/ml. The assay substrate was 4-nitrophenyl-α-D-glucopyranoside. The substrate was prepared in a phosphate buffer and kept at -20ºC until required. The final substrate concentration required was 1mM. Acarbose was used as a positive control for the assay. Acarbose was dissolved in distilled water and was then tested at concentrations ranging from 10 µM-25 mM.

3.3.1.4. α-amylase inhibition assay

The α-amylase inhibition assay was carried out with some modifications to the method described by Funke and Melzig (2005). HEPES (4-(2-hydroxyethyl)-1-piperazineethanesulfonic acid) buffer was prepared at a concentration of 50 mM, and the pH of the buffer was 7.1 at 37°C. A stock concentration of porcine pancreas α-amylase was prepared in distilled water as 250 U/ml and stored at -20°C. The final enzyme concentration used in the assay was 125 U/ml. The assay substrate 4-nitrophenyl-α-D-maltohexaside was prepared in assay buffer and stored at -20ºC until required. The final substrate concentration required was 1.5mM. Acarbose was used as a positive control for the assay and was dissolved in distilled water then tested at concentrations ranging from 300 nM-1 mM.

3.3.1.5. PTP 1B inhibition assay

The PTP 1B inhibition assay was carried out with some modifications to the method described by Zhang *et al.* (2006). The assay buffer was made by dissolving 25 mM HEPES, 50 mM sodium chloride, 2 mM dithiothreitol (DTT), 2.5 mM ethylene-diamine-tetraacetic acid (EDTA) and 0.01 mg/ml bovine serum albumin (BSA) in 500 mL distilled water. The buffer pH was calibrated to pH 7.2. Catalase (0.25/ml) was

added to the assay buffer to scavenge any ROS that occur as a result of interaction between DTT and natural products. ROS can inhibit PTP 1B and hence generate false positives. The enzyme buffer consisted of 25 mM HEPES 5 mM DTT, 1 mM EDTA and 0.05% (v/v) NP-40. The final PTP 1B enzyme concentration used was 2 nM. The assay substrate was 6,8-difluoro-4-methylumbelliferyl phosphate (DiFMUP) and was prepared in DMSO as a stock concentration of 10 mM. The final substrate concentration required was 10 µM. Bis(4-trifluoromethylsulfonamidophenyl)-1,4-diisopropylbenzine (TFMS) was used as a positive control for the assay. TFMS was then tested at concentrations ranging from 0.03 µM -100 µM.

3.3.1.6. PL inhibition assay

The PL inhibition assay was carried out with some modifications to the method described by Zhang *et al.* (2015). The assay buffer was 0.1 mM Tris-HCL and the solution pH was 8 at 37ºC. PL (type II from porcine pancreas) was the enzyme used in this assay and the substrate was 4-methyl umbelliferyl oleate. The substrate was prepared in assay buffer as 50 U/ml and kept at -20ºC until required. The final substrate concentration required was 200 µM. Orlistat was used as a positive control. Orlistat was dissolved in distilled water and was then tested at concentrations ranging from 10 nM-30 µM.

3.3.1.7. DPPIV inhibition assay

The DPPIV inhibition assay was carried out with some modifications to the method described by Scharpé *et al.* (1988). The buffer was prepared by dissolving 100 mM Tris-HCl and 0.1 mg/ml BSA in 500 mL of distilled water to yield a concentration of 100 mM. The final buffer solution was at pH 8 at 37ºC. DPPIV was dissolved in assay buffer to produce 0.27 µM of the enzyme which was stored -20°C until required. A stock solution of 0.6 nM (containing 5.6 µl of enzyme) was prepared and added to 2.5 mL of DPPIV buffer to produce a final concentration of 0.3 nM. The assay substrate was gly-pro-7-amido-4-methylcoumarin hydrobromide (Gly-pro). The required final substrate working concentration was 30 µM. P32/98, a known DPPIV inhibitor was used as a positive control tested at concentrations ranging from 1 nM-3 µM.

3.3.1.8. Calculation of inhibition

All extracts and isolated compounds were tested in triplicate as a minimum and the results were compared with the control and expressed as a percent inhibition. The control was assumed to have a 0% inhibitory effect in the enzymatic assays. The percent inhibition was calculated using the following equation:

$$\% \text{ inhibition} = \frac{control\ reading - sample\ reading}{control\ reading}\ X\ 100$$

3.3.2. Anti-diabetic assessment on Caco2 and HepG2 cells

3.3.2.1. Cell culture of Caco2 and HepG2 cells

Cells were incubated and grown in a humidified incubator at 37°C with 5% CO_2. They were cultured in DMEM culture media supplemented with 10% (v/v) Foetal Calf Serum (FCS), 1% penicillin-streptomycin, 1% L-glutamine, and 1% non-essential amino acids (NEAA).

Tissue culture flasks, size 75cm^2, were seeded at 1x10^4 cells/cm^2. Cells were grown to 75-85% confluency before being used for assays. The cells were washed with HBSS before being dissociated with 2.5 ml TripLE Express. Then, cells were incubated for 5 min to dissociate the cells from the flask before the addition of 7.5 ml of culture media to stop the action of TripLE Express. The cells were transferred into a 15ml centrifuge tube and centrifuged for 2 min at 1000 RPM. The supernatant was discarded and the cell pellet resuspended in culture media before being counted under the microscope.

3.3.2.2. Cytotoxicity assessment on Caco2 and HepG2 cells

Cytotoxicity assays were carried out to ensure the samples were not cytotoxic to the cell line prior to enzyme assays being carried out. Cells were seeded in 96-well clear

plates at $1x10^5$ cells/ml. Plates were incubated for 48h in a humidified incubator at 37°C with 5% CO_2 prior to adding samples.

Samples were diluted in DMEM culture media; 30 µg/ml for extracts or 30 µM for isolated compounds. Stock samples were prepared at concentrations of 120 µg/ml or 120 µM as they were diluted four times in the assay plate. Twenty-five µl of samples were added to the pre-plated 75 µl of cells. Triton X (a cytotoxic agent) was used as a positive control for the assay, while cells only were used as a negative control. Samples/cells were incubated for 4h before adding 10 µl of alamarBlue® reagent and then further incubated for 4h in a humidified incubator at 37°C with 5% CO_2. The plates were read using fluorescence (560nm excitation, 590nm emission) on a M5 Spectramax Plate Reader using Softmax Pro software. The cell viability was calculated using the formula below:

$$\%\ \text{inhibition} = \frac{control\ reading - sample\ reading}{control\ reading}\ X\ 100$$

3.3.3. DPPIV inhibition assay in Caco2 cell line

Caco2 cells were seeded at $20x10^4$ cells/ml (50 µl per well) in 96-well half-area clear-bottom black plates. Cells were left to differentiate in the plate for 5 days, and media was changed on day 3 of differentiation. On day 5 of differentiation, tested samples and P32/98 were prepared in PBS in a 96-well round bottom dilution plate – stock was placed in column 12, and then serially diluted starting from 100 µM to 0.03 µM.

Samples on the other hand were prepared at 60 µg/ml or 60 µM as they were diluted twice in the assay plate. Media from the seeded assay plate was removed. Cells were washed twice with 50 µl PBS solution. Then, 20 µl of samples and P32/98 were added to the cells and allowed to incubate in a humidified incubator at 37°C with 5% CO_2 for 20 min. Following incubation, 20 µl of 250µM Gly-pro was added to all wells and for a further 20 min. The plate was read on a Wallac Victor plate reader at excitation 355 nm and emission 460 nm. The above procedure was repeated at least three times.

3.3.4. Glucose uptake levels in HepG2 cells using a Glucose Uptake-Glo™ kit

A Glucose Uptake-Glo™ kit was used per the manufacturer's instructions.

3.3.4.1. 2DG6P Detection Reagent

This reagent was prepared by adding the following components in Table 3.1.

Table 3. 1: Components used in the preparation of the Glucose Uptake-Glo™ assay.

Component	Per reaction	Per 5 ml
Luciferase	50 µl	5 ml
NADP+	0.5 µl	50 µl
G6PDH	1.25 µl	125 µl
Reductase	0.25 µl	25 µl
Reductase Substrate	0.03125 µl	3.125 µl

The reagent was prepared fresh, one hour prior to performing the assay and not stored. The total volume prepared was adjusted according to the number of reactions/wells needed; 50 µL 2DG6P Detection Reagent is required per reaction/well; 2-deoxyglucose (100 mM) was diluted to 1mM using PBS.

3.3.4.2. 2DG6P standard

2DG6P was diluted in PBS to produce a curve with a concentration range of 0.5–30 µM; 25 µl used per well.

3.3.4.3. Glucose uptake in HepG2 cell line

HepG2 cells were seeded in half-area black plates with a clear bottom at 1 x 10^4 cells/well (50 µl/well) and were allowed to adhere overnight in a humidified incubator at 37°C with 5% CO_2. The next day, samples were prepared as 60 µg/ml or 60 µM as it was diluted 1:1 with cells to give a final sample concentration of 30 µg/ml or 30 µM. Insulin (100 nM) was used as a positive control which is known to enhance glucose

uptake in HepG2 cells, whereas cytochalsin B (50 µM) was used as a known inhibitor of glucose transport in cells. The samples were incubated with the cells for 5h in a humidified incubator at 37°C with 5% CO_2. As HepG2 is plated using DMEM which contains glucose that can interfere with the assay, the media was removed and replaced with 50 µl of 1mM 2DG. The plate was incubated at room temperature for 10 min after being shaken for 1 min using a plate-shaker. Twenty-five µl of stop buffer and 25 µl of neutralisation buffer were added to all wells. Then, 50 µl of 2DG6P detection reagent was added to all wells and the plate was incubated at room temperature for 3h after being shaken again for 1 min. Luminescence with an integration time of 0.5 seconds/well was read on a M5 Spectramax Plate Reader using Softmax Pro software.

3.3.4.4. Statistical analysis

ANOVA with a Dunnet's post-test in PraphPad Prism 4.0 was used to perform statistical analysis, $P < 0.05$ was considered statistically significant.

3.4. Results

3.4.1. Anti-diabetic assays on isolated enzymes

3.4.1.1. α-Glucosidase assay

All the extracts and isolated compounds were tested against α-glucosidase activity that had been serially diluted. Highest concentration of extracts was 30 µg/ml, whereas 30 µM used for pure compounds. Acarbose was used as a positive control (Figure 3.10) and produced an IC_{50} of 0.38 mM.

3.4.1.1.1. LL tuber extracts and isolates

LLT EA extracts strongly ($P < 0.05$) inhibited α-glucosidase with an IC_{50} of 9.5 µg/ml (Figure 3.11), while LLT Hex extract showed approximately 40% enzyme inhibition when tested at 30 µg/ml and this activity disappeared at lower concentrations; LLT MeOH extract was inactive. The compounds obtained from LLT EA were BA, lupeol, and a mixture of sitosterol/stigmasterol and their effects on α-glucosidase are shown

in Figure 3.12. Lupeol showed 50% and 30% inhibition ($P < 0.05$) when tested at 30 and 10 µM, respectively. Sitosterol/stigmasterol showed no activity against α-glucosidase. BA was a strong ($P < 0.05$) inhibitor of α-glucosidase with an IC_{50} of 5.5 µM.

3.4.1.1.2. LL leaf extracts

LLL Hex showed some ($P < 0.05$) inhibition activity against α-glucosidase when tested at 30, 10, and 3 µg/ml, LLL EA showed the strongest ($P < 0.05$) inhibition activity against α-glucosidase among all the tested samples, with an IC_{50} of 0.6 µg/ml, LLL MeOH strongly ($P < 0.05$) inhibited α-glucosidase with an IC_{50} of 4.3 µg/ml as shown in Figure 3.13.

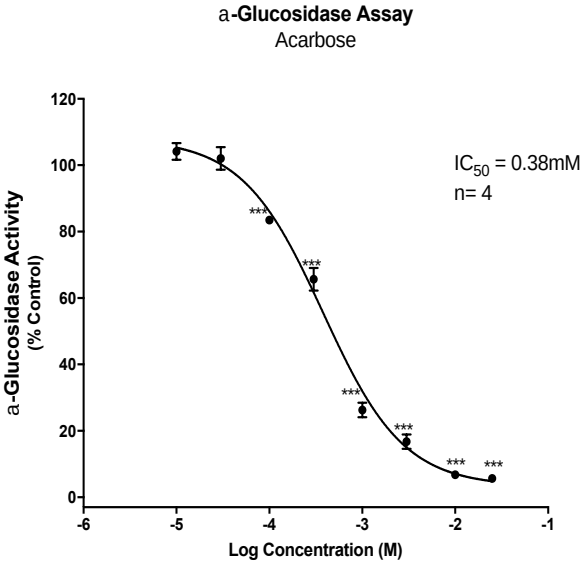

Figure 3. 10: The inhibitory effects of various concentrations of acarbose on α-glucosidase activity. Data was analysed using One-Way ANOVA with a Dunnet Post-Test. ***P<0.001 vs control, **P<0.01 vs control.

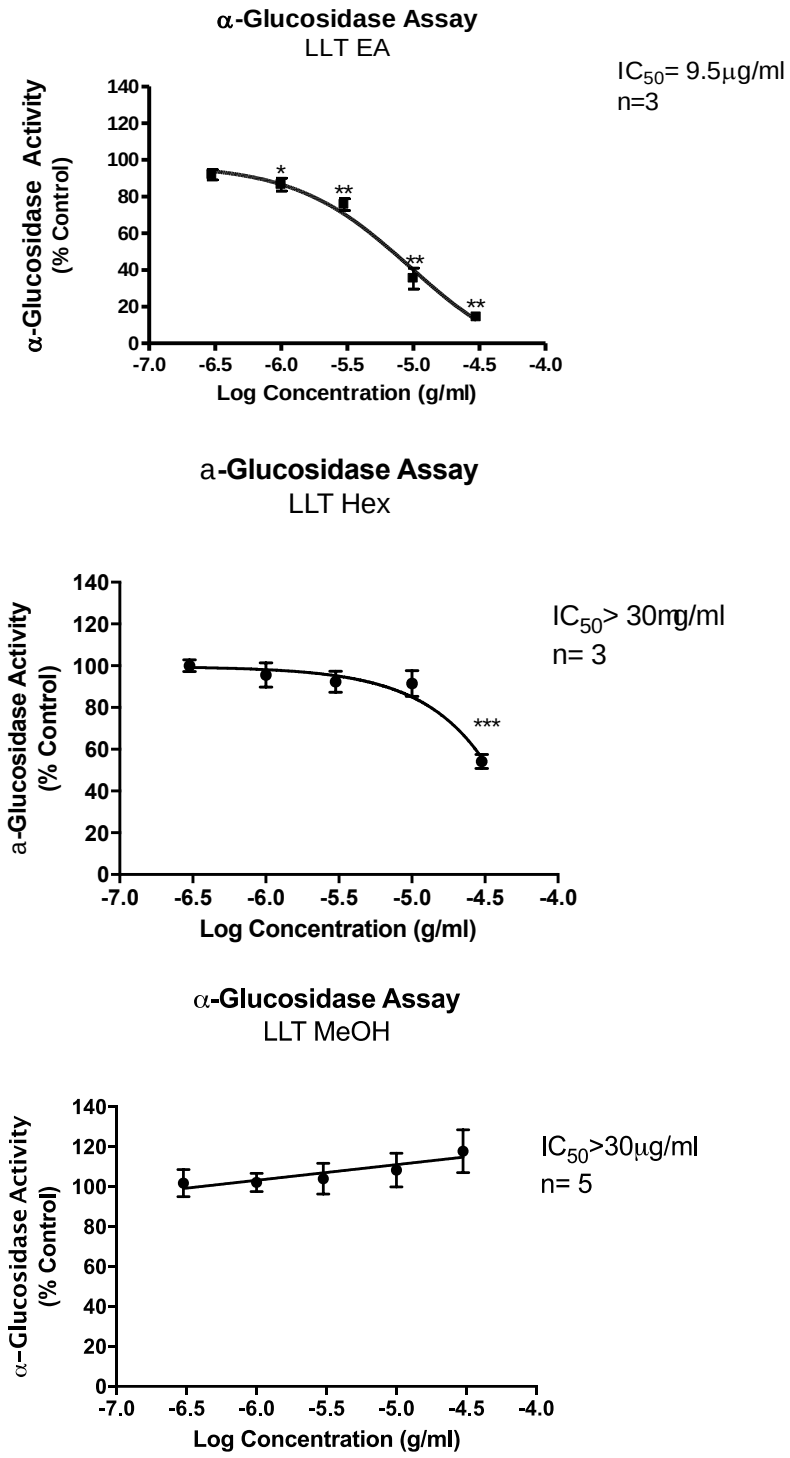

Figure 3. 11: The inhibitory effects of various concentrations of extracts of LL tubers on α-glucosidase activity. Data was analysed using One-Way ANOVA with a Dunnet Post-Test. ***P<0.001, **P<0.01, *P<0.05 vs control.

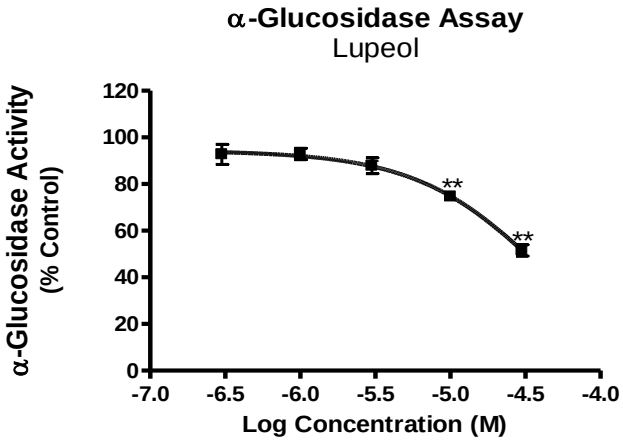

IC_{50}>30μM
n=3

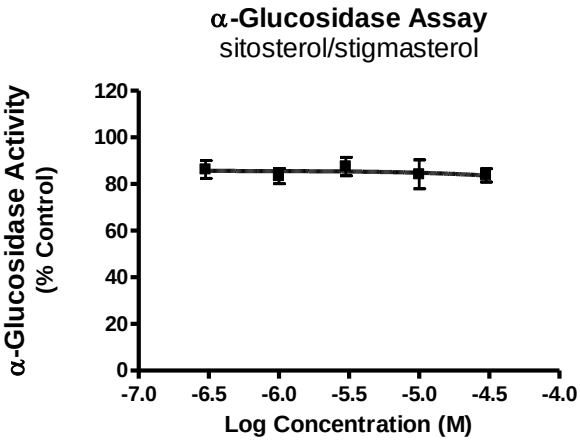

IC_{50}>30μM
n=3

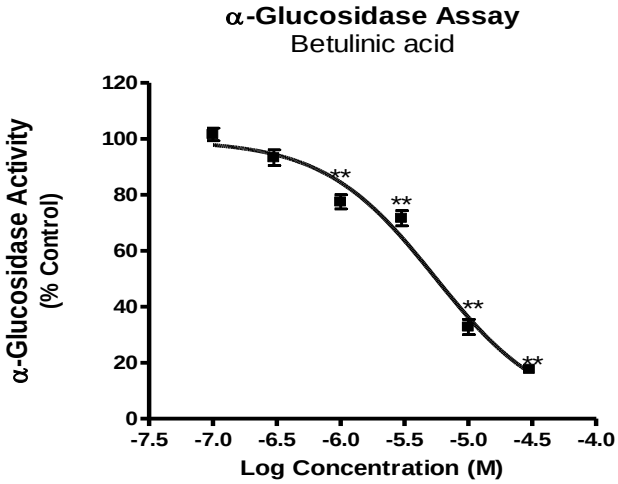

IC_{50}= 5.5μM
n=3

Figure 3. 12: The inhibitory effects of various concentrations of lupeol, mixture of sitosterol/stigmasterol and BA on α-glucosidase activity. Data was analysed using One-Way ANOVA with a Dunnet Post-Test. **P<0.01, *P<0.05 vs control.

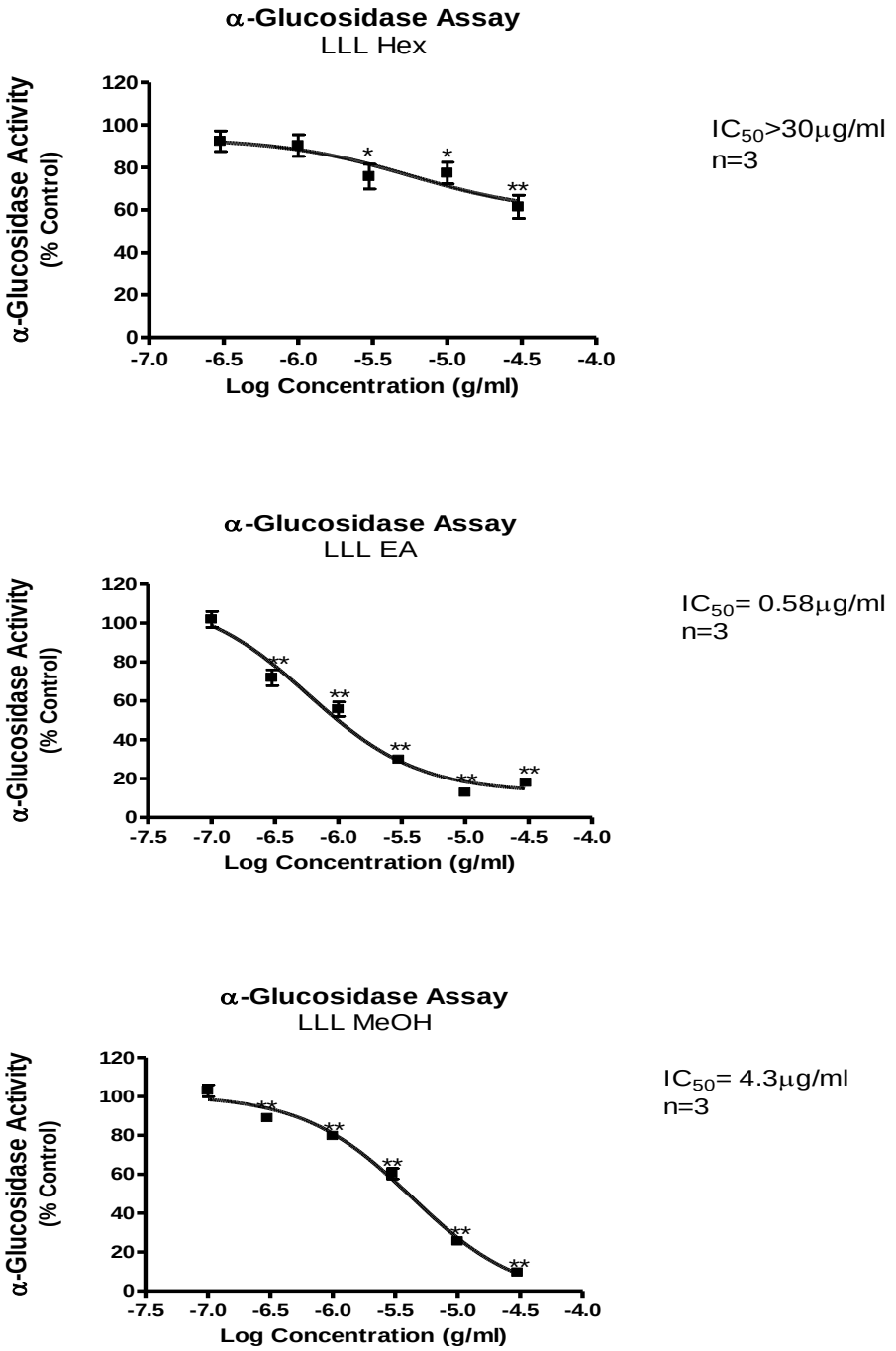

Figure 3. 13: The inhibitory effects of various concentrations of extracts of LL leaves on α-glucosidase activity. Data was analysed using One-Way ANOVA with a Dunnet Post-Test. ***P<0.001, **P<0.01, *P<0.05 vs control.

3.4.1.1.3. Summary of α-glucosidase assay results

Four samples from LL extracts and isolated compounds showed α-glucosidase inhibition, the IC_{50} values are summarised in Table 3.2.

Table 3. 2: Summary of the activity of the LL extracts and isolated compounds on α-glucosidase. Red indicates inhibition of α-glucosidase.

Part of LL	Sample ID	IC_{50}
Tubers	LLT Hex	>30 µg/ml
	LLT EA	9.5 µg/ml
	LLT MeOH	>30 µg/ml
	BA	5.5 µM
	Lupeol	>30 µM
	sitosterol/stigmasterol	>30 µM
Leaves	LLL Hex	>30 µg/ml
	LLL EA	0.58 µg/ml
	LLL MeOH	4.3 µg/ml

3.4.1.2. α-Amylase assay

Following the α-glucosidase assay results, samples were tested against their ability to inhibit α-amylase. Acarbose was used as a positive control and inhibited the enzyme with an IC_{50} of 1.2 mM and results were statistically significant ($P < 0.01$) (Figure 3.14).

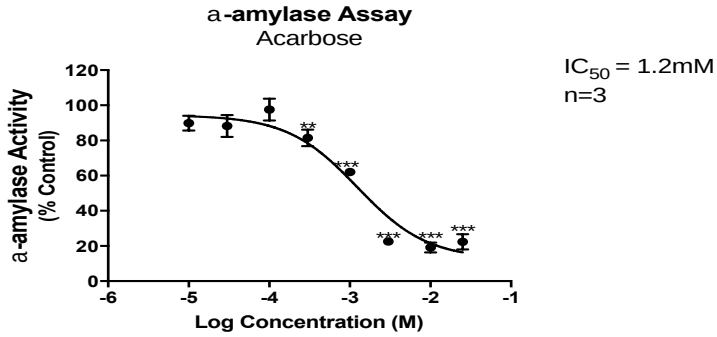

Figure 3. 14: The inhibitory effects of various concentrations of acarbose on α-amylase activity. Data was analysed using One-Way ANOVA with a Dunnet Post-Test. ***P<0.001, **P<0.01 vs control.

3.4.1.2.1 LL extracts and isolated compounds

All the extracts of the tubers and the leaves as well as the isolated compounds were inactive against α-amylase, the assay results are shown in Appendix 1.

3.4.1.3. PL assay

Orlistat, current licenced anti-obesity drug, was used as a positive PL inhibitor in this assay. Orlistat inhibited PL with an IC_{50} of 0.23 µM and results were statistically significant ($P < 0.05$) as shown in Figure 3.15.

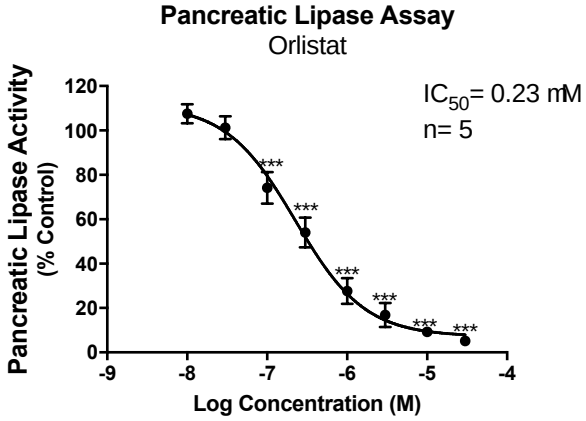

Figure 3. 15: The inhibitory effects of various concentrations of Orlistat on PL activity. Data was analysed using One-Way ANOVA with a Dunnet Post-Test. ***P<0.001 vs control.

3.4.1.3.1. LL tuber extracts and isolated compounds

LLT EA showed 50% inhibition ($P < 0.05$) of PL when tested at 30 µg/ml as in Figure 3.16, whereas LLT MeOH and LLT Hex extracts were inactive at the tested concentrations. Lupeol and the mixture of stigmasterol/sitosterol produced no inhibitory activity against PL as shown in Figure 3.17, BA produced comparable results to LLT EA extract, causing 50% reduction in the PL activity when tested at 30 µM.

3.4.1.3.2. LL extracts of the leaves

LLL Hex extract showed some inhibitory effect (30%) against PL when tested at 30 µg/ml, and the results were statistically significant ($P < 0.05$) as per Figure 3.18. LLL EA and LLL MeOH extracts did not inhibit PL at the tested concentrations.

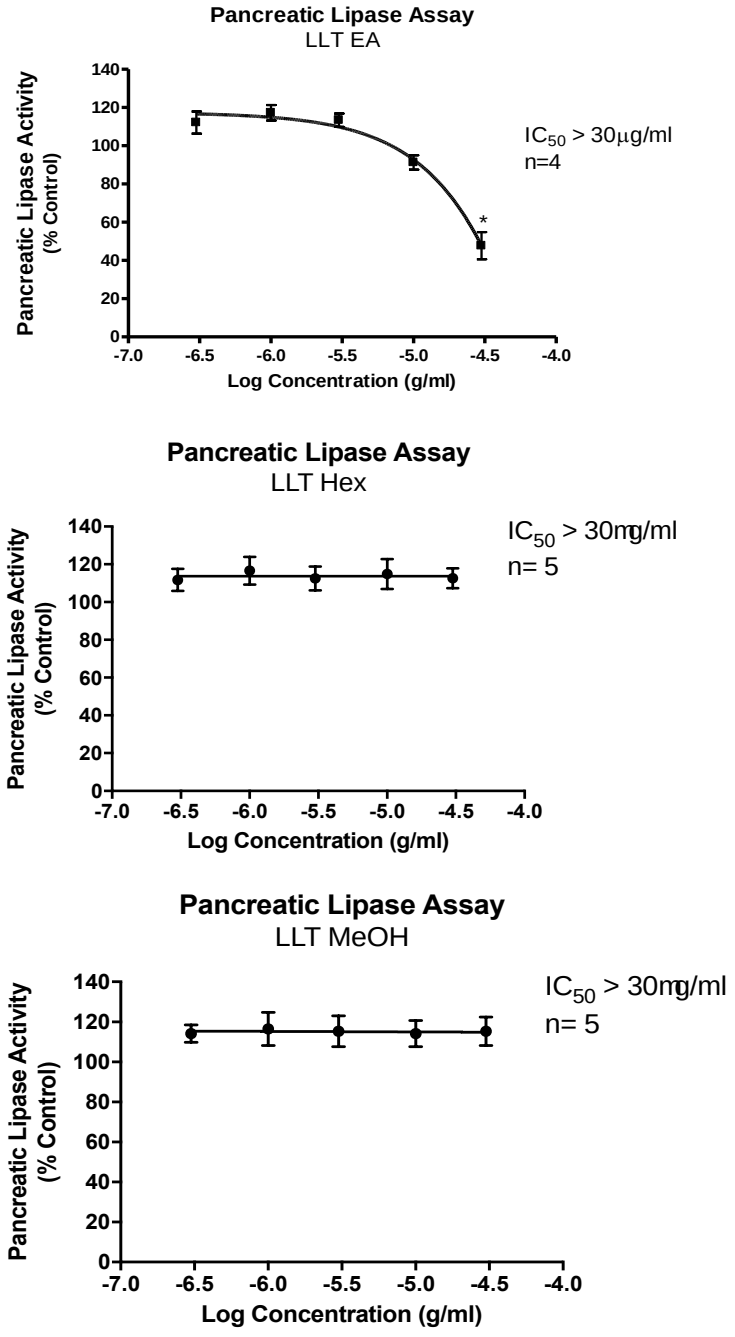

Figure 3. 16: The inhibitory effects of various concentrations of extracts of LL tubers on PL activity. Data was analysed using One-Way ANOVA with a Dunnet Post-Test. *P<0.05 vs control.

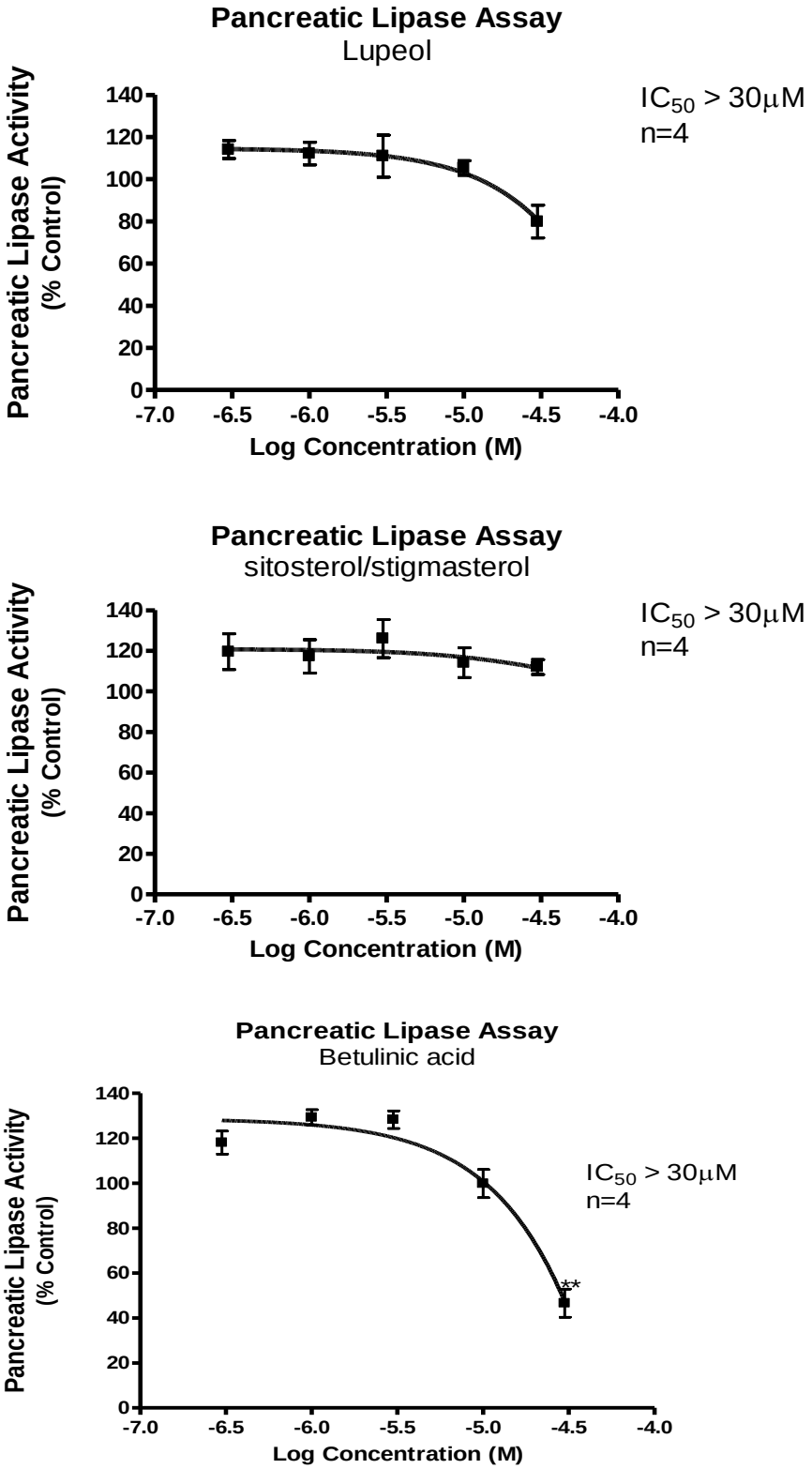

Figure 3. 17: The inhibitory effects of various concentrations of lupeol, mixture of sitosterol/stigmasterol and BA on PL activity. Data was analysed using One-Way ANOVA with a Dunnet Post-Test.

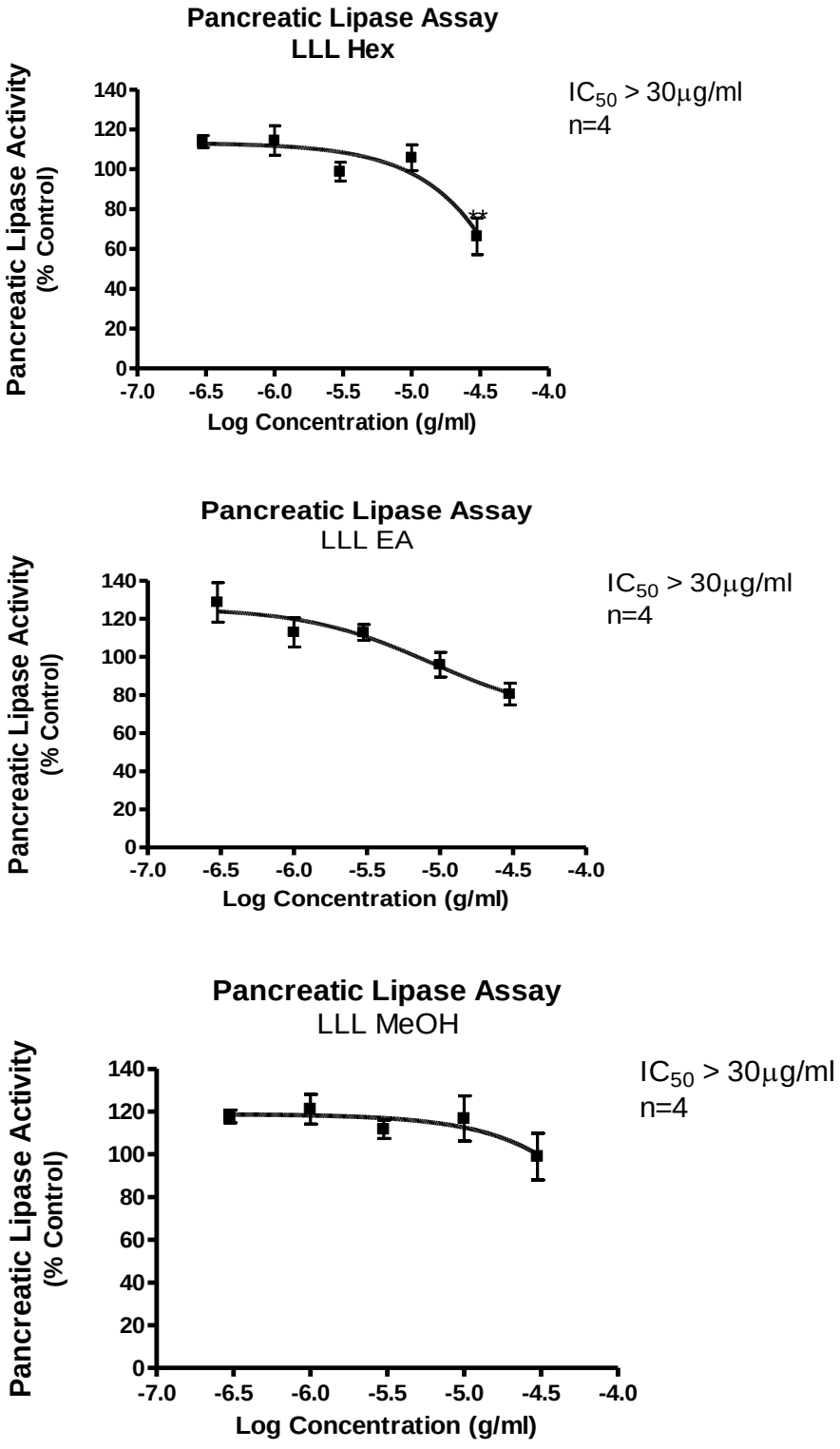

Figure 3. 18: The inhibitory effects of various concentrations of extracts of LL leaves on PL activity. Data was analysed using One-Way ANOVA with a Dunnet Post-Test. **P<0.01 vs control.

3.4.1.3.3. Summary of PL assay results

Three samples from LL extracts and isolated compounds showed PL inhibition, the % inhibition values are summarised in Table 3.3.

Table 3. 3: Summary of the activity of the LL extracts (30 µg/ml) and isolated compounds (30 µM) on PL. Red indicates inhibition of PL.

Part of LL	Sample ID	% Inhibition of PL
Tubers	LLT Hex	Inactive
	LLT EA	50
	LLT MeOH	Inactive
	BA	50
	Lupeol	Inactive
	sitosterol/stigmasterol	Inactive
Leaves	LLL Hex	30
	LLL EA	Inactive
	LLL MeOH	Inactive

3.4.1.4. PTP1B screening assay

In this screening assay, TFMS was used as a positive inhibitor for PTP 1B and strongly ($P < 0.05$) inhibited the activity of the enzyme with an IC_{50} of 5 µM (Figure 3.19).

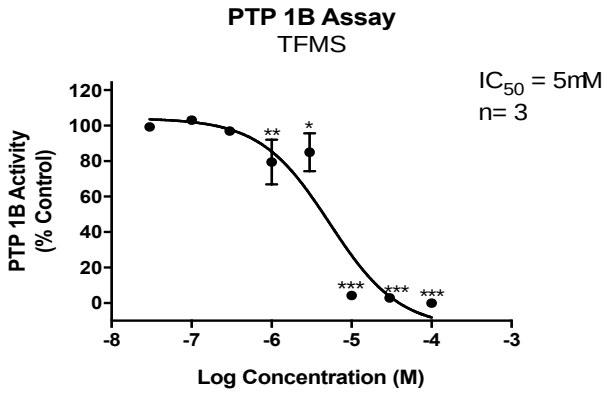

Figure 3. 19: The inhibitory effects of various concentrations of TFMS on PTP 1B activity. Data was analysed using One-Way ANOVA with a Dunnet Post-Test. ***P<0.001, **P<0.01, *P<0.05 vs control.

3.4.1.4.1. LL extracts and isolated compounds

All the extracts of the tubers and the leaves as well as the isolated compounds were inactive against PTP1B, the assay results are shown in Appendix 1.

3.4.1.5. DPPIV screening assay

All samples from LL were tested for their ability to inhibit DPPIV enzyme. P32/98, known DPPIV inhibitor, strongly ($P < 0.05$) inhibited DPPIV with an IC_{50} of 77.6 nM as shown in Figure 3.20.

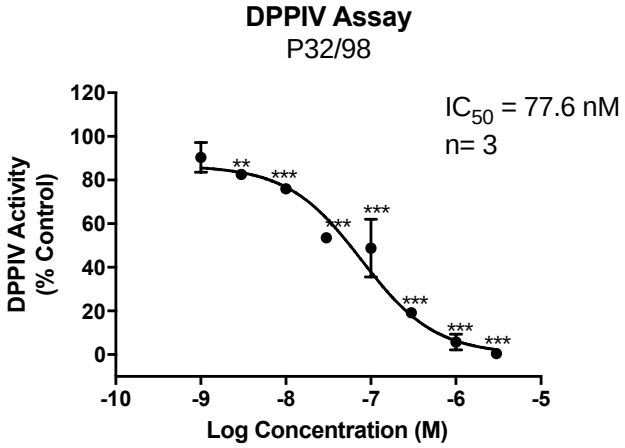

Figure 3. 20: The inhibitory effects of various concentrations of P32/98 on DPPIV activity. Data was analysed using One-Way ANOVA with a Dunnet Post-Test. ***P<0.001, **P<0.01 vs control.

3.4.1.5.1. LL tuber extracts and isolated compounds

LLT EA showed 20% reduction ($P < 0.05$) in DPPIV activity when tested at 30 µg/ml (Figure 3.21), while LLT MeOH was inactive against DPPIV at the tested concentrations, and 20% enzyme inhibition ($P < 0.05$) was obtained with LLT Hex extract at 30 µg/ml. None of the isolated compounds from LLT EA showed any positive results against DPPIV at the tested concentrations (Appendix 1).

3.4.1.5.2. LL extracts of the leaves

All LLL extracts showed 20% DPPIV inhibition at 30 µg/ml; results were statistically significant ($P < 0.05$) as per Figure 3.22.

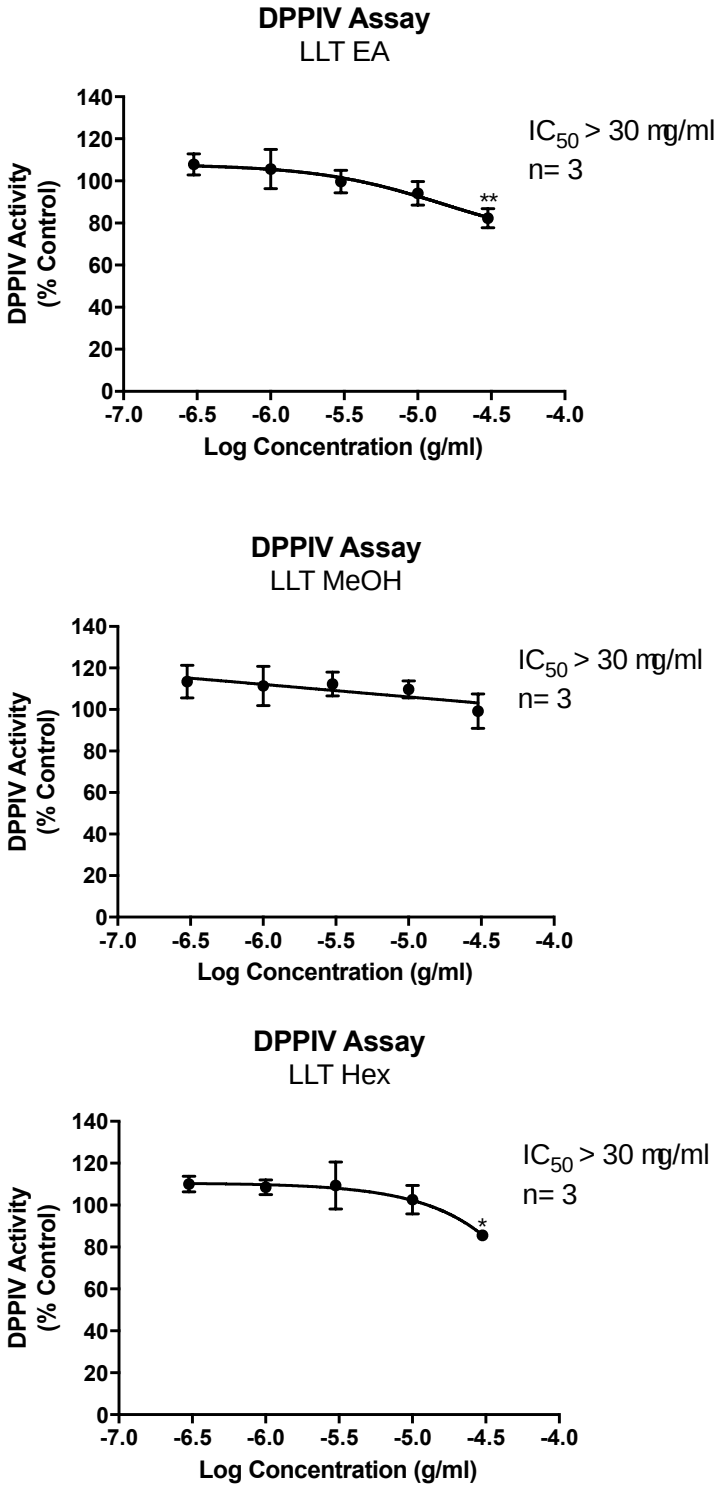

Figure 3. 21: The inhibitory effects of various concentrations of extracts of LL tubers on DPPIV activity. Data was analysed using One-Way ANOVA with a Dunnet Post-Test. **P<0.01, *P<0.05 vs control.

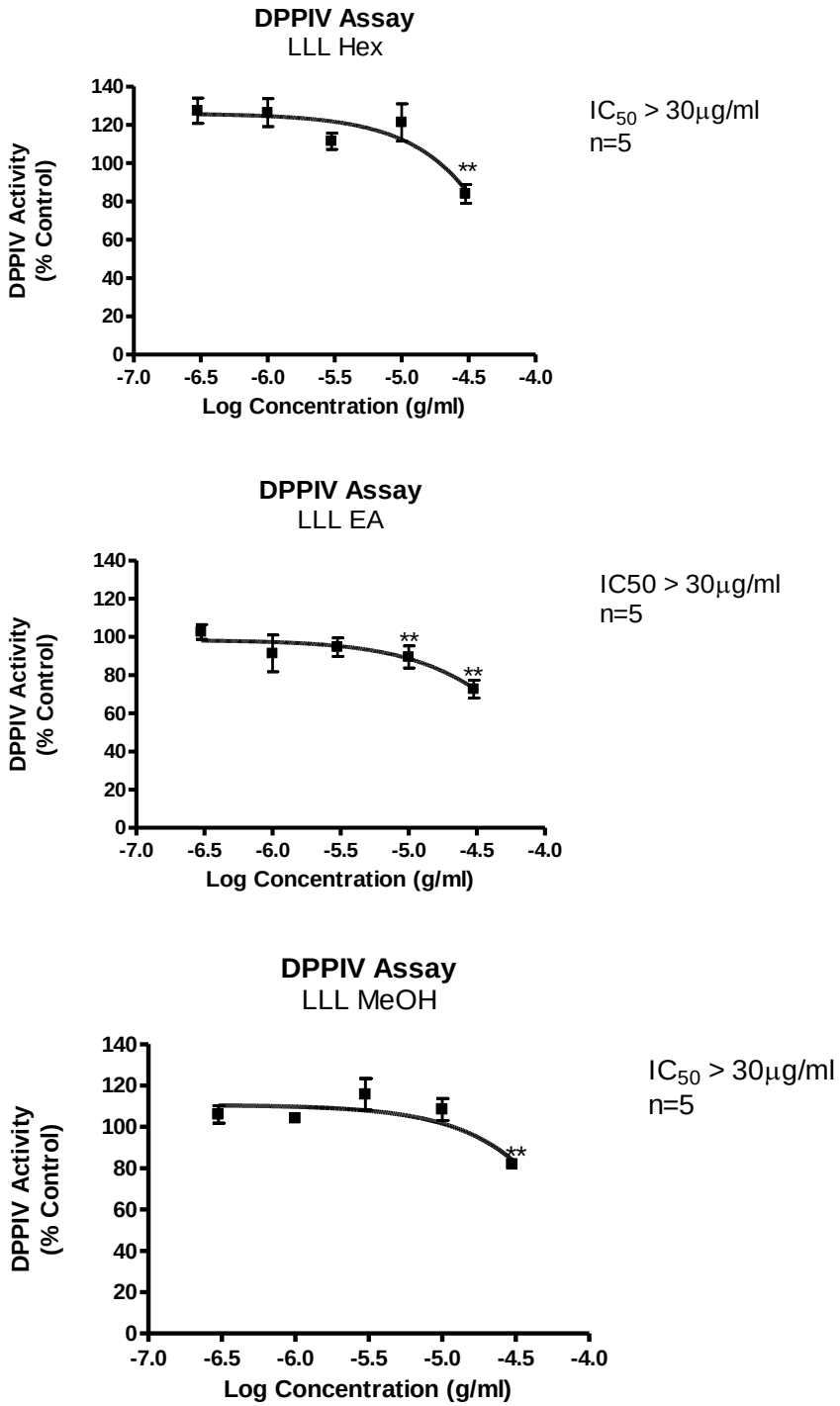

Figure 3. 22: The inhibitory effects of various concentrations of extracts of LL leaves on DPPIV activity. Data was analysed using One-Way ANOVA with a Dunnet Post-Test. **P<0.01 vs control.

3.4.2. Cell Viability: alamarBlue® Assay

3.4.2.1. Caco2 and HepG2 cells

All samples were tested for cytotoxic effects on Caco2 and HepG2 cells before carrying out the DPPIV inhibition assay in Caco2 cells and glucose uptake assay in HepG2 cells to ensure samples were not cytotoxic to the cells. Samples were tested at 30 µg/ml for extracts and 30 µM for isolates. All tested samples were not cytotoxic to Caco2 and HepG2 cells as shown in Figure 3.23.

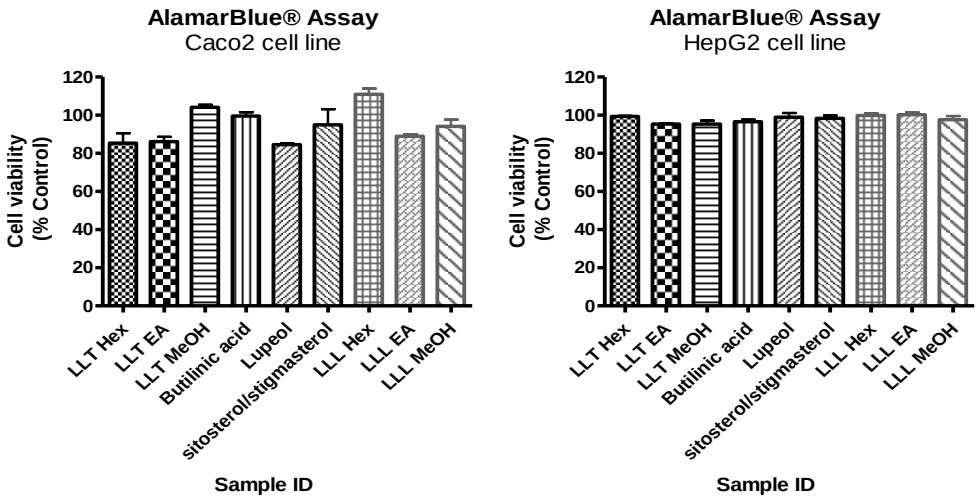

Figure 3. 23: The effect of LL extracts and isolated compounds on Caco2 and HepG2 cells. Data represents mean ± SEM, n=3.

3.4.3. DPPIV assay in Caco2 cells

3.4.3.1. LL extracts of tubers and leaves and the isolated compounds.

All LL extracts and isolated compounds were not capable of inhibiting the activity of DPPIV enzyme when tested at concentrations of 30 µg/ml for the extracts and 30 µM for the isolated compounds (Appendix 1).

3.4.5. Glucose Uptake-Glo™ in HepG2 cell line

2DG6P standard was used to ensure the assay was run at optimum performance, 2DG6P range of concentrations (30 µM to 0 µM) showed a curve with r^2 of 0.995 which indicates a good curve fit as shown in Figure 3.24.

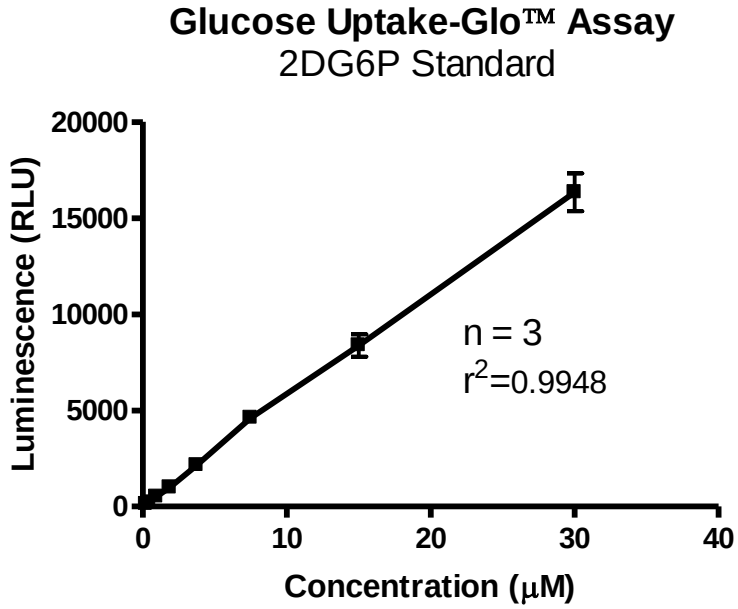

Figure 3. 24: Standard curve for 2DG6P used in the Glucose Uptake-Glo™ assay. Data represents mean ± SEM, n=3.

3.4.5.1. LL extracts and isolated compounds

The results obtained with LL extracts and isolated compounds are summarised in Figure 3.25. Insulin (100 nM) was used as a positive control and increased glucose uptake in HepG2 cells by 50% ($p<0.05$), whereas cytochalsin B (50 µM) was used as a known inhibitor of glucose transport and it caused 60% ($p<0.05$) reduction in glucose uptake. All tested concentrations were 30 µg/ml for extracts and 30 µM for isolated compounds. LLT Hex showed comparable results to insulin; it was the only tuber extract that increased glucose uptake by approximately 50% ($p<0.05$). LLL EA and LLL MeOH as well as the mixture of sitosterol/stigmasterol showed 30% reduction in glucose uptake and results were statistically significant ($p<0.05$). The other tested extracts and isolated compounds showed no effects ($P>0.05$) on glucose uptake at the tested concentrations.

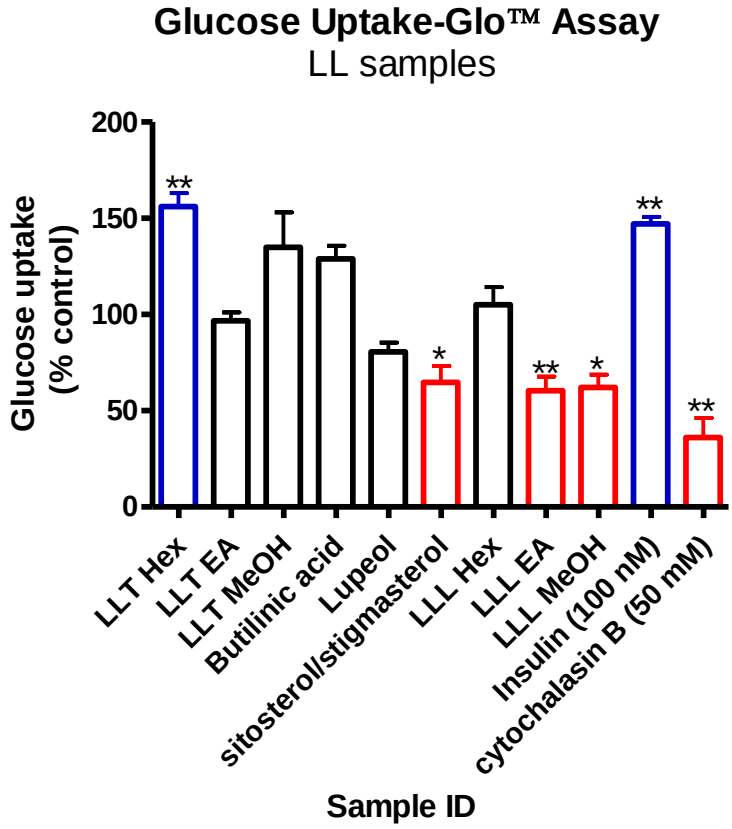

Figure 3. 25: The effects of LL extracts and isolated compounds on glucose uptake levels in HepG2 cell lines. Blue represents increased glucose uptake, red represents decreased glucose uptake and black represents unchanged in glucose uptake. Data represents mean ± SEM, n=3. **P<0.01, *P<0.05 vs control.

3.5. Discussion and Conclusions

Diabetes is a complex disease that involves complex signaling pathways. Therefore, LL extracts and isolated compounds were tested against five anti-diabetic assays, α-glucosidase, α-amylase, DPPIV, PTP 1B and PL assays, to assess the anti-diabetic effects in different pathways. All of the chosen assays are useful for high throughput screening (HTS).

3.5.1. Inhibitory effects of LL extracts and isolated compounds on α-glucosidase activity

α-glucosidase enzyme plays an important role in increasing postprandial hyperglycaemia, as it enhances carbohydrate digestion. Its critical role is in the

catalysis of monosaccharide cleavage, starting from disaccharides and oligosaccharides (Chen *et al.*, 2016). Therefore, α-glucosidase activity inhibition is preferred in diabetic patients to decrease postprandial hyperglycaemia. Currently, there are a number of effective α-glucosidase inhibitors on the market and these include acarbose, voglibose, and miglitol. Despite the effectiveness of these drugs, they are associated with a number of unpleasant side effects, including abdominal pain, liver disorders, diarrhoea and flatulence; such undesirable effects can lead to patient non-compliance (Peng *et al.*, 2016). As a consequence of this, there is a need to find new potent α-glucosidase inhibitors with fewer unwanted side effects. LL tubers and leaves were assessed for their ability to inhibit α-glucosidase, with acarbose as a positive control.

Acarbose confirmed the efficiency of the assay as it inhibited α-glucosidase activity with an IC_{50} of 380 µM, the IC_{50} is comparable with the ones obtained from the literature (180-500 µM) (Figueiredo-González *et al.*, 2016; Elya *et al.*, 2011; Habtemariam, 2011; Kang *et al.*, 2011). In this study, the tested samples were only considered active when the IC_{50} was $\leq$ 30 µg/ml for crude extracts or 30 µM for isolated compounds.

LLT Hex and LLT MeOH crude extracts were inactive against α-glucosidase. However, LLT EA extract showed strong α-glucosidase inhibition activity with an IC_{50} of 9.5 µg/ml. The LLT EA extract contains several compounds of which four were isolated (lupeol, a mixture of stigmasterol/sitosterol and BA) and tested against α-glucosidase. Lupeol and the stigmasterol/sitosterol mixture showed no activity in this assay. Ortiz-Andrade *et al.* studied the inhibitory effects of an MeOH extract of *Tournefortia hartwegiana* (METh) against α-glucosidase (Ortiz-Andrade *et al.*, 2007). Seven compounds were isolated from METh, and three of them were lupeol, stigmasterol and sitosterol. METh significantly inhibited α-glucosidase with an IC_{50} of 3.16 mg/ml, which is 100 times more than the highest concentration used for the LL extracts. This suggests that the concentration of compounds in METh is also much higher than that of the ones used in this study. The isolated compounds from METh were not tested against α-glucosidase and so it is not possible to relate the α-

glucosidase inhibition activity to lupeol, stigmasterol and sitosterol. In another study by Mbaze *et al.*, in which lupeol and a mixture of stigmasterol and sitosterol was isolated from *Fagara tessmannii* and subjected to α-glucosidase inhibition assay, none of the compounds showed inhibitory effects against α-glucosidase when tested at 800 µM, and this supports the findings obtained in the current research (Mbaze *et al.*, 2007). BA from LLT EA extract was a potent inhibitor of α-glucosidase activity with an IC_{50} of 5.5 µM. BA was almost twice more potent than its parent extract, LLT EA and 70 times stronger than acarbose in inhibiting α-glucosidase. Therefore, it is highly likely that LLT EA activity against α-glucosidase is due to the presence of BA. He *et al.* showed that BA isolated from the fruits *of Malus domestica* inhibited glucosidase activity with an IC_{50} of 14 µM, which is comparable to the findings in this study (He *et al.*, 2014). A study by Ding *et al.* showed that the mechanisms of action of BA on α-glucosidase was achieved by the formation of a BA-α-glucosidase complex (Ding *et al.*, 2018). BA was found to bind to the active side of α-glucosidase and therefore prevent the enzyme substrate binding and hence, the enzyme activity decreased.
For the first time, LL leaves were tested against α-glucosidase enzyme. LLL EA and LLL MeOH extracts of LL leaves were strong inhibitors of α-glucosidase with an IC_{50} of 0.58 µg/ml and 4.3 µg/ml, respectively. LLL Hex showed an $IC_{50} > 30$ µg/ml against α-glucosidase. More phytochemistry work needs to be performed on LLL MeOH and LLL EA extracts to find out the responsible compounds for the α-glucosidase inhibition activity. There are several classes and compounds which have been isolated and shown to possess α-glucosidase inhibition activity. Triterpenoids saponins isolated from the roots of *Gypsophila oldhamiana* (Luo *et al.*, 2008), alkaloids isolated from *Campanulaceae Lobelia* species (Ikeda *et al.*, 1999), quinones isolated from Himalayan *rhubarb Rheum* (Babu *et al.*, 2004) and flavonoids isolated from *Machilus philippinensis* (Lee *et al.*, 2008) have all shown α-glucosidase inhibition activity.

Inhibitors of α-glucosidase are not only beneficial for enhancing insulin release and lowering postprandial blood glucose, they are also hunger suppressants and satiety enhancers (Hao *et al.*, 2017). GLP-1 activity is prolonged by α-glucosidase inhibitors and this has been directly linked with delayed gastric emptying (DGE) which enhances satiety, reduces hunger and limits calorie intake (Lee *et al.*, 2002). Kaku *et al.* carried

out a randomised clinical trial on 20 healthy volunteers to investigate the anorexigenic effects of miglitol (MG), α-glucosidase inhibitor (Kaku *et al.*, 2012). The study looked at the effects of 50 mg MG on the levels of GLP-1, peptide YY (PYY) and ghrelin (appetite inducer) and simultaneously determined the appetite scores using visual analogue scales (VAS) over a 3h period following the ingestion of a 592 kcal cookie. MG (50 mg) was administered to 12 individuals three times a day for one week and both hormone levels and VAS were recorded. GLP-1 and PYY levels were significantly enhanced by MG treatment, whereas ghrelin level was suppressed. Moreover, MG treatment suppressed appetite and enhanced satiety as per VAS and the gastric emptying rate was inhibited following the cookie ingestion. These findings correlate with the historical use and anecdotal reports of LL tubers as appetite suppressants which seems to be mediated by their ability to inhibit α-glucosidase and prolong GLP-1 activity, which increases the feeling of satiety.

In summary, the leaves and tubers of LL contain chemical constituents capable of strongly inhibiting the α-glucosidase enzyme. Consequently, LL showed promising results to be a potential new source for anti-diabetic agents through the inhibition of α-glucosidase. Therefore, LL extracts and isolated compounds were then tested against α-amylase, a target for T2DM treatment.

3.5.2. Inhibitory effects of LL extracts and isolated compounds on α-amylase activity

The enzyme α-amylase is similar to α-glucosidase, it breaks down disaccharides and oligosaccharides into monosaccharides in the intestines that are absorbed and increase postprandial hyperglycaemia (Sales *et al.*, 2012).

The current study investigated the effects of the leaves and tubers of LL as possible α-amylase inhibitors, following their potent inhibition of α-glucosidase. Acarbose was used as a positive control and inhibited the enzyme activity with an IC_{50} of 1.2 mM. None of the LL extracts or the isolated compounds were active against α-amylase. BA did not inhibit α-amylase which confirms the study by Noguera-Artiaga *et al.* (2018) in which pistachio kernels (*Pistacia vera L.*) were found to have a high content of BA,

but did not inhibit α-amylase. Moreover, lupeol isolated from *Phyllanthus amarus* was tested at 100 µM and showed no inhibition against α-amylase. This is consistent with the findings of the current study (Yonemoto *et al.*, 2014). Despite the fact that α-amylase and α-glucosidase have similar activity on carbohydrate hydrolysis, several plants were found to be potent inhibitors to one but not to the other. Yilmazer-Musa *et al.* showed that green tea extract, Teavigo® and white tea extract were potent α-glucosidase inhibitors with IC_{50} values < 2.5 µg/ml, but that they were inactive against α-amylase and showed IC_{50} values > 30 µg/ml (Yilmazer-Musa *et al.*, 2012). This trend was seen with LLT and LLL extracts and BA in the current study.

3.5.3. Inhibitory effects of LL extracts and isolated compounds on PL activity

Approximately 95% of dietary fats are consumed in the form of triglycerides which are then initially hydrolysed in the stomach by gastric lipase (Gupta, 2019). Triglyceride hydrolysis is further continued in the duodenum by synergistic actions of gastric and colipase-dependent PL. This continued hydrolysis leads to monoglycerides as well as FFA formation. Enterocytes absorb FFA and start synthesising new triglycerides, which are distributed into various body organs by lipoproteins and chylomicrons, in particular following meal consumption (Sellami *et al.*, 2017). The majority of dietary fats (50-70%) are hydrolysed by PL. Therefore, agents inhibiting PL can help in managing obesity and T2DM. This study tested extracts of LL leaves and tubers as well as the isolated compounds against PL. Orlistat, was used as a positive control and gave an IC_{50} of 0.23 µM. LLT EA extract at 30 µg/ml and BA at 30 µM showed 50% inhibition of PL activity; the results were statistically significant. Moreover, LLL Hex extracts from the leaves showed 30% enzyme inhibition at 30 µg/ml which was statistically significant. BA in this study showed the highest inhibition for PL among all the tested samples, the anti-obesity activity of BA was published by several researchers. Kim *et al.* investigated the anti-obesity activity of BA following the oral administration of lipid emulsion in rats (Kim *et al.*, 2012). BA was found to inhibit PL in a dose dependent manner, with an IC_{50} of 21 µM. Moreover, elevation of triglyceride plasma levels was inhibited by BA, 2 h following the administration of a lipid emulsion. In addition to this, BA administration to 3T3L1 adipocytes inhibited the development of adipogenesis confirming its anti-obesity

activity. Therefore, BA is one of the compounds responsible for PL inhibition by LL. However, more fractionation for LL extracts and in particular LLL Hex is required to identify other lipase inhibitors. To summarise, these results support the use of LL for the management of obesity and T2DM. Future work would involve assessing the LL extracts *in vivo* using diabetic/ obese rats such as Zucker rats and monitor the effects on the BW and food consumption.

3.5.4. Inhibitory effects of LL extracts and isolated compounds on PTP 1B

PTP 1B is induced by inflammation - it is known to negatively regulate insulin signaling pathways (Zabolotny *et al.*, 2008). PTP 1B inhibitors can reduce postprandial glucose levels and enhance insulin release (de Moura *et al.*, 2013). LLT and LLL extracts were tested against PTP 1B in the presence of catalase enzyme. As the assay buffer contained dithioreitol, it is known that interaction between natural products and dithioreitol can lead to ROS and particularly hydrogen peroxide which can generate false positives. Catalase was included in the assay buffer to eliminate ROS formation. TFMS was used as a positive control which inhibited PTP 1B and gave an IC_{50} of 5 µM. However, none of the tested LL extracts or isolated compounds showed PTP 1B inhibition at the tested concentrations and this might indicate that the LL anti-diabetic mechanism of action does not involve PTP 1B inhibition.

3.5.5. Inhibitory effects of LL extracts and isolated compounds on DPPIV

Other approaches to decrease postprandial glucose levels include the prolongation of incretins such as GLP-1 and GIP. These two incretins act as insulinotropic gut hormones, involved in blood glucose regulation. Following a meal ingestion, GLP-1 and GIP trigger insulin secretion and inhibit glucagon secretion which result in decreased BG (Lutz *et al.*, 2014). DPPIV is an incretin inhibitor, and therefore finding agents inhibiting DPPIV can be beneficial for the management of T2DM.

Extracts of LL tubers and leaves as well as isolated compounds were studied in a DPPIV assay. P32/98 was used as a positive DPPIV inhibitor and showed an IC_{50} of 77.6 nM. The samples that showed significant activity were the LLT EA, LLT Hex,

and all the extracts of LL leaves. LLT EA was found to be a potent α-glucosidase inhibitor and showed some inhibition against DPPIV. The inhibition of these two enzymes is linked with increasing GLP-1 which is known to increase satiety and suppress appetite. However, this activity was considered weak as all these samples showed no more than 20% inhibition and the IC_{50} was > 30 µg/ml. As this was performed on an isolated enzyme assay, this was followed-up in Caco2 cells which are known to express DPPIV. However, no effect on Caco2 DPPIV was observed in all the tested extracts and isolated compounds. To summarise, extracts of LL in this study did not show strong DPPIV inhibition, and therefore LL might have anti-diabetic effects by a different mechanism of action.

From all the five anti-diabetic and anti-obesity assays used to assess the biological activity of the extracts of LL tubers and leaves as well as the isolated compounds, LL possesses some potential anti-diabetic and anti-obesity effects particularly through the inhibition of α-glucosidase and PL enzymes. The selectivity of LL to α-glucosidase might be beneficial for diabetic patients. The selectivity of drugs is associated with high efficacy and less side effects which therefore can improve patient compliance (Hung and Chen, 2014). Hence, the possibility of LL extracts and isolated compounds to enhance glucose uptake in the HepG2 cell line was investigated.

3.5.6. Effects of LL extracts and isolated compounds on glucose uptake in HepG2 cells

Glucose uptake in hepatic cells (HepG2) was used as a follow-up study for the extracts of tubers and leaves of LL. The HepG2 cell line was chosen in this experiment because such cells possess glucose transporters. Moreover, HepG2 cells do not need to be differentiated and so are less time consuming when compared to other cells such as adipocytes (3T3-L1 cells) which requires a differentiation process (Arimochi *et al.*, 2016). Insulin (100 nM) was used as a positive control which increased glucose uptake by 50%; whereas cytochlastin B (50 µM) was used as it is known to inhibit glucose transport and reduce glucose uptake by approximately 60%. LLT Hex produced comparable results to that of insulin which was statistically significant, while LLT EA and lupeol showed results similar to the control (untreated cells). LLT MeOH extract

and BA increased glucose uptake by 25%, but the results were statistically insignificant. The mixture of sitosterol and stigmasterol decreased glucose uptake by 30% ($p<0.05$). LLL Hex extract was similar to the control, whereas LLL EA and LLL MeOH extracts decreased glucose uptake by approximately 30 % and the results were statistically significant.

A number of discussion points emerge from the results obtained in this assay. To start with, the LLT Hex enhanced glucose uptake in HepG2 cells, and this extract showed slight inhibition in the DPPIV assay, confirming the possibility of it acting as a potential anti-diabetic agent. Secondly, samples which showed no or a slight increase in glucose uptake might be beneficial for management of T2DM, but by different mechanisms. To illustrate this, LLT EA extract and BA were potent inhibitors for α-glucosidase and did not increase glucose uptake in HepG2 cells. This might mean such samples act as anti-diabetics by inhibiting enzymes that are responsible for breaking down carbohydrates to smaller molecules such as glucose, and not by enhancing glucose uptake into cells. Samples which reduced glucose uptake in HepG2 (stigmasterol/sitosterol, LLL EA, and LLL MeOH), might act as anti-diabetic agents by different mechanisms. To make this clear, LLL EA, and LLL MeOH were potent inhibitors of α-glucosidase, but did not enhance glucose uptake in HepG2. Lastly, the action of LL samples in HepG2 cells might differ when tested in other cells. Therefore, it is recommended that this test would be repeated using pancreatic, skeletal muscles and adipocyte cells as LL extracts might be more selective to specific cells.

To conclude, from the findings obtained in this chapter, LLT and LLL extracts possess anti-diabetic activity by the inhibition of α-glucosidase. BA and LLT EA extract were found to be strong α-glucosidase inhibitors. Moreover, LLT and LLL extracts inhibited PL, which suggest that they might be beneficial for T2DM and obesity. Lastly, the LLT Hex extract enhanced glucose uptake in HepG2 cells and showed a similar response to that of insulin. These results led to further investigation regarding the possibility of the plant containing anti-inflammatory and anti-oxidant constituents which could also be beneficial in managing diabetes as detailed in Chapter 4.

Chapter 4

4. The potential anti-oxidant and anti-inflammatory activity of *L. linifolius*

4.1. Introduction

The link between T1DM and inflammation is established and well-reviewed (Bending *et al.*, 2012; Gouda *et al.*, 2018; Fatima *et al.*, 2016). However, relationships between T2DM and inflammation are quite a recent concept (Tsalamandris *et al.*, 2019). The concept that links inflammation and metabolic conditions, including obesity and insulin resistance, was first mooted in 1993 by Hotamisligil *et al.* Their publication showed that the pro-inflammatory cytokine TNFα was highly expressed in the adipose tissues of obese animals, and this TNFα expression was linked to increased insulin resistance (Hotamisligil *et al.*, 1993). These animals showed improved insulin resistance when the TNFα was neutralised using soluble TNFα receptor. These observations gave the first link between insulin resistance and an increased level of a pro-inflammatory cytokine (Dandona *et al.*, 2004). T2DM and obesity are considered to be risk factors for developing ischemic heart disease and premature atherosclerosis (Imai *et al.*, 2013). Both of these conditions are now linked to inflammation and oxidative stress (Sjoholm and Nystrom, 2006). Therefore, following positive anti-diabetic findings from Chapter 3, tuber and leaf extracts of LL were assessed in inflammatory and oxidative stress assays. These assays are introduced and described below:

4.1.1. Anti-inflammatory

4.1.1.1. NF-ƙB luciferase assay

NF-ƙB is a protein that consists of a number of Rel family transcriptional factors such as p50, p65, and c-Rel (Dąbek *et al.*, 2010, Bolshakova *et al.*, 2013). These factors are known to be stimulated by stress, immune, and inflammatory responses. In normal situations where cells are unstimulated, NF-ƙB is inhibited by a cytoplasmic inhibitor of kappa B (IƙB) proteins (Giridharan and Srinivasan, 2018). Activation of IƙB kinase (IKK) by pro-inflammatory cytokines, LPS, and growth factors lead to IƙB phosphorylation to cause it to be degraded (Giridharan and Srinivasan, 2018; Uehling

and Harris, 2015). Degradation of IκB results in freeing NF-κB complexes and causes them to translocate into the nucleus where they bind to the NF-κB DNA response elements and therefore transcriptional factors are induced (Lawrence, 2009). Cells can be transfected with a NF-κB luciferase reporter vector. Once NF-κB is activated, this vector is bound to the NF-κB and luciferase will be detected by luminescence at 961nm wavelength. Therefore, anti-inflammatory agents show low luminescence readings while inflammatory agents show high luminescence readings.

4.1.2. Anti-oxidant assays

4.1.2.1. 2,2-Diphenyl-1-picrylhydrazyl (DPPH) Assay

The DPPH assay is a widely used anti-oxidant assay in natural product research due to its simplicity and sensitivity (Aqil *et al.*, 2014). The basic principle of the assay is the fact that anti-oxidant reagents are hydrogen donors. DPPH free radical (DPPH●) is a stable free radical that is available commercially. DPPH● is a purple coloured radical that accepts hydrogen from anti-oxidant materials to form DPPH that is yellow in colour (Figure 4.1) (Kedare and Singh, 2011). DPPH● has its highest absorption level when at 517nm and therefore the anti-oxidant activity can be detected using optical density at 517nm wavelength (Akar *et al.*, 2017). Generally, samples and DPPH are incubated in the dark for 20 min at room temperature before being read (OD 517nm). To sum up, anti-oxidant samples turn the DPPH colour from purple to yellow and decrease the absorbance at 517nm.

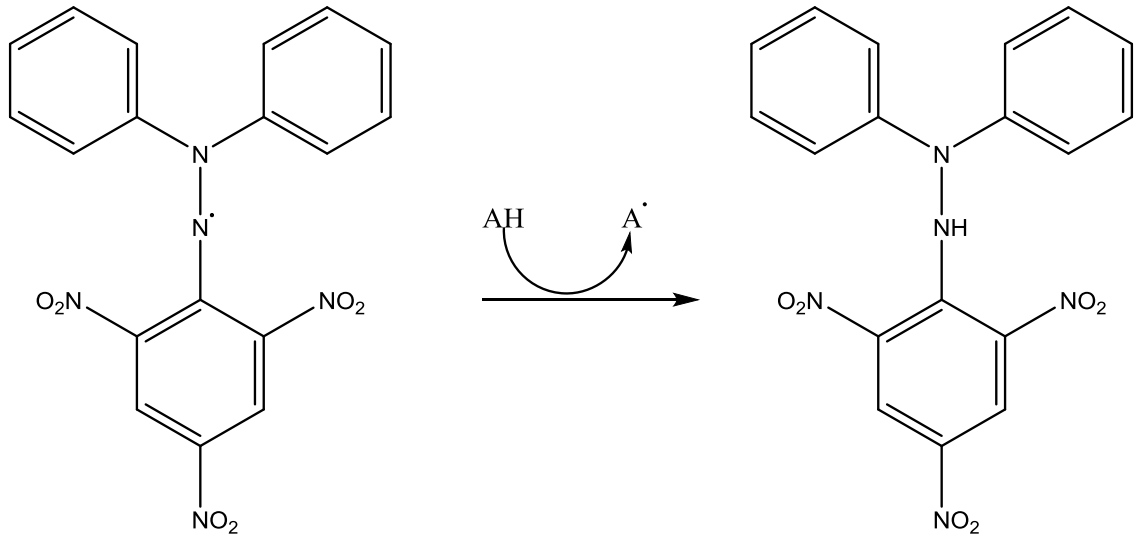

Oxidised DPPH
(purple)

Reduced DPPH
(yellow)

Figure 4. 1: Unstable purple DPPH is reduced by anti-oxidant agents to yield a yellow DPPH colour.

4.1.2.2. DCFDA / H2DCFDA - Cellular Reactive Oxygen Species Detection Assay

This assay uses 2',7'–dichlorofluorescein diacetate (DCFDA or H2DCFDA) which is a cell permeable reagent (Eruslanov and Kusmartsev, 2010). DCFDA is a dye that measures ROS activity such as hydroxyl and peroxyl free radicals in cells (Wojtala *et al.*, 2014). DCFDA enters the cells by diffusion and cellular esterases deacetylate it to a non-fluorescent reagent (Oukarroum *et al.*, 2013). This compound is oxidised by ROS to form 2', 7'–dichlorofluorescein (DCF) which is a highly fluorescent agent that can be detected by fluorescence spectroscopy at an excitation wavelength of 485nm and an emission wavelength of 535nm (Wang *et al.*, 2019). ROS scavenging compounds show low fluorescence readings, while ROS generating compounds show high fluorescence readings.

4.1.2.3. Glutathione (GSH)

Glutathione (GSH) is a tripeptide molecule that consists of three amino acids: glutamic acid, cysteine, and glycine (Bachhawat and Yadav, 2018). The thiol group in the cysteine amino acid gives the molecule its importance (De Flora *et al.*, 2018). This group acts as an antioxidant and plays a fundamental role in the detoxification process of toxins. GSH exists in two forms, the oxidised form (GSSG) and the reduced form (GSH) (Figure 4.2) (Winterbourn, 2019). In normal healthy cells, the ratio of GSH concentration to GSSG concentration is greater than 10 (Zitka *et al.*, 2012). Glutathione reductase (GSR) is the enzyme responsible for converting GSSG to the GSH in the presence of nicotinamide adenine dinucleotide phosphate (NADPH) (see the equation below) (Bradshaw, 2019).

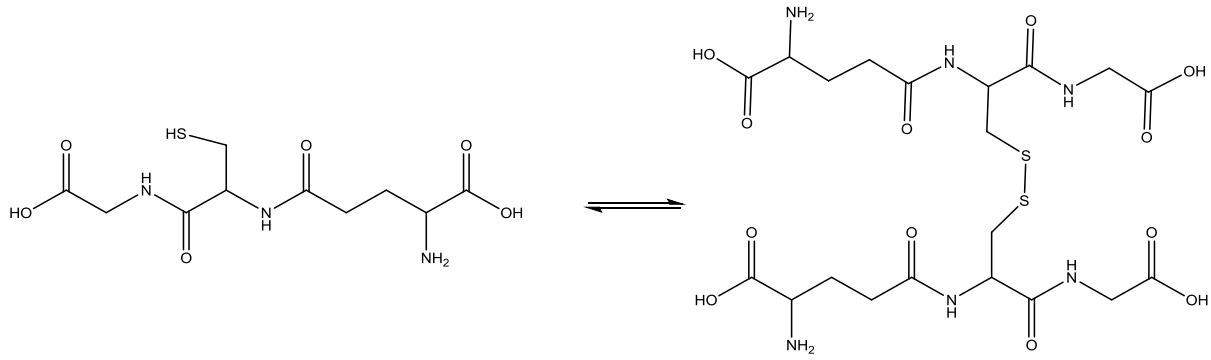

Glutathionr reduced form (GSH)

Glutathione oxidised form (GSSG)

Figure 4. 2: The structure of the two forms of GSH.

The following equations represent the redox states of GSH:

$$GSSG + NADPH + H+ \xrightarrow[\text{reductase}]{\text{Glutathione}} 2GSH + NADP+$$

$$2GSH + H2O2 \xrightarrow[\text{peroxidase}]{\text{Glutathione}} GSSG + 2\,H2O$$

GSH is one of the most abundant low molecular weight molecules in the body. The cytosol, the mitochondria, and the nucleus are the pools of GSH. The GSH concentrations can vary from 0.1 mM to 5 mM depending on the cell types. The highest concentrations (5 mM) are seen in the liver, which can be justified by the fact that the detoxification mechanisms occur mainly in the hepatocytes (Chen *et al.*, 2013).

In this research, LL extracts and isolated compounds were subjected to testing for their potential for being anti-oxidant and anti-inflammatory agents.

4.2. Aims and Objectives

This chapter aims to evaluate the potential of LL extracts and isolated compounds to possess anti-inflammatory and anti-oxidant properties. These will be achieved by:

1. Testing the extracts and isolated compounds on their ability to protect the L929 cell line (mouse fibroblast cells commonly used for anti-inflammatory studies), from cytotoxicity following exposure to TNFα.
2. Testing the extracts and isolated compounds on their ability to inhibit NF-ƙB release (pro-inflammatory factor) in the NCTC cell line (human skin cells transfected with a NF-ƙB luciferase reporter vector).
3. Evaluating the inhibitory action of LLT and LLL extracts and isolated compounds on DPPH activity.
4. Testing the ability of LLT and LLL extracts and isolated compounds to generate/inhibit ROS using the DCF assay in various cells, SHSY-5Y (commonly used to investigate diabetic neuropathy caused by ROS), HepG2 (liver), and Panc1 (pancreas) cells.
5. Studying the effects of LL extracts and isolated compounds on GSH levels in the HepG2 cell line.

4.3. Methods

4.3.1. Anti-inflammatory assays in cells

Cells were incubated and grown at 37°C with 5% CO2 and 100% humidity. The L929 cell line was cultured in DMEM culture media supplemented with 10% (v/v) FBS, 1% penicillin-streptomycin, and 1% L-glutamine. The NCTC cell line was cultured in M199 culture media which contained 10% (v/v) FBS, 1% penicillin-streptomycin, and 1% L-glutamine.

4.3.1.1. alamarBlue® Assay

Cytotoxicity assays were carried out to ensure the plant samples were not cytotoxic to the cells prior to carrying out the anti-inflammatory assays. Cells were seeded using 96-well clear plates at $1x10^5$ cells/ml, and $2x10^5$ cells/ml for L929 and NCTC cell lines, respectively and an alamarBlue® cell viability assay was carried out as per section 3.3.2.2.

4.3.1.2. TNFα assay in L929 cell line

On day 1 of the assay, L929 cells were seeded in a 96-well clear plate at a seeding density of $1x10^4$ cells/well, 75 µl per well. Seeded plates were incubated overnight in a humidified incubator at 37°C with 5% CO_2. On day 2, 25 µl of media was removed from the plate and replaced with 25 µl test agent. All test agents were tested at 30 µg/ml or 30 µM. The plate was then incubated for 30 min in a humidified incubator at 37°C with 5% CO_2. Next, 12.5 µl of 10 µM Actinomycin D was added to all wells containing samples including wells A1-D1, E12-H12. The plate was then incubated for a further 30 min at 37°C before 12.5 µl of 80 µM TNFα being added to all wells containing samples and wells E1-H1, E12-H12. Then, the plate was incubated overnight as before. On day 3, 10 µl of alamarBlue® was added to all wells, and the plate was incubated for 5 h at 37˚C as before. At the end of this experiment, the plate was read in fluorescence mode (ex 560, em590) on a M5 Spectramax Plate Reader using Softmax Pro software.

4.3.1.3. NF-ƙB Luciferase assay in NCTC cell line

On day 1, NCTC cells were seeded at $5x10^4$ cells/well in a volume of 200 µl/well using 96-well black clear bottom plates. The plates were seeded using 10% (v/v) FBS in M199 medium and incubated for 48 h in a humidified incubator at 37°C with 5% CO_2. On Day 3, media from all wells was removed and replaced with 50 µl of phenol red free DMEM (without FBS) and incubated for 30 min. In the meantime, samples were prepared using phenol red free DMEM containing 0.75 ng/ml TNFα. MG132 (a proteasome inhibitor that blocks TNFα activity), was used as a positive control whilst media with no TNFα was used as a negative control/background. DMSO (solvent control) was tested as for the samples. Samples and DMSO were tested at 30 µM for pure samples and 30 µg/ml for non-pure samples. Fifty µl of samples/DMSO/MG132 were added to the plate and incubated for 4 h at 37°C. Then, all media were removed and 50 µl of 1:1 Bright-Glo: DMEM was added to each well. The plate was covered with foil and kept at room temperature (15-25°C) for 10 min in the dark. The plate was then read using luminescence on a M5 Spectramax Plate Reader using Softmax Pro software.

4.3.2. Anti-oxidant assays

4.3.2.1. DPPH assay

4.3.2.1.1. DPPH preparation

DPPH was stored at 4°C until used. A stock concentration of 10 mM was made by dissolving 7.98 mg of DPPH in 2 ml ethanol. The working DPPH solution concentration was 200 µM and therefore the solution was prepared at 400µM as it was diluted twice in the assay plate. For an assay plate, 60 µl of the stock was added to 3ml ethanol.

4.3.2.1.2. Preparation of Samples

Plant extracts were prepared at 30 µg/ml and isolated compounds were prepared at 30 µM.

4.3.2.1.3. Standard/inhibitor preparation

Ascorbic acid was used as a positive control as it is a known anti-oxidant (Baba and Malik, 2015). The displacement curve of ascorbic acid was obtained by using a range of ascorbic acid concentrations from 100 µM to 30 nM.

4.3.2.1.4. Assay assembly

The assay was performed in a 96-well half-area clear flat bottom plate. Twenty µl of ascorbic acid or 20 µl of sample were added to wells. Then, 20 µl of DPPH was added to all wells and the plate was covered with foil and incubated for 20 min at room temperature. Optical density (OD) was read at a wavelength of 512 nm on a M5 Spectramax Plate Reader using Softmax Pro software. The percent inhibition of DPPH was calculated as follows:

$$\%\ DPPH\ inhibition = \frac{(OD\ control - OD\ sample)}{OD\ control}\ X\ 100$$

4.3.2.2. DCFDA assay on SHSY-5Y, Panc1, and HepG2 cells

4.3.2.2.1. Cell culture

All cells were cultured in DMEM culture media supplemented with 10% (v/v) FBS, 1% penicillin-streptomycin, and 1% L-glutamine.

4.3.2.2.2. AlamarBlue® Assay

Cytotoxicity assays were carried out to ensure that the samples were not cytotoxic to the cell lines prior to performing the DCFH-DA and GSH-Glo™ assays. Cells were

seeded using 96-well clear plates at $2x10^5$ cells/ml, 75 µl per well, before performing the alamarBlue® cell viability assay as per section 3.3.2.2.

4.3.2.3. DCFDA assay in SHSY-5Y, HepG2, and Panc1 cell lines

On day 1, SH-SY5Y, HepG2, and Panc1 cells were seeded at 1.5x105 cells/well in a volume of 50µl/well using half-area 96-well black clear bottom plates and placed in a humidified incubator at 37°C with 5% CO_2. On Day 2, media from all cells were removed and 50 µl of phenol red free HBSS (containing 10% FBS) was used to wash the cells once. Then, 50 µl of 10 µM DCFH-DA was added to wells A1-H11, and 50µl of phenol red free HBSS was added to column 12 (wells A12-H12) and then the plate was placed in a humidified incubator at 37°C with 5% CO_2 for 30 min.

In the meantime, samples were prepared using FBS phenol red free HBSS (containing 10% v/v FBS) at concentrations of 30 µg/ml for non-pure samples or 30 µM for pure samples. Following the DCFH-DA incubation, DCFH-DA was removed and cells were washed once with 50 µl of phenol red free HBSS (containing 10% v/v FBS). Then, 45µl of samples were added to wells A2-H11, 45µl buffer was added to wells E1-H1, and 50 µl buffer was added to wells A1-D1; the plate was incubated in a humidified incubator at 37°C with 5% CO_2 for 40 min.

Then, 5µl of 1mM of t-BuOOH was added to wells E1-H1 and A2-H11 and the plate was incubated for 30 min in a humidified incubator at 37°C with 5% CO_2. The plate was then read at fluorescence (ex485nm/em535nm) on a M5 Spectramax Plate Reader using Softmax Pro software.

4.3.2.4. GSH-Glo™

The assay was carried out as per the manufacturer's instructions. HepG2 cells were seeded in half-area black plates with a clear bottom at 1 x 10^4 cells/well (50 µl/well) and were allowed to adhere overnight in a humidified incubator at 37°C with 5% CO_2. The next day, samples were prepared as 60 µg/ml or 60 µM as they would be diluted 1:1 with cells and give a final sample concentration as 30 µg/ml or 30 µM. The samples

were incubated with the cells for a further 5 h. As the HepG2 cells were plated using DMEM which contains serum and phenol red, which can interfere with the assays, the media had to be completely removed before the next step. Then, 50 µl of GSH-Glo™ reagent 1X was added to all wells. The plate was incubated at room temperature for 30 min after being shaken for 1 min using a plate-shaker. Fifty µl of Luciferin Detection Reagent was added to all wells. The plate was incubated at room temperature for 15 min after being shaken for 1 min using a plate-shaker. Luminescence with an integration time of 0.5 seconds/well was read on a M5 Spectramax Plate Reader using Softmax Pro software.

4.4. Results

4.4.1. Anti-inflammatory assays

4.4.1.1. AlamarBlue® Assay

Cytotoxicity testing using an alamarBlue® cell viability assay was carried out on all samples prior to performing the TNFα and NF-ƙB luciferase assays in L929 and NCTC cells. All samples were non-cytotoxic to L929 and NCTC cell lines at the tested concentrations (30 µg/ml for extracts and 30 µM for isolated compounds, Figure 4.3) and therefore these were the top concentrations used in the TNFα and NF-ƙB luciferase assays.

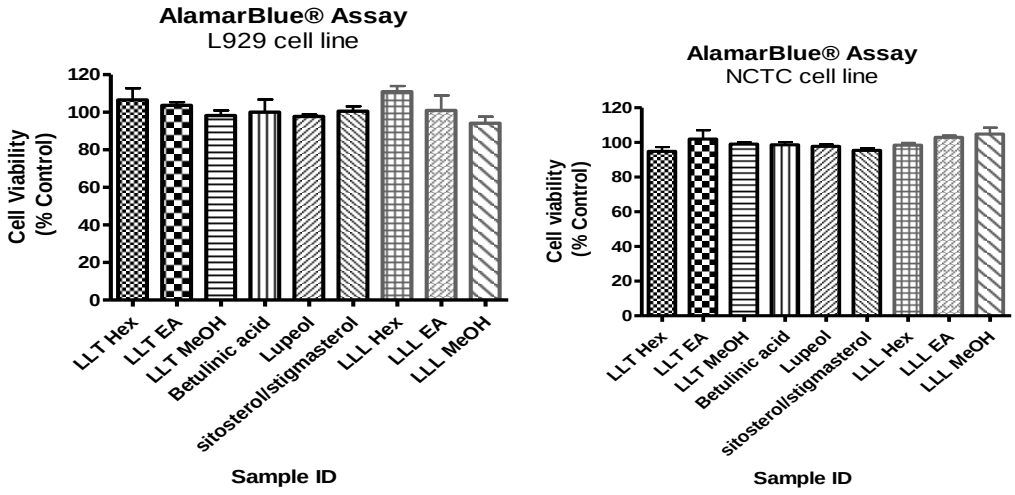

Figure 4. 3: The effect of LL extracts and isolated compounds on the L929 and NCTC cells. Data represents mean ± SEM, n=3.

4.4.1.2. TNFα assay

All extracts as well as the isolated compounds were tested for their ability to protect the L929 cell line from the cytotoxic effects of TNFα (10 µM causes 50% cell death). LLT and LLL extracts as well as the isolated compounds showed at least 90% cell protection ($P < 0.01$) against TNFα cytotoxicity, BA was the most protective sample at 110% as shown in Figure 4. 4.

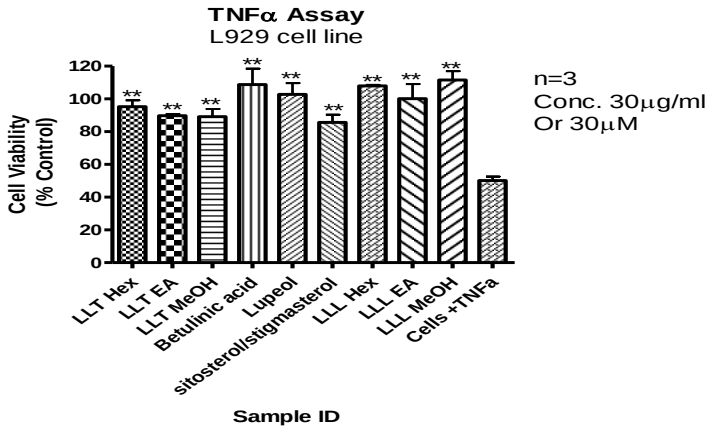

Figure 4. 4: The protective effects of LL tuber extracts and isolated compounds against TNFα on the L929 cell line. Data represents mean ± SEM, n=3. Data was analysed using One-Way ANOVA with a Dunnet Post-Test. **P<0.01 is significant increase in cell viability vs Cells + TNFα.

4.4.1.3. NF-ƙB assay

All the extracts as well as the isolated compounds were tested for their ability to inhibit NF-ƙB in the NCTC cell line. MG132 was used as a standard inhibitor of NF-ƙB to ensure the assay was at optimum conditions. MG132 inhibited NF-ƙB with an IC_{50} of 2.4 µM as illustrated in Figure 4.5.

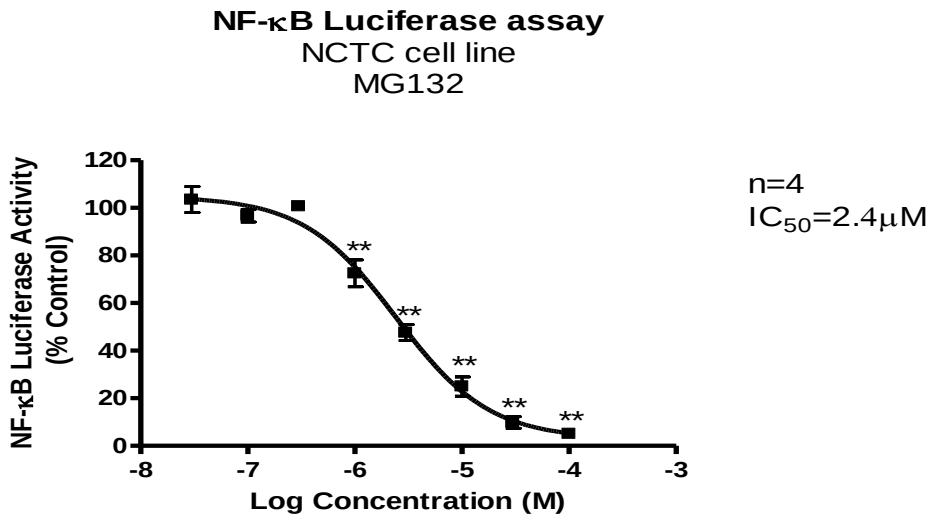

Figure 4. 5: The percentage inhibition of NF-ƙB luciferase by MG132 (positive control). Data represents mean ± SEM, n=3. Data was analysed using One-Way ANOVA with a Dunnet Post-Test. **P<0.01 is a significant decrease in NF-ƙB luciferase activity vs control.

4.4.1.3.1. LL extracts and isolated compounds

NF-ƙB activity was not affected by LLT Hex, LLT MeOH, LLL MeOH, lupeol and stigmasterol/sitosterol as shown in Figure 4.6. LLT EA showed 40% reduction in NF-ƙB activity and this was statistically significant ($P < 0.05$). BA, isolated from LLT EA, was the strongest NF-ƙB inhibitor among the tested LLT and LLL samples as it gave approximately 70% inhibition when tested at 30 µM. Therefore, a serial dilution of BA was carried out and a dose-response curve generated (Figure 4.7). The IC_{50} of BA was just under 23 µM.

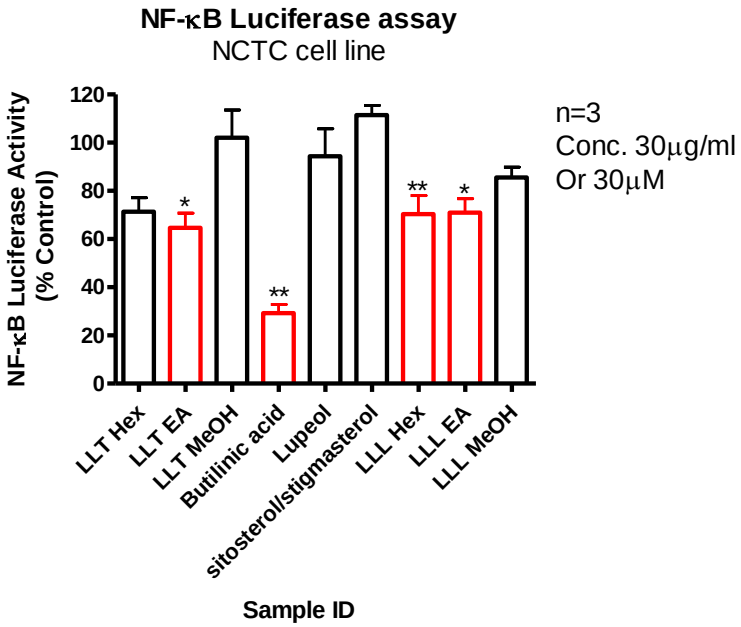

Figure 4. 6: The percentage activity of NF-ƙB luciferase following the treatment with LL tuber extracts and isolated compounds. Data represents mean ± SEM, n=3. Red colour indicates inhibition of NF-ƙB luciferase. Data was analysed using One-Way ANOVA with a Dunnet Post-Test. **P<0.01 vs control, *P<0.05 vs control.

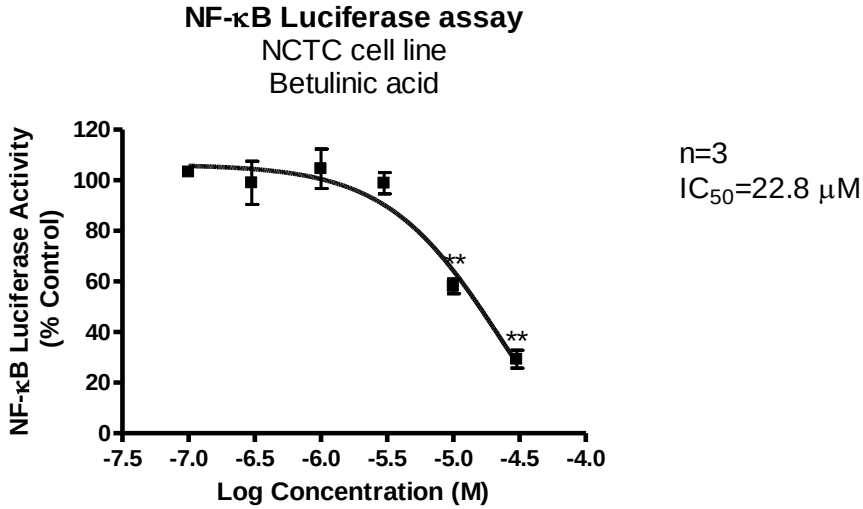

Figure 4. 7: The percentage activity of NF-ƙB luciferase following treatment with various concentrations of BA. Data represents mean ± SEM, n=3. Data was analysed using One-Way ANOVA with a Dunnet Post-Test. **P<0.01 is significant decrease in NF-ƙB luciferase activity vs control.

4.4.2. Anti-oxidant assays

4.4.2.1. DPPH Assay

LLT extracts, LLL extracts and isolated compounds were investigated for their ability to scavenge DPPH activity. Ascorbic acid, a known anti-oxidant, was used as a positive control and tested at a range of concentrations where 100µM was the highest. Ascorbic acid significantly ($P < 0.05$) scavenged the DPPH activity at concentrations 100 µM, 30 µM, and 10 µM, it had an IC_{50} value of 20 µM as shown in Figure 4.8.

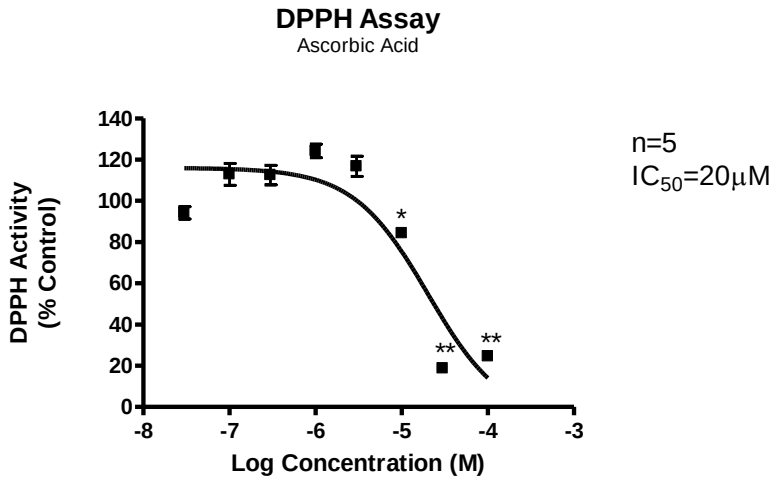

Figure 4. 8: The percentage inhibition of DPPH by Ascorbic acid (standard). Data represents mean ± SEM, n=5. Data was analysed using One-Way ANOVA with a Dunnet Post-Test. **P<0.01, *P<0.05 is significant decrease in DPPH activity vs control.

4.4.2.1.1. LL tuber extracts and isolated compounds.

LLT extracts, BA, lupeol and stigmasterol/sitosterol showed no inhibition activity against DPPH when tested at 30 µg/ml or 30 µM and lower concentrations (results in Appendix 2).

4.4.2.1.2. Extracts of LL leaves

LLL Hex extracts did not scavenge the DPPH activity as shown in Figure 4.9 when tested at 30 µg/ml. On the other hand, LLL EA significantly ($P < 0.05$) inhibited DPPH

activity at concentrations 30, 10, 3, and 1 µg/ml, with an IC_{50} of 6.5 µg/ml. Moreover, LLL MeOH extract also significantly ($P < 0.05$) inhibited DPPH activity at concentrations of 30 and 10 µg/mL and produced an IC_{50} of 24.8 µg/ml.

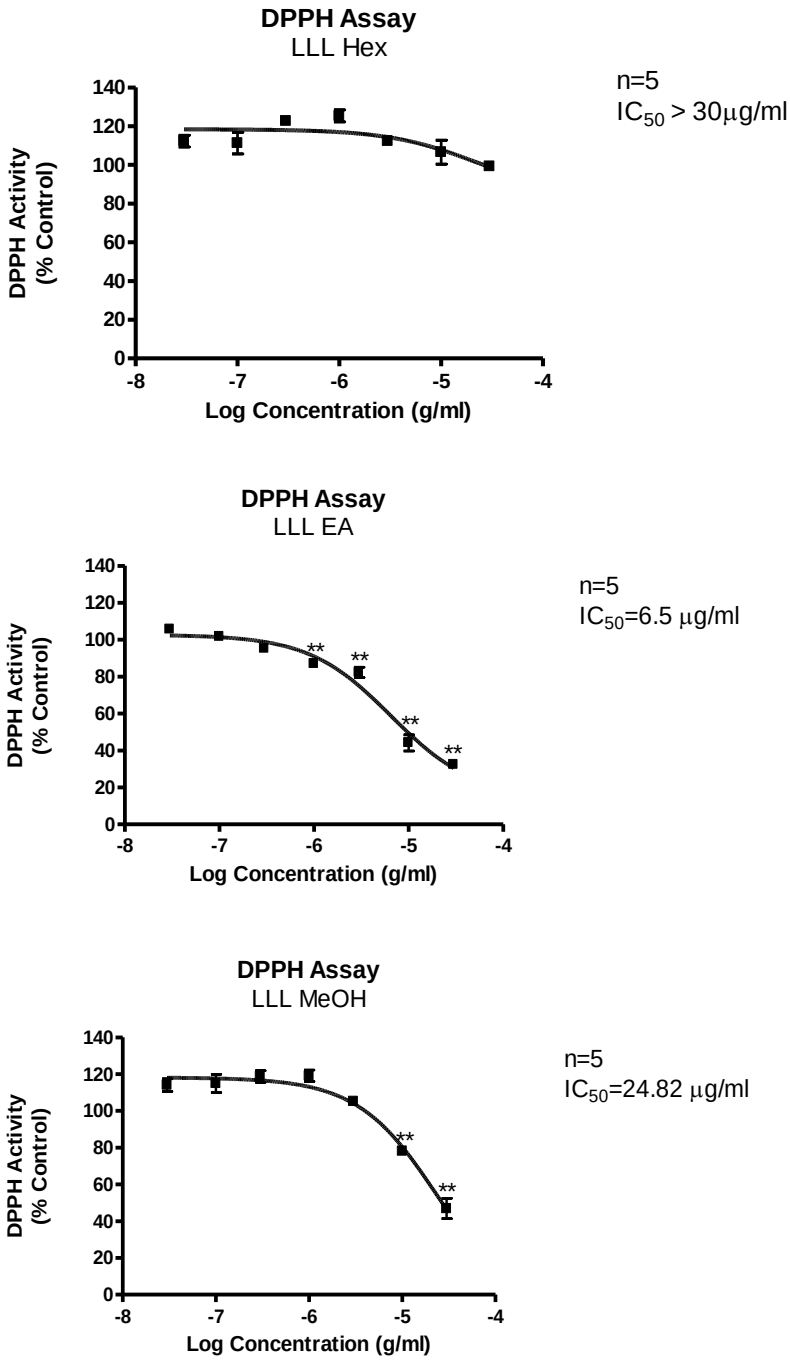

Figure 4. 9: The percentage inhibition of DPPH by LLL extracts. Data represents mean ± SEM, n=5. Data was analysed using One-Way ANOVA with a Dunnet Post-Test. **P<0.01 is significant decrease in DPPH activity vs control.

4.4.2.2. alamarBlue® Assay

Cytotoxicity testing using an alamarBlue® cell viability assay was carried out on all samples prior to performing the DCFH-DA and GSH assays. Samples were tested at 30 µg/ml for extracts and 30 µM for pure compounds. All samples were non-cytotoxic to SH-SY5Y, Panc1, and HepG2 cells at the tested concentrations (Figure 4.10) and therefore all of the samples were used at these concentrations or below in the DCFH-DA and GSH assays.

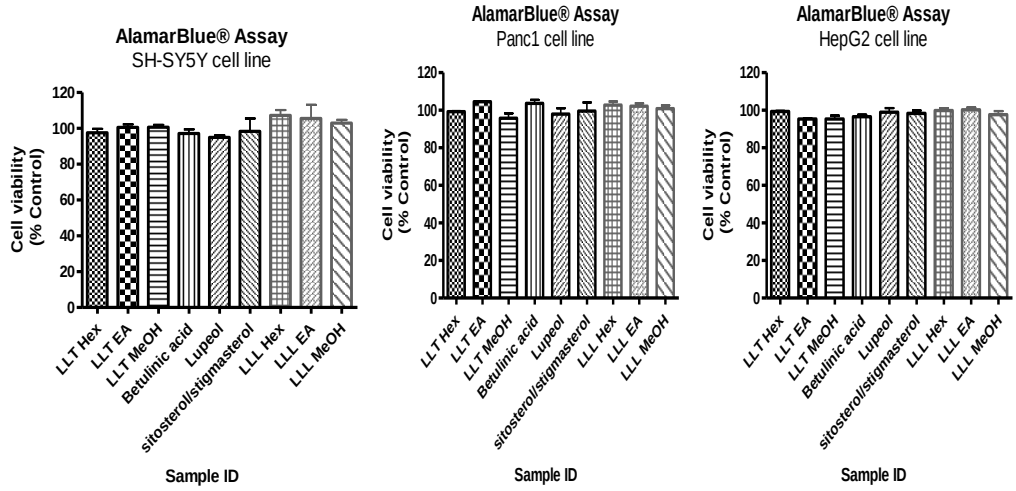

Figure 4. 10: Percentage of SH-SY5Y cell viability in alamarBlue® assay following treatment with LL extracts and isolated compounds. Data represents mean ± SEM. Data was analysed using One-Way ANOVA with a Dunnet Post-Test.

4.4.2.3. DCFH-DA assay

The DCFH-DA was carried out to assess the ability of the extracts and isolated compounds to generate ROS. The results were compared to the control which had only cells and DCFH-DA. All LL (tuber and leaf) extracts and isolated compounds showed comparable results to those for the control when tested at 30 µg/mL for extracts and 30 µM for isolated compounds in SY5Y, Panc1, and HepG2 cells, except for lupeol in HepG2 cells as shown in Figure 4.11 A1-A3. Lupeol increased ROS by more than three times in comparison with the control in HepG2 and the result was statistically significant ($P < 0.01$). Then, extracts and isolated compounds were tested in the same cells for their ability to protect cells against t-BuOOH, known as a ROS generator; a

summary of the results is shown in Figure 4.11 B1-B3. All tested samples significantly ($P < 0.01$) protected cells from ROS generated by t-BuOOH apart from lupeol in HepG2 cells which caused more ROS to be generated ($P<0.01$).

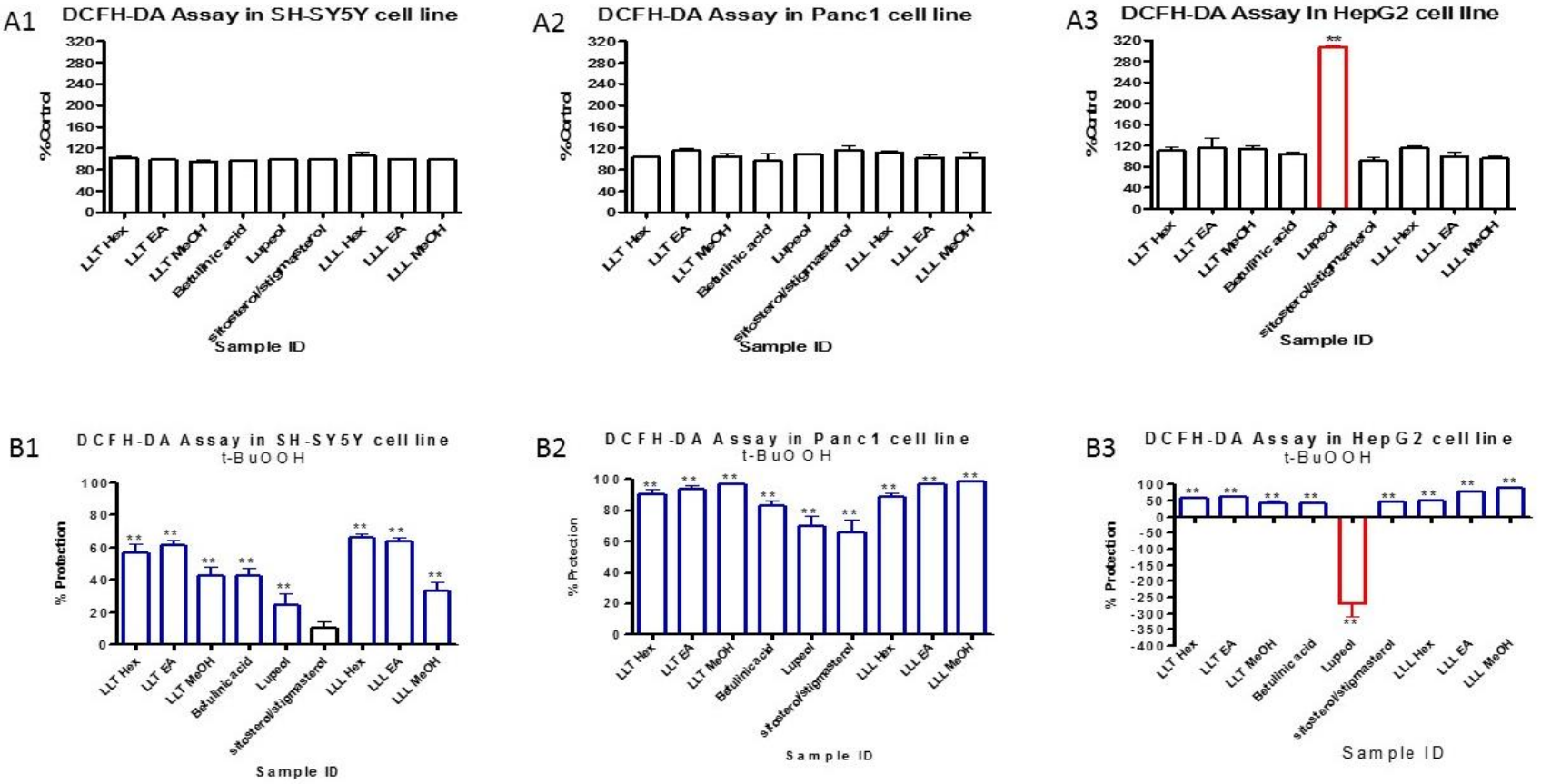

Figure 4. 11: The percentage induction of ROS generated by LL extracts and isolated compounds in A1-A3 where a red colour indicates significant increase in ROS ($P<0.01$); whereas B1-B3 show the ability of tested samples to protect cells from ROS generated by t-BuOOH where a blue colour indicates significant protection ($P<0.01$) and red represents significant contribution to ROS generation ($P<0.01$).

4.4.2.4. GSH-Glo™ Assay

GSH standard was used to ensure the assay is at optimum performance. At a range of concentrations (5 µM to 0 µM) a curve was generated with r^2 of 0.9859 which indicates a good curve fit as shown in Figure 4.12.

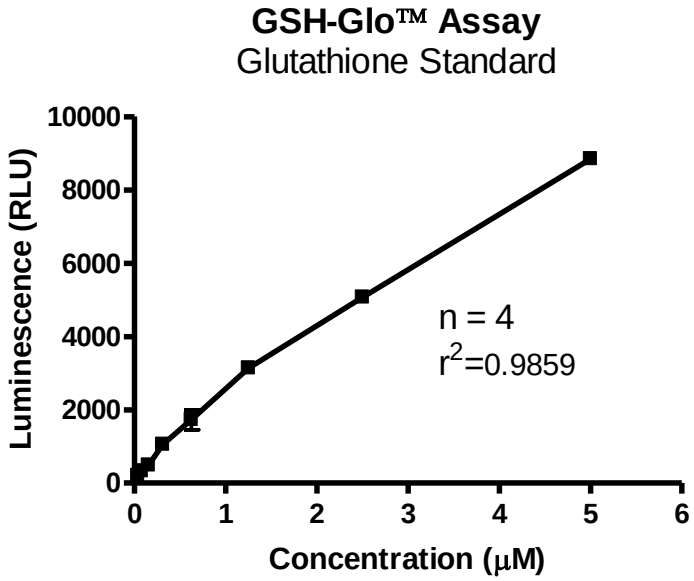

Figure 4. 12: GSH standard curve generated from the GSH-Glo™ Assay. Data represents mean ± SEM, n=4.

4.4.2.4.1. LL extracts and isolated compounds.

LLT MeOH and BA showed a 20% increase in GSH levels ($P < 0.05$), LLT Hex elevated GSH levels by 50% ($P < 0.05$), and LLT EA doubled GSH levels in HepG2 cells ($P < 0.05$). Lupeol decreased GSH levels by approximately 15%, but this decrease was statistically insignificant ($P > 0.05$). However, the mixture of sitosterol and stigmasterol decreased GSH levels by 30% and results were statistically significant ($P < 0.05$). Extracts of LLL were comparable to the control, except for LLL Hex extract which increased GSH levels by 50% ($P < 0.05$). A summary of these findings is shown in Figure 4.13, and Table 4.1.

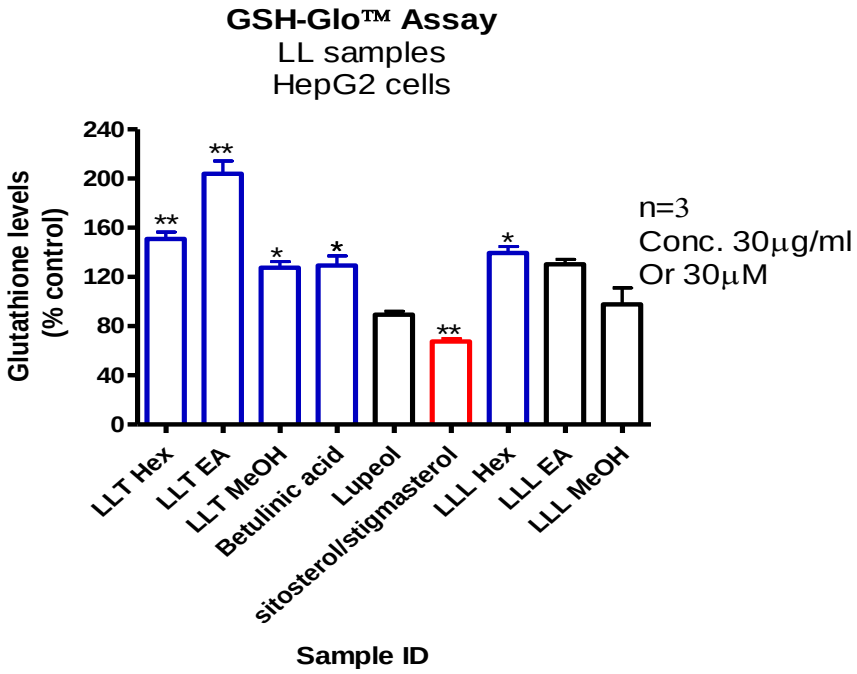

Figure 4. 13: The effects of LLT extracts and isolated compounds on GSH levels in HepG2 cells. Data represents mean ± SEM, n=3. Blue columns represent significant increase in GSH, red represents significant decrease in GSH and black indicates no significant change in GSH levels. Data was analysed using One-Way ANOVA with a Dunnet Post-Test. **P<0.01, *P<0.05 vs control.

Table 4. 1: GSH concentrations quantified following treatment with LL extracts and isolated compounds.

Sample ID		GSH Conc. (µM)
	Control	1.62
Tubers	LLT Hex	2.44
	LLT EA	3.29
	LLT MeOH	2.06
	BA	2.08
	Lupeol	1.44
	Sitosterol/ stigmasterol	1.09
Leaves	LLL Hex	2.25
	LLL EA	2.11
	LLL MeOH	1.59

4.5. Discussion and Conclusions

Extracts of LL tubers and leaves showed positive results in the anti-diabetic and anti-obesity assays as described in Chapter 3. Thus, it was pertinent to test these samples in some anti-inflammatory and anti-oxidant assays. Inflammation and oxidative stress have recently been linked to the development of diabetes and obesity. Therefore, this chapter explored the potential use of tubers and leaves of LL as anti-inflammatory and anti-oxidant agents.

4.5.1. Anti-inflammatory assays

The anti-inflammatory and anti-oxidant properties of LL were assessed in *in vitro* assays using L929 and NCTC cells. Non-cytotoxic concentrations of the extracts and compounds were used as determined by an alamarBlue® cell viability assay.

4.5.1.1 TNFα assay in L929 cell lines

Studies in rodents have shown that TNFα plays a major role in insulin resistance (da Costa *et al.*, 2016; Liang *et al.*, 2008; Togashi *et al.*, 2002). Suppression of TNFα in rodents have shown improvements to insulin resistance in obese animals (Schaeffler, 2017). Interestingly, all extracts of both tubers and leaves as well as the isolated compounds of LL showed almost 100% protection ($P < 0.01$) against 10 μM of TNFα, the concentration that was found to be cytotoxic to 50% of the cells. Among all of the tested samples, BA and LLL MeOH extract were the most protective samples against TNFα giving approximately 120% protection to L929 cells. The BA protection against TNFα has been shown in a number of publications as follows. To begin with, Yoon *et al.* demonstrated that treatment with BA in human umbilical vein endothelial cells (HUVEC) were found to be strong inhibitors of the vascular inflammation process which was mediated by TNFα (Yoon *et al.*, 2010). The study showed that BA pre-treatment on HUVEC stopped the expression of cell adhesion molecules such as intracellular adhesion molecule-1 (ICAM-1), vascular cell adhesion molecule-1 (VCAM-1), endothelial cell selectin (E-selectin) as well as gelatinase in TNFα-activated HUVEC that occur when TNFα is induced. Therefore, the study suggested that BA could be used as an anti-inflammatory agent in vascular inflammation.

Moreover, Dash *et al.* revealed that BA pre-treatment showed protection against inflammation produced by doxorubicin, a chemotherapeutic agent that is used to treat certain types of cancer (Dash *et al.*, 2015). Lupeol and stigmasterol were potent TNFα suppressors in this study and this is concordant with the literature. Kangsamaksin *et al.* quantified TNFα gene expression, by RT-qPCR, from HUVEC treated with 5 µM lupeol and stigmasterol. These two compounds reduced TNFα expression by 40% ($P < 0.05$) despite the fact that the concentrations of the compounds were 6 times lower than the ones in the current study (Kangsamaksin *et al.*, 2017).

Extracts of LL leaves and tubers require further phytochemistry work to isolate and identify compounds responsible for the TNFα inhibition activity. Several compounds from various plants were found to be potent TNFα inhibitors. *Neouvaria foetida* was shown to inhibit TNFα and the active compound identified was 17-O-acetylacuminolide which inhibited expression of TNFα in a dose-dependent manner with an IC_{50} of 2.7 µg/ml (Mouna *et al.*, 2010). Moreover, Dexheimer *et al.* have studied the effects of ethanol and hexane extracts of *Calyptranthes grandifolia* O.Berg (Myrtaceae) on Caco-2 cell line. Caco-2 was stimulated with LPS and treated with plant extracts ranging from 25 to 200 µg/ml (Dexheimer *et al.*, 2017). Then, the total RNA was extracted for gene expression analysis. The ethanolic extract was found to decrease TNFα expression at concentrations of 100 and 200 µg/ml. *C. grandifolia* decreased TNFα expression when it was given at high concentrations showing that this plant was not highly potent. From the points discussed above, it can clearly be said that tubers and leaves of LL have some potential anti-inflammatory effects by protecting L929 cells from treatment with TNFα. Pro-inflammatory cytokines such as TNFα are known to activate NF-ƙB and mediate inflammation (Shanmugam *et al.*, 2015). As a result of this, it was desirable to evaluate the effects of LL extracts from tubers, leaves, and isolated compounds on NF-ƙB activity.

4.5.1.2. NF-ƙB assay in NCTC cell line

NF-ƙB is an inflammatory mediator that has been implicated in diabetes; NF-ƙB inhibition was shown to improve insulin resistance (Schaeffler, 2017). Therefore, LL

extracts and isolated compounds were investigated in terms of their ability to inhibit or decrease NF-ƙB expression in NCTC cells.

MG132, used as a positive inhibitor for the expression of NF-ƙB in monocytes, showed an IC_{50} of 2.4 µM. This finding confirms the MG132 inhibition of NF-ƙB expression in the human monocyte cell line U937 that was found by Ortiz‐Lazareno et al. (2008).

Tuber extracts and isolated compounds from LL showed no significant ($P > 0.05$) inhibitory effects on the expression of NF-ƙB apart from LLT EA extract and BA which showed approximately 40% and 70% inhibition, respectively. A dose-response BA study was performed and it was found to inhibit NF-ƙB expression with an IC_{50} of 22.8 µM. On the other hand, LLL MeOH extracts showed no inhibition whereas LLL Hex and LLL EA extracts showed 30% inhibition ($P < 0.05$). This data supports the findings which were obtained from the TNFα assay in the L929 cell line in which the tested samples were considered to be anti-inflammatory. The study by Yoon *et al.* (2010) showed that BA inhibited NF-ƙB expression in HUVEC and this confirms the findings obtained in the current study. Moreover, pretreatment with BA in LPS-stimulated BV2 microglial cells significantly ($P < 0.05$) inhibited IKB degradation, which caused NF-ƙB to be in the cytoplasm. Therefore, translocation of NF-ƙB was suppressed by BA (Kim, 2013).

For future work, LL should be considered for *in vivo* experiments to examine the effects on NF-ƙB and glucose homeostasis. Li *et al.* looked at the activity of *Gynura divaricata* (L.) DC (GD), a plant which has been reported to possess therapeutic effects in animals as well as humans (Li *et al.*, 2018). GD was studied to identify the mechanisms by which the plant improves insulin resistance in obese mice which were given STZ to induce diabetes. The aqueous extract of GD significantly reduced fasting BG levels, recovered the pancreatic function and reversed the dyslipidemic state. Moreover, obese mice showed improvements to their BW. The study also showed that in HepG2 cells, the expression of NF-ƙB was highly decreased by GD water extract whereas molecules involving insulin pathways such as insulin receptor substrate 1

(IRS-1), protein kinase B (PKB), and glucose transporter 1 (GLUT1) were enhanced in the treated mice. One of the major complications of uncontrolled diabetes is the development of cardiovascular abnormalities. Bagul *et al.* (2015) demonstrated that resveratrol, a phytoalexin, protected and improved the cardiac hypertrophy and electrocardiographic (ECG) abnormalities as well as oxidative stress which was seen in hearts of SD rats which were on a fructose diet for 8 weeks (Bagul *et al.*, 2015). The diabetic rats' hearts were found to express high levels of NF-ƙB-p-65 and showed a decreased expression of sertuin-1 (SIRT-1). Resveratrol was found to express its therapeutic effects on the diabetic rats' hearts by the activation of SIRT-1 which was associated with decreased activities of both NF-ƙB-p65 and NADPH oxidase (NOX). Therefore, LL extracts and isolated compounds should be investigated further for their ability to activate SIRT-1 in order to get a better picture of the mechanisms by which LLT EA extract and isolated BA showed decreased levels of NF-ƙB.

Thus, LL could be beneficial to the management of T2DM and in particular LLT EA extract and isolated BA as they showed a strong inhibition for α-glucosidase and decreased PL activity. In this chapter they also showed anti-inflammatory activities by protecting L929 cells against TNFα, and inhibiting the expression of NF-ƙB in a NCTC cell line. These results were followed up by exploring the anti-oxidant activity of LL extracts and isolated compounds as oxidative stress is implicated in diabetes and inflammation.

4.5.2. Anti-oxidant assays

The anti-oxidant activity of LLT and LLL extracts and isolated compounds were tested in DPPH, DCFDA and GSH assays.

4.5.2.1. DPPH assay

It is now clear that free radicals or ROS are implicated in a number of diseases including inflammation, atherogenesis, neurodegeneration, cancer and diabetes (Deng *et al.*, 2011). A DPPH assay was used to assess the ability of samples to scavenge ROS; this assay has a number of advantages. DPPH is stable, sensitive, simple, feasible

and the most reliable anti-oxidant assay for plant extracts (Sanna *et al.*, 2012). Therefore, LLT and LLL extracts and isolated compounds were firstly tested in a DPPH assay.

Ascorbic acid was used in this assay as positive control due to its known anti-oxidant activity; it inhibited DPPH with an IC_{50} of 20 µM. Tuber extracts as well as the isolated compounds showed no anti-oxidant activity in the DPPH assay when tested at concentrations < 30 µg/ml or 30 µM. BA was found to be inactive in the DPPH assay and this finding is concordant with a published study by Cesari et al. (2013). The LLL Hex extract was inactive, whereas LLL EA and LLL MeOH extracts showed activity against DPPH with IC_{50} of 6.5 µg/ml and 24.8 µg/ml, respectively. However, these two extracts of LL leaves require fractionation and isolation of compounds to identify those responsible for the DPPH inhibition activity. Sylvie *et al.* investigated the types of compounds present in methanol extracts of *Garcinia lucida*, *Hymenocardia lyrata* and *Acalypha racemosa* which are DPPH inhibitors (IC_{50} 1.74 µg/ml 2.61 µg/ml) (Sylvie *et al.*, 2014). The phytochemical screening of these extracts showed the presence of various classes of compounds, including alkaloids, tannins, glycosides, terpenoids and flavonoids.

4.5.2.2. DCFDA assay

There are various methods for detecting ROS in cells and one of these is the use of suitable fluorescent probes. DCFDA was used firstly by Brandt as a fluorescent probe to detect hydrogen peroxide (H_2O_2) (Brandt, 1965). Later, it was discovered that DCFDA oxidation was not limited to hydrogen peroxide, peroxyl and hydroxyl radicals are also DCFDA oxidisers (Gomes *et al.*, 2005). Therefore, LLT and LLL extracts and isolated compounds were subjected to a DCFDA assay to further investigate whether they contribute to oxidative stress in SH-SY5Y, Panc1 and HepG2 cells. All of the tested samples were non-cytotoxic to the cells at the tested concentrations by the alamarBlue® cytotoxicity assay. All of the extracts and isolated pure samples showed negative results in producing ROS in the tested cells apart from lupeol which produced positive results only in HepG2 cells. Therefore, it was desirable to study the potential of the tested samples to protect cells from a known ROS-

producing agent. Thus, the DCFDA assay was repeated, but in the presence of tBuOOH, a known ROS generator.

In the SH-SY5Y cell line, tuber extracts and isolated compounds protected cells from tBuOOH with statistical significance ($P < 0.01$) apart from sitosterol/stigmasterol. LLT EA extract was the most protective sample (70%) followed by LLT Hex extract (60%). LLT MeOH extract and BA showed 50% protection and lupeol gave 30% protection. Extracts of LL leaves also showed a reduced ROS generation by tBuOOH in SH-SY5Y. ROS decreased by 70% in LLL Hex and LLL EA extracts and 40% in LLL MeOH extract ($P < 0.01$). In Panc1 cells, extracts and isolated compounds were the most protective. ROS generated by tBuOOH were decreased to less than 10% and in some samples reached 0% ($P < 0.01$) by LL extracts and BA. Lupeol and sitosterol/stigmasterol showed the lowest protection properties with 80% protection ($P < 0.01$). The results with HepG2 indicated that all of the samples tested showed protection against ROS generated by tBuOOH by at least 50% except for lupeol which increased generated ROS to over 280%. This research showed that lupeol generates ROS in HepG2 cells and this is not concordant with the literature. Preetha *et al.* showed that *in vivo* lupeol possesses hepatoprotective activity against ROS generated by alfatoxins, which are known hepatotoxic and hepatocarcinogenic agents (Preetha *et al.*, 2006). Moreover, cadmium is hepatotoxic and has its action by generating ROS and changing the hepatic redox state; lupeol was administered at 150 mg/kg daily for three days prior to injecting rats with cadmium chloride, lupeol changed the hepatic redox state and scavenged ROS. However, the mismatch between the results obtained in this project and the literature can be due to two reasons; 1) *in vitro* studies do not always correlate with *in vivo* studies; 2) HepG2 are human hepatic cells, whereas the previous studies were on rats and therefore the difference in species can generate opposing results. In general, the DCFDA assay showed that all LL extracts and isolated compounds did not produce ROS in the tested or protected cells from ROS generated by tBuOOH except for lupeol in HepG2 cells.

4.5.2.3. GSH-Glo™ Assay

All of the tuber extracts showed an increase in GSH levels. LLT EA increased synthesis of GSH by 100% reaching 3.3 µM while the control sample showed 1.6 µM GSH. LLT Hex and LLT MeOH extracts showed GSH levels of 2.4 µM (60% increase) and 2.1 µM (30% increase), respectively. Isolated BA from LLT EA extract significantly ($P < 0.05$) increased GSH levels by 30% (2.1 µM). Lupeol insignificantly ($P > 0.05$) decreased GSH levels by 10% (1.4 µM) and this decrease was expected because ROS generators in HepG2 cells can decrease GSH levels. This was confirmed in a study by Luqman *et al.* where ROS-generators such as tBuOOH depleted GSH levels in HepG2 cells (Luqman *et al.*, 2009). Sitosterol/stigmasterol significantly ($P <0.01$) reduced GSH levels by 30% (1.1 µM). By looking at the effects of extracts of LL leaves on GSH levels, GSH synthesis increased to 140 % (2.25 µM) and 130% (2.1 µM) when HepG2 cells were treated with LLL Hex and LLL EA extracts, respectively and the results were statistically significant ($P < 0.05$). LLL MeOH extracts showed comparable results to the control which showed a GSH concentration of 1.59 µM ($P > 0.05$). However, compounds in the LL leaves need to be isolated and identified in order to find out the agents responsible for elevating GSH levels. To sum up, tuber and leaf extracts of LL as well as isolated compounds (except sitosterol/stigmasterol) showed enhancement of GSH synthesis. This indicates that this plant has compounds that have anti-oxidant activity by raising GSH levels; BA increased GSH concentration in HepG2 cells ($P < 0.05$) in this study and this is comparable to the findings in the literature. A study by Cho *et al.* examined the neuroprotective effects of *Betula platyphylla* bark (BPB) in an β-amyloid-induced amnesic mouse model (Cho *et al.*, 2016). The study showed that the memory and cognitive function in mice were improved by treatment with BPB, botulin and BA. These samples were found to increase GSH levels in the hippocampus. The study concluded that these samples could be used for the management of Alzheimer's disease (AD), a disorder characterised by progressive neurodegeneration that is age-linked and which can eventually result in dementia development (Ahmed *et al.*, 2015). A study carried out by de la Monte and Wands (2005) showed that AD was associated with abnormalities in energy metabolism and glucose uptake (de la Monte and Wands, 2005). Moreover, deficiencies in insulin, insulin growth factor (IGF), and insulin receptors (IR) in AD

were linked to insulin resistance in the neuropathology of AD (Craft, 2012). All of the above evidence that links both insulin resistance and AD has resulted in the term type III diabetes to be coined for AD, which is considered a brain-specific type of diabetes (Schaeffler, 2017).

A study by Dinçer *et al.* (2002) investigated the relationship between reduced GSH levels and glycaemic control in diabetic patients; poorly controlled T2DM showed lower GSH levels in blood samples in comparison with well-controlled T2DM patients (Dinçer *et al.*, 2002). Minette *et al.* justified the decrease in GSH levels in T2DM patients as this was as a result of compromised GSH synthesis and metabolising enzyme levels (Minette *et al.*, 2015). The study showed that transforming growth factor beta (TGF-β) was increased in plasma samples from T2DM patients. TGF-β is a cytokine that decreases the synthesis of reduced GSH. TNFα and other cytokines were also associated with decreased levels of GSH in T2DM. All the above points suggest that one of the mechanisms by which LL can improve glucose homeostasis is by increasing levels of GSH.

In conclusion, LL maybe a promising plant to be used for the management of T2DM as it contains potent inhibitors for α-glucosidase, strong protection against TNFα mediated cell death and increases GSH levels. These findings directed the project to look back at the animal study by Woods (2017) where rats were fed LL tubers. Pancreatic tissues of the animals were therefore subjected to RNA sequencing analysis (Chapter 5) to examine the changes in affected pathways and genes caused by the tuber treatment and investigate whether there is some evidence at the gene expression level supporting the findings obtained so far in this project.

Chapter 5

5. RNA Sequencing of Pancreatic Tissues

5.1. Introduction

The project findings in Chapters 2-4 suggested that the tubers and leaves of LL possess anti-diabetic and anti-obesity activities. BA was isolated from the LLT EA extract (Chapter 2), and as the compound is known to have some anti-diabetic activity (Ding *et al.*, 2018). Both LL tuber and leaf extracts as well as the isolated BA inhibited α-glucosidase and PL, and enhanced glucose uptake in HepG2 cells (Chapter 3); protected against TNFα mediated cell death in L929 cells and inhibited NF-ƙB expression in NCTC cells (Chapter 4); and acted as an anti-oxidant by inhibiting DPPH, protecting against ROS in SH-SY5Y, Panc1 and HepG2 cells, and increased GSH levels in HepG2 cells (Chapter 4). Following on from the above findings, it was thought pertinent to investigate the changes in gene expression of pancreatic tissue from animals treated with LL tubers by Woods (2017).

One of the most advanced technologies which enables investigation of samples of interest and looks at gene expression is RNA sequencing (RNA-Seq). RNA-Seq applies next generation sequencing (NGS) technologies to quantify and confirm the presence of RNA molecules in biological samples (Li and Li, 2018). RNA-Seq has replaced conventional Complementary DNA (cDNA) gene expression microarrays due to a number of advantages. Generally, RNA-Seq analysis is carried out in five main steps: (1) The initial step involves the fragmentation of RNA samples prior to reverse transcription and cDNA synthesis, and then sequenced using high-throughput platforms. (2) A genome or a transcriptome is mapped from the generated sequenced cDNA. (3) The next step involves the estimation of expression levels of each gene or isoform. (4) Normalisation of mapped data is carried out using statistical and machine learning techniques to identify differentially expressed genes (DEGs) following treatment. (5) The data is evaluated using a biological context.

5.2. Aims and objectives

This chapter aims to apply RNA-Seq to investigate the effects of LLT on rat pancreatic tissue. This was achieved by:

1. Isolating total RNA from the pancreas of control rats and rats treated with an extract from the LLT.
2. Carrying out a transcriptome-wide gene expression analysis from these groups using RNA-Seq.
3. Conducting a bioinformatics analysis of the RNA-Seq differentially expressed genes to try to understand the effects of the LLT extract on rat pancreatic tissues.
4. Performing quantitative PCR experiments on the key genes highlighted from the RNA-Seq analysis.

5.3. Materials and methods

5.3.1. Animals

Ten male SD rats aged 12 weeks were obtained from Charles River Laboratories, and treatment started when the rats were 15 weeks old (Woods, 2017). Briefly, the animals were divided into two groups with 5 rats per group. Group 1, the control received 0.9% (v/v) saline by oral gavage on day 1 of the experiment. Group 2 were treated with 42 mg/kg of LL tubers on day 1 of the experiment. The LL tubers were ground into powder and dissolved in 1ml of deionised (dH2O) water before being administered by oral gavage. Both groups were then monitored for 7 days and the tuber dose was increased on day 7 to 210 mg/kg. Four hours later, the animals were anaesthetised with pentobarbitone sodium tartrazine (20% v/v, 0.1ml per 100g BW). Then, cardiac punctures were performed and dissection of the rats carried out in which pancreatic tissues were removed. All tissues were immersed in RNA*L*ater solution for 24 hours at 4°C to preserve the RNA. Then, the RNA solution was removed and the tissues were stored at -80°C until required.

5.3.2. RNA extraction

Total RNA from the pancreatic tissue was isolated using a RNeasy Plus Universal Midi Kit. Typically, 100 mg of tissue was added to a 2 ml microcentrifuge tube with 1 ml of QIAzol lysis reagent. A 6mm cone ball was added and the tissue homogenised using a MM-300 bead-mill for one min at 30Hz. The resultant disrupted sample was processed as per the RNeasy Plus Universal Midi Kit protocol. Total RNA was eluted from the spin column with 250 µl of RNase-free water and stored at -80°C until required.

5.3.3. RNA quality and integrity

The concentrations of the extracted RNA were measured using a NanoDrop ND-2000C™ spectrophotometer. The RNA integrity was assessed using a Bio-Rad Experion™ automated electrophoresis system and Experion StdSens Analysis; the procedure was carried out per the manufacturer's protocol.

5.3.4. RNA sequencing

Four RNA samples (two controls and two treated) were selected for RNA-Seq analysis. The selection of samples was based on the RNA integrity scores obtained from the Bio-Rad Experion™ StdSens Analysis Kit. Samples were submitted to BGI-Tech (Shenzhen, China) to perform RNA-Seq using Illuminia HiSeq4000 technology, with 20Mb clean reads per sample. RNA-Seq was applied to outline the effects of LL tubers on rat pancreatic tissues. Pairwise experiments were carried out on six experimental groups. These were: (1) control 11 *versus* control 14; (2) control 11 *versus* repeated tuber-treated 18; (3) control 11 *versus* repeated tuber-treated 20; (4) control 14 *versus* repeated tuber-treated 18; (5) control 14 *versus* repeated tuber-treated 20; (6) tuber-treated 18 *versus* tuber-treated 20. These comparison results were then illustrated using the interaction of heatmap and heatmap correlation.

5.3.5. Pathway enrichment analysis

Cytoscape Software (version 3.3.0) (Shannon *et al.*, 2003) with ClueGO plugin (version 2.2.4) (Lotia *et al.*, 2013) that has the ability to relate a group of genes to a

particular biological activity was used to analyse the RNA-Seq results received from BGI. The ClueGo plugin is a visualising tool that is capable of relating a group of genes to their functions, displaying a cluster network of results. The following parameters (Table 5.1) were applied with the ClueGo plugin:

Table 5. 1: Parameters applied with the ClueGo plugin.

Parameter	**Applied in ClueGo**
Statistical test	Two-sided hypergeometric option with Benjamini-Hochberg correction
Pathway	Significant KEGG (Kyoto Encyclopedia of Genes and Genomes) pathway enrichment ($P < 0.05$)
Kappa score	3
GO Term/Pathway selection	(3/4%)

5.3.6. Real time quantitative PCR (RT-qPCR)

RT-qPCR was carried out to validate the results obtained from the RNA-Seq analysis. RNA-Seq analysis is very expensive and as such was performed on only four samples out of ten. RT-qPCR was therefore used on all of the ten pancreatic RNA samples to increase the depth of investigation by examining more of the biological replicates. The expression of selected genes related to obesity, diabetes, and inflammation was analysed using RT-qPCR for ten samples (five controls, and five tuber treated).

5.3.7. Complementary DNA (cDNA) synthesis

For gene expression analysis, the isolated RNA samples must be converted to cDNA to function as a template to be used in RT-qPCR. A Tetro cDNA Synthesis Kit was used per the manufacturer's instructions to synthesise cDNA from the ten pancreatic RNA samples. Five µg of RNA,1 µl of Random Hexamer primer, 1 µl of 10mM dNTP mix, 4µl of 5xRT Buffer, 1µl of RiboSafe RNase Inhibitor, 1 µl of MMLV Reverse Transcriptase and DEPC-treated water up to a total reaction volume of 20 µl (final cDNA concentration 250 ng/µl) were mixed and termed as RT (+) samples. Random hexamers were used as the primer for these experiments due to the level of degradation present in the RNA from the pancreatic tissues. In parallel to the preparation of RT (+)

samples, RT (-) samples were prepared which used 1 µl DEPC-treated water to substitute for 1µl of MMLV Reverse Transcriptase. RT (-) samples were used to check for genomic DNA contamination. Moreover, a no-template control (NTC) was also prepared in the absence of RNA with and without reverse transcriptase (NTC (+) and NTC (-)). Following sample preparation, the samples were incubated for 30 min at 45°C in a DNA thermal cycler, the reaction was stopped by further incubation at 85°C. Samples were removed from the incubator and placed on ice for cooling; they were used immediately for RT-qPCR or stored at -20°C until needed. To permit a number of RT-qPCR technical replicates to be performed on each batch, the cDNA was further diluted 1:5 with 1xRT Buffer with 80 µl of buffer added to the 20 µl of cDNA.

5.3.8. Primer design

Three candidate reference genes were examined in this study with their selection based on the current literature for reference genes for pancreatic samples. These were: Beta-2-microglobulin (*B2m*), hypoxanthine phosphoribosyltransferase 1 (*Hprt1*), and TATA box binding protein (*Tbp*). Seven target genes were selected based on the RNA-Seq results; these were: adiponectin (*Adipoq*), interleukin 1 beta (*Il1b*), TNF receptor superfamily member 19 (*Tnfrsf19*), CD40 molecule (*Cd40*), CD40 ligand (*Cd40lg*), leptin (*Lep*), and C-C motif chemokine ligand 20 (*CCL20*).

The PrimerBLAST website from NCBI (https://www.ncbi.nlm.nih.gov/tools/primer-blast/) was used to design primers for reference and target genes. Designed primers had a product size of 130-150bp, and the melting temperature (T_m) was between 59-61°C. All primers were checked against the mRNA and genomic DNA database to ensure there were no other potential targets or amplicons generated. Additional details of the designed primers are shown in Tables 5.2 and 5.3.

The oligonucleotide PCR Primers were synthesised by IDT (Integrated DNA Technologies, Leuven, Belgium) and were diluted in ultrapure water to give 100 µM stock primer concentration. Ten µl of the 100 µM stock solutions were further diluted 1:10 with water (90 µl) and used in the RT-qPCR reactions.

Table 5.2: Primer sequences for the reference genes.

Reference Gene Name	Gene Symbol	Accession No.	Designed Primers (5' to 3')	Primer T_m (°C)	Amplicon Length (bp)
Beta-2-microglobulin	*B2m*	NM_012512.2	F: CTTGTCTCTCTGGCCGTCGTGC	60.22	147
			R: ATTTGAGGTGGGTGGAACTGAGACAC	59.62	
Hypoxanthine phosphoribosyltransferase 1	*Hprt1*	NM_012583	F: ATACAGGCCAGACTTTGTTGGA	59.62	150
			R: GCCGCTGTCTTTTAGGCTTTG	60.40	
TATA box binding protein	*Tbp*	NM_001004198	F: AGCTCCAAAATATTGTATCCACCG	59.18	148
			R: ATCAACGCAGTTGTTCGTGG	59.41	

F=Forward, R=Reverse

Table 5. 3: Primer sequences for the target genes

Reference Gene Name	Gene Symbol	Accession No.	Designed Primers (5' to 3')	Primer T_m (°C)	Amplicon Length (bp)
Adiponectin	*Adipoq*	NM_144744	F: CCACCCAAGGAAACTTGTGC	59.61	136
			R: GACCAAGAACACCTGCGTCT	60.25	
Interleukin 1 beta	*Il1b*	NM_031512	F: GGCTTCCTTGTGCAAGTGTC	59.69	144
			R: AAGGGCTTGGAAGCAATCCT	59.59	
TNF receptor superfamily member 19	*Tnfrsf19*	NM_001044229	F: CGCCATTCTCCTAGTCGGTC	59.97	149
			R: CGAAGCCACATTCCTTGGAC	59.20	
CD40 molecule	*Cd40*	NM_134360	F: ACCGACTAGTTAGCCACTGC	59.47	133
			R: AGCCCTTGATTGAGTTCGCA	59.96	
CD40 ligand	*Cd40lg*	NM_053353	F: GCATCTGTTCTTCAGTGGGC	59.19	158
			R: CGTTGACTCAAAGGTTCCCG	59.13	
Leptin	*Lep*	NM_013076	F: TCCTGTGGCTTTGGTCCTATC	59.44	131
			R: GGATACCGACTGCGTGTGT	59.79	
C-C motif chemokine ligand 20	*Ccl20*	NM_019233	F: GCACCTCCTCAGCCTAAGAAC	60.41	140
			R: CACAAATCAGGTCTGTGCAGTG	60.03	

F=Forward, R=Reverse

5.3.9. SYBR-Green RT-qPCR

PowerUp™ SYBR™ Green Master Mix was used per the manufacturer's instructions. RT-qPCR reactions were performed in triplicate in separate wells in MicroAmp® Fast Optical 96-well reaction plates. The total volume per reaction was 10 µl consisting of PowerUp™ SYBR™ Green Master Mix, primers, nuclease-free water, and cDNA as shown in Table 5.4; reaction mixtures were stored at room temperature until needed for RT-qPCR. ABI StepOne Plus Real-Time PCR System (Applied Biosystems, Paisley, UK) with fast cycle conditions (Table 5.5) was used for running all the reactions.

Table 5.4: The components required for each RT-qPCR reaction

Constituent	**Volume (µl)**
PowerUp™ SYBR™ Green Master Mix (2x)	5 µl
Forward primer (10pmol/ul)	0.5 µl
Reverse primer (10pmol/ul)	0.5 µl
Nuclease-free water	3 µl
cDNA	1 µl

Table 5.5: ABI StepOne Plus Real-Time PCR System with fast cycle conditions used for RT-qPCR experiments.

Step	**Temperature (°C)**	**Duration**	**Cycles**
UDG Activation	50	2 min	Hold
Dual-Lock™ DNA Polymerase	95	2 min	Hold
Denature	95	3 sec	40
Anneal/Extend	60	30 sec	

5.3.9.1. Reference gene stability

Prior to testing the control and treated cDNA samples with the RT-qPCR primers of interest, reference gene stability was established. One control and one treated sample

were tested against the three reference genes *Hprt1*, *Tbp*, and *B2m*. The results were compared using RefFinder platform (http://www.leonxie.com/referencegene.php), which compares the results using integrated computational programmes, BestKeeper, geNorm, Normfinder and the comparative ΔΔCt method.

5. 3.9.2. RT-qPCR product sequencing

RT-qPCR products from each of the RT+ gene expression assays underwent agarose gel separation. Each band was cut out and purified per Illustra GFX PCR DNA and Band Purification Kit's instructions. Purified PCR products were sent to GATC Biotech AG (Köln, Germany) for Sanger sequencing to confirm the identity of the RT-qPCR products.

5.4. Results

5.4.1. RNA extraction and quality control

5.4.1.1. Nanodrop analysis

The pancreatic RNA samples were analysed using a Nanodrop 2000c spectrophotometer to quantify and assess the quality and purity of the isolated RNA. The summary of these findings is shown in Table 5.6. The RNA purity was assessed by the absorbance ratio at 260nm and 280nm (optimum RNA purity has a ratio close to 2). In addition, the quality of RNA is also assessed by the ratio of 260/230, where a ratio of 2-2.2 is ideal. Therefore, the obtained results for all ten pancreatic RNA samples were considered as acceptable for these studies.

Table 5.6: A summary of the RNA extraction results from rat pancreatic tissues (see Appendix 3 for Nanodrop traces)

Group	Sample no.	Weight of sample (mg)	RNA Conc. (ng/µl)	A260/A280	A260/A230
Controls	11	149	2349.1	2.06	2.21
	12	239	3196.0	2.08	2.25
	13	228	2290.6	2.06	2.22
	14	250	2027.6	2.07	2.23
	15	225	2505.9	2.06	2.28
Tuber-Treatment	16	197	3693.3	2.07	2.25
	17	250	2540.0	2.07	2.31
	18	248	2879.8	2.07	2.27
	19	214	2465.5	2.06	2.30
	20	224	1674.8	2.07	2.27

5.4.1.2.Experion™ RNA StdSens Analysis

An Experion™ RNA StdSens kit was used in addition to the Nanodrop due to its ability to assess RNA quality and integrity through RNA quality indicator (RQI) or RNA Integrity Number (RIN) determination. RQI is an RNA integrity determination scale which ranges from 1-10, 1 being extensive RNA degradation and 10 is intact RNA and is similar to the RIN standard developed by Agilent for their similar BioAnalyzer systems (Denisov *et al.*, 2008). For optimum RNA-Seq analysis and RT-qPCR assay, RQI is preferred to be 7 or greater.

The Experion™ RNA StdSens kit also measures the amount of ribosomal RNA (rRNA), mainly 28S and 18S rRNA, which can also give an indication of the RNA integrity. Eighty percent of total RNA is rRNA of which 28S and 18S are the majority. 28S rRNA is at least twice the size of 18S rRNA. Therefore, 28S to 18S ratio of 2 is accepted for intact RNA, a ratio of greater than 1 is also acceptable. A virtual gel is produced by Experion™ RNA StdSens kit for all the 10 pancreatic RNA samples as shown in Figure 5.1.

For BGI to perform RNA-Seq analysis, samples are required to have RIN with values of ≥7. All the isolated pancreatic RNA samples had RIN values ranging from 5.7 to 6.3, and 28S/18S ratio was in the range of 0.59-0.66 as shown in Table 5.7. It is challenging to isolate RNA with high quality from the pancreas, this is mainly due to the presence of high endogenous levels of RNases, DNases, and proteases in the pancreas which enhance autolysis immediately following dissection (Augereau *et al.*, 2016). Following communication of these findings to BGI, their experts confirmed that RNA sequencing could be performed on samples with RIN values of 5-6, but could not be guaranteed to be successful. Hence, it was decided to send four samples instead of six to minimise the risks and costs if the experiments were not successful. Samples no. 11 and 14 showed the highest RIN values in the control group, while samples no. 18 and 20 had most intact RNA in comparison to the others in the treated group. Therefore, these four samples were sent to BGI for RNA-Seq analysis.

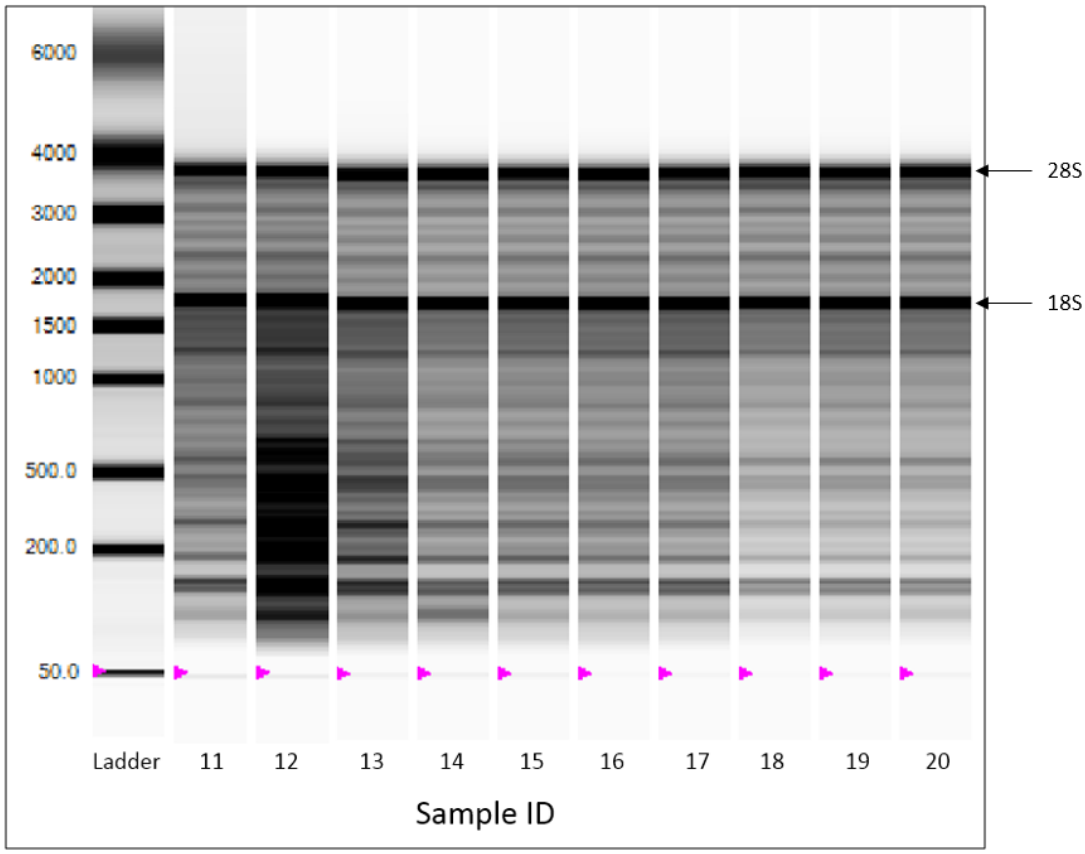

Figure 5.1: A virtual gel is produced by Experion™ RNA StdSens kit for all the 10 pancreatic RNA samples.

Table 5.7: Ratio of 28S:18S and RQI values for all the extracted ten RNA samples.

Group	Sample No.	Ratio (28S/18S)	RQI
Control	11	0.62	5.9
	12	0.61	5.7
	13	0.67	5.9
	14	0.66	6.0
	15	0.59	5.9
Tuber Treatment	16	0.64	6.0
	17	0.61	5.9
	18	0.66	6.3
	19	0.62	6.1
	20	0.64	6.2

5.4.2. RNA-Seq analysis

The purpose of the RNA-Seq analysis was to obtain an overview of the effects on pancreatic tissues of tuber treated rats. This information was obtained to act as guidance for future work and the next steps involved in this project.

BGI were able to successfully perform the RNA-Seq analysis on the samples despite the low RIN values. The average raw sequence reads were 22,364,443, and 22,364,810 for the control and treated groups respectively, while 22,318,249, and 22,257,793 were the average of clean sequence reads for both the control and treated groups, respectively. A summary of the alignment statistics is shown in Table 5.8.

Table 5. 8: Alignment statistics for the four pancreatic RNA samples, provided by BGI.

Group	Sample no.	Total Clean Reads	Total Mapped Reads (%)	Unique Match (%)	Multi-position Match (%)	Total Unmapped Reads (%)
Control	11	22,327,263	91.31	77.63	13.69	8.69
	14	22,309,235	92.19	78.12	14.07	7.81
Treated	18	22,231,442	92.41	76.99	15.43	7.58
	20	22,284,144	92.37	77.51	14.86	7.63

5.4.2.1. Gene expression

Total clean reads were mapped against transcriptome, reference genome UCSC rn6, (17,449 genes) to quantify the number of genes expressed among the four samples (Figure 5.2). When mapping genes against transcriptome, some genes are expected to be lost due to unannotated transcripts. Therefore 70-90% of expressed genes is considered to be acceptable. However, the samples from this study showed approximately 66% of gene expression. This slightly low percentages can be a result of the degraded pancreatic RNA samples sent to BGI. These underreportings of gene expressions are to be expected.

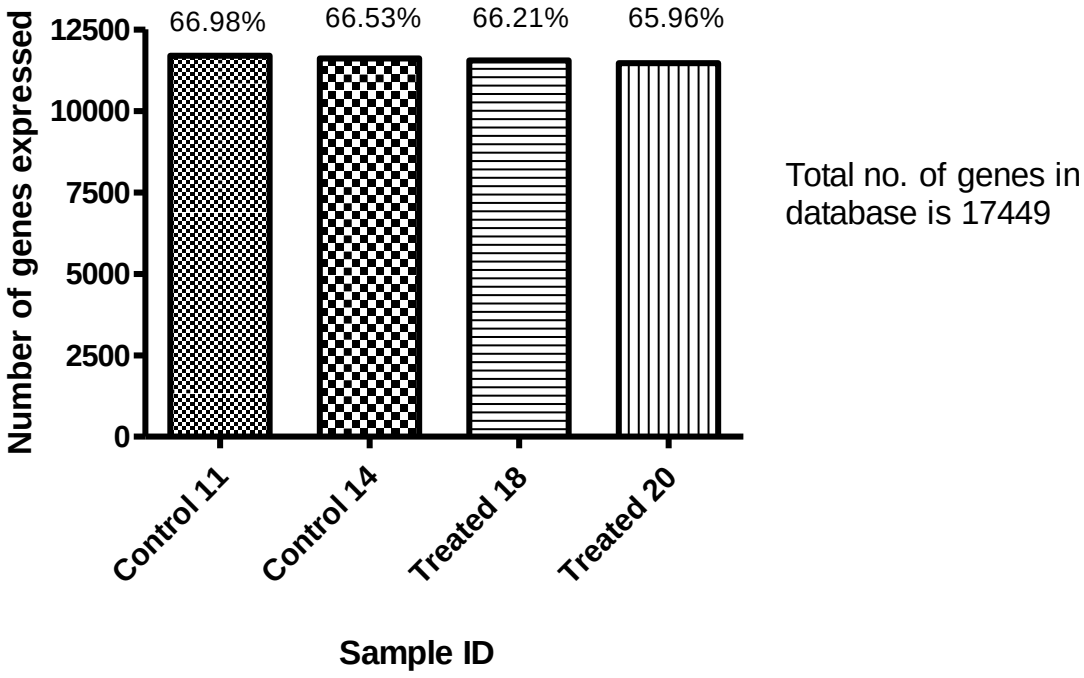

Figure 5.2: Total clean reads were mapped against transcriptome (17,449 genes) to quantify the number of genes expressed among the four samples.

5.4.2.2. Correlation between samples

The relationship between the four samples in terms of the expressed genes was assessed using Pearson values (Huang, 2008). Values closer to 1 show a high correlation between samples. Pearson values were 0.997 and 0.998 for control 11 vs control 14, and treated 18 vs treated 20, respectively (Figure 5.3). Hence, there was a high correlation between samples of the same group. The comparisons of the treated samples with the control samples showed less correlation and this indicates there is a difference between the two groups. By considering treated samples 18 and 20, sample no. 20 was found to be more similar to the control groups (0.985, 0.988) than sample no. 18 (0.975, 0.978).

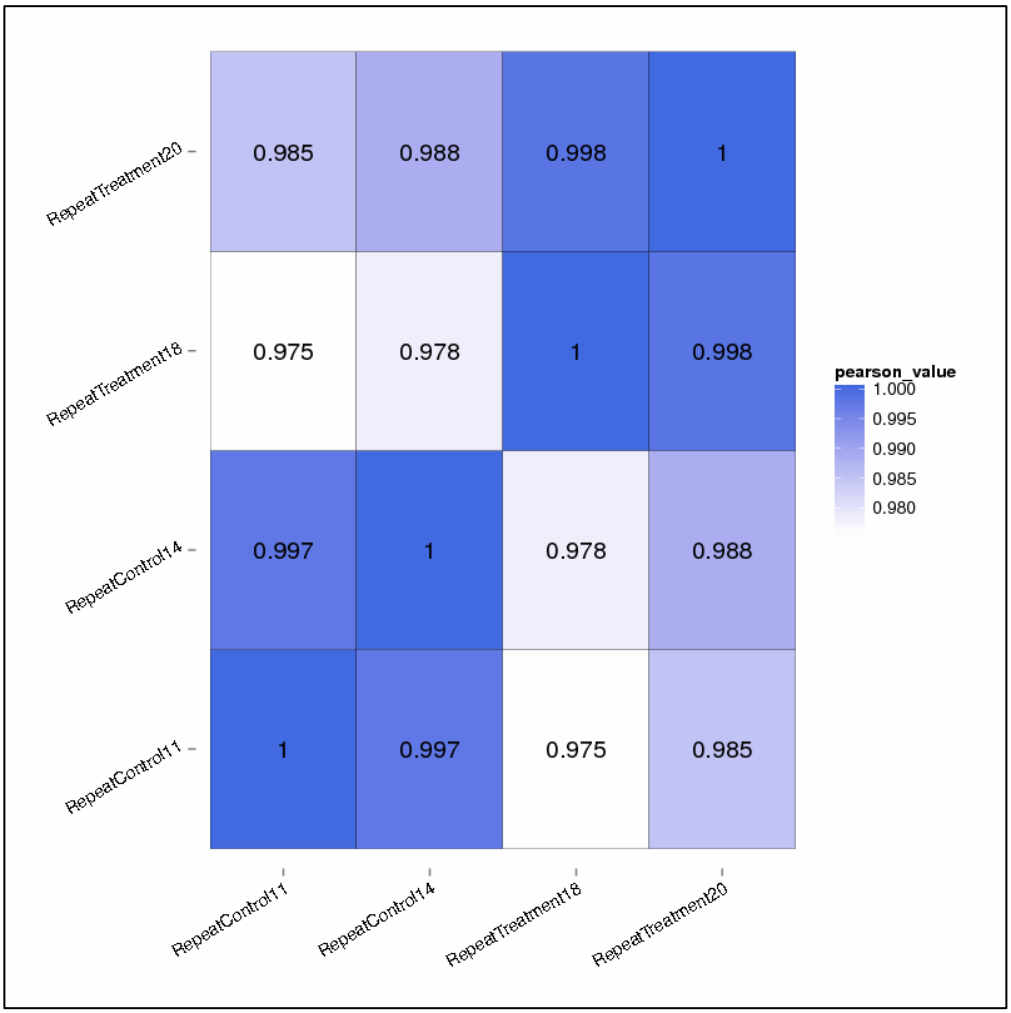

Figure 5.3: Heatmap correlation for all four samples that were RNA sequenced.

5.4.2.3. Differentially expressed genes (DEGs)

Four pairwise comparisons were carried out in terms of the differentially expressed genes (DEGs) and a summary of these results is given in Figures 5.4-5.7. These results mimic the heatmap correlations shown in Figure 5.8. When comparing treated samples with control 11, higher DEGs were obtained, while lower DEGs were seen with control 14.

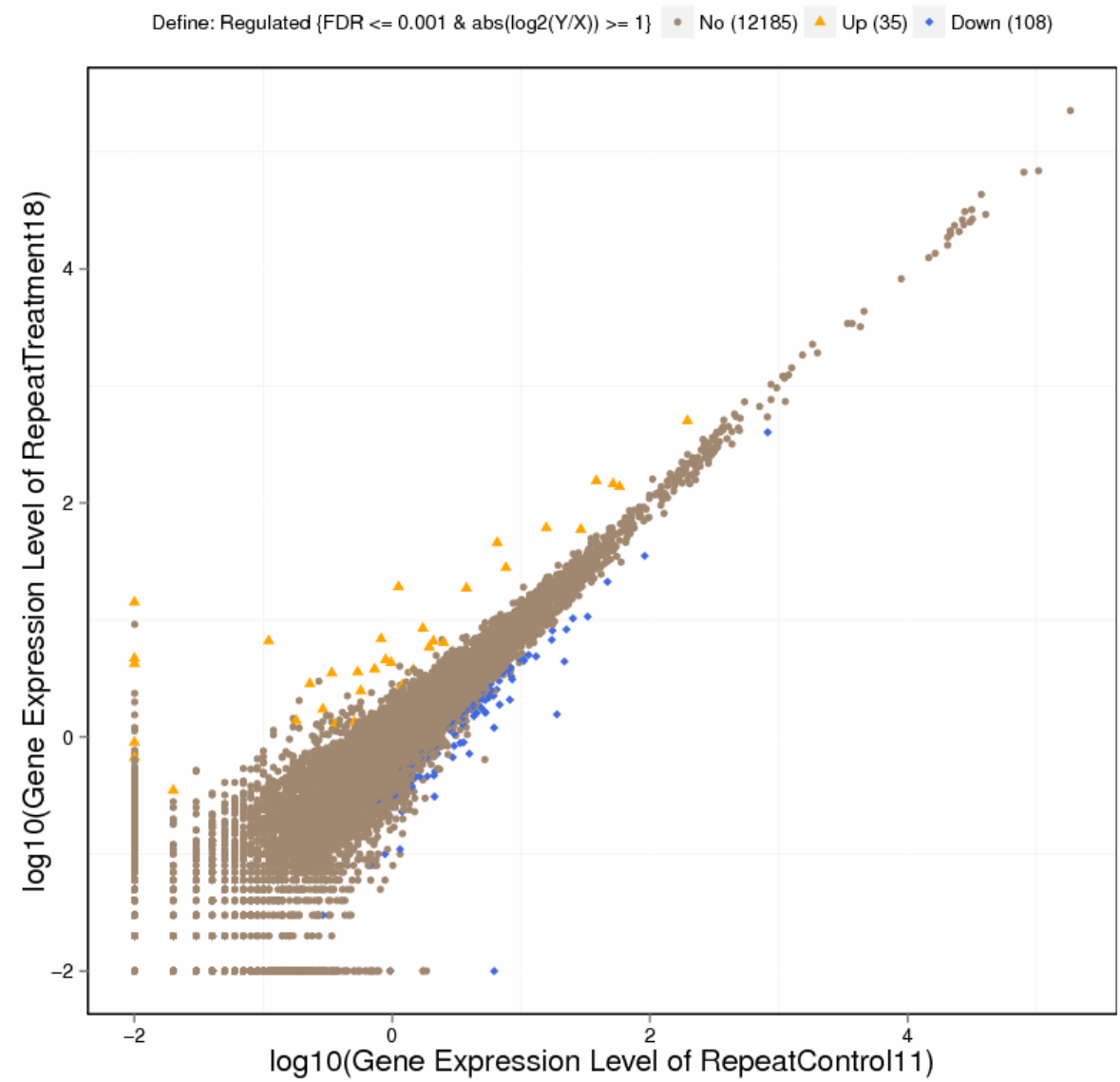

Figure 5. 4: Differentially expressed genes (DEG) between control 11 and treated 18 with pairwise comparisons.

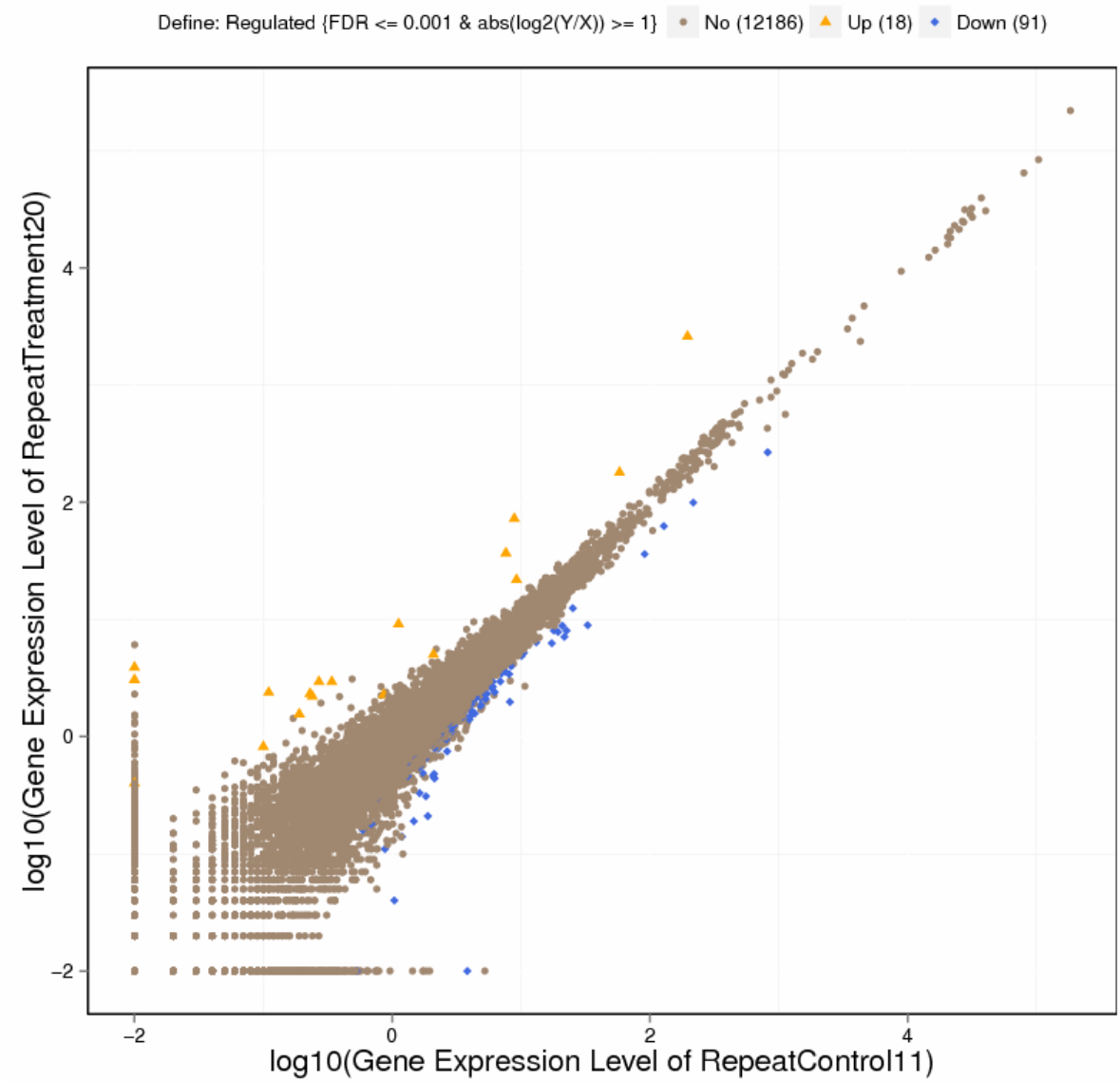

Figure 5. 5: Differentially expressed genes (DEG) between control 11 and treated 20 with pairwise comparisons.

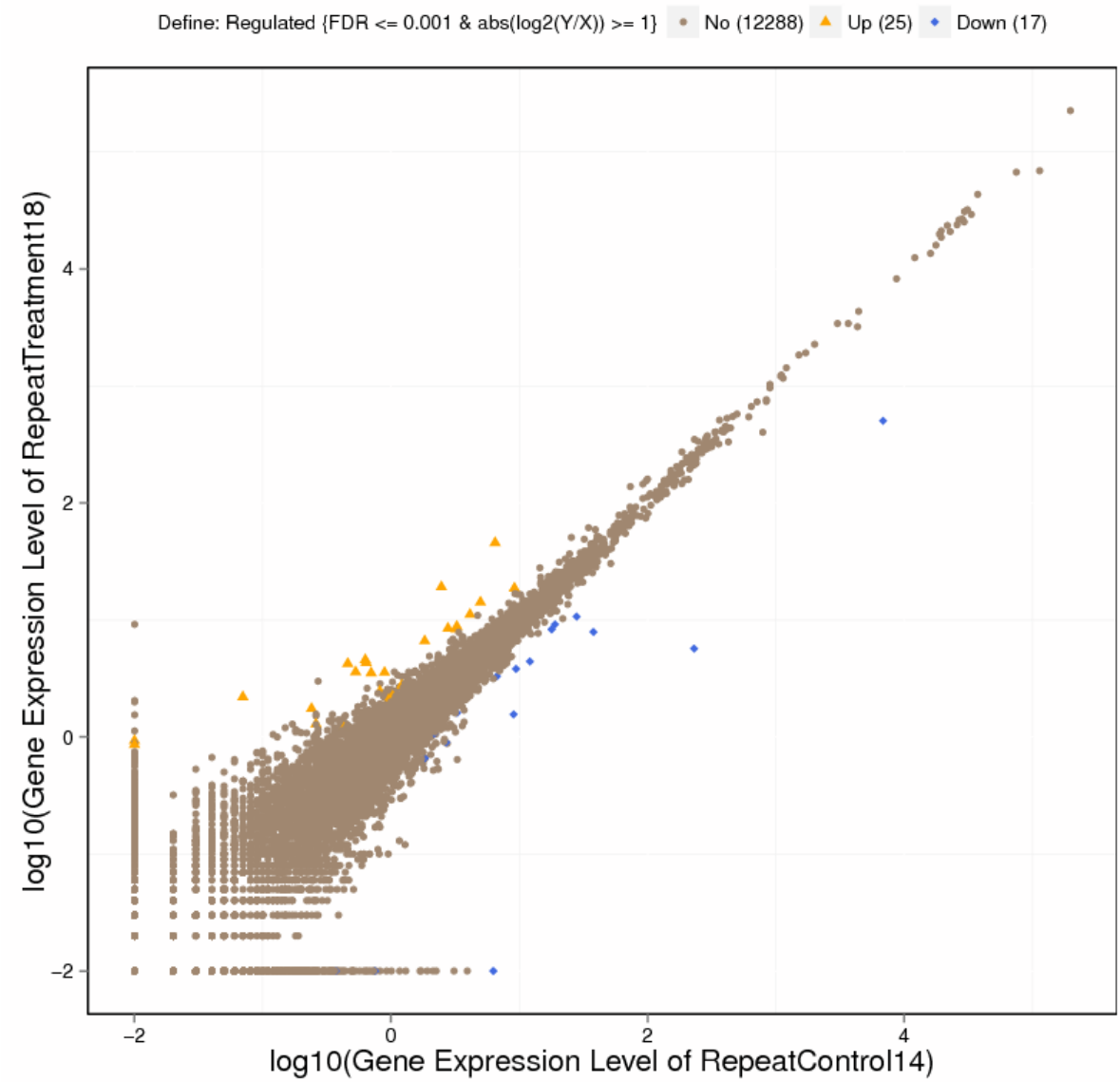

Figure 5. 6: Differentially expressed genes (DEG) between control 14 and treated 18 with pairwise comparisons.

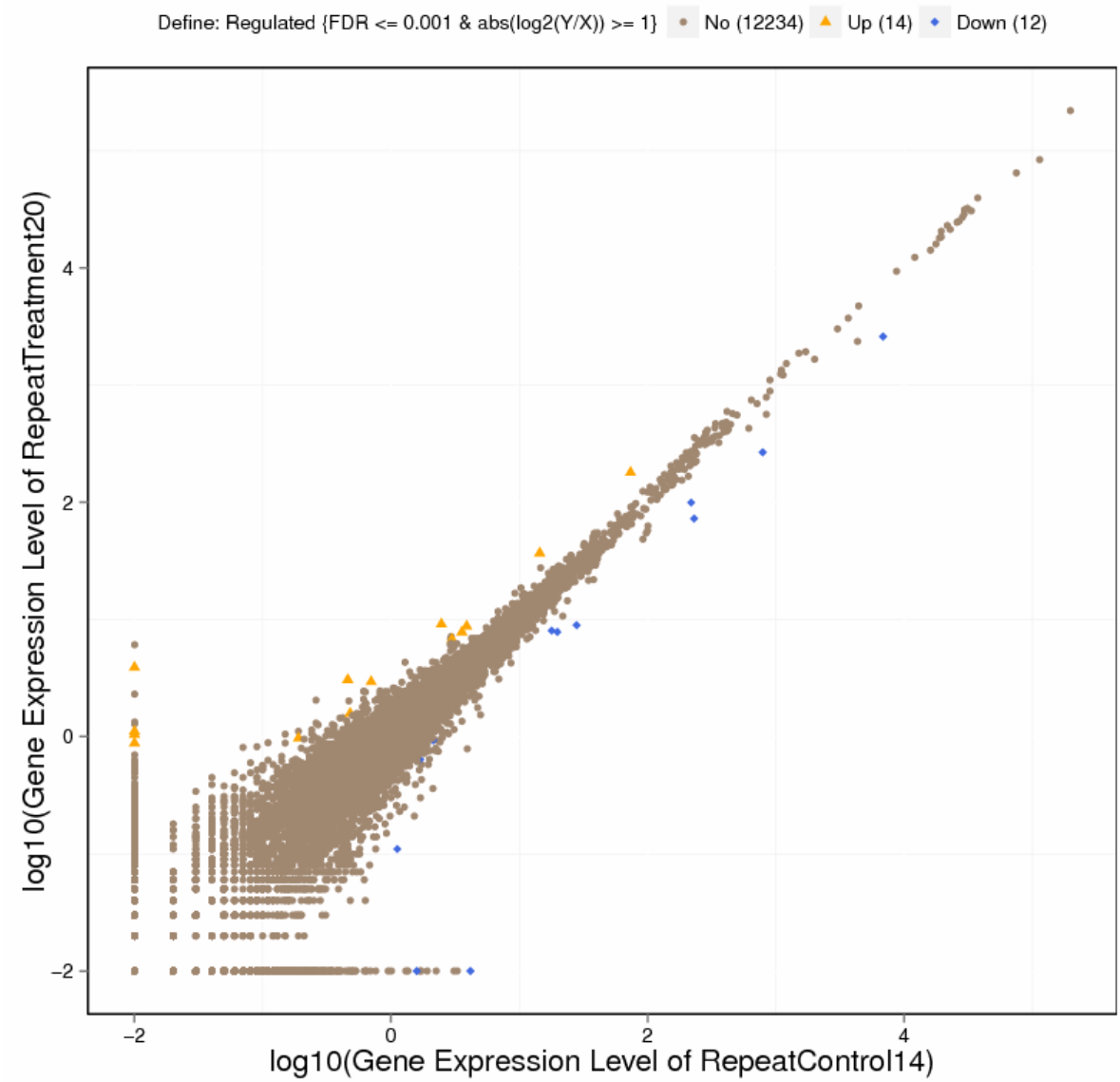

Figure 5. 7: Differentially expressed genes (DEG) between control 14 and treated 20 with pairwise comparisons.

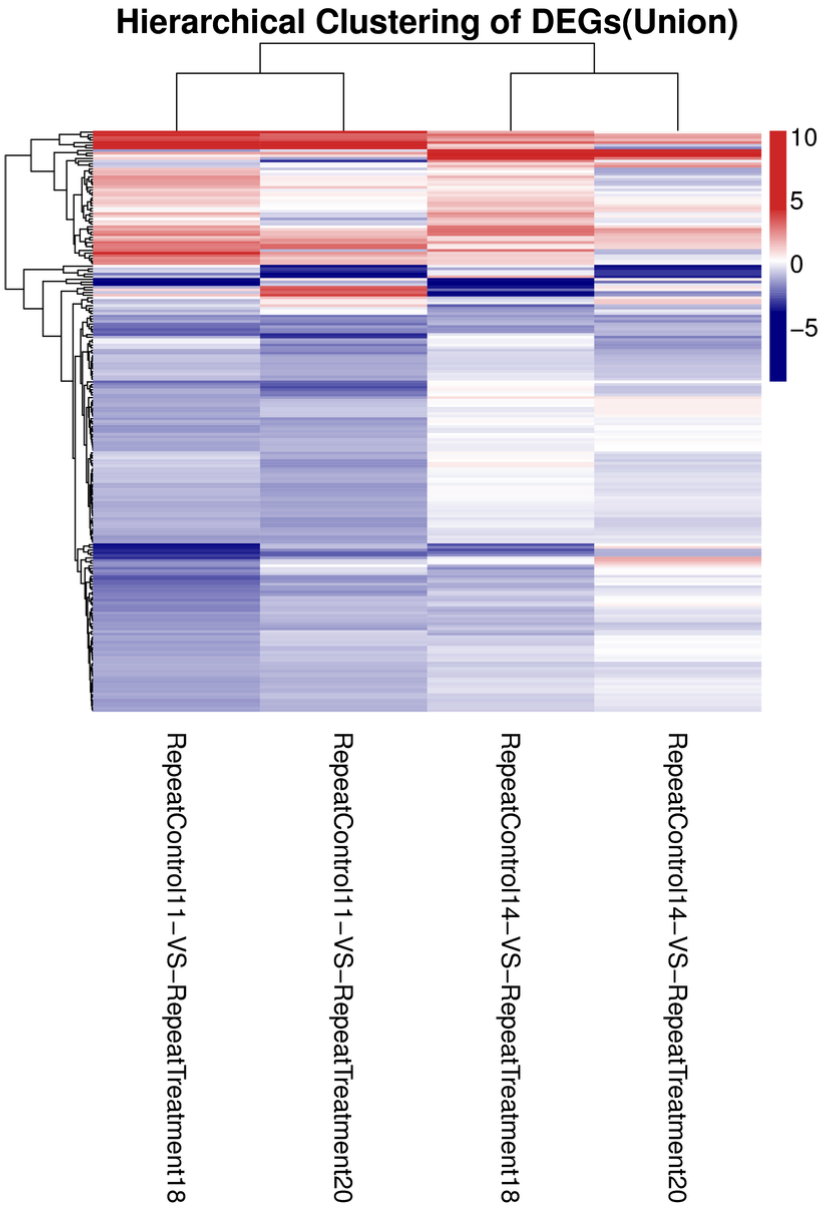

Figure 5. 8: Heatmap of clustering analysis of differentially expressed genes using Java Treeview software. Red colour indicates up-regulated genes; blue indicates down-regulated genes; white indicates no change. Pairwise comparisons are represented in each column, whereas the rows represent DEGs. Branches on the left represent gene clusters, which are based on the expression patterns.

5.4.2.4. Pathway enrichment analysis

Deep analysis of the RNA-Seq data provided by BGI was carried out using Cytoscape software with a ClueGo plugin. Only Significant ($P<0.05$) affected gene ontology (GO) from KEGG pathway was selected. The genes that showed at least two-fold change in comparison with the control were only considered in this analysis. A summary of the ClueGo results is shown in Figures 5.9-5.12, Tables 5.9-5.12. When comparing control 11 with treated 18, there were 1, 5, 1 significant GO terms associated with all genes, up-regulated genes, and down-regulated genes, respectively. On the other hand, comparison of control 11 vs treated 20 showed 12 GO terms associated with all genes together, only 2 GO terms were associated with up-regulated genes, and 9 GO terms associated with down-regulated genes. The two treated samples were then compared with control 14 to investigate the trend of the results. A comparison of control 14 vs treated 18 produced 5 GO terms associated with all genes in general, 4 GO terms with only up-regulated genes, and no significant GO terms were affected by down-regulated genes. The last comparison was with control 14 vs treated 20 and resulted in 3 GO terms associated with all genes, 1 GO term associated with both up-regulated genes, and down-regulated genes.

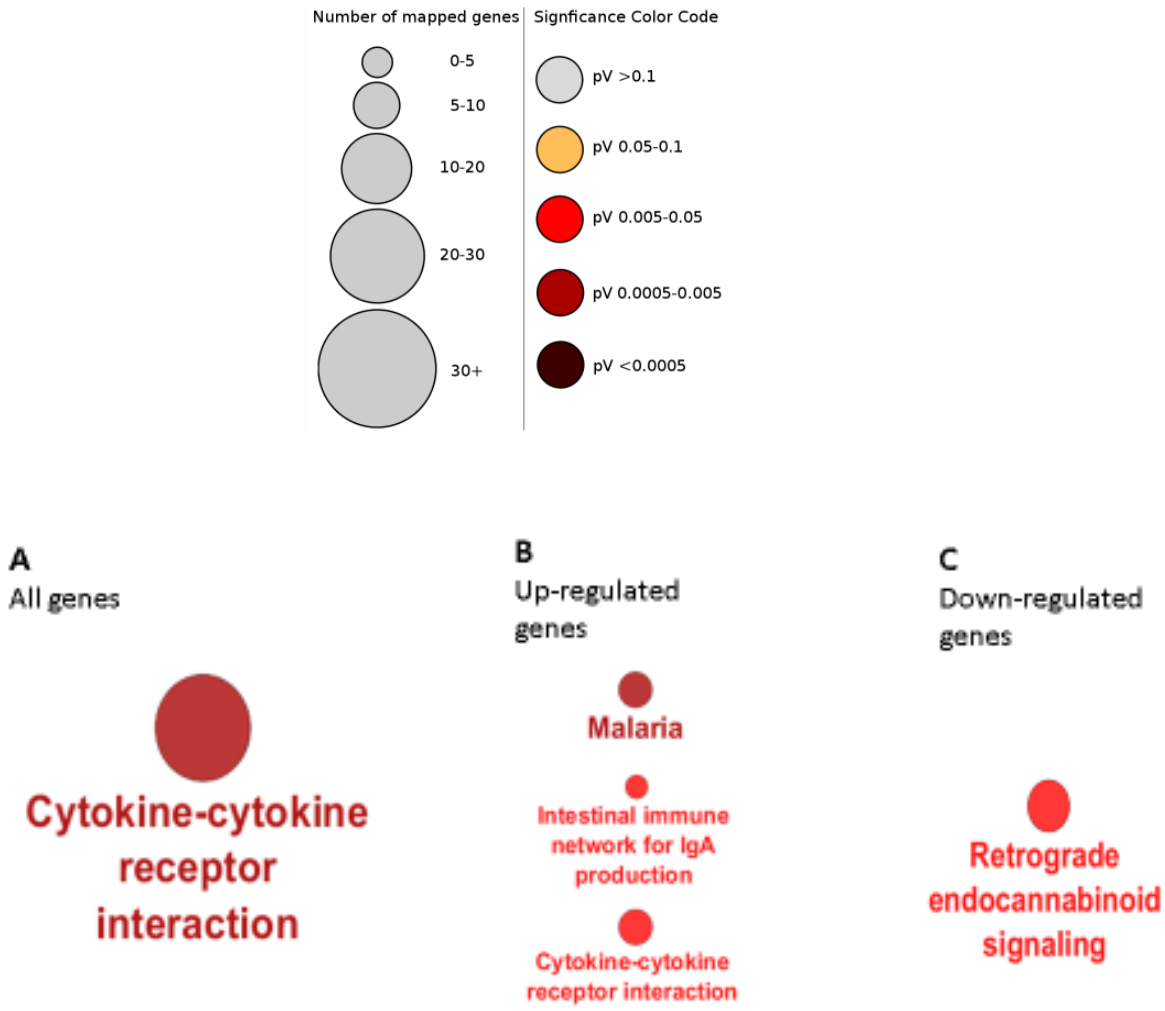

Figure 5.9: Cluster results obtained from Cytoscape GlueGO using DEGs in the control 11 vs treated 18. (A) Represents all the DEGs, up-regulated, and down-regulated combined together. (B) Represents up-regulated DEGs alone. (C) Represents down-regulated DEGs alone. Size of the circles is directly related to the number of genes in each GO, the circle's colour is linked to the significance of the affected pathway.

Table 5.9: Lists of significant genes linked with particular gene ontology when comparing control 11 vs treated 18. The number of genes involved in particular GO from the submitted list is indicated, the percentage is the proportion of affected genes in this experiment from the total number of genes associated with that KEGG pathway.

KEGG Pathway	P-value	(%)	Number of genes	List of genes
All genes (up-regulated, and down-regulated are combined together)				
Cytokine-cytokine receptor interaction	0.000005	14.93	33	*Ccl19, Ccl20, Ccl7, Ccr1, Ccr10, Ccr5, Ccr7, Ccr9, Cd40, Cd40lg, Clcf1, Csf2ra, Csf2rb, Cxcl10, Cxcl13, Cxcr3, Flt3, Hgf, Ifnlr1, Il12rb1, Il17rb, Il18, Il1b, Il20ra, Il23a, Lep, Ngfr, Tnfrsf17, Tnfrsf19, Tnfrsf25, Tnfrsf4, Tnfsf13b, Tnfsf9*
Up-regulated genes				
Cytokine-cytokine receptor interaction	0.0002	8.14	18	*Ccl20, Ccr1, Ccr5, Ccr9, Cd40, Cd40lg, Csf2rb, Cxcl13, Cxcr3, Flt3, Hgf, Il17rb, Il1b, Lep, Tnfrsf17, Tnfrsf19, Tnfrsf4, Tnfsf13b*
Intestinal immune network for IgA production	0.0001	16.33	8	*Ccr9, Cd40, Cd40lg, Itga4, RT1-DMb, RT1-DOb, Tnfrsf17, Tnfsf13b*
Malaria	0.00001	16.95	10	*Cd40, Cd40lg, Hba-a1, Hbb, Hbb-b1, Hgf, Il1b, Klrb1b, LOC689064, Thbs2*
Down-regulated genes				
Retrograde endocannabinoid signalling	0.0005	10.68	11	*Gabrb3, Gabrg2, Gabrr3, Gnb3, Gng3, Gria4, Kcnj3, Kcnj9, Mapk10, Prkcb, Slc17a8*

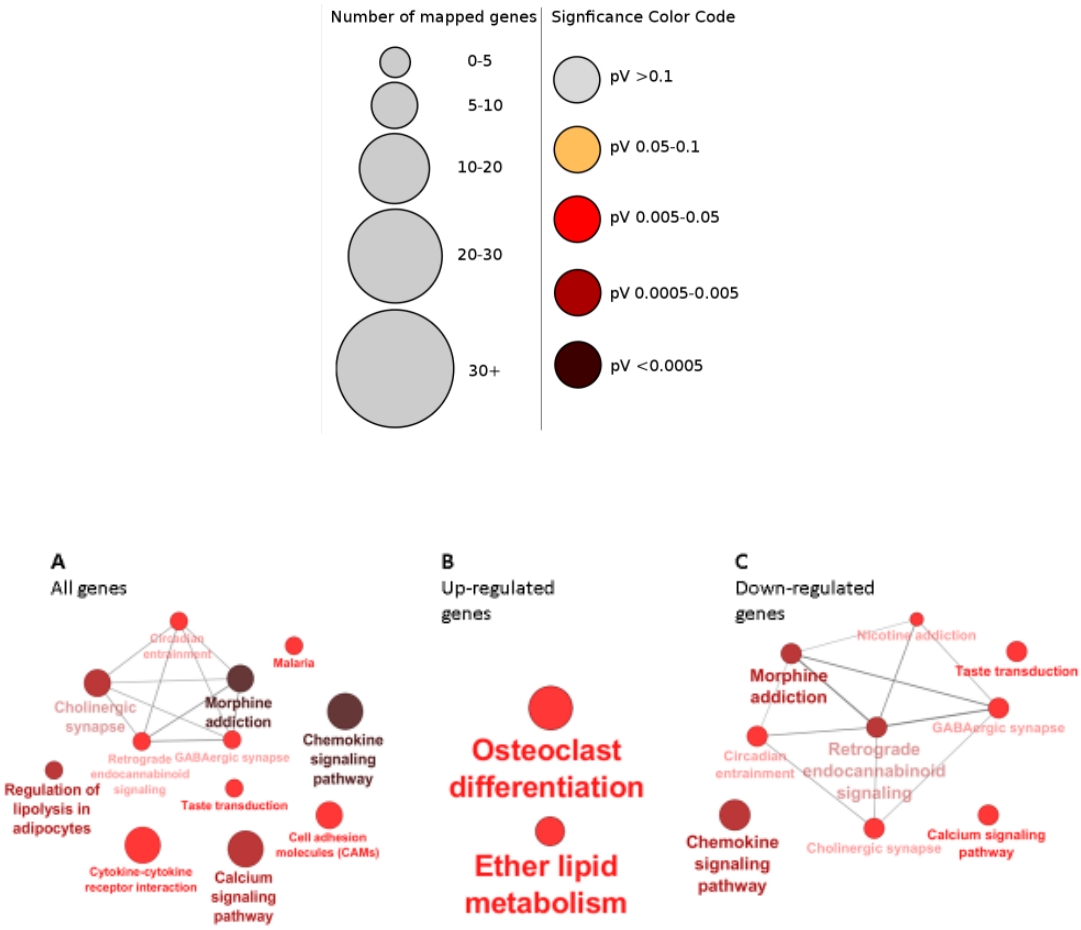

Figure 5.10: Cluster results obtained from Cytoscape GlueGO using DEGs in the control 11 vs treated 20. (A) Represents all the DEGs, up-regulated, and down-regulated are combined together. (B) Represents up-regulated DEGs alone. (C) Represents down-regulated DEGs alone. Size of the circles is directly related to the number of genes in each GO, the circle's colour is linked to the significance of the affected pathway.

Table 5.10: Lists of significant genes linked with particular gene ontology when comparing control 11 vs treated 20. The number of genes involved in particular GO from the submitted list is indicated, the percentage is the proportion of affected genes in this experiment from the total number of genes associated with that KEGG pathway.

KEGG Pathway	P-value	(%)	No. of genes	List of genes
All genes (up-regulated, and down regulated are combined together)				
Calcium signalling pathway	0.00001	16.04	30.00	*Adcy2, Adcy4, Adcy7, Adcy8, Adrb3, Agtr1b, Atp2b2, Avpr1a, Avpr1b, Cacna1b, Cacna1c, Cacna1g, Cacna1h, Camk2b, Camk4, Chrna7, Gna15, Hrh1, Nos1, Oxtr, P2rx2, P2rx6, Pde1a, Pde1b, Pde1c, Phkg1, Plcd4, Slc8a3, Tbxa2r, Tnnc1*
Cytokine-cytokine receptor interaction	0.00007	14.48	32.00	*Amhr2, Ccl19, Ccl2, Ccl28, Ccl7, Ccr1, Ccr10, Ccr5, Ccr7, Cntfr, Cxcl11, Cxcr5, Cxcr6, Flt3lg, Hgf, Il10ra, Il12rb1, Il12rb2, Il18, Il18r1, Il1b, Il20ra, Il20rb, Il23a, Il2ra, Il2rg, Osm, Pf4, Tnfrsf18, Tnfrsf19, Tnfrsf25, Tnfrsf4*
Malaria	0.00004	23.73	14.00	*Ccl2, Comp, Hba-a1, Hgf, Il18, Il1b, Klrb1a, Klrk1, LOC689064, RGD1565355, Sele, Selp, Thbs3, Tlr4*
Chemokine signalling pathway	0.00000005	19.10	34.00	*Adcy2, Adcy4, Adcy7, Adcy8, Akt3, Ccl19, Ccl2, Ccl28, Ccl7, Ccl9, Ccr1, Ccr10, Ccr5, Ccr7, Cxcl1, Cxcl11, Cxcr5, Cxcr6, Gnb3, Gnb5, Gng3, Gng8, Grk3, Hck, Pf4, Pik3cd, RSA-14-44, Rac2, Rasgrp2, Shc2, Shc3, Shc4, Vav1, Was*
Cell adhesion molecules (CAMs)	0.00019	15.12	26.00	*Cd274, Cd80, Cd86, Cldn1, Cldn15, Cldn20, Cldn23, Cntn2, Itgb8, Mpz, Ncam1, Nectin1, Negr1, Nlgn2, Nrxn1, Nrxn2, Ntng2, RT1-CE1, RT1-CE15, RT1-CE2, RT1-DMb, RT1-DOa, RT1-M1-2, Sele, Selp, Vtcn1*
Taste transduction	0.000034	20.22	18.00	*Adcy4, Adcy8, Cacna1c, Gabra4, Gnat3, Gnb3, Htr1b, P2rx2, Pde1a, Pde1b, Pde1c, Scn2a, Scn3a, Scnn1a, Tas1r1, Tas1r3, Tas2r137, Trpm5*
Regulation of lipolysis in adipocytes	0.000009	25.42	15.00	*Adcy2, Adcy4, Adcy7, Adcy8, Adora1, Adrb3, Akt3, Aqp7, Cga, Irs3, Npy, Npy1r, Pik3cd, Plin1, Tshr*
Circadian entrainment	0.0001	18.56	18.00	*Adcy2, Adcy4, Adcy7, Adcy8, Cacna1c, Cacna1g, Cacna1h,*

				Camk2b, Gnb3, Gnb5, Gng3, Gng8, Gria4, Gucy1b2, Kcnj3, Kcnj9, Nos1, Per3
Retrograde endocannabinoid signalling	0.00008	18.45	19.00	*Adcy2, Adcy4, Adcy7, Adcy8, Cacna1b, Cacna1c, Gabra4, Gabrg1, Gabrg2, Gabrr3, Gnb3, Gnb5, Gng3, Gng8, Gria4, Kcnj3, Kcnj9, Mapk11, Slc17a8*
Cholinergic synapse	0.00003	18.75	21.00	*Ache, Adcy2, Adcy4, Adcy7, Adcy8, Akt3, Cacna1b, Cacna1c, Camk2b, Camk4, Chrna3, Chrna7, Chrnb2, Gnb3, Gnb5, Gng3, Gng8, Kcnj12, Kcnj3, Pik3cd, Slc5a7*
GABAergic synapse	0.0001	18.89	17.00	*Adcy2, Adcy4, Adcy7, Adcy8, Cacna1b, Cacna1c, Gabra4, Gabrg1, Gabrg2, Gabrr3, Gad2, Gnb3, Gnb5, Gng3, Gng8, Plcl1, Slc38a1*
Morphine addiction	0.0000001	22.83	21.00	*Adcy2, Adcy4, Adcy7, Adcy8, Adora1, Cacna1b, Gabra4, Gabrg1, Gabrg2, Gabrr3, Gnb3, Gnb5, Gng3, Gng8, Grk3, Kcnj3, Kcnj9, Pde1a, Pde1b, Pde1c, Pde7b*
Up-regulated genes				
Ether lipid metabolism	0.0002	15.91	7.00	*Chpt1, Enpp6, Lpcat2, Pafah1b3, Pafah2, Pla2g3, Pla2g5*
Osteoclast differentiation	0.0004	8.96	12.00	*Camk4, Ctsk, Fosl1, Il1b, Lilra5, Lilrb3l, Mapk11, Ncf2, Nox1, Oscar, Spi1, Trem2*
Down-regulated genes				
Taste transduction	0.0003	13.48	12.00	*Adcy4, Adcy8, Cacna1c, Gabra4, Gnat3, Gnb3, Htr1b, Pde1b, Scn3a, Tas1r1, Tas1r3, Trpm5*
Circadian entrainment	0.00004	14.43	14.00	*Adcy4, Adcy7, Adcy8, Cacna1c, Cacna1g, Cacna1h, Camk2b, Gnb3, Gng3, Gria4, Kcnj3, Kcnj9, Nos1, Per3*
Retrograde endocannabinoid signalling	0.00002	14.56	15.00	*Adcy4, Adcy7, Adcy8, Cacna1b, Cacna1c, Gabra4, Gabrg1, Gabrg2, Gabrr3, Gnb3, Gng3, Gria4, Kcnj3, Kcnj9, Slc17a8*
Cholinergic synapse	0.00005	13.39	15.00	*Ache, Adcy4, Adcy7, Adcy8, Akt3, Cacna1b, Cacna1c, Camk2b, Chrnb2, Gnb3, Gng3, Kcnj12, Kcnj3, Pik3cd, Slc5a7*
GABAergic synapse	0.00008	14.44	13.00	*Adcy4, Adcy7, Adcy8, Cacna1b, Cacna1c, Gabra4, Gabrg1, Gabrg2, Gabrr3, Gad2, Gnb3, Gng3, Plcl1*
Morphine addiction	0.000005	16.30	15.00	*Adcy4, Adcy7, Adcy8, Cacna1b, Gabra4, Gabrg1, Gabrg2,*

				Gabrr3, Gnb3, Gng3, Grk3, Kcnj3, Kcnj9, Pde1b, Pde7b
Nicotine addiction	0.0002	20.00	8.00	*Cacna1b, Chrnb2, Gabra4, Gabrg1, Gabrg2, Gabrr3, Gria4, Slc17a8*

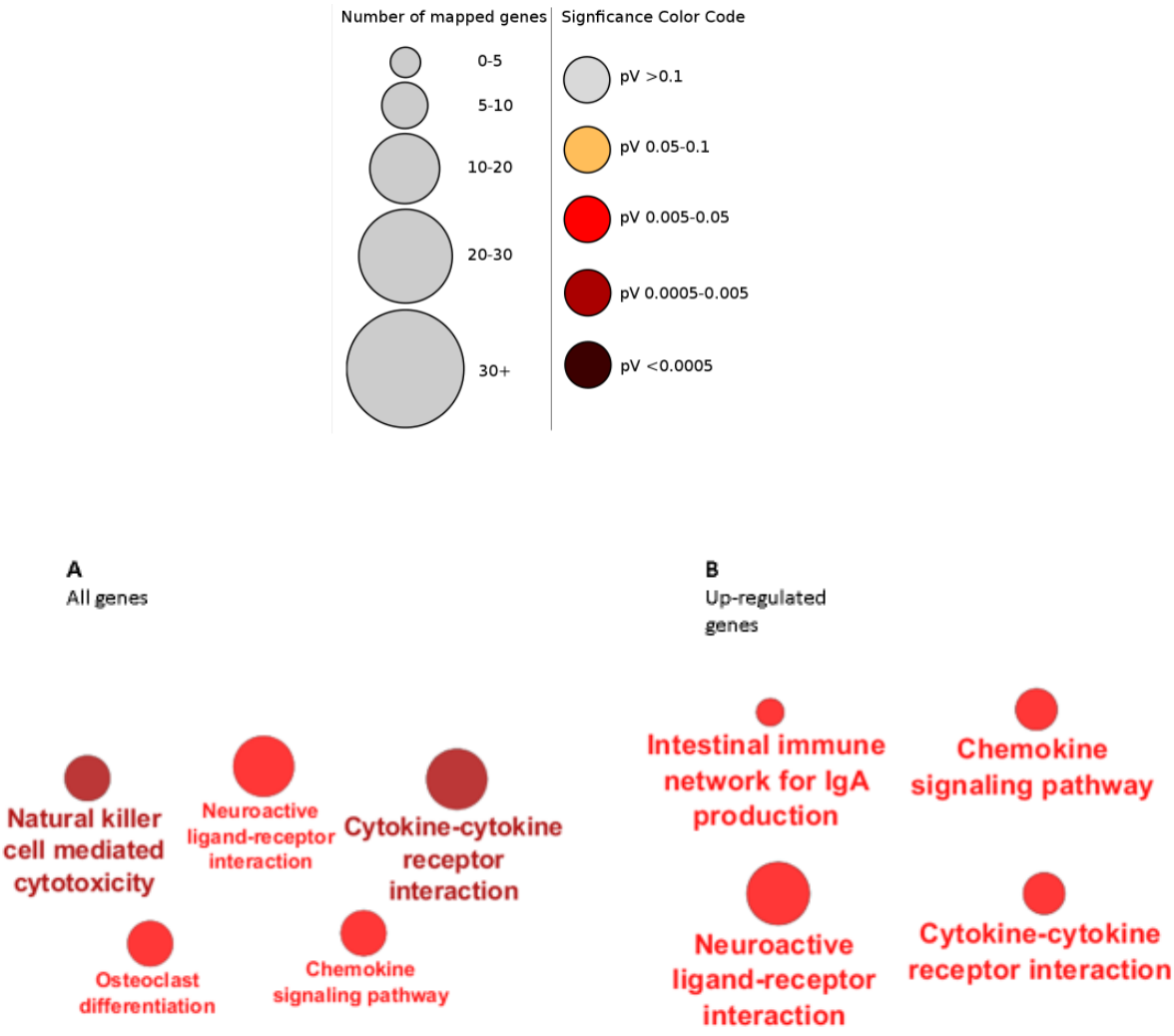

Figure 5.11: Cluster results obtained from Cytoscape GlueGO using DEGs in the control 14 vs treated 18. (A) Represents all the DEGs, up-regulated, and down-regulated are combined together. (B) Represents up-regulated DEGs alone. Size of the circles is directly related to the number of genes in each GO, the circle's colour is linked to the significance of the affected pathway.

Table 5.11: Lists of significant genes linked with particular gene ontology when comparing control 14 vs treated 18. The number of genes involved in particular GO from the submitted list is indicated, the percentage is the proportion of affected genes in this experiment from the total number of genes associated with that KEGG pathway.

KEGG Pathway	P-value	(%)	No. of genes	List of genes
All genes (up-regulated, and down-regulated are combined together)				
Cytokine-cytokine receptor interaction	0.000006	15.84	35.00	*Acvr2b, Ccl20, Ccl22, Ccl27, Ccl3, Ccr10, Ccr9, Cd40, Cd40lg, Csf2ra, Csf2rb, Cxcl11, Cxcl13, Cxcl9, Cxcr3, Cxcr4, Cxcr6, Epor, Ifnlr1, Il11, Il12rb1, Il18r1, Il1b, Il20ra, Il21r, Il23a, Lep, Ngfr, Thpo, Tnfrsf18, Tnfrsf19, Tnfrsf9, Tnfsf13b, Tnfsf4, Tnfsf9*
Chemokine signalling pathway	0.00007	15.73	28.00	*Ccl20, Ccl22, Ccl27, Ccl3, Ccr10, Ccr9, Cxcl1, Cxcl11, Cxcl13, Cxcl9, Cxcr3, Cxcr4, Cxcr6, Gnb4, Gng13, Gng7, Gngt2, Grk3, Grk4, Hck, Pak1, Pik3r3, Prkcb, Rac2, Rasgrp2, Shc3, Src, Vav3*
Neuroactive ligand-receptor interaction	0.00009	13.36	39.00	*Adora2a, Adra2a, Adrb3, Agtr1b, C5ar1, Chrna2, Chrna3, Cysltr1, Ednra, F2rl2, F2rl3, Gabra4, Gabrb2, Gabrb3, Gabrg1, Galr1, Galr3, Gcgr, Glp2r, Glra2, Gpr83, Grik5, Grin1, Grin2d, Hcrtr1, Hrh1, Hrh3, Lep, Lpar1, P2rx2, P2rx7, P2ry13, Ptger2, Ptger4, Ptgir, Pth1r, S1pr4, Tshr, Vipr2*
Osteoclast differentiation	0.0002	16.42	22.00	*Blnk, Btk, Fcgr1a, Fcgr2a, Fcgr2b, Fcgr3a, Fosl1, Fosl2, Il1b, Lck, Lcp2, Lilra5, Lilrb4, Ncf4, Nfatc2, Nox1, Oscar, Pik3r3, Pparg, Socs1, Spi1, Tyrobp*
Natural killer cell mediated cytotoxicity	0.00002	19.80	20.00	*Bid, Fcgr2a, Fcgr3a, Gzmb, Klrd1, Klrk1, Lat, Lck, Lcp2, Ncr1, Nfatc2, Pak1, Pik3r3, Prkcb, Rac2, Shc3, Tnfrsf10b, Tyrobp, Vav3, Zap70*
Up-regulated genes				
Cytokine-cytokine receptor interaction	0.0004	8.60	19.00	*Acvr2b, Ccl20, Ccl27, Ccr9, Cd40, Cd40lg, Csf2rb, Cxcl13, Cxcl9, Cxcr3, Cxcr4, Cxcr6, Epor, Il1b, Il21r, Lep, Tnfrsf18, Tnfrsf19, Tnfsf13b*
Chemokine signalling pathway	0.0002	9.55	17.00	*Ccl20, Ccl27, Ccr9, Cxcl1, Cxcl13, Cxcl9, Cxcr3, Cxcr4, Cxcr6, Gnb4, Gng13, Gngt2, Hck, Rac2, Shc3, Src, Vav3*
Neuroactive ligand-receptor interaction	0.0002	8.22	24.00	*Adrb3, Agtr1b, C5ar1, Cysltr1, F2rl2, Gabra4, Gabrb2, Gabrg1, Glp2r, Glra2, Grik5, Grin1, Grin2d,*

				Hcrtr1, Hrh1, Hrh3, Lep, Lpar1, P2ry13, Ptger4, Pth1r, S1pr4, Tshr, Vipr2
Intestinal immune network for IgA production	0.0003	16.33	8.00	*Ccr9, Cd40, Cd40lg, Cd86, Cxcr4, Itga4, RT1-Bb, Tnfsf13b*

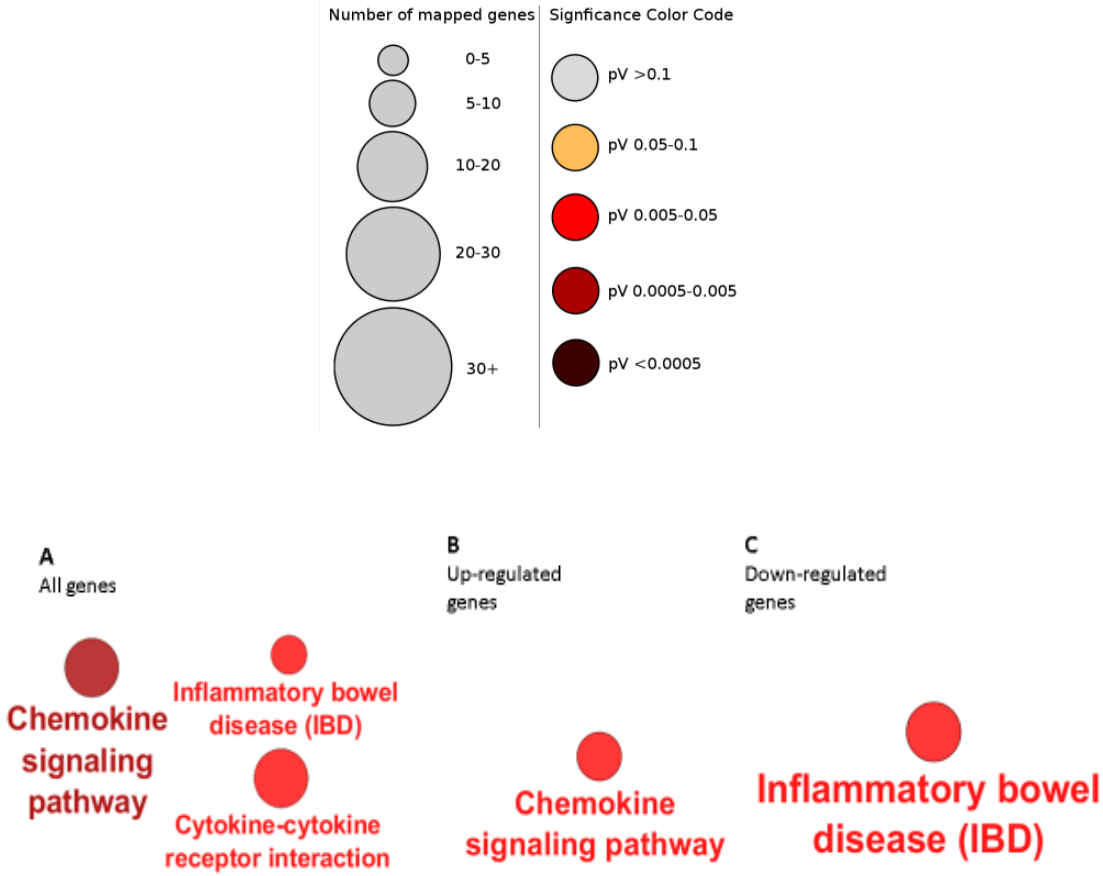

Figure 5.12: Cluster results obtained from Cytoscape GlueGO using DEGs in the control 14 vs treated 20. (A) Represents all the DEGs, up-regulated, and down-regulated are combined together. (B) Represents up-regulated DEGs alone. (C) Represents down-regulated DEGs alone. Size of the circles is directly related to the number of genes in each GO, the circle's colour is linked to the significance of the affected pathway.

Table 5.12: Lists of significant genes linked with particular gene ontology when comparing control 14 vs treated 20. The number of genes involved in particular GO from the submitted list is indicated, the percentage is the proportion of affected genes in this experiment from the total number of genes associated with that KEGG pathway.

KEGG Pathway	P-value	(%)	No. of genes	List of genes
All genes (up-regulated, and down-regulated are combined together)				
Cytokine-cytokine receptor interaction	0.0002	13.12	29.00	*Acvr2b, Amhr2, Ccl2, Ccl22, Ccl27, Ccl28, Ccl3, Ccr10, Cntfr, Cxcl10, Cxcr5, Il10ra, Il11, Il12rb1, Il12rb2, Il17rb, Il18r1, Il1b, Il20rb, Il21r, Il23a, Il2ra, Osm, Pf4, Thpo, Tnfrsf17, Tnfrsf19, Tnfrsf9, Tnfsf4*
Chemokine signalling pathway	0.00002	15.17	27.00	*Adcy7, Akt3, Ccl2, Ccl22, Ccl27, Ccl28, Ccl3, Ccl9, Ccr10, Cxcl1, Cxcl10, Cxcr5, Gnb4, Gng13, Gng3, Gng7, Gng8, Gngt2, Hck, Pak1, Pf4, Pik3r3, RSA-14-44, Rasgrp2, Shc4, Vav3, Was*
Inflammatory bowel disease (IBD)	0.0002	20.00	13.00	*Il12rb1, Il12rb2, Il18r1, Il1b, Il21r, Il23a, LOC688090, RT1-Bb, RT1-DOb, Stat4, Tbx21, Tlr4, Tlr5*
Up-regulated genes				
Chemokine signalling pathway	0.0006	7.87	14.00	*Ccl2, Ccl27, Ccl9, Cxcl1, Cxcl10, Cxcr5, Gnb4, Gng13, Gng8, Gngt2, Hck, RSA-14-44, Shc4, Vav3*
Down-regulated genes				
Inflammatory bowel disease (IBD)	0.00006	15.38	10.00	*Il12rb1, Il12rb2, Il18r1, Il23a, LOC688090, RT1-DOb, Stat4, Tbx21, Tlr4, Tlr5*

After analysing the results using Cytoscape ClueGo plugin, cytokine-cytokine receptor interaction was the only common KEGG pathway significantly affected among the four control-treated comparisons. Despite the existence of the cytokine-cytokine receptor interaction pathway in all comparisons, only two common genes were found, interleukin 1 beta (*Il1b*), and TNF receptor superfamily member 19 (*Tnfrsf19*). The log2 fold change of *Il1b* and *Tnfrsf19* are shown in Figures 5.13 and 5.14.

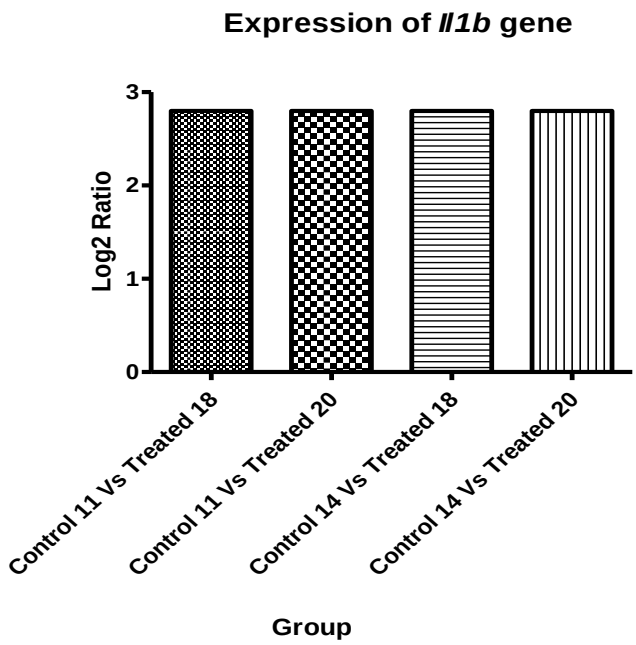

Figure 5. 13: A bar chart showing the Log2 ratio of *Il1b* RNA-Seq gene expression among the four comparisons. Log2 ratio was 2.8 for all comparisons. Tuber treatment shows up-regulated ($P < 0.05$) *Il1b* gene expression.

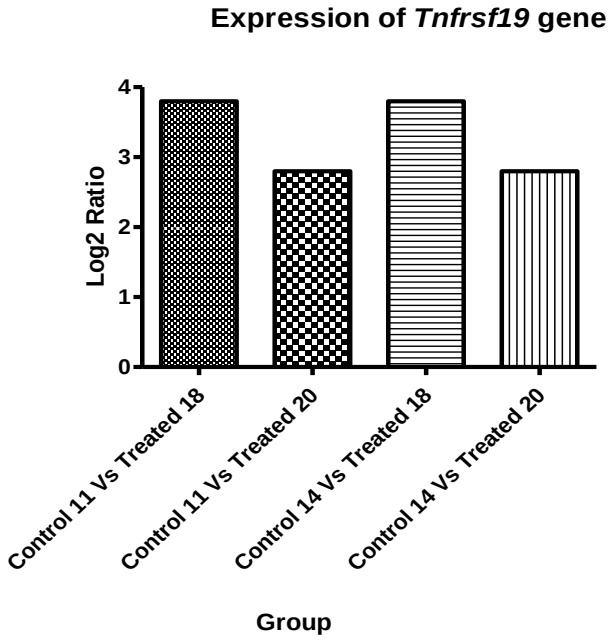

Figure 5. 14: A bar chart showing the Log2 ratio of *Tnfrsf19* RNA-Seq gene expression in pancreatic RNA among the four comparisons. Log2 ratio was 2.8 when comparing the two controls with treated 18, while a 3.8 ratio was obtained from comparing both controls with treated 20. Tuber treatment shows up-regulated ($P < 0.05$) *Tnfrsf19* gene expression.

5.4.2.5. Adiponectin

The adiponectin gene (*Adipoq*) has been up-regulated by the tuber treatment as shown in Figure 5.17. This gene is of interest in the context of diabetes and obesity as it produces the adiponectin protein which plays a fundamental role in glucose regulation and fatty acid metabolism.

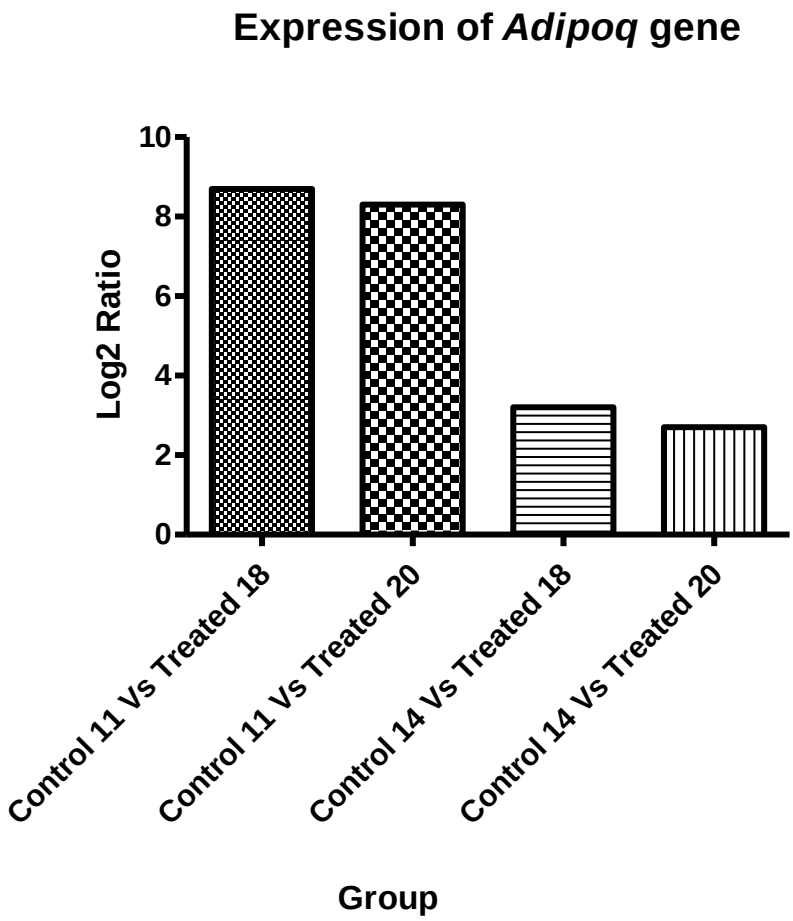

Figure 5. 15: A bar chart showing the Log2 ratio of *Adipoq* gene expression among the four comparisons. Log2 ratio was 8.5 when comparing the two treated samples with control 11, while a 3 ratio was obtained from comparing both treated samples with control 14. Tuber treatment has statistically ($P < 0.05$) up-regulated the *Adipoq* gene expression.

5.4.3. Real time quantitative PCR (RT-qPCR)

5.4.3.1. Reference gene stability

Prior to testing the control and treated cDNA samples with the RT-qPCR primers of interest, reference gene stability was established. The results were compared using the RefFinder tool which compares the results using integrated computational programmes, BestKeeper, geNorm, Normfinder and the comparative ΔΔCt method as shown in Figures 5.16-5.20. The results from the comprehensive gene stability method were examined and *Hprt1* was found to be the most stable gene out of the three assessed. *Hprt1* was therefore used as a reference gene for the RT-qPCR experiments.

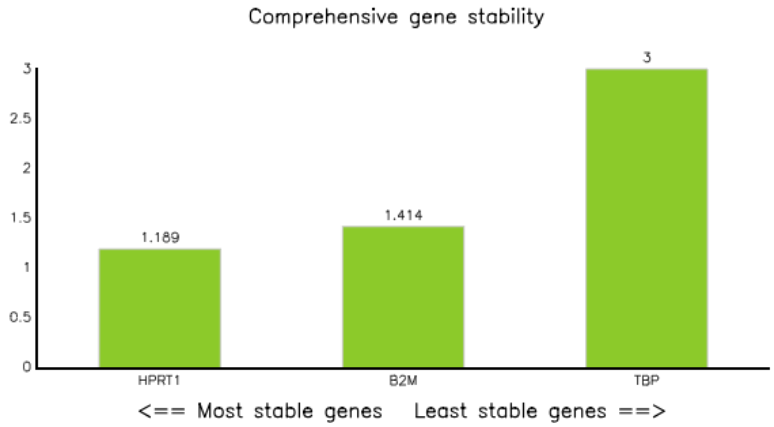

Figure 5.16: Comprehensive gene stability provided by RefFinder tool.

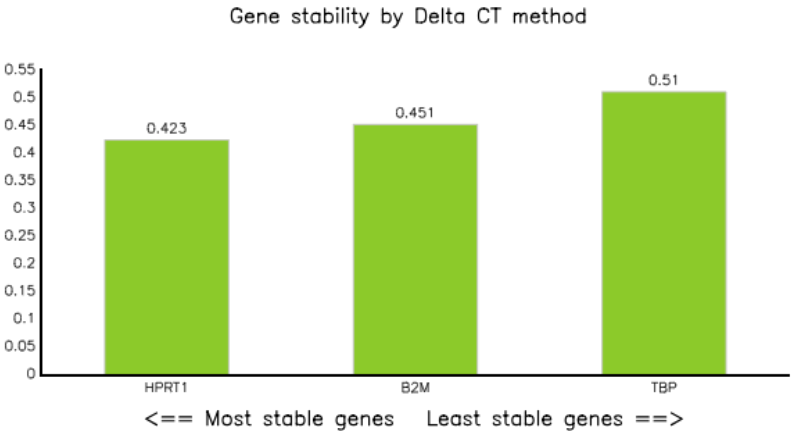

Figure 5.17: Delta CT gene stability provided by RefFinder tool.

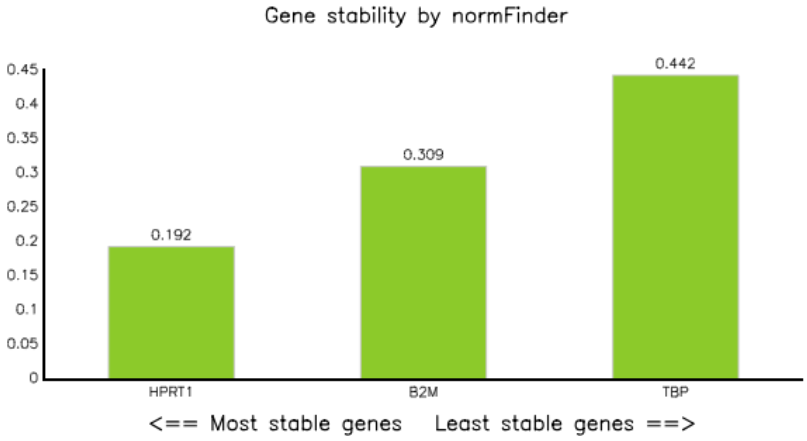

Figure 5.18: normFinder gene stability provided by RefFinder tool.

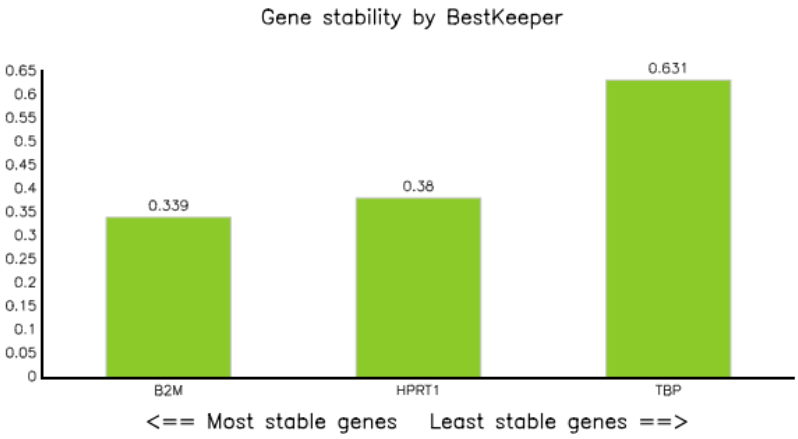

Figure 5.19: BestKeeper gene stability provided by RefFinder tool.

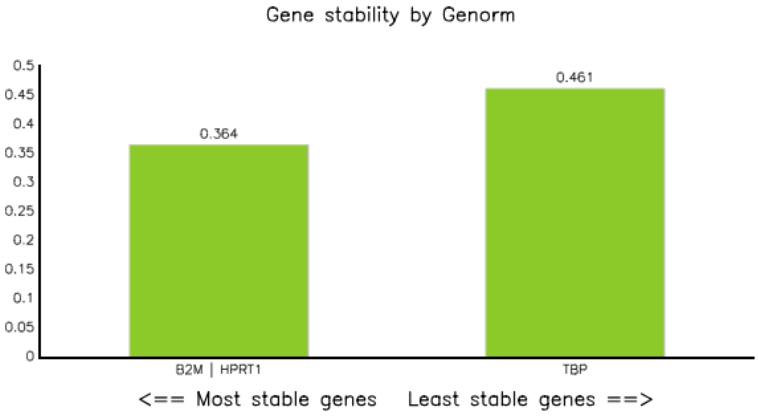

Figure 5.20: Genorm gene stability provided by RefFinder tool.

5.4.3.2. Melt curve analysis (MCA)

The primers and reaction conditions can determine the specificity of the RT-qPCR assay. It is possible that even well-designed primers can form primer-dimers or amplify non-specific products. Moreover, it is possible that the RNA samples can be contaminated with genomic DNA which can then be amplified in the RT-qPCR assay (Akey *et al.*, 2001; Ahmed *et al.*, 2017). MCA is an approach used to assess the specificity of the of RT-qPCR reactions. Cyber-green used in this RT-qPCR is only fluorescent when it is bound to double-stranded DNA (dsDNA) and not to single-stranded DNA (ssDNA) or when the dye is free in solution. The thermal cycler used for the RT-qPCR is programmed to produce melt curves following the completion of the amplification cycles. At the end of the assay run, the thermal cycler starts at a temperature above the primer melting temperature (T_m) and measures the fluorescence intensity. Then, incremental increases in the temperature of the sample are carried out and the fluorescence is measured. As the temperature rises, dsDNA becomes denatured ssDNA and this results in cyber-green dissociation and hence the fluorescence decreases (Downey, 2014). The slope change of the curve is then plotted to produce MCA for the tested samples.

All primers of interest were tested against all control and treated samples and normalised to *Hprt1* gene. Each primer was tested against non-template control (NTC), RT- and RT+.

5.4.3.2.1. Non-template control (NTC)

All of the designed primers were tested in the absence of cDNA samples to ensure the RT-qPCR reactions do not generate false positive products from contamination of the reaction or reaction components. In the MCA of NTC samples, there were no sharp single peaks generated by any of the primers as shown in Figure 5.21. This is, along with the undetermined cycle threshold (Cts) obtained confirmed that the designed primers did not generate false positive products in the PCR reactions.

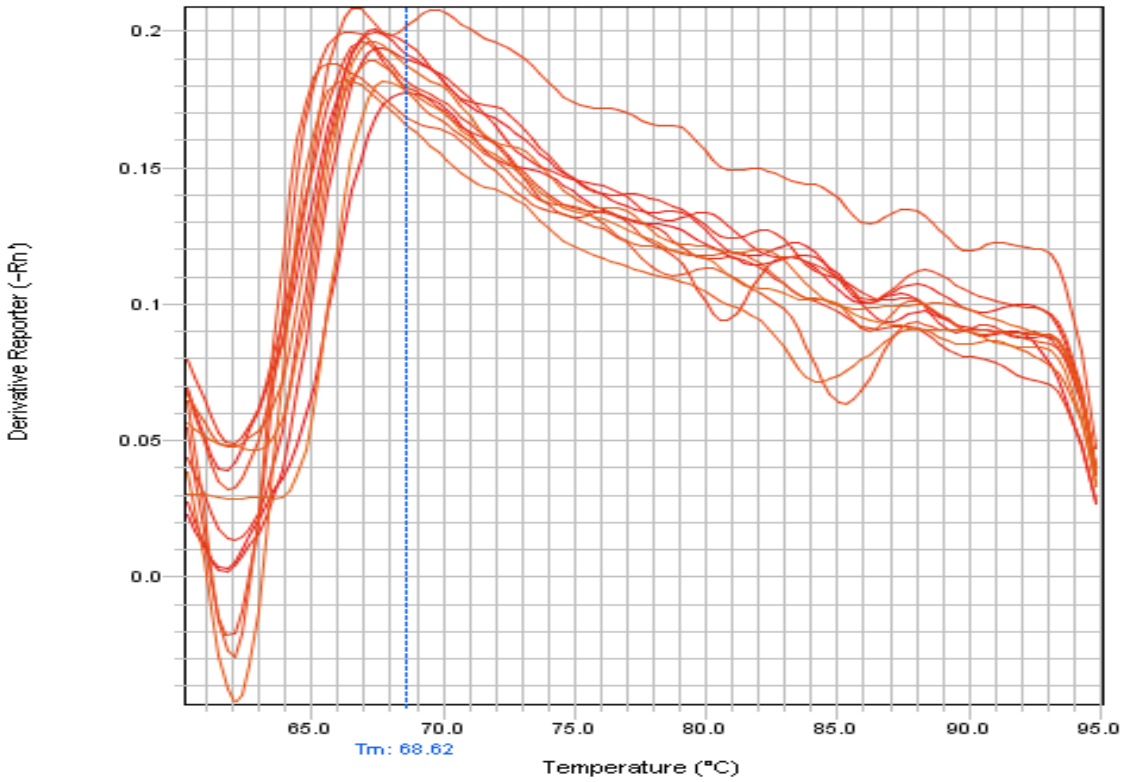

Figure 5.21: MCA of qRT-PCR products from of *Hprt1, Adipoq, IL1b, Tnfrsf19, Cd40, Cd40ig, Lep*, and *Ccl20* genes. No amplicons were generated using the primer sets for the target genes. Curves are representative of all NTC samples in the RT-qPCR assay analyses.

5.4.3.2.2. cDNA synthesis in the absence of Reverse Transcriptase (RT-)

The conversion of mRNA in the pancreatic total RNA samples to cDNA requires reverse transcriptase (RT). RT- samples, where no reverse transcriptase was used in the cDNA synthesis reaction, do not produce single peaks in the MCA unless they are contaminated with genomic DNA which may have been carried over from the RNA isolation. All the RT- samples did not produce peaks in the MCA indicating that they were not contaminated with genomic DNA and would not produce false positive PCR amplicons as in Figure 5.22.

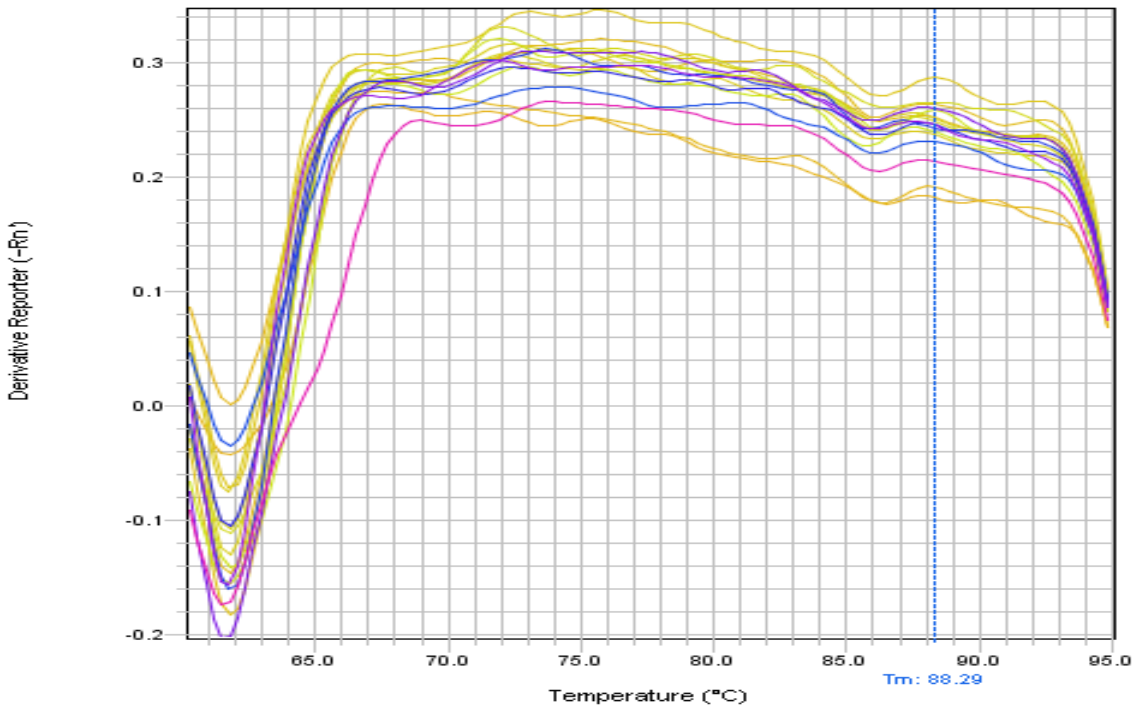

Figure 5.22: MCA of RT-qPCR products from the *Hprt1*, *Adipoq*, *IL1b*, *Tnfrsf19*, *Cd40*, *Cd40ig*, *Lep*, and *Ccl20* gene expression assays. No amplicons were generated using the primer sets for the target genes and no distinct single peaks were observed in melt curve analyses. Curves are representative of all RT- samples in the RT-qPCR assay analysis.

5.4.3.2.3. cDNA synthesis in the presence of Reverse Transcriptase (RT+)

All RNA samples were converted to cDNA in the presence of reverse transcriptase and then RT-qPCR was performed against the reference and target primers of interest. All samples showed single sharp peaks on the MCA as shown in Figures 5.23-5.30. This indicates that the designed primers were specific and selective to their target genes of interest.

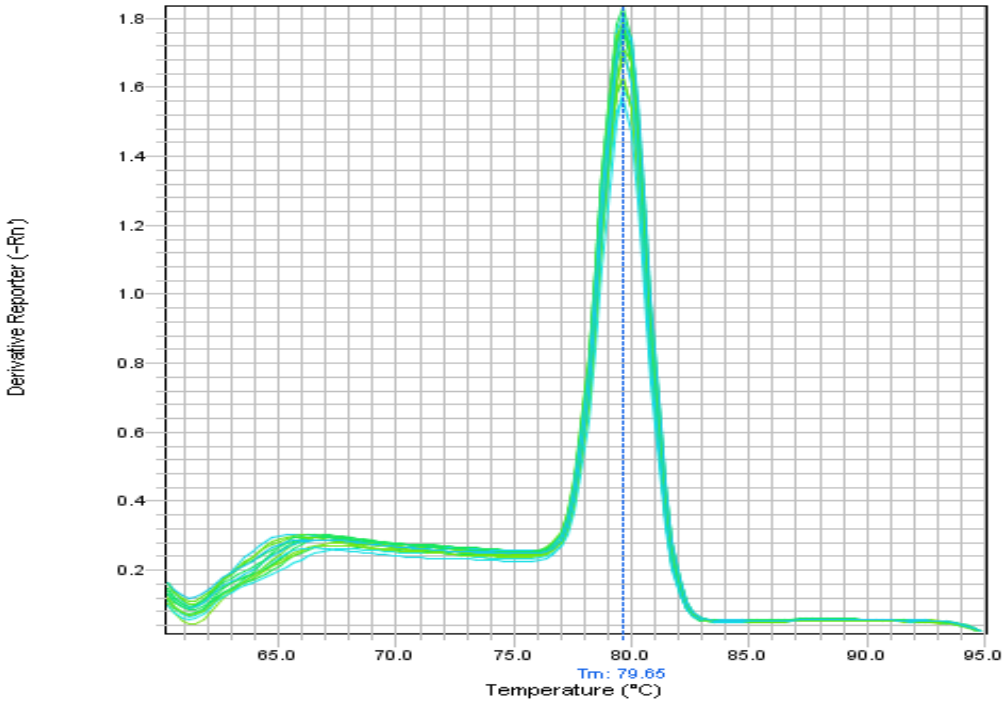

Figure 5.23: MCA of RT-qPCR products from the *Hprt1* gene expression assay. Single amplicons were generated using the primer sets for the target gene, which produced single peaks in melt curve analyses. Curves are representative of all *Hprt1* RT+ samples in the RT-qPCR assay analysis.

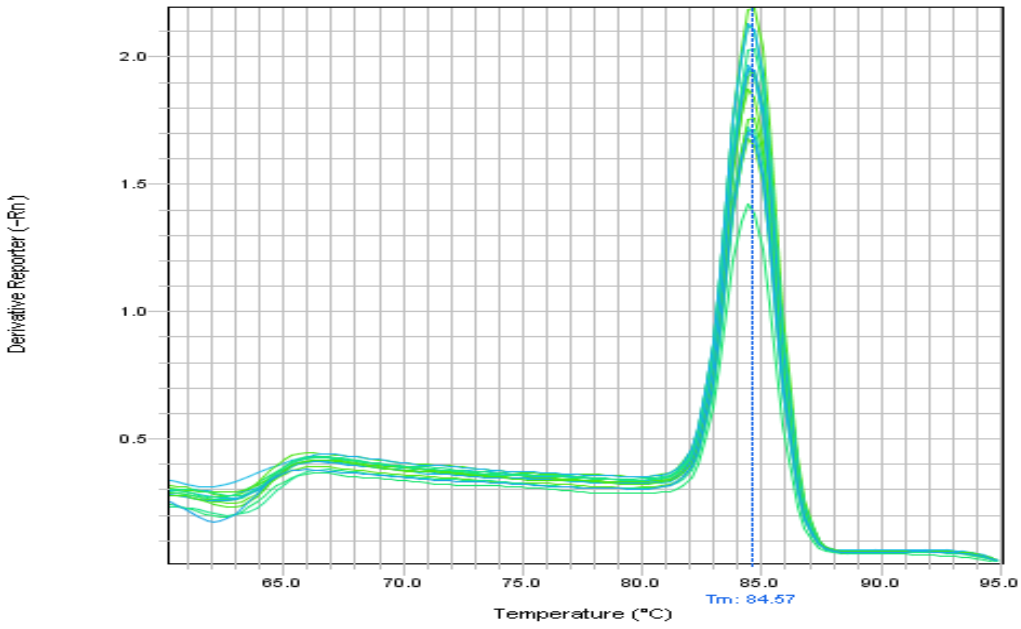

Figure 5.24: MCA of RT-qPCR products from the *Adipoq* gene expression assay. Single amplicons were generated using the primer sets for the target gene, which produced single peaks in melt curve analyses. Curves are representative of all *Adipoq* RT+ samples in the RT-qPCR assay analysis.

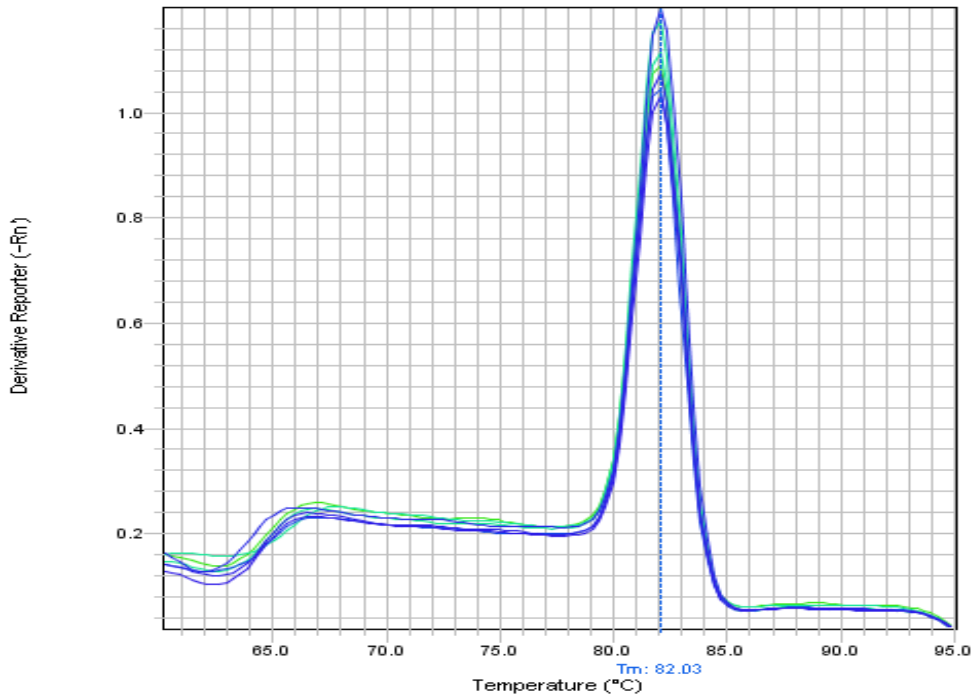

Figure 5.25: MCA of RT-qPCR products from the *Il1b* gene expression assay. Single amplicons were generated using the primer sets for the target gene, which produced single peaks in melt curve analyses. Curves are representative of all *Il1b* RT+ samples in the RT-qPCR assay analysis.

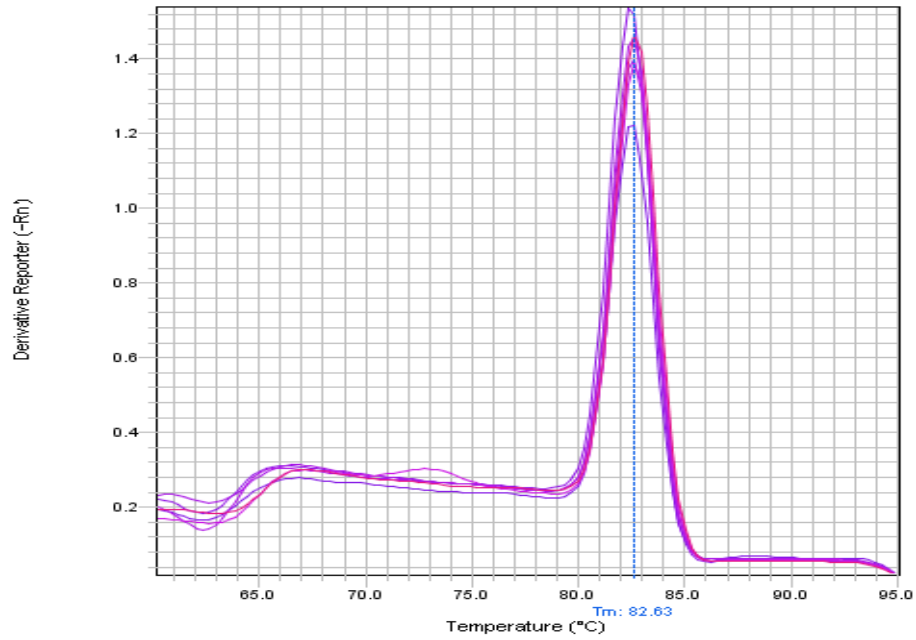

Figure 5.26: MCA of RT-qPCR products from the *Tnfrsf19* gene expression assay. Single amplicons were generated using the primer sets for the target gene, which produced single peaks in melt curve analyses. Curves are representative of all *Tnfrsf19* RT+ samples in the RT-qPCR assay analysis.

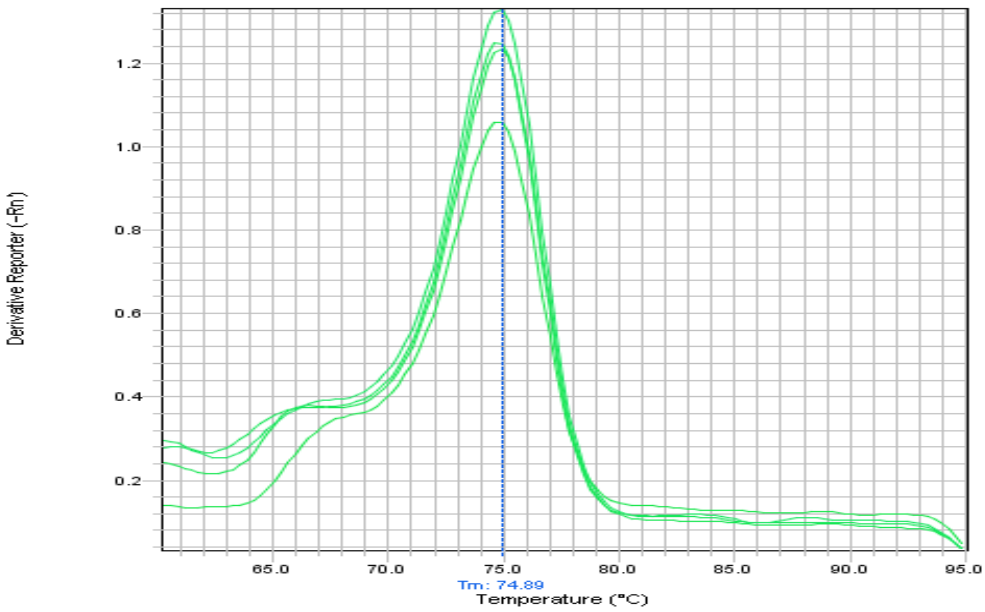

Figure 5.27: MCA of RT-qPCR products from of *Cd40* gene expression assay. Single amplicons were generated using the primer sets for the target gene, which produced single peaks in melt curve analyses. Curves are representative of all *Cd40* RT+ samples in the RT-qPCR assay analysis.

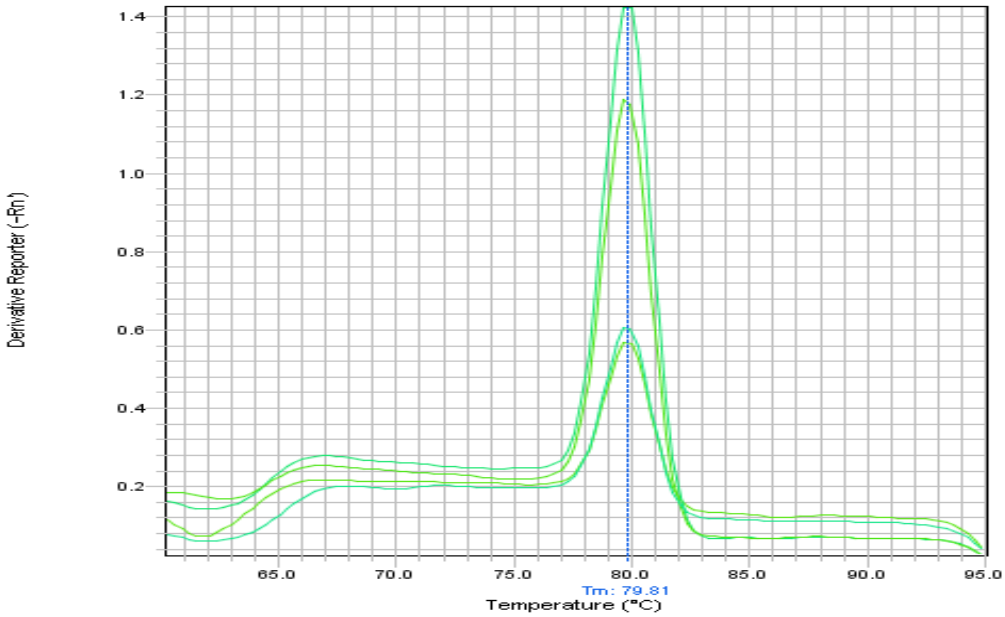

Figure 5.28: MCA of RT-qPCR products from the *Cd40ig* gene expression assay. Single amplicons were generated using the primer sets for the target gene, which produced single peaks in melt curve analyses. Curves are representative of all *Cd40ig* RT+ samples in the RT-qPCR assay analysis.

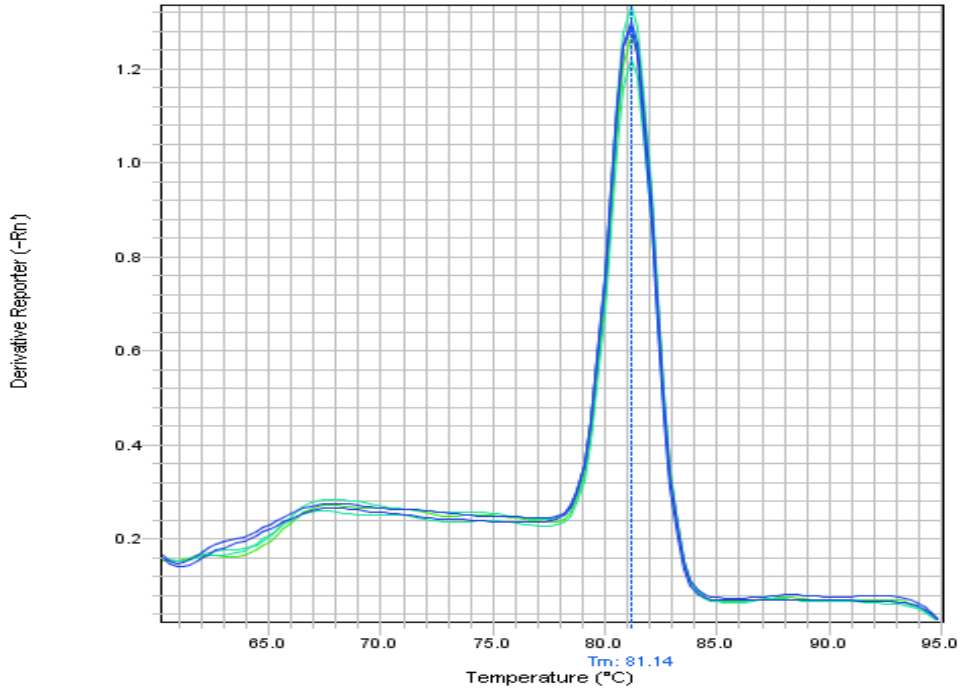

Figure 5.29: MCA of RT-qPCR products from the *Lep* gene expression assay. Single amplicons were generated using the primer sets for the target gene, which produced single peaks in melt curve analyses. Curves are representative of all *Lep* RT+ samples in the RT-qPCR assay analysis.

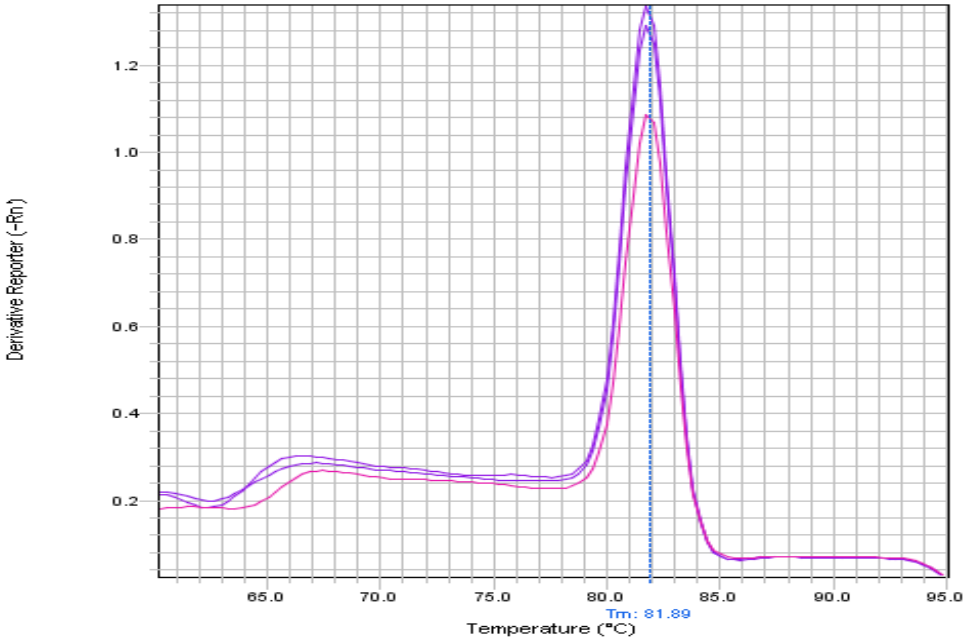

Figure 5.30: MCA of RT-qPCR products from the *Ccl20* gene expression assay. Single amplicons were generated using the primer sets for the target gene, which produced single peaks in melt curve analyses. Curves are representative of all *Ccl20* RT+ samples in the RT-qPCR assay analysis.

5.4.3.3. Gel electrophoresis

All generated products from RT-qPCR experiments were run on an electrophoresis gel and only RT+ samples produced single bands, NTC and RT- samples showed no detected bands on the gels as shown in Figures 5.31 and 5.32. This also confirms that the designed primers were specific and selective to target genes.

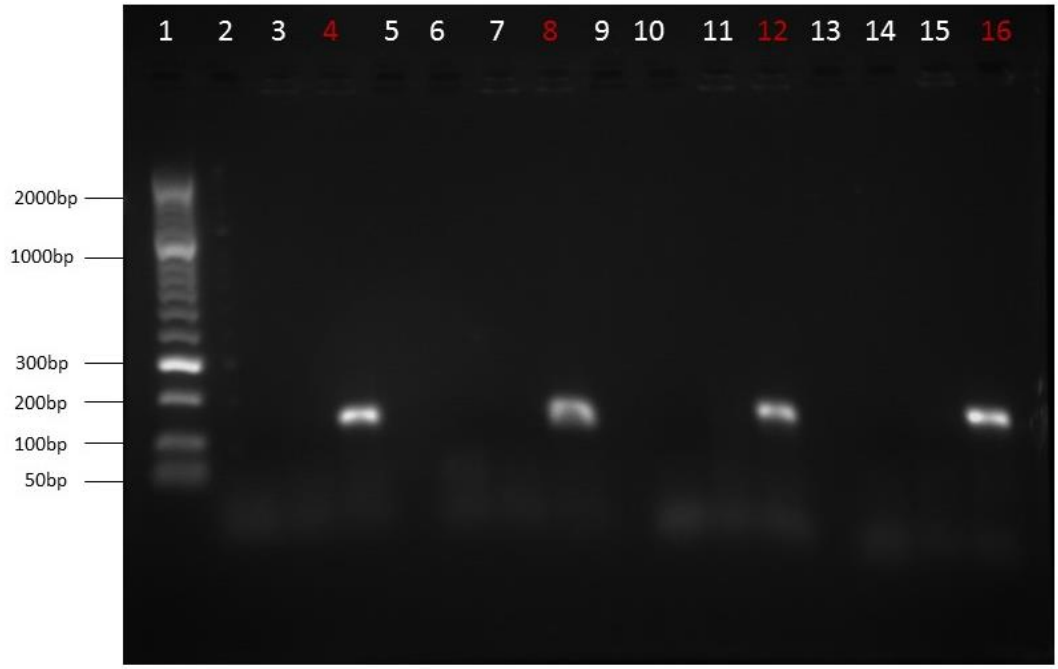

Figure 5. 31: Gel electrophoresis results for *Hprt1*, *Adipoq*, *Il1b*, and *Tnfrsf19* primers. Applied samples all used the same order NTC, RT-, and RT+. *Hprt1* primers in wells 2-4, *Adipoq* primers in wells 6-8, *Il1b* primers in wells 10-12, and *Tnfrsf19* primers in wells 14-16. Hyperladder II™ 50bp was loaded in well 1. All RT + (wells 4,8,12,16) showed single bands confirming the amplification of a single amplicon at the expected band size, while NTC and RT – samples (wells 2,3,6,7,10,11,14,15) showed no bands indicating that there were no false-positive amplications.

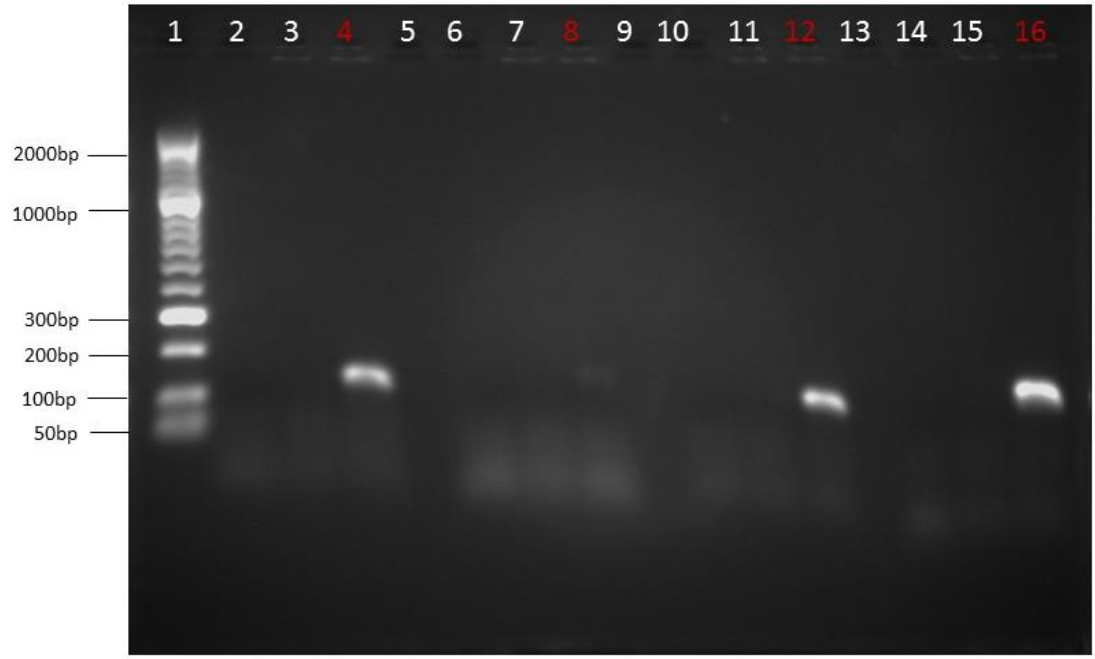

Figure 5. 32: Gel electrophoresis results for *Cd40*, *Cd40ig*, *Lep*, and *Ccl20* primers. Applied samples all used the same order NTC, RT-, and RT+. *Cd40* primers in wells 2-4, *Cd40ig* primers in wells 6-8, *Lep* primers in wells 10-12, and *Ccl20* promers in wells 14-16. Hyperladder II™ 50bp was used in well 1. All RT + (wells 4,8,12,16) showed single bands confirming the amplification of a single amplicon at the expected band size, while NTC and RT – samples (wells 2,3,6,7,10,11,14,15) showed no bands indicating that there were no false-positives.

5.4.3.4. RT-qPCR product sequencing

RT-qPCR products from each of the RT+ gene expression assays were run on agarose gel. Each band was cut out and purified per Illustra GFX PCR DNA and Band Purification Kit's instructions. Purified PCR products were sent to GATC Biotech AG (Koln,Germany) for Sanger sequencing. Sequencing of the RT-qPCR product aligned with the intended target transcripts confirming the specificity of the RT-qPCR assays.

5.4.3.5. Summary of RT-qPCR experiments

RT-qPCR was carried out on seven target genes, which were selected from the RNA-Seq results. All genes were normalised to *HPRT1* which was found to be most stable reference gene. LL tuber treatment significantly ($P < 0.05$) up-regulated *Adipoq*

expression and down-regulated *Il1b*, *Tnfrsf19*, and *Lep*. The effect of LL tuber treatment was not statistically significant ($P > 0.05$) on *Cd40*, *Cd40lg* and *Ccl20*. A summary of the RT-qPCR on the selected genes is shown in Figure 5.33.

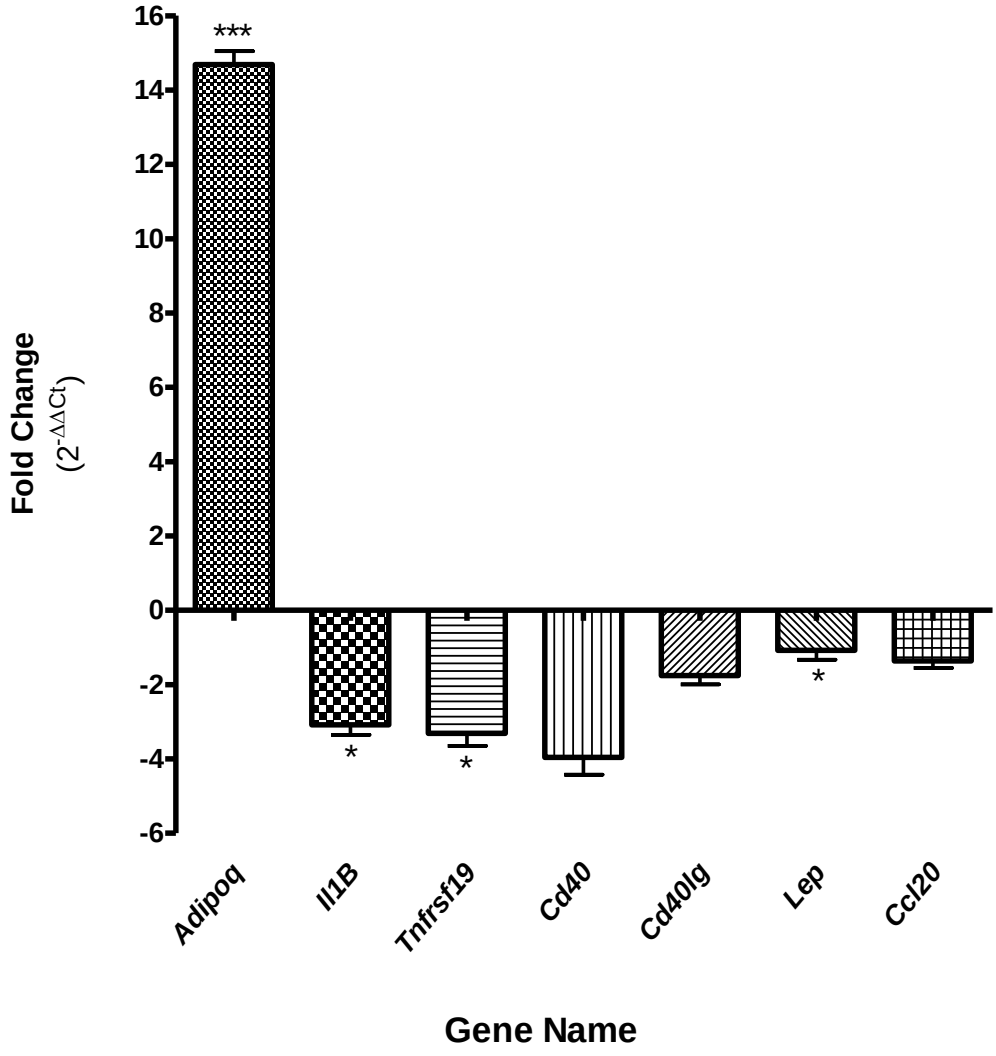

Figure 5. 33: Effects of LL tuber treatment on seven selected genes (chosen from the RNA-Seq results), results obtained from RT-qPCR experiments. Data represents mean ± SEM, n=15. ***P<0.001, *P<0.05 vs control.

5.5. Discussion and Conclusions

RNA-Seq is a cutting-edge life science technology that can enable the discovery of molecular mechanisms of actions, improve disease diagnosis, and enhance the discovery of new effective therapeutic agents (Costa *et al.*, 2013). Due to the limited information available on the biological activity of the LL tubers in this study as detailed in Chapter 1, there was a need to explore the molecular effects on body organs (Dello Jacovo *et al.*, 2019, Nilsson *et al.*, 2008). RNA-Seq is the new gold standard when it comes to whole transcriptome analysis (Everaert *et al.*, 2017), and so was used in this study in order to examine the transcriptome of the rat pancreas following administration of LL tubers. It was hoped that this would provide information on the action of tubers on an organ which plays a vital role in the digestive process and blood glucose regulation, in terms of changes to genes related to diabetes following tuber treatment. Isolating high quality intact RNA is crucial when carrying out deep molecular analysis such as RNA-Seq and RT-qPCR. The isolated RNA samples showed RIN of 5-6, which is indicative of degraded RNA samples. This was despite taking all necessary precautions by harvesting the tissue, immediately stabilising it in RNALater, storing the stabilised tissues at -80°C, and conducting RNA extraction using Qiagen's Total RNeasy Plus Universal. Generally, it is challenging to isolate high quality RNA from the pancreas mainly due to the presence of high endogenous levels of RNases, DNases, and proteases which enhance autolysis immediately following dissection (Augereau *et al.*, 2016). Future work should consider speeding-up the dissection of animals and pancreatic tissue to be removed as the first organ and be immersed immediately in RNALater to minimise the degradation process.

Typically, 70-90% of expressed genes are detected following RNA-Seq analysis and this is considered to be acceptable. However, the RNA-Seq of the samples from this study found the level to be approximately 66%, which is a slightly lower percentage of gene expression and is linked to the low RIN values obtained. Moreover, such RNA degradation can result in an incomplete overview of what was going on in the rat pancreatic tissues following tuber treatment.

5.5.1. Effect of LL treatment on the cytokine-cytokine receptor interaction pathway

The main finding of the RNA-Seq analysis from the use of Cytoscape ClueGo was the effect of LL tuber treatment on the cytokine-cytokine receptor interaction pathway. Cytokines are soluble extracellular proteins that are crucial for innate and adaptive immune responses. They are important for cell growth, cell death, cell differentiation, angiogenesis, and repair mechanisms for cells (Brandsma *et al.*, 2016). There were a number of cytokines up-regulated, in RNA-Seq, following the tuber treatment, however, only two cytokines were consistently up-regulated in all comparisons. These were *Il1β* and *Tnfrsf19* in the RNA-Seq analysis, however these two genes were found to be down-regulated in the RT-qPCR. This mismatch between RNA-Seq and RT-qPCR has been observed previously; Everaert *et al.* evaluated the correlation between RNA-Seq data and the RT-qPCR, correlation plots revealed that a high number of genes showed an opposite direction when quantified by RNA-Seq and compared with RT-qPCR (Everaert *et al.*, 2017). This trend was also seen in hypothalamus RNA samples in the study by Woods (2017). Moreover, RNA samples were highly degraded and failed to meet BGI's minimum RQI submission guidelines and hence this might have affected the RNA-Seq results. Furthermore, only four samples (2 controls, 2 treated) were sent to BGI in comparison with 10 RNA samples used in the RT-qPCR; this gives rise to more confidence in the results obtained from the RT-qPCR. RNA-Seq analysis found that the cytokine-cytokine interaction pathway was mainly affected by tuber treatment and thus guided the direction of the subsequent RT-qPCR investigation. Within this pathway the following cytokines were chosen for RT-PCR experiments: *Adipoq, Il1β, Tnfrsf19, Cd40, Cd40ig, Lep,* and *Ccl20*.

All primers of interest were tested against all control and treated samples and normalised to *Hprt1* as the reference gene. Each primer set was tested against NTC, RT- and RT+. None of the RT-qPCR assays generated false positive amplicons in the NTC and RT- samples. All of the RT-qPCR assays performed well with the RT+ samples and showed single melt curves and the amplification of a single, target-specific amplicon as predicted.

5.5.1.1. Effect of LL on *Adipoq*

RNA-Seq and RT-qPCR have shown that tuber treatment significantly ($P < 0.05$) increased *Adipoq* expression by more than 15-fold in RT-qPCR and 8-fold in RNA-Seq. Adiponectin, a product of *Adipoq*, is 30kDa in size and circulates in the blood at very high levels (2–10 $\mu g\,ml^{-1}$ in humans) (Kandasamy *et al.*, 2012). It is unlike other adipokine proteins and it acts as an anti-inflammatory, anti-atherogenic, and insulin-sensitising hormone. Reduced adiponectin levels are known to be prevalent in obese and T2DM patients, thus suggesting its role in obesity and diabetes. There are a number of studies reporting the effects of adiponectin on pancreatic β-cells. In one *ex vivo* study, Okamoto *et al.* investigated adiponectin effects on isolated mouse islets and found that insulin secretion from these cells was stimulated (Okamoto *et al.*, 2008). The study showed that the adiponectin mode of action was through the enhancement of exocytosis of insulin granules. Moreover, a 24 h treatment in mice islets with adiponectin was shown to augment glucose-stimulated insulin secretion (GSIS) and elevate insulin gene expression. Pancreatic and duodenal homeobox 1 (*Pdx-1*), and *MafA* genes, transcriptional factors known to be involved in insulin production pathway and play a role in maintaining β-cells viability, were also increased following adiponectin treatment (Wijesekara *et al.*, 2010). Adiponectin was found to protect pancreatic β-cells, by its anti-apoptotic activity, from apoptosis induced by both IL1β and interferon-γ (Rakatzi *et al.*, 2004). Adiponectin was also found to exhibit β-cell protection from chronic effects of glucotoxicity. In addition, adiponectin is an activator of adenosine monophosphate-activated protein kinase (AMPK), AMPK activation was found to suppress lipogenesis stimulated by glucose in MIN6 cells (pancreatic β-cells) (Huypens *et al.*, 2005).

In vivo studies have confirmed the beneficial and involved role of adiponectin in the regulation of glucose homeostasis. A study by Kubota *et al.* showed that adiponectin knockout mice were intolerant to glucose despite the fact that they had normal or low insulin levels, thus indicating that high glucose levels alone were not sufficient to enhance insulin release in the tested animals (Kubota *et al.*, 2002). Moreover, Yamauchi *et al.* administered globular adiponectin to transgenic *ob/ob* mice and tested animals showed higher insulin sensitivity and secreted more insulin when

compared with non-transgenic mice (Yamauchi *et al.*, 2003). The ability of adiponectin enhancement on insulin secretion was found to be independent of BW. A study by Kandasamy *et al.* showed that adiponectin gene therapy in high-fat, high-sucrose (HFHS)-fed mice for 13 weeks prevented weight gain and showed glucose tolerance improvement in comparison with the control HFHS mice (Kandasamy *et al.*, 2012). In addition, giving adiponectin intravenously to C57BL/6 mice enhanced insulin secretions (Okamoto *et al.*, 2008). All these results propose that adiponectin might exhibit its activity by maintaining pancreatic β-cells viability (Lee *et al.*, 2011b).

Adiponectin has been identified to possess anti-inflammatory effects, it is involved in suppressing proinflammatory cytokines such as TNFα and IL6 and induction of anti-inflammatory factors (Tilg and Wolf, 2005). Conditions characterised by high levels of inflammation, such as T2DM and obesity show low levels of adiponectin (Li *et al.*, 2009). Moreover, a negative relationship has been noted between adiponectin and C-reactive protein protein (CRP, an inflammation marker).

Adiponectin is currently unavailable to be administered in humans, however, there are a few studies that looked at the relationship between adiponectin and insulin. Hung *et al.* carried out an observational study on Asian children and found the adiponectin level was inversely proportional to BW, BMI, and pro-insulin levels in children irrespective of the gender (Hung *et al.*, 2006). Adiponectin levels were also found to negatively correlate with proinsulin levels and ratio between pro-insulin and insulin which are a known feature of β-cell damage (Bacha *et al.*, 2004). These findings suggest that low levels of adiponectin in humans leads to damage to pancreatic β-cells.

T1DM and T2DM share the fact that they have some β-cell mass reduction by the process of apoptosis. Adiponectin is believed to also act as an anti-apoptotic agent on pancreatic β-cells. Recent studies have shown that adiponectin suppresses apoptosis by enhancing the activity of ceramidase which increases the levels of sphingosine-1-phosphate (an anti-apoptotic factor). However, this role in diabetic patients remains

unclear and is not established yet (Choi *et al.*, 2018). A summary of adiponectin's role in protecting pancreatic β-cells is illustrated in Figure 5.34.

The LL tubers appear to result in an overexpression of the adiponectin gene in the rat pancreatic tissues. Over-expression of pancreatic *Adipoq* is associated with improved regulation of glucose homeostasis and protection of pancreatic β-cells from apoptosis, this finding correlates with the anti-diabetic and anti-inflammatory activities of the tubers which are detailed in Chapters 3 and 4 of this thesis. It would be useful to study the protective effects of LL *in vivo* following the administration of STZ, an apoptotic inducer in β-cells.

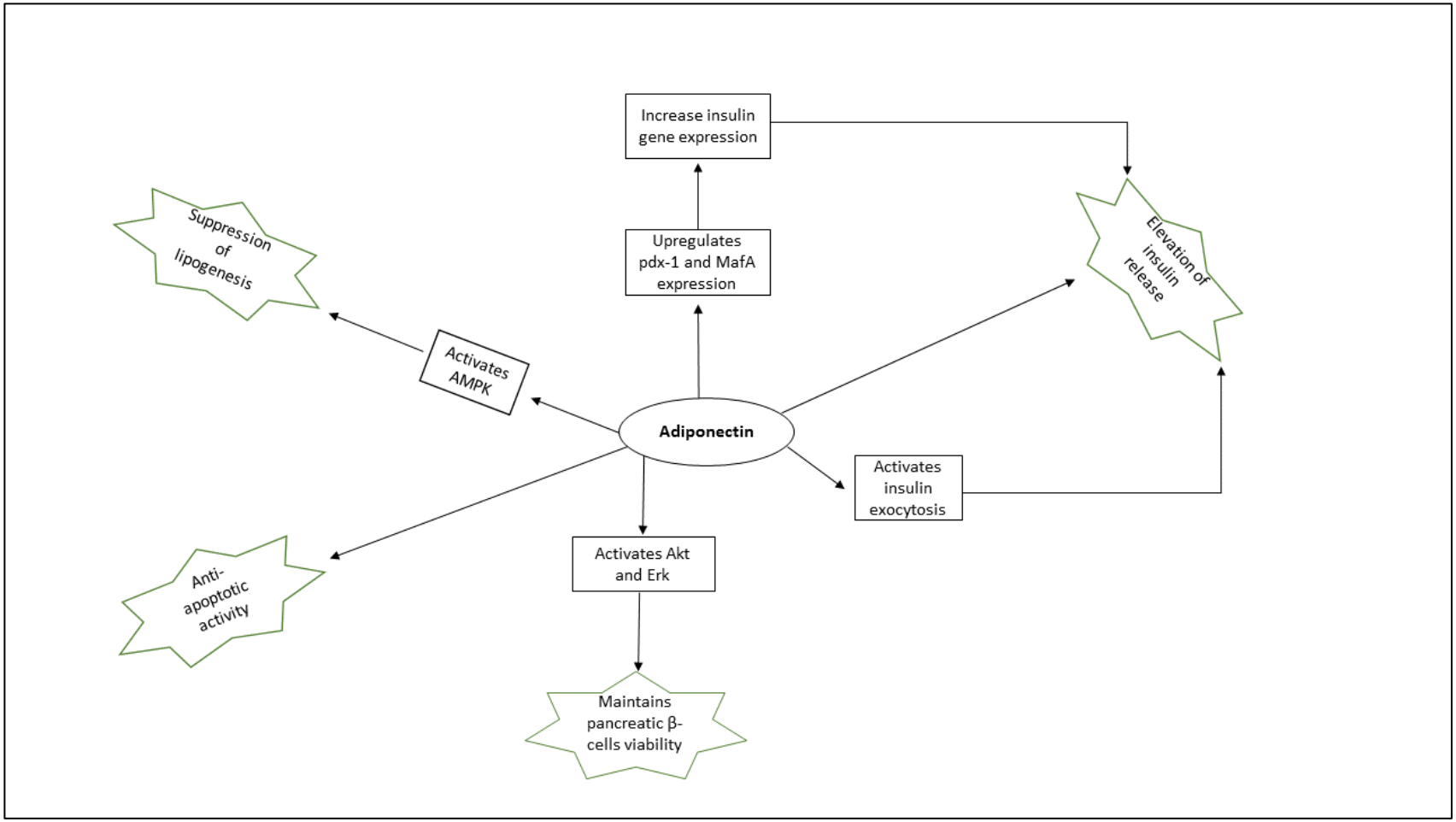

Figure 5. 34: Adiponectin pathways in protecting pancreatic β-cells and enhancing insulin release.

5.5.1.2. Effect of LL on *Il1β*

T1DM is characterised by destroyed pancreatic β-cells, which leads to an inability to produce insulin and hence hyperglycaemia develops. β-cell loss is well known to be a result of pro-inflammatory cytokines, in particular Il1β that plays a fundamental role (Wang *et al.*, 2010). The RT-qPCR results showed that levels of *Il1β* in the tuber treated rats' pancreatic tissues were down-regulated by 3.1 fold ($P < 0.05$). IL1β synthesis in cells begins in an immature form called pro-IL1β. Pro-IL1β is 31kDa in size and remains cytosolic before being converted to IL1β by proteolysis cleavage by IL-1 converting enzyme (ICE) and caspase-1 (CASP1) (Banerjee and Saxena, 2012, Lopez-Castejon *et al.*, 2011). Mature IL1β is smaller in size at 17.5 kDa and some of it is excreted outside the cells by unrevealed mechanisms (Monteleone *et al.*, 2018). Diabetes, in particular T1DM, is characterised by β-cells mass loss in the pancreas, which leads to less insulin being produced (Esposito *et al.*, 2003). β-cell mass loss is explained as result of a mediated immune response that is enhanced by cytokines and in particular IL1β; IL1β is also implicated in T2DM. NF-ƙB activation through the MyD88 pathway contributes to increased IL1β signaling (Guest *et al.*, 2008). Results from the RT-qPCR confirm the obtained findings in Chapter 4 which found tuber extracts and BA have inhibition activity on NF-ƙB (*in vitro* studies) and this was reflected in *Il1β* down-regulation in the RT-qPCR results.

In addition, prolonged IL1β over-expression in the pancreas can lead to pancreatic β-cell dysfunction (Venieratos *et al.*, 2010), and this is linked with elevated IL1β levels in patients with T2DM (Dogan *et al.*, 2006). In *in vitro* studies, IL1β alone causes pancreatic β-cells to be dysfunctional by inducing apoptosis signaling pathways (Maedler *et al.*, 2002). In β-cells, IL1β is capable of activating the c-jun N-terminal kinase (JNK) pathway (Major and Wolf, 2001), and JNK is able to activate the mitogen activated protein kinase (MAPK) family which is involved in apoptosis activation (Miyauchi *et al.*, 2009). JNK has a critical role in mediating cytokine apoptotic pathways of β-cells. In addition, JNK suppresses the transcription of the insulin genes in β-cells (Kaneto *et al.*, 2002). To link this with the findings in Chapter 2, BA isolated from LL tubers might be responsible for *Il1β* down-regulation. A study by Jingbo *et al.* investigated BA as a possible anti-osteoarthritis agent and used human

osteoarthritis chondrocytes which were pre-treated with BA then 10 ng/ml Il1β was added to cells (Jingbo *et al.*, 2015). The findings were that BA inhibited IL1β and NF-ƙB release in a dose-dependent manner. Pancreatic *Il1β* down-regulation is also suggesting the LL role in protecting β-cells.

5.5.1.3. Effect of LL on *Tnfrsf19*

The TNF receptor superfamily 19 (*Tnfrsf19*) gene encodes for a 417 amino acid protein which possesses a TRAF-binding site for NF-ƙB that is important for initiating inflammatory responses (Bondareva *et al.*, 2007). Over-expression of *Tnfrsf19* gene activates JNK pathways and eventually leads to apoptosis. From the RT-qPCR investigation, LL tuber treatment resulted in the down-regulation ($P < 0.05$) of rat pancreatic *Tnfrsf19* gene by 3.5 fold. Down-regulation of *Tnfrsf19* is beneficial in diabetes as it protects β-cells from damage. This is illustrated in a number of studies, Schön *et al.* showed that *Tnfrsf19* is an activator of NF-ƙB, which induces pancreatic β-cells apoptosis (Schön *et al.*, 2014). Moreover, research carried out by Machado-Lima *et al.* looked at human serum albumin (HSA) that was obtained from poorly-controlled T2DM patients and, *Tnfrsf19* was found to be up-regulated in comparison with well-controlled T2DM patients (Machado-Lima *et al.*, 2015). Therefore, down-regulation of *Tnfrsf19* by LL tubers suggests that the plant can protect pancreatic β-cells from apoptotic mechanisms. Furthermore, these findings support the fact that the tubers inhibited NF-ƙB *in vitro* (Chapter 4). This suggests that tubers maintain pancreatic β-cell viability by protecting from apoptosis mediated by Il1β, NF-ƙB, and Tnfrsf19.

5.5.1.4. Effect of LL on *Cd40* and *Cd40lg*

The study also quantified *Cd40* gene expression by RT-qPCR. *Cd40* belongs to the TNF receptor family and is known to be expressed in a number of tissues with the pancreas being one of them (Barbé-Tuana *et al.*, 2006, Klein *et al.*, 2005). LL tuber extract down-regulated *Cd40* gene expression by approximately 4 fold ($P > 0.05$). In non-haematopoietic cells, such as pancreatic duct cells, the activation of CD40 receptor results in non-specific inflammation (Vosters *et al.*, 2004). CD40 activation

enhances synthesis and release of pro-inflammatory mediators such as cytokines and chemokines (Ohta and Hamada, 2004). In pancreatic cells, CD40 activation of other inflammatory mediators has been reported to cause damage to pancreatic β-cells and decrease cell viability, therefore insulin production and secretion is affected (Piemonti *et al.*, 2002). Vosters *et al.* showed that in *in vitro* studies, *Cd40* activation in pancreatic duct cells enhances the secretions of both IL1β and TNFα which then leads to dendritic cell activation (Vosters *et al.*, 2004). Activated dendritic cells cause apoptotic effects in adjacent pancreatic β cells (Movahedi *et al.*, 2004). Moreover, *CD40* up-regulation can be achieved by incubation with inflammatory mediators such as IL1β and TNFα and CD40 is also implicated in activating NF-ƙB (Klein *et al.*, 2005). Barbé-Tuana *et al.* showed that *Cd40* activates pro-inflammatory mediators IL-6, IL-8, monocyte chemoattractant protein (MCP)-1and MIP-1β, macrophage inflammatory protein 1β (Barbé-Tuana *et al.*, 2006). This activation occurs through Raf/mitogen extracellular kinase (MEK)/extracellular signal–regulated kinase (ERK) and NF-ƙB pathways. Moreover, CD40 activation up-regulates other genes which are involved in inflammation responses, these include ICAM-1. The *Cd40lg* gene is responsible for expressing CD40 ligand which is a protein required for Cd40 activity (Di Pietro *et al.*, 2009). RT-qPCR in the present study showed that in treated rat pancreatic tissues the cytokine genes were down-regulated 2-fold. All these findings suggest that LL tubers may have a protective role on pancreatic tissues, and could potentially be considered for use in diabetes management. Effect of LL on STZ-treated rats should be investigated in the future to confirm its protective role for β-cells.

5.5.1.4. Effect of LL on *Ccl20*

The current study also looked at *Ccl20* gene expression in the tested animals. *Ccl20* belongs to the cytokine C-C family, expressed in various tissues including the pancreas. However, healthy pancreatic β-cells are characterised by low or undetectable levels of *Ccl20* (Burke and Collier, 2015). Pro-inflammatory cytokines such as IL1β are known to up-regulate CCL20; IL1β stimulation of CCL20 is believed to be through NF-ƙB transcriptional activity (Burke *et al.*, 2015a). RT-qPCR in this study found a slight down-regulation of *Ccl20* (1.4 fold, $P > 0.05$). This finding was expected since *IL1β* was shown to be down-regulated; down-regulation of such genes is beneficial for

diabetes management (Brandsma *et al.*, 2016, Burke *et al.*, 2015b). To illustrate this, Lee *et al.* showed that resveratrol is a possible therapeutic agent for diabetes. Subcutaneous injection of diabetic mice with resveratrol showed a decrease in *Ccl20* gene expression and improved glucose homeostasis (Lee *et al.*, 2011a). Again, these findings support the hypothesis that the LL tuber may protect pancreatic β-cells from apoptosis and enhance insulin release.

5.5.1.5. Effect of LL on *Lep*

Leptin is a cytokine protein that encodes for 167 amino acids and its synthesis and secretion is largely in adipose tissue. It is therefore known as the adiposity hormone (Elinson *et al.*, 2006). There is some evidence to suggest that leptin plays a role in glucose metabolism and particularly in adipose tissues, but the mechanisms by which it regulates BG are not fully understood (Meek and Morton, 2016, D'souza *et al.*, 2017, Denroche *et al.*, 2012). In the pancreas, leptin is found to inhibit insulin secretion in β-cells, this was confirmed in *in vitro*, and *in vivo* studies (Marroquí *et al.*, 2012). Insulin release was decreased following leptin administration in doses ranging from 0.5-100 nM in β-TC6 (mouse pancreatic β-cells), HIT-T15 (hamster pancreatic β-cells), and INS-1 (rat pancreatic β-cells) (Kulkarni *et al.*, 1997, Zhao *et al.*, 1998, Tsiotra *et al.*, 2001). Moreover, decreased insulin secretion was also shown in isolated pancreatic islets obtained from *ob/ob* and in islets from normal mice and rats following leptin (1 pM- 100 nM) treatment (Zhao *et al.*, 1998). Additionally, leptin has inhibitory activity on insulin gene expression in β-cells. Incubation with leptin at low doses (0.625-10 nM) for 16-40 h led to a decrease in the expression of the proinsulin gene (*Ins*) in β-TC6, HIT-T15, and INS-1 cells (Kulkarni *et al.*, 1997, Tsiotra *et al.*, 2001). Studies on rat isolated islets showed a reduction on *Ins* mRNA levels when dosed with 1-10 nM leptin; similar findings were also seen in *in vivo* studies on mice (Kulkarni *et al.*, 1997). Human isolated islets incubated with leptin (6.25 nM) for two days showed reduced *Ins* mRNA levels (Seufert *et al.*, 1999).

Leptin inhibitory action on the insulin gene is believed to be achieved by activating the JAK/STAT signalling pathway (Marroquí *et al.*, 2012). Following JAK2 proteins phosphorylation, STAT proteins are recruited to act as transcriptional factors in the

nucleus (Morton et al., 2011, Hekerman et al., 2007). Leptin is involved in STAT3 protein activation and the promotion of STAT protein DNA binding in nuclear extracts from RINm5F cells (Morton et al., 2011). It was also shown that STAT5b is involved in leptin-mediated inhibition of insulin 1 in INS-1 cells (Seufert *et al.*, 1999). Leptin activates JAK2 and involves STAT3, and STAT5b, despite the fact that INS-1 cells have STAT1, STAT3, and STAT5b (Marroquí *et al.*, 2012). Leptin activity was shown to be through indirect interaction between STAT3 and STAT5b with a pro-insulin promoter (Laubner et al., 2005, Hekerman et al., 2007). Leptin enhances the expression of suppressor of cytokine signalling 3 (SOCS3) by STAT-dependant pathways (Laubner et al., 2005, Seufert, 2004). SOCS3 is responsible for inhibiting the pro-insulin promoter gene (Fruhbeck, 2006). LL tubers showed a slight down-regulation in pancreatic leptin expression in the RT-qPCR experiment. All these findings give a strong indication of the potential of the LL tuber having an anti-diabetic action.

In conclusion, RNA-Seq and RT-qPCR findings from rat pancreatic tissues showed that LL tubers used in this project are promising agents for the management of both T1DM and T2DM. The adiponectin gene was highly up-regulated by tuber treatment. This indicated that the tuber impacts on important roles in the pancreas. To start with, it increases insulin secretion by activating insulin exocytosis. Secondly, the tuber appears to activate AMPK pathways which could lead to inhibition of lipogenesis, PL was inhibited by LL extracts as shown in Chapter 3. Moreover, the adiponectin gene protects β-cells from apoptosis and maintains cell viability, which leads to increased insulin secretion. The tuber may contribute to maintaining pancreatic β-cell viability by protecting from apoptosis mediated by its effects on *Il1β, Nf-ƙB,* and, *Cd40, Cd40lg, Tnfrsf19* gene expression. Pancreatic leptin was also down-regulated by tuber treatment, which enhances insulin release from the pancreas.

Based on the results obtained in this chapter, it was decided to examine the effects of the tubers on obese/diabetic animals such as *ob/ob* Zucker rats, rather than normal SD rats. Therefore, these findings will be followed up in Chapter 6, where LL tubers were

administered to obese male and female Zucker rats and the effects on the animal's BW, FI, WI, and BG were investigated.

Chapter 6

6. Animal Study on Obese Zucker Rats (OZR)

6.1. Introduction

LL tubers and leaves have shown promising findings for the plant to be used for the purpose of managing diabetes and obesity. In Chapter 2, BA was isolated from LLT EA extract; a compound which is known to have some anti-diabetic properties (Ahangarpour *et al.*, 2018). LL tuber and leaf extracts and isolated compounds were tested for their potential anti-diabetic activity as detailed in Chapter 3. LL tubers and leaf extracts and BA strongly inhibited α-glucosidase, an enzyme that is implicated in diabetes, and PL, an enzyme that is implicated in obesity. Moreover, the plant extracts and BA increased glucose uptake in HepG2 hepatic cells. This was then followed by testing the plant's anti-inflammatory and anti-oxidant activities where positive results were obtained in which LL and isolated compounds protected cells *in vitro* from cytotoxic effects of TNFα and increased GSH levels in HepG2 cells (Chapter 4). Investigation was then carried out *ex vivo*, by examining the transcriptomics of rat pancreatic tissues in animals treated with the tubers by Woods (2017). The results showed high up-regulation in the *Adipoq* gene - a positive regulator for both obesity and diabetes. Other genes known to suppress insulin release and destroy β-cell function were down-regulated in normal SD male rats administered tubers as described in Chapter 5. Therefore, it was thought to be pertinent to further investigate the activity of the tuber *in vivo* using an obese rat model such as Zucker rats. BW and FI of animals were monitored daily as LL might have anti-diabetic and anti-obesity effects by reducing BW and FI. BG levels were also monitored.

Many medicinal plants have been investigated *in vivo* for their anti-diabetic potential. Most studies are carried out on STZ-induced diabetic mice or rats and db/db diabetic mice (Fang *et al.*, 2019). Other studies have used different animal models; these include OZR (Mezei *et al.*, 2003), diabetic Zucker rats (ZDF) (Dong *et al.*, 2016), high-fat diet mice/rats (Kumar *et al.*, 2018; Al-Trad *et al.*, 2019), high-sucrose diet rats (Ehsanifard *et al.*, 2017) and albino rats (Sikarwar and Patil, 2010). OZR were first discovered in 1961 after a cross between Merck M-strain and Sherman rats (King,

2012). OZR have a mutation in the leptin receptor that results in hyperphagia which causes obesity by the age of four weeks (Phillips *et al.*, 1996). They are also hyperinsulinaemic, hyperlipidaemic, hypertensive and have impaired glucose tolerance (Srinivasan and Ramarao, 2007). Hence, they were chosen in this study as the obesity and diabetic state do not require STZ or a high fat diet to be developed, and they are more obese when compared to their substrain ZDF (King, 2012).

Different types of studies have been carried out and many plants have been reported to exhibit anti-hyperglycaemia effects; some of these were studied *in vivo* for anti-diabetic activity. Soy intake has been linked with various therapeutic effects including improved insulin resistance and better glycaemic control (Bhathena and Velasquez, 2002). Isoflavones such as genistein, daidzein and glycitein are some of the bioactive phytochemicals present in soy (Clarkson, 2002). Mezei *et al.* (2003) investigated the anti-diabetic activity of a high isoflavone soy (HIS) protein on male and female OZR. Treatment was given over a period of 8 and 11 weeks for male OZR and female OZR, respectively. OZR HIS-fed diet groups showed significantly ($P < 0.05$) improved glucose tolerance when compared to untreated groups. Morover, both male and female OZR on HIS-diet showed a decrease ($P < 0.05$) in liver weight, hepatic cholesterol and triglyceride levels in comparison with the untreated groups.

Leaves of *Camellia sinensis* are used to produce green tea which is known to possess various biological activities including hypoglycaemic effects. Sabu *et al.* looked at the effects of green tea polyphenols (GTP) on alloxan diabetic rats (Sabu *et al.*, 2002). GTP extracts were administered daily for 15 days at a dose of 100 mg/kg BW showed a significant reduction ($P <0.05$) in serum glucose levels. Moreover, GTP extract at 50 mg/kg BW and 100 mg/kg BW reduced serum glucose levels induced by alloxan administration by 29% amd 44%, respectively. Kao *et al.* looked at the effects of epigallocatechin gallate (EGCG), which is a known component in GTP on the BW of OZR (Kao *et al.*, 2000). EGCG was administered by intraperitoneal injection at 92 mg/kg BW for 4 days and showed a significant ($P < 0.05$) reduction in BW. Reduction on BW was linked to the reduced FI and leptin levels following EGCG administration.

Citrus grandis (CG) is a plant which has been used generally to promote health (Vijaylakshmi and Radha, 2015). Kim *et al.* investigated the anti-diabetic and anti-oxidant actvity *in vitro* of CG fruit (Kim *et al.*, 2009). Extracts of CG fruit showed significant ($P < 0.05$) α-glucosidase and α-amylase inhibition, and they were scavengers for ROS generated by peroxyl and hydroxyl radicals. The *in vivo* effects of water extract of CG fruit on energy metabolism were studied by Raasmaja *et al.* (2013). OZR were fed HFD and treated with extracts of CG at 300 mg/kg BW, 600 mg/kg BW and 1200 mg/kg BW. Treatment was administered daily by intragastric gavage for 12 weeks. BW and FI were monitored weekly, while serum glucose and lipid were measured before commencing the experiment and after 2, 4, 8 and 12 weeks. Levels of GLP-1 were significantly lower in the treated groups, while ghrelin levels were higher. Glucose and lipid profile was unchanged by the extracts administration. The above studies showed that OZR are a suitable model for investigating LL biological effects.

6.2. Aims and Objectives

This chapter describes the effects of LL tubers on male and female OZR to provide *in vivo* biological evidence supporting their traditional use. This was achieved by:

1. Optimising the way in which tubers could be fed to rats, rather than using gastric gavages. SD male rats were chosen as a cheaper option to OZR and tubers were incorporated in rusks, normally given as a "treat".
2. Feeding trial in male and female OZR with LL tubers, since OZR are an established model for obesity and diabetes.
3. Studying the effects of LL on BW, it was hypothesised that animals might lose weight as tubers were historically used to suppress appetite. RNA-Seq on pancreatic tissues of SD male rats in Chapter 5 showed significant elevation of *Adipoq* following treatment with LL tubers. *Adipoq* is known as an anti-obesity and anti-diabetic gene.
4. Studying the effects of the tubers on FI and WI, it was expected that appetite suppressants would cause reduction in FI and WI of OZR.

5. Determining serum glucose levels in the OZR, BA was the major component in the extract of LL and showed potent α-glucosidase inhibition as detailed in Chapter 3. Therefore, administration of tubers could have an effect on BG.

6.3. Materials and methods

6.3.1. Feeding optimisation study

6.3.1.1. Animal husbandry

The feeding study was optimised using six male, in-house bred SD rats aged 9 weeks with a starting weight of 319-347g. The animals were allowed to acclimatise for two weeks before starting the feeding trial. Rats were treated when they were 11 weeks old. Access to food and water was provided *ad libitum* except when the optimisation was being carried out (a period of 30 min). Moreover, cages were fitted with Red Polycarbonate Shelter Huts to block visible light in order to make the rats feel more secure and improve their environment. Each rat had a space in the cage of a minimum of 900 cm^2. Three rats were housed together per cage and they were only separated when feeding optimisation was being carried out. The room was at a temperature of 21°C with 55% humidity and 12-hour day-night light cycle.

6.3.1.2. Feeding study

All protocols conducted in this study were covered under Home Office UK Licence number P73667397. Dry Farley's rusks were initially introduced to rats for three days. Then, rusks (3 g) were mixed with deionised water (3 ml) and this mixture was introduced as a treat for the rats. Rusks were introduced to the rats for 5 days and then the animals were randomly placed into two groups, control and treated groups with 3 rats in each group. The control group continued to receive wet rusks for a further 5 days, whereas the treated group received LL tuber powder mixed in with the wet rusks. The body weight of each animal was measured first thing in the morning and the tuber dose was calculated and prepared as 100 mg/kg. Rusks containing tuber were given to the rats in the morning and left for approximately 30 min in the cage.

6.3.2. Feeding study on obese rats

6.3.2.1. Animal husbandry

Ten male OZR rats aged 9 weeks and 8 female OZR aged 10 weeks were purchased from Charles River Laboratories. Animals were allowed to acclimatise for three days and then dry rusks were introduced to the animals for a further three days before they were separated and housed individually. This was then followed by seven days of wet rusks feeding (as in section 6.3.1.2) to ensure that the animals were used to them before incorporating the tuber into the mixture as per Figure 6.1. Treatment started when the Zucker rats were aged 11 and 12 weeks for males and females, respectively.

6.3.2.2. Tuber treatment

The animals were separated randomly into four groups.
Group 1: control males (n=5)
Group 2: treated males (n=5)
Group 3: control females (n=4)
Group 4: treated female (n=4)

Animals in Groups 1 and 3 received daily wet rusks (3 g rusks mixed with 3 ml water) for 22 days. On the other hand, Groups 2 and 4 were given wet rusks from day 1 to day 5. Then, on day 6 a tuber dose of 100 mg/kg was mixed with the wet rusks and given to the animals (Figures 6.2 and 6.3). This dose was continued for a further four days before the dose was increased to 150 mg/kg in day 11 and this continued for another 4 days. On day 16 of the experiment, treated animals were dosed with 200 mg/kg tubers until the end of the experiment (day 22).

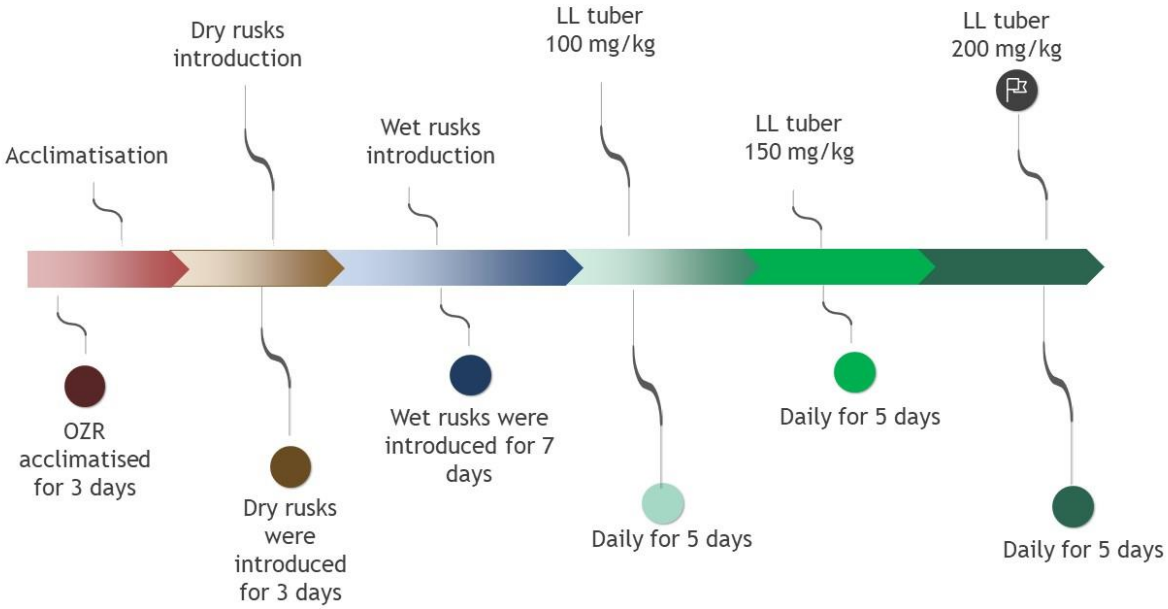

Figure 6. 1: Timeline showing the treatments carried out on OZR.

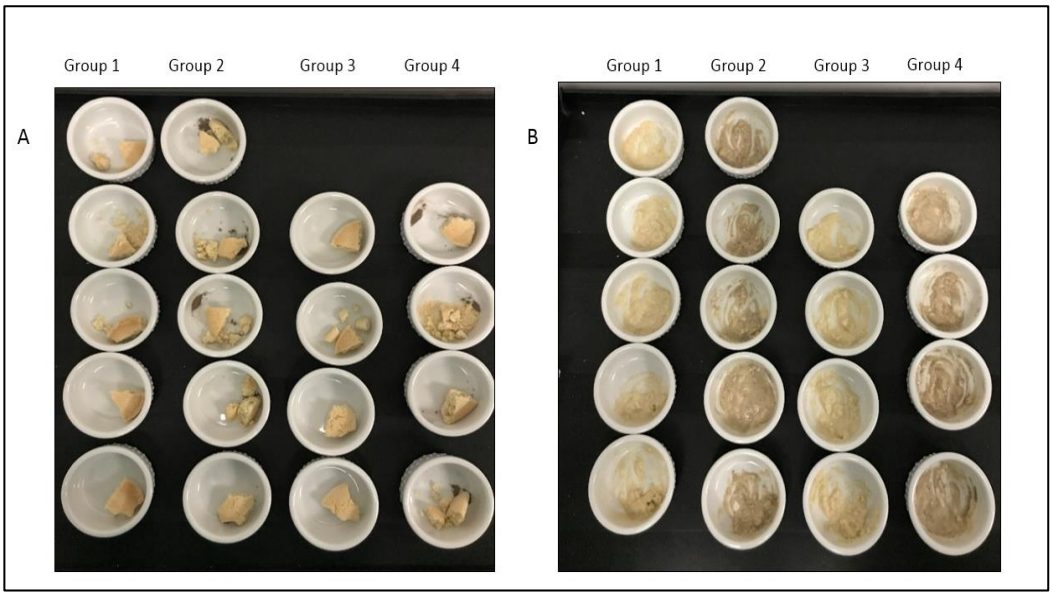

Figure 6. 2: Wet rusks with and without the tuber powder which was used during the animal study. Three g of dry rusks were prepared for each animal as in A, then 3 ml deionised water was added to dissolve rusks as in B before introducing the mixture to OZR.

Figure 6. 3: Wet rusks with and without tuber powder were administered to each rat and in general the rats took 5-10 minutes to consume the contents.

6.3.2.3. Animal monitoring

6.3.2.3.1. Body weight (BW)

The animals were taken out of the cage and placed in a beaker and their weight was recorded using an electronic balance with 1 g tolerance. BW measurements were recorded every day and initiated 5 days before starting the treatment and continued for 17 days following the treatment.

6.3.2.3.2. Food intake (FI)

The normal chow was placed in a metal hopper and weighed daily to record the amount of food consumed per OZR. The food was topped up daily and was never left to fall below 100g. FI was taken on a daily basis for 4 days prior to treatment and 17 days following the treatment.

6.3.2.3.3. Water intake (WI)

The animals' cages were fitted with a plastic bottle that had a stainless steel feeding tube. The amount of water in millilitres consumed per OZR was recorded daily. WI measurements started 4 days before the start of treatment and continued for 17 days following the treatment.

6.3.2.3.4. Blood glucose (BG)

BG measurements (mmol/l) were performed using a rodent glucose meter (AlphaTRAK 2 glucose monitor) with appropriate test strips purchased from Abbott Laboratories. Animals were placed on a table and their face covered with a piece of cloth. Then a sterile needle was used to introduce a puncture at the tip of the tail, a drop of blood was placed on the test strip and the glucose concentration measured. To reduce the stress to the animals, BG was monitored every other day during the study. BG was recorded 2 days (day 4) before the treatment to act as the baseline for the study, and was then taken on days 6, 8, 10, 12, 14, 16, 18, 20 and 22 following the treatment.

6.3.3. Dissection of animals

Animals were dosed with sodium pentobarbital by intraperitoneal (IP) route at a dose of 0.1mg/100 mg body weight for euthanasia. Then, blood samples collected by cardiac puncture were stored at 4 °C in a fridge for 24 h before being centrifuged at 2500 RPM for 15 min. The serum was removed and stored at -80 °C in a freezer until required.

Brain, hypothalamus, liver, pancreas, skeletal muscle, adipose tissues, kidneys, testes and ovarian tissues were harvested and placed in tubes containing RNA*later* solution and stored at 4°C for 24 hours to stabilise tissues' RNA. Then, RNA*later* solution was removed and tissues were stored at -80 °C in a freezer for long-term storage.

6.3.4. Statistical analysis

Values are shown as the mean ± standard error of the mean (S.E.M.). Statistical analysis were performed using Student's t-test. Differences with a value of $P < 0.05$ were considered statistically significant.

6.4. Results

6.4.1. Feeding study optimisation on SD rats

The feeding study that was carried out on male SD rats which involved mixing the baby rusks with the tubers (in powder form) was successful. All animals in the control group consumed all of the given wet rusks. The animals in the treated group consumed the wet rusks which contained LL tubers. Based on this, a feeding study on OZR was considered.

6.4.2. Feeding study on OZR

6.4.2.1. Effects of LL treatment on BW

6.4.2.1.1. Male OZR

Ten male ob/ob Zucker rats were monitored 5 days before the start of tuber treatment and their BW was recorded daily. As shown in Figure 6.4, both of the control and treated groups had similar BW for the first 3 days, however, on day 4 (2 days before administering the treatment) the two groups started to separate despite the fact that they were receiving only wet rusks. Following the tuber treatment on day 6, the average BW of those in the treated group continued to be lower than those in the control group. This separation trend was shown to be slightly increased by increasing the tuber dose to 150 mg/kg and 200 mg/kg. However, this difference in BW was statistically insignificant ($P > 0.05$).

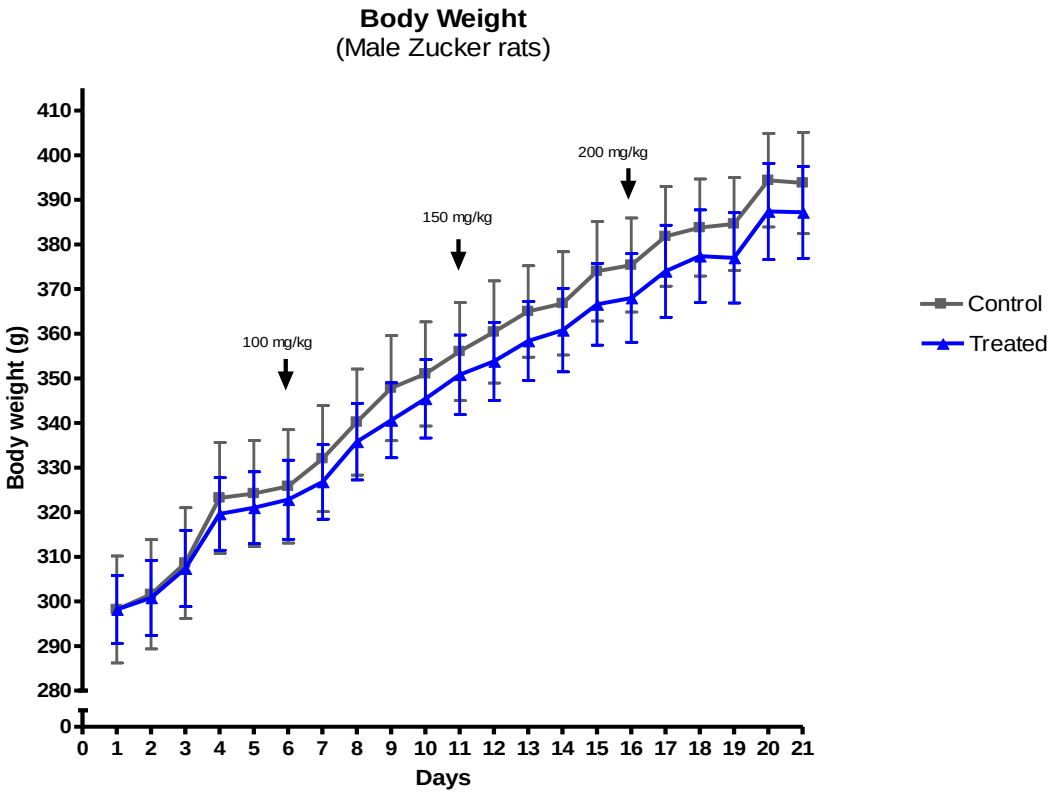

Figure 6. 4: The effect of LL on male Zucker rat BW (n=5). BW measurements were recorded every 24h ± 30 mins.

6.4.2.1.2. Female OZR

The BW of 8 female ob/ob Zucker rats were monitored as per section 6.4.2.1.1. As in Figure 6.5 and contrary to the findings of the male group, LL treatment in the female group showed a greater increase in BW of the treated group in comparison with the control group. As the LL dose increased, the BW of the treated group increased and differed more from the control group. However, this increase in BW was statistically insignificant ($P > 0.05$).

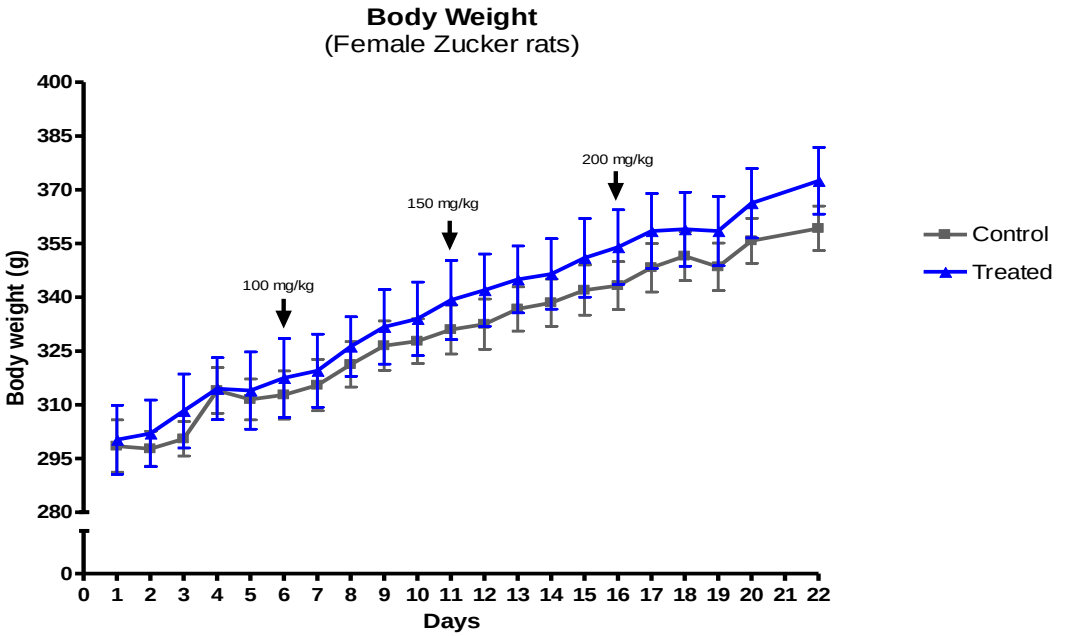

Figure 6. 5: The effect of LL on female Zucker rat BW (n=4). BW measurements were recorded every 24h ± 30 mins.

6.4.2.2. Effect of LL treatment on WI

6.4.2.2.1. Male OZR

WI was recorded daily for every rat and started 4 days prior to initiating the LL treatment. As shown in Figure 6.6, all animals consumed between 20 to 30 ml of water daily. Both the control and treated groups had a similar daily WI prior to initiating the treatment. On day 6 at the start of treatment, both groups showed an increase in WI and this was decreased for both groups on day 7. From day 9, the treated group started to differ from the control group and showed a reduction in WI. This separation remained fairly constant irrespective to the dose of LL. However, these results were not of a statistical significance ($P > 0.05$).

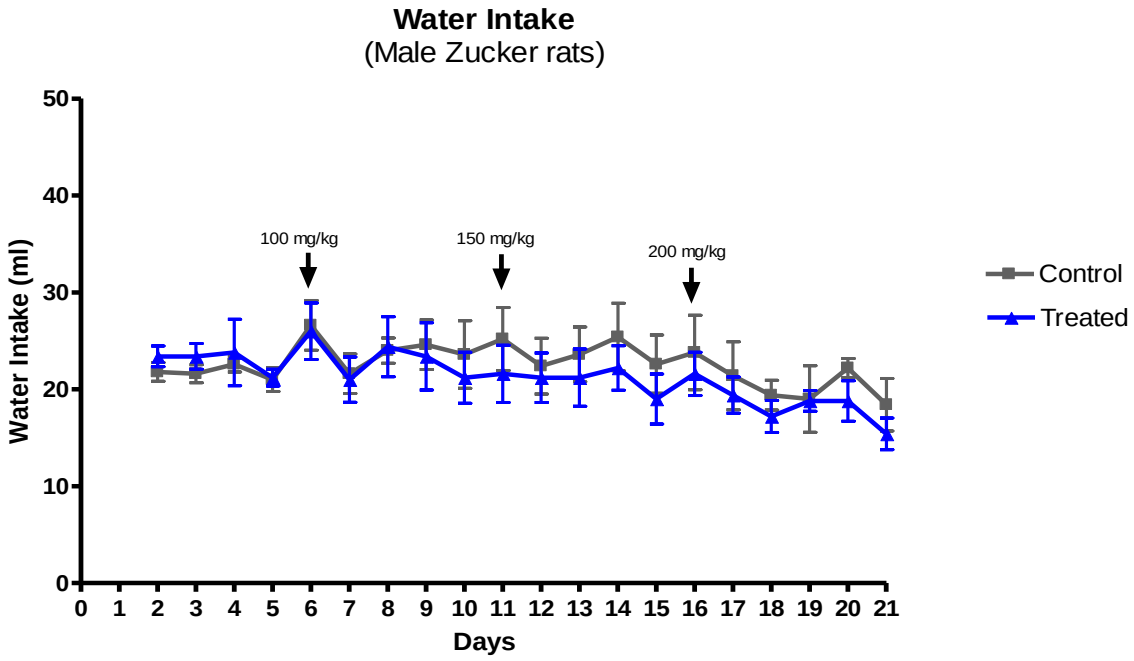

Figure 6. 6: The effect of LL on male Zucker rat WI (n=5). WI measurements were recorded every 24h ± 30 mins.

6.4.2.2.2. Female OZR

Prior to the initiation of the LL treatment, both the control and treated groups showed comparable daily WI and this continued for 3 days following the treatment, as shown in Figure 6.7. On day 9, the treated group had a higher WI and this increase returned back to level with that of the control group on the following day. On days 12-14, the treated group showed a reduction in WI in comparison with the control group, but these results were statistically insignificant ($P > 0.05$). On days 15-17, both groups showed similar levels of daily WI. The treated group showed a reduction in daily WI on days 17 and 18. However, on days 20-22, the treated group had more WI than the control group ($P > 0.05$). Thus, LL treatment at the tested doses and for the period of study did not show any significant increase or decrease in the WI of the tested female Zucker rats.

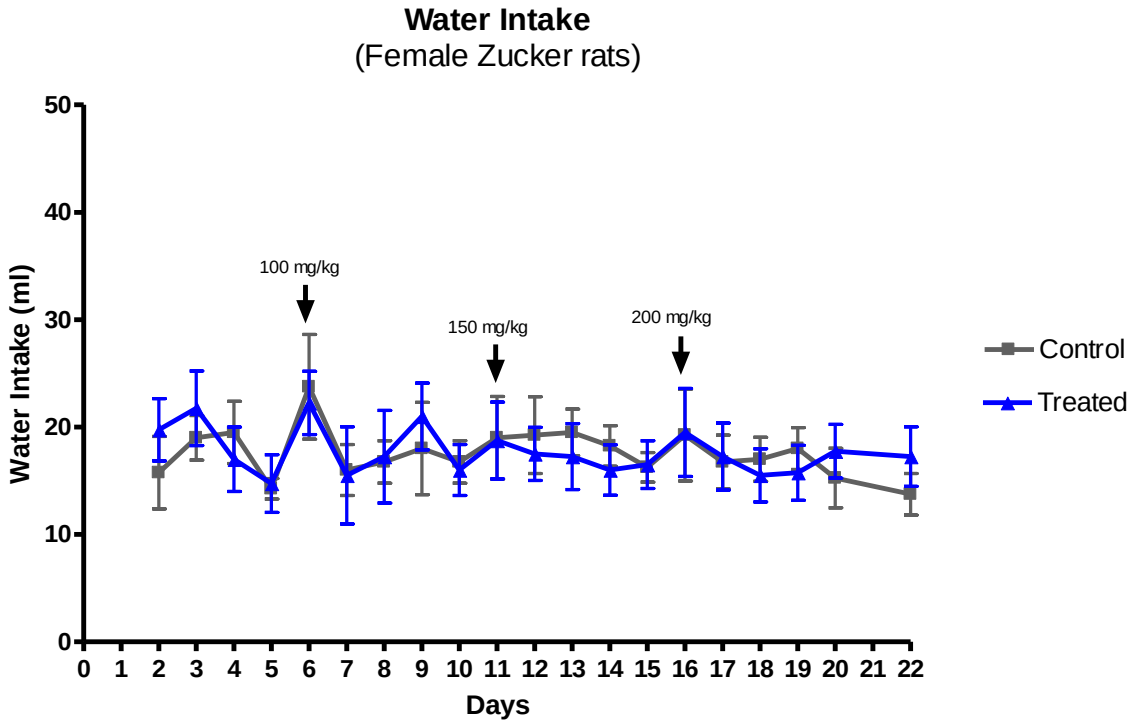

Figure 6. 7: The effect of LL on female Zucker rat WI (n=4). WI measurements were recorded every 24h ± 30 mins.

6.4.2.3. Effect of LL treatment on FI

6.4.2.3.1. Male OZR

FI was recorded daily for all rats and started 4 days prior to initiating the LL treatment. As shown in Figure 6.8, all animals consumed 20-30 g of food daily. Both the control and treated groups had similar daily FI prior to initiating the treatment and for 2 days post-treatment. On day 9, the treated group showed a significant ($P < 0.05$) reduction in FI when compared with the control group and this reduction continued, but was only significant on day 13. A boxplot was generated for the significant findings in days 9 and 13 as per Figure 6.9.

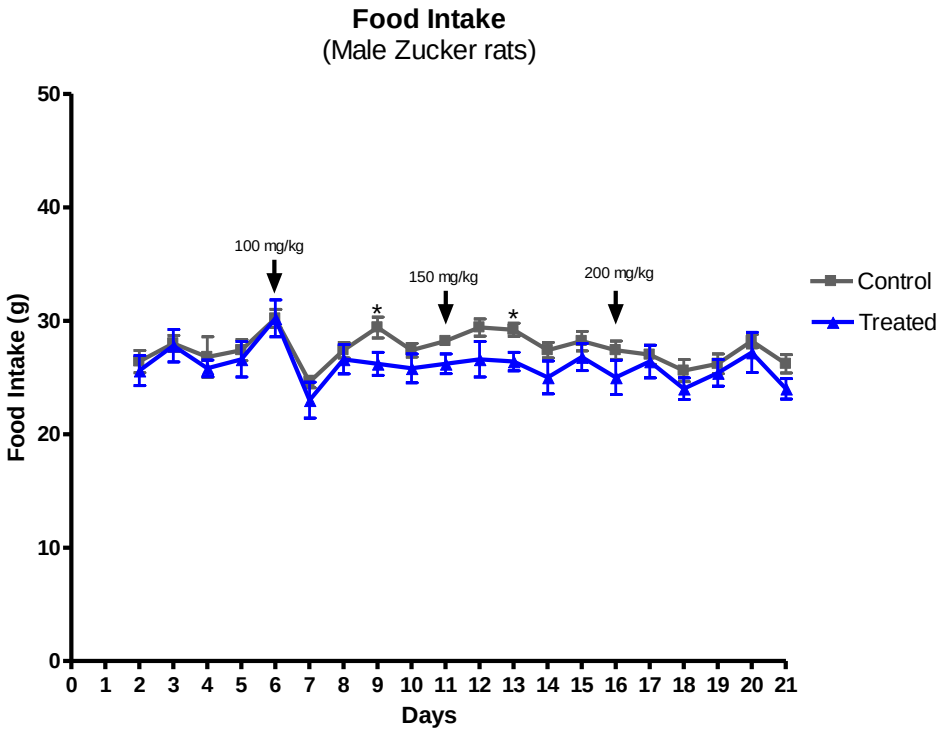

Figure 6. 8: The effect of LL on male Zucker rat FI (n=5). FI measurements were recorded every 24h ± 30 mins. Data was analysed using Student's t-test. * p value < 0.05.

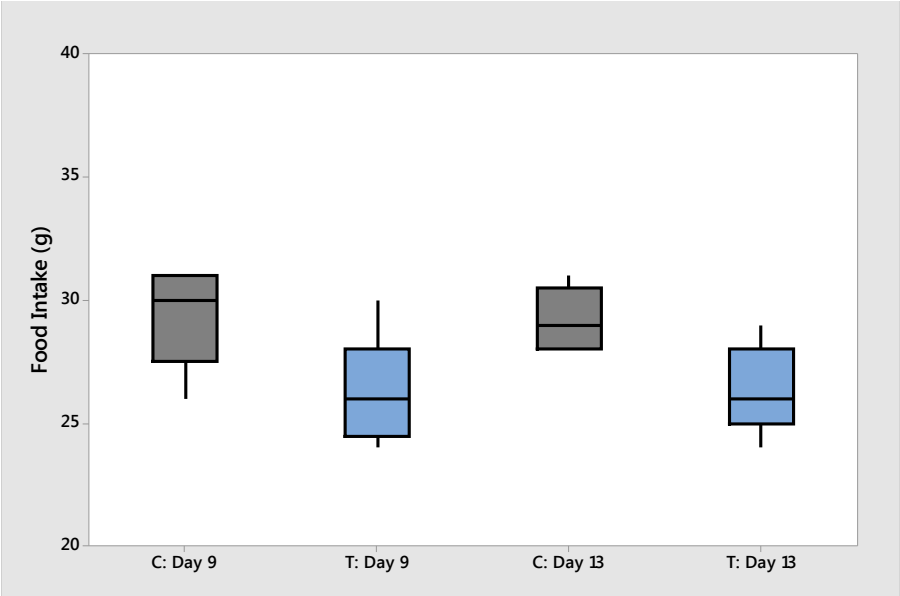

Figure 6. 9: A boxplot showing the effect of LL on male Zucker rat FI (n=5) in days 9 and 13 of the experiment. C= control, T= Treated. FI measurements were recorded every 24h ± 30 mins.

6.4.2.3.2. Female OZR

Control and treated female OZR consumed approximately 20 g of food per animal daily. Both groups showed comparable results before and post-treatment and the results were not of statistical significance (Figure 6.10) apart from day 7 where the treated group showed more food intake when compared with the control group ($P < 0.05$), as shown in Figure 6.11.

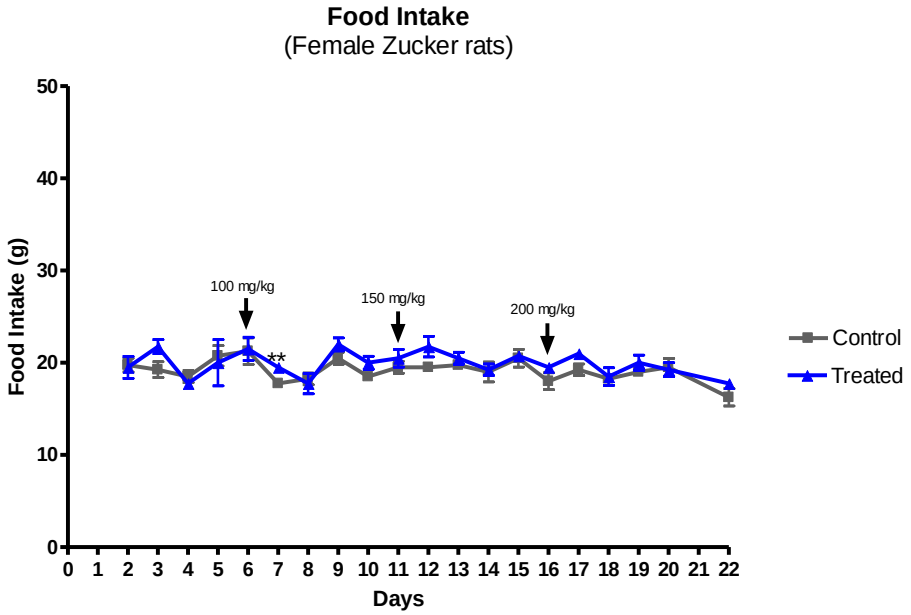

Figure 6. 10: The effect of LL on female Zucker rat FI (n=4). FI measurements were recorded every 24h ± 30 mins. Data was analysed using Student's t-test. ** p value < 0.01.

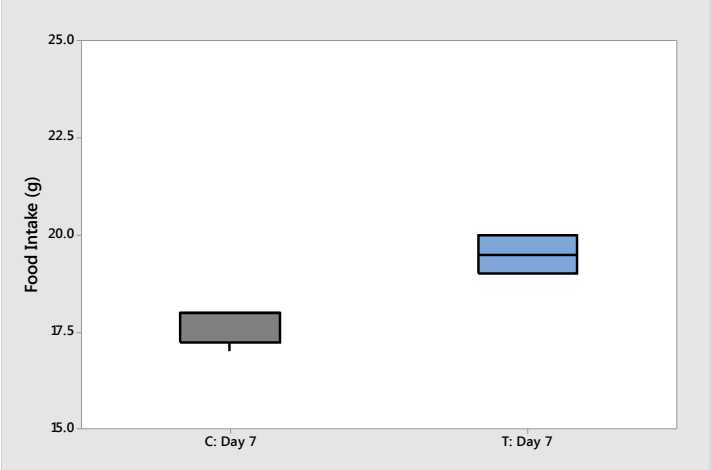

Figure 6. 11: A boxplot showing the effect of LL on female Zucker rat FI (n=4) in day 7 of the experiment. C= control, T= Treated. FI measurements were recorded every 24h ± 30 mins.

6.4.2.4. Effects of LL tuber treatment on BG

6.4.2.4.1. Male OZR

The first BG measurement was taken 2 days prior to the start of treatment where both groups were almost identical and had an average BG of 5.6 mmol/l as shown in Figure 6.12. On day 6, i.e. 2 days into the treatment period, the treated group had the highest BG measurement in the study which was slightly higher but not significant ($P > 0.05$) compared with the control group. This increase in BG decreased on day 8 and was below that of the control group for the first time. Then, the treated group maintained lower BG levels when compared to the control group until the end of the study.

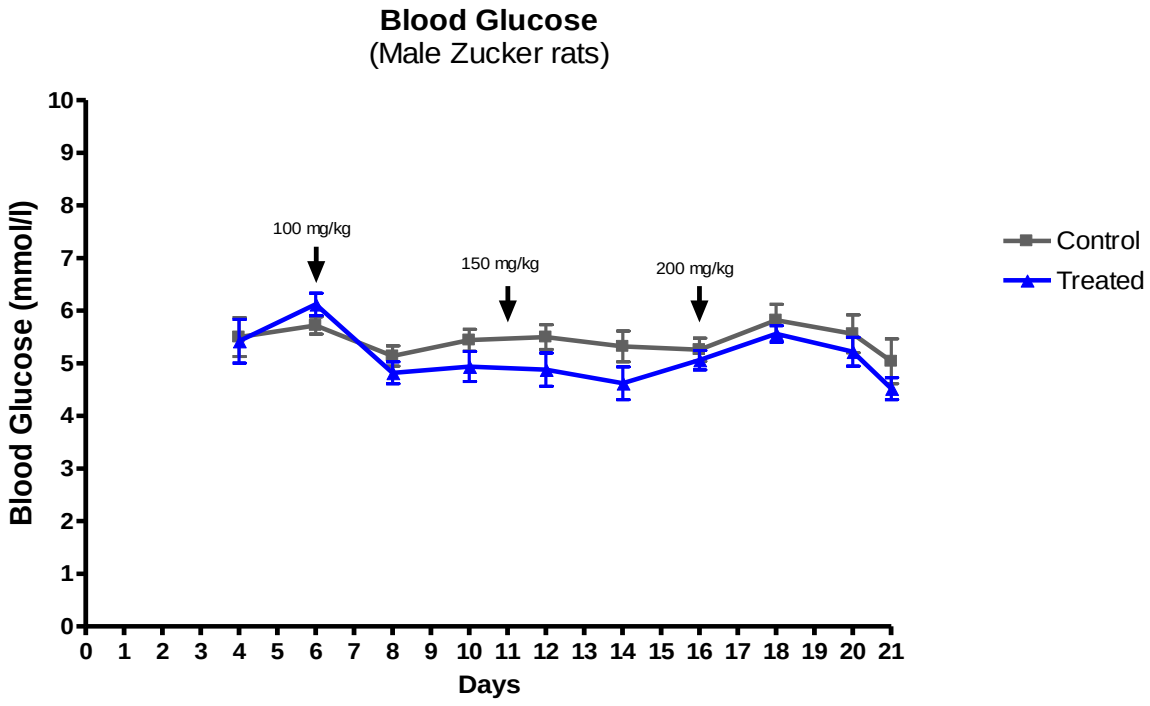

Figure 6. 12: The effect of LL on male Zucker rat BG (n=5). BG measurements were recorded every 48h ± 30 mins.

6.4.2.4.2. Female OZR

In the first two BG measurements, both the treated and the control group showed similar results as in Figure 6.13. On days 8-14, the treated group showed slightly

higher BG levels when compared with the control group ($P > 0.05$). Average BG levels of both groups were very similar on days 16-20, but the treated group BG increased on day 22 whereas the BG of the control group remained constant ($p > 0.05$).

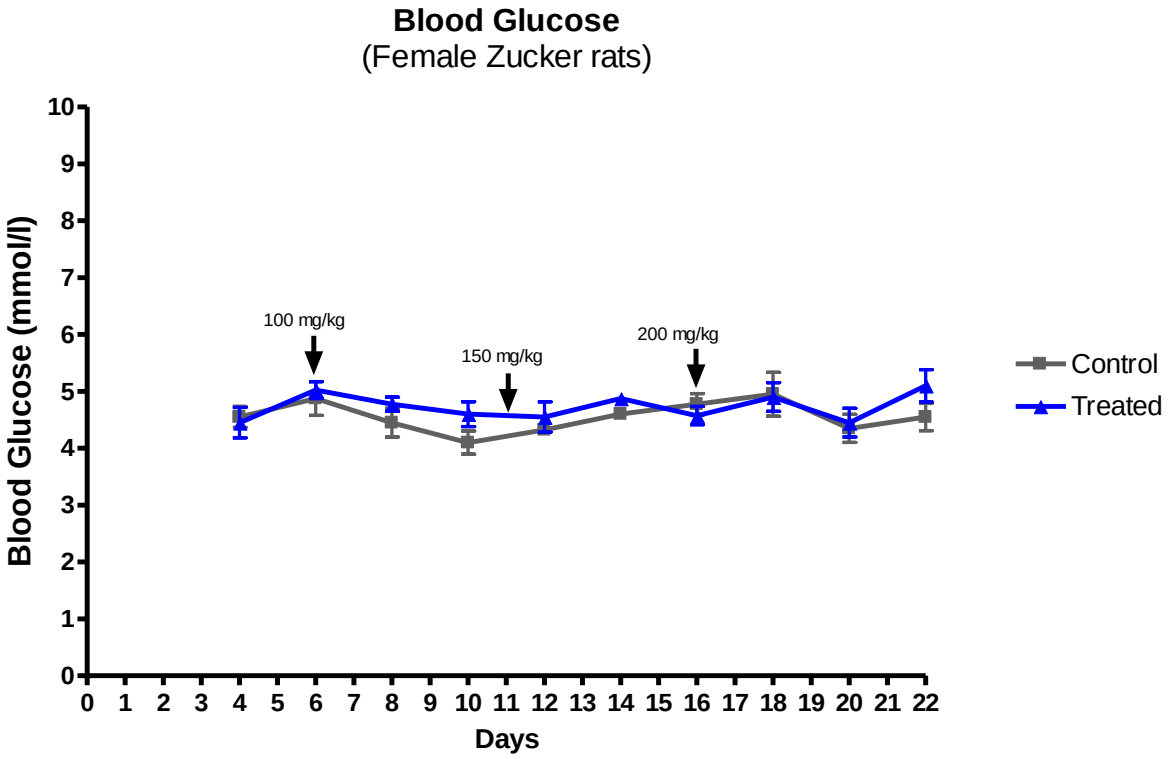

Figure 6. 13: The effect of LL on female Zucker rat BG (n=4). BG measurements were recorded every 48h ± 30 mins.

6.4.2.5. Collection of tissues

The following tissues were collected at the end of the animal experiment: liver, brain, hypothalamus skeletal muscles, adipose tissues, pancreas, kidney, testis and ovarian tissues. Some of the extracted tissues are shown in Figure 6.14. There were some lesions in the livers of two of the treated male OZR as shown in Figure 6.15.

The tissues were then placed in tubes containing RNA*later* solution and stored at 4°C for 24 hours to stabilise tissues' RNA. Then, RNA*later* solution was removed and the tissues stored at -80 °C in a freezer for long-term storage.

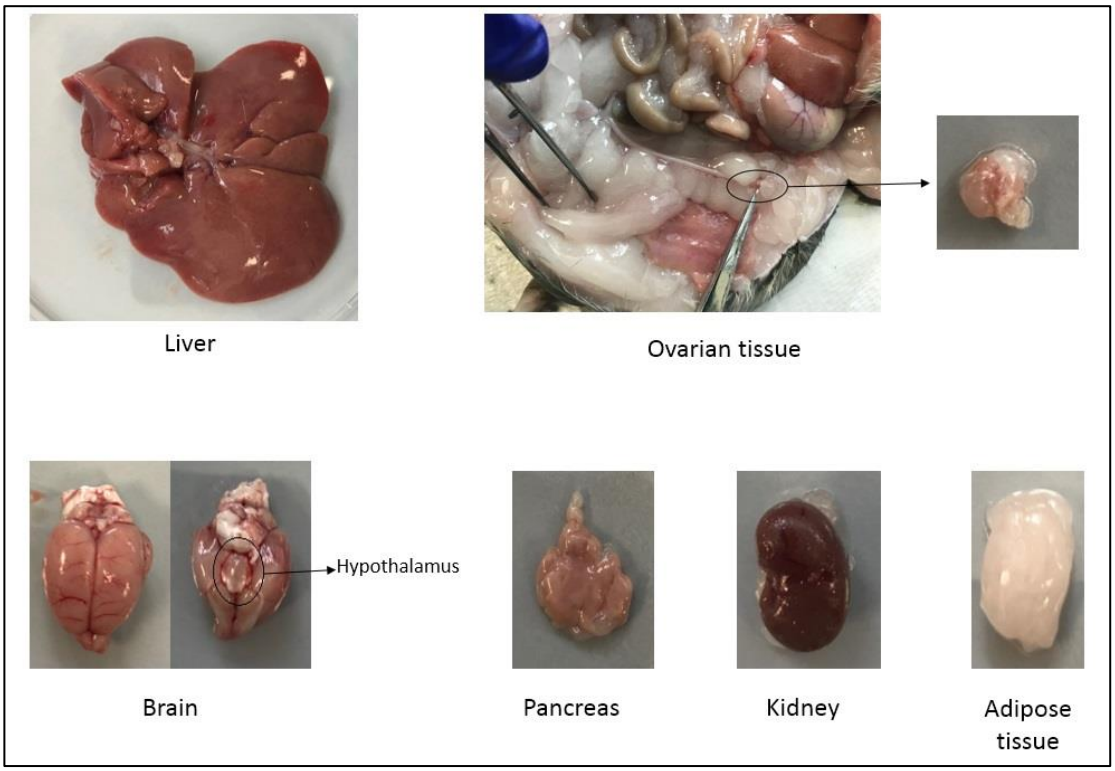

Figure 6. 14: Some of the extracted tissues following the end of the animal study. All tissues are representative for the other animals used in this study.

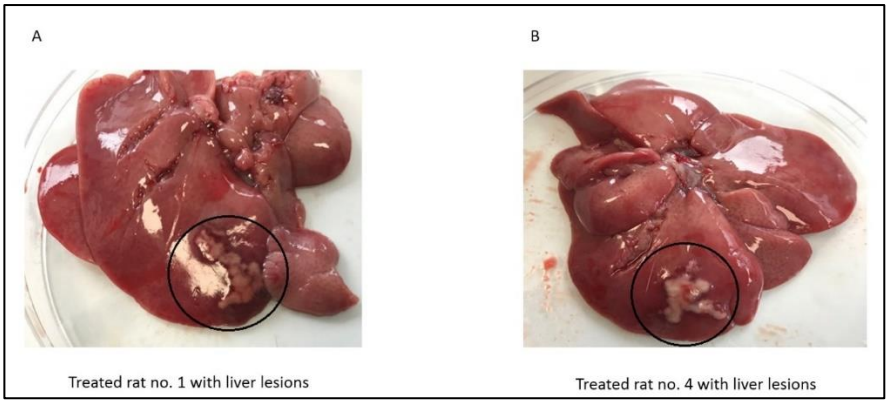

Figure 6. 15: Liver lesions were seen in two of the treated male Zucker rats.

6.4.2.5.2. Weight of the extracted tissues

Brain, kidney, liver and testis of the tested animals were weighed and the findings presented in Figures 6.16-6.19. There were no significant differences in the weight of the tissues, indicating LL treatment had no effect on their weight at the tested concentrations and time-frame of experiment.

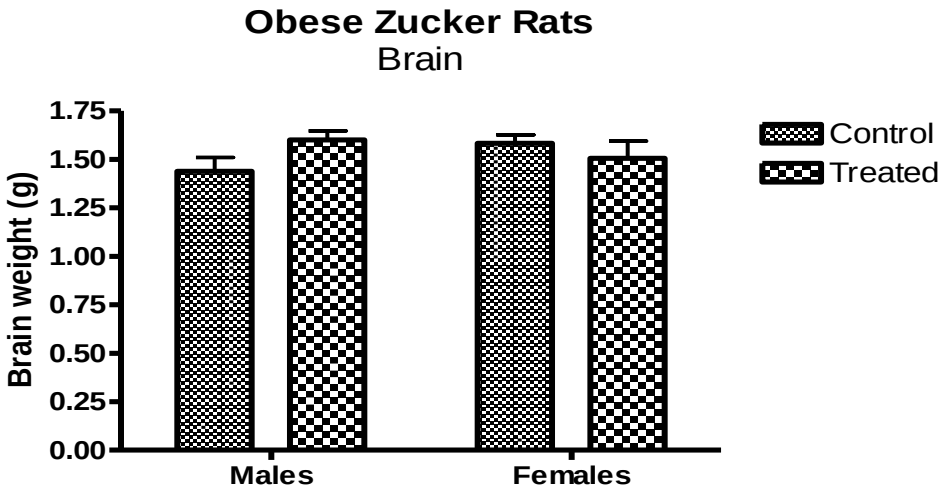

Figure 6. 16: The effect of LL treatment on the weight of the brain of male and female Zucker rats.

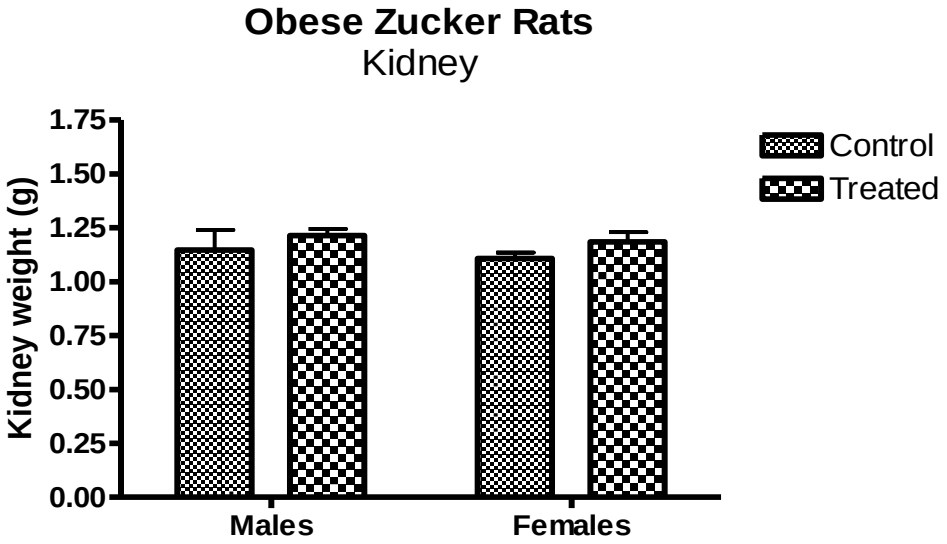

Figure 6. 17: The effect of LL treatment on the weight of the kidney (right kidney) of male and female Zucker rats.

Figure 6. 18: The effect of LL treatment on the weight of the liver of male and female Zucker rats.

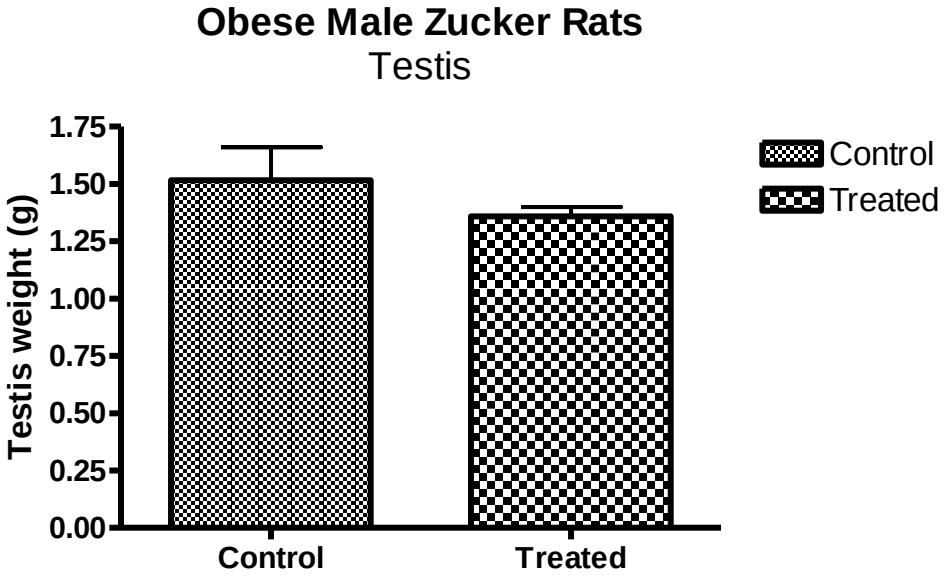

Figure 6. 19: The effect of LL treatment on the weight of the testis (right testis) of male Zucker rats.

6.5. Discussion and Conclusions

LL extracts and isolated compounds showed potential anti-diabetic, anti-inflammatory, anti-oxidant properties and the ability to change gene expression of pancreatic RNA. These results led to a trial on genetically obese animals.

Woods (2017) examined the effects of LL on male SD rats and the results showed no effect on BW, WI and FI. Therefore, the current feeding study was amended in the following ways to determine if the rat model used had not been the appropriate one. Firstly, OZR were used instead of SD rats. This is because they have a higher BW and therefore changes in BW could be detected more easily; Zucker rats are genetically obese and have insulin resistance and glucose intolerance and this make them a better model for this type of study (Phillips *et al.*, 1996; Srinivasan and Ramarao, 2007). Secondly, the current study employed male and female rats to determine if there are any gender differences in response to LL. Thirdly, the route of administration was modified so that the tubers were eaten rather than delivered by oral gavage as in Woods (2017) study. It was deemed that direct delivery to the stomach removed the possibility that chewing the tuber would remove some of the activity due to buccal cavity absorbance. Therefore, the current study incorporated ground tuber in Farley's rusks mixed with water. A preliminary test was carried out in SD rats before purchasing OZR which are more expensive. The rusks-tuber mixture was orally consumed by all of the rats and following this success, Zucker rats were purchased. Another amendment which was made in this study was to increase the LL dose to 100 mg/kg and titrated up to 200 mg/kg by the end of the study instead of 42 mg/kg which was given only once in the previous study.

Despite the fact that many amendments and changes were put into place to maximise the effects of LL, the findings showed no clear differences between the control and treated groups. LL slightly reduced the BW of male OZR and this reduction was increased when the dose of the tuber was increased. This showed that there was a dose-response effect, however, the results were statistically insignificant ($P > 0.05$). The effect of LL on BW was not evident as both the control and treated groups started to separate two days prior to the start of the treatment. Contrary results were obtained

from the female OZR; the control group continued to show a lower BW in comparison to the treated group. Again, these results were statistically insignificant ($P > 0.05$). These trends of results were also obtained when looking at the effects of LL tubers on WI of OZR. There was no statistical difference between the control and treated groups and this was true for both male and female rats. FI measurements produced similar results to the BW and WI in that the results were statistically insignificant ($P > 0.05$). LL did not affect the BG levels of male and female OZR either.

The lack of significant findings on either male or female OZR can be as a result of several factors. To start with, BW, FI and WI measurements were taken 24 hours post treatment and hence any effects that occurred before this time were not detected. BG was measured 2 hours post-treatment and this might have been too short of a time for LL to affect BG levels. A study by Candasamy *et al.* looked at the effect of glibenclamide (drug used for T2DM) and fenofibrate (drug used to lower cholesterol levels) on the BG of normal adult Wistar rats (Candasamy *et al.*, 2014). Glibenclamide and fenofibrate were administered orally at 0.45 mg/kg BW and 18.1 mg/kg BW repectively. BG levels were measured before and after drug treatments at 0, 0.5, 1, 2, 3, 4, 6, 8, 10, 12 and 16h by puncturing the tail vein and placing a drop of blood on a BG strip which was read by an Accu-Chek Active glucometer. Glibenclamide showed a significant BG reduction from 1h and this reduction was at its lowest level ($P < 0.01$) 4 hours following the treatment. Fenofibrate showed comparable results to that of the control ($P > 0.05$) for the first 3h of the treatment and at 4h, it was found to significantly ($P < 0.05$) decrease BG levels. Therefore, future work should involve collecting blood samples at different time points in order to find out the optimum time for monitoring BG following LL treatment.

Another possibility is the fact that rats are nocturnal (Tempel *et al.*, 1989). This means that rats usually consume more food during the dark phase (Terrón *et al.*, 2013). LL tubers were given to the rats during the light phase. The tubers may have contained appetite suppressant agents, however no effects were seen on BW, WI or FI because these agents' potential might have been diminished by the dark phase where rats eat more food. Metformin is an anti-diabetic drug that is effective in lowering BG and is

associated with reducing BW. Kim *et al.* investigated the effects of metformin on neuronal activity in obese mice . (Kim *et al.*, 2016). Obesity in male C57BL/6 mice was introduced by a high-fat diet for 16 weeks before starting metformin treatment. The experiment was carried out over a 3-day period where the control group received 0.9% saline (vehicle) for 3 days, the single metformin (SM) treatment group received vehicle for the first 2 days and 300 mg/kg BW metformin in the third day and the repeated metformin (RM) treatment group received 300 mg/kg BW metformin for 3 days. All treatments were administered by oral gavage immediately before the dark cycle (6pm). The BW of the SM and control groups were comparable ($P > 0.05$), whereas the RM group showed a significant reduction ($P < 0.05$) in BW vs SM and the control groups. Hence, future work could involve administering the tubers just before the dark phase.

Moreover, it was possible that the LL dose was not sufficient to initiate effects on BW, WI, FI or BG. In addition to that, the length of the treatment may have been too short to allow for biological responses. *Cyperus rotundus* tubers (CRT) is an Indian medicinal plant that is used as a slimming agent. Lemaure *et al.* studied the effects of 45 or 220 mg/kg BW hexane extract of CRT on the BW of OZR (Lemaure *et al.*, 2007). The study was performed over a 60-day period in which the CRT were administered daily. The study found that CRT significantly ($P < 0.05$) reduced the BW of OZR without changing the food consumption and the response was dose-dependent. Therefore, future work would involve repeating the current study for a longer period of treatment (60 days) to maximise the effects of LL tubers.

BA is one of the isolated compounds which is detailed in Chapters 2, 3 and 4 and was found to be a potential anti-diabetic, anti-obesity, anti-inflammatory and anti-oxidant agent in cells and isolated enzyme studies. As the LL tubers contain a mixture of compounds, this might have caused an antagonism effect and therefore resulted in negative findings of LL on the BW, WI, FI and BG of OZR, although this is not likely to be the reason as the tubers were traditionally eaten as a whole. Another possibility is that the BA concentrations in the administered LL tubers were at sub-therapeutic levels and hence no positive effects were seen. BA yield in the tuber was found to be

1.3% and this indicates that the BA concentration used in this animal study was 1.3-2.6 mg/kg BW. BA was shown to possess anti-diabetic activity in a number of published research papers. Xie *et al.* investigated the protective activity of BA on STZ-induced diabetic SD rats (Xie *et al.*, 2017). Rats were injected (IP) with STZ 35 mg/kg to induce diabetes. Seven days later, BA 20 mg/kg or 40 mg/kg was given daily and administered orally for 30 days. BG, insulin, Il1β and TNFα levels in the serum were monitored. BA significantly ($P < 0.05$) decreased BG, insulin Il1β and TNFα in a dose dependent manner. The % yield of BA isolated from LLT EA was 1.3 which means that approximately 1.3-2.6 mg/kg BW of BA was administered daily to OZR in this study and this is 8-16 times less than that used in the study by Xie *et al.* (2017). This might explain the reason why BA from LLT did not decrease the BG of OZR.

In another study by de Melo *et al.*, BA isolated from *Clusia nemorosa* was investigated for its biological effects in mice on HFD (de Melo *et al.*, 2009). Due to solubility issues, BA was initially suspended in 2% (v/v) Tween 80 and then dissolved in water. BA was given as 50 mg/L in drinking water for 15 weeks and the water was changed twice a week. The BA + HFD group showed significant decreases ($P < 0.05$) in BW, BG, total cholesterol and plasma triglycerides when compared to the HFD only group. Moreover, BA treatment increased plasma insulin and leptin levels significantly ($P < 0.05$), whereas ghrelin levels were decreased. All of the above studies suggest that the BA used in this research was at sub-therapeutic levels and that the length of treatment was insufficient for biological effects to occur.

Oral administration is preferred because it is less invasive compared to other methods for example, intravenous (IV), subcutaneous (s/c) and intraperitoneal injection (IP). However, the bioavailability of oral drugs is affected by many factors including degradation in the stomach and metabolism by gut and liver in which these are avoided by IV, IP and s/c routes. Tubers were orally administered to OZR to mimic their traditional use of being eaten by humans. However, humans and rats are different species and they possess different hepatic metabolising enzymes, particularly in cytochromes P450 (CYP450). CYP450 are metabolising enzymes that are commonly involved in metabolism of xenobiotics (Martignoni *et al.*, 2006). Tubers are a mixture

of compounds in which some might be activated after metabolism (pro-drugs) by specific human enzymes that are not present in the rats so therefore, no biological effects were seen in this study. Moreover, first pass hepatic metabolism is challenging for oral drugs and results in reduced bioavailability. Therefore, IC, IP and s/c routes are advantageous as they are not affected by first pass metabolism and therefore they have increased bioavailability. To illustrate this with an example, Kao *et al.* compared the biological effects of oral and IP administration of EGCG on SD rats (Kao *et al.*, 2000). IP EGCG at 85 mg/kg BW showed significant reduction in the BW of OZR, whereas its oral administration did not affect the BW. This study suggests that the LL route of administration should consider IP method in a future animal study.

This study only looked at the LL effects on BW, FI, WI and BG however, these are not the only parameters by which anti-diabetic and anti-obesity agents work. In the study by Woods (2017), LL treatment did not affect any of the parameters measured (BW, FI, WI) in SD rats. However, RNA samples isolated from pancreatic tissues of these rats revealed the fact that several genes involved in obesity and diabetes were affected as detailed in Chapter 5. *Adipoq* expression was significantly upregulated ($P < 0.001$) by LL treatment. This gene is known for its anti-diabetic and anti-obesity effects and its expression in the pancreas is linked with enhancing insulin release and protecting pancreatic β-cells from apoptosis. Moreover, genes such as *Il1β* and *Tnfrsf19* were down-regulated ($P<0.05$). The expression of such genes is linked with diabetes and damage to β-cells of the pancreas. Therefore, it is possible that the anti-diabetic and anti-obesity activity of LL might initially start by affecting the gene expression which may require time in order to be reflected by parameters such as BW, WI, FI and BG. Future work should consider investigating the effects of LL on gene expression (hypothalamus, pancreas, liver and adipocytes) of OZR.

In addition to this, it is possible that OZR were not the ideal model to assess the appetite suppressant activities of the LL tubers. Anecdotal evidence provided by Dr. Brian Moffat indicated that the effects of the LL tuber starts 1-1.5 h following its consumption and would suppress the appetite in humans by decreasing the feeling of a "desire to eat". Several plants have been tested as appetite suppressants that reduced

the BW of humans, but not in rats. *Garcinia cambogia* is a plant that is endogenous to Southeast Asia. Its hydroxycitric acid (HCA) extract is available commercially to suppress appetite and reduce BW *(*Semwal *et al.*, 2015). HCA has been traditionally used with meals and reported to increase feeling of satiety. Preuss *et al.* investigated the activity of HCA on 60 human volunteers who were given a 2000 kcal diet/day and an oral dose of placebo or 4.7 g HCA three times per day 30-60 minutes before meals for 8 weeks (Preuss *et al.*, 2004). The study monitored the BW, BMI, lipid profiles, serum leptin, serotonin and excretion of urinary fat metabolites at 0, 4 and 8 weeks of treatment. At the end of the study, BW and BMI decreased by 5.4% and 5.2%, respectively. FI, serum leptin, LDL, triglyceride and total cholesterol levels were significantly lower in the treated group, whereas HDL, serotonin levels and fat metabolites excretion were increased significantly when compared with the control group. The study reported no significant adverse effects and therefore demonstrated the safety and efficacy of HCA in humans. However, a year later, Saito *et al.* investigated the effect of HCA on 6-week old male OZR (Saito *et al.*, 2005). The rats were fed various doses of HCA, 0, 2.0, 10.1, 20.1 and 30.2, g HCA/kg diet for 92 days. The findings were that HCA showed no effect on the FI and BW of male OZR. Both of these studies suggest that LL tubers should be administered to humans for future work in order to investigate the appetite suppressant activity. Traditionally, LL tubers were eaten and there are no reported adverse effects associated with them.

Moreover, sample size plays an important role when it comes to designing animal experiments. An insufficient sample size can lead to mis-capturing of real effects and differences between groups. On the other hand, a sample size that is too large can result in wastage of resources and animals involved in the study. According to Charan and Kantharia there are a number of sample size calculation methods which can be applied when it comes to designing animal studies (Charan and Kantharia, 2013). One of these methods is called the "resource equation" method. It is advantageous to use this method when it is not possible to make assumptions about the effect of sample size and therefore it is the preferred method for exploratory studies. In this method, "E" value is calculated. E is the degree of freedom of analysis of variance (ANOVA). For

significant results, the E value is recommended to be between 10 and 20. E value is calculated using the following formula:

$$E = Number\ of\ animals\ in\ the\ study - number\ of\ groups\ in\ the\ study$$

By applying the sample size used in the current study, 10 male OZR were divided into two groups and this gives E a value of 8, whereas the female OZR group had an E value of 6. Therefore, the sample size used in the current study was too small and this might have caused significant results not to be seen. By choosing an E value of 16, this experiment should have had 9 animals per group instead of 5 and 4 in male and female groups, respectively. This was meant to be a preliminary study so the number chosen was deemed correct.

The weight of tissues from the treated groups was comparable with their controls. Two male Zucker rats from the treated group developed some hepatic lesions, however, none in the female treated group did. Hence, 40% of the treated male group and 22% of the total treated animals in the study developed liver lesions. It is challenging at this time to determine the cause of this hepatic damage for a number of reasons. It is more likely that this damage to the liver was pre-existing as such lesions are known to be a consequence of chronic exposure to hepatotoxins and the LL was administered for only two weeks. Moreover, only 2 out of the 9 treated rats showed any hepatic effects and this again supports the possibility that these lesions existed before the treatment started. Furthermore, Woods (2017) did not report any liver damage to SD rats following treatment with LL. Future work will involve histopathological studies to identify the nature and possible causes for liver damage.

In conclusion, LL tubers did not show any significant effects on the BW, FI, WI or BG of the tested male and female OZR. Further investigation is required to be carried out on the gene expression effects of LL on OZR. This will be carried out in the next few months by other students and it will be interesting to compare the results with the normal rats.

Chapter 7

7. Summary, Future work and Conclusions

As indicated in Chapter 1, the objective of this research was to evaluate the anti-diabetic and anti-obesity activities of LL tubers and leaves by *in vitro* and *in vivo* methods. LL tubers were historically used during medieval times as appetite suppressants when food was scarce however, there is a lack of scientific research investigating their appetite suppressant activity. There is no historical use reported for LL leaves, but they were included in this project as this part of the plant is renewable. NMR was used to identify the constituents present in each extract. LLT EA extract was shown to exhibit inhibitory effects on α-glucosidase by Woods (2017), but the compounds responsible for the activity were not isolated. Therefore, the current research fractioned LLT EA extract to isolate bioactive compounds. For the first time, BA, lupeol and a mixture of stigmasterol and sitosterol were isolated from LL. BA was found to be the major compound in LLT EA extract and its % yield was 1.3 which is high in comparison to other plants (Prakash Chaturvedula *et al.*, 2003; Begum *et al.*, 2002; Chien *et al.*, 2004; Fang *et al.*, 2006; Fu *et al.*, 2005). This indicates that LL is a potential good source for BA.

The isolated compounds are known to possess various biological activities and include anti-hyperglycaemia, anti-HIV, anti-malarial, anti-inflammatory, anti-oxidant and anti-mutagenic effects (Bori *et al.*, 2012; Guo *et al.*, 2018; Gabay *et al.*, 2010; Gupta *et al.*, 2011). Therefore, these isolated compounds as well as the LL extracts were subjected to *in vitro* testing against isolated enzymes implicated in diabetes and obesity (α-glucosidase, α-amylase, PTP 1B, PL and DPPIV) as presented in Chapter 3. In the α-glucosidase assay, only LLT EA extract and BA from the tubers were potent α-glucosidase inhibitors ($P < 0.05$) with IC_{50} of 9.5 µg/ml and 5.5 µM, respectively. Moreover, LLL EA and LLL MeOH extracts of LL leaves were also strong inhibitors of α-glucosidase ($P < 0.05$) with IC_{50} of 0.58 µg/ml and 4.3 µg/ml, respectively. Inhibitors of α-glucosidase are not only beneficial for enhancing insulin release and lowering postprandial BG, they are also hunger suppressants and satiety enhancers (Hao *et al.*, 2017). GLP-1 activity is prolonged by α-glucosidase inhibitors

and this has been directly linked with delayed gastric emptying (DGE) which enhances satiety, reduces hunger and limits calorie intake (Lee *et al.*, 2002). It is possible that the activity of LLT EA extract on α-glucosidase is as a result of BA which is found to be the major compound present in both these extracts. Despite the fact that α-glucosidase and α-amylase have similar physiological actions, none of the extracts or tested compounds were inhibitors for α-amylase. This indicates that LL may possess selective α-glucosidase inhibitors. None of the tested LL extracts or isolated compounds showed inhibition against PTP 1B and DPPIV at the tested concentrations and this might indicate that the LL anti-diabetic mechanism of action does not involve PTP 1B and DPPIV inhibition. This was followed up by testing samples against PL. LLT EA at 30 µg/ml and BA at 30 µM showed 50% enzyme inhibition ($P<0.05$) and one extract from the leaves (LLL Hex) showed 30% inhibition, which was statistically significant. The isolated enzymatic assays suggest that LL can be potentially therapeutic for diabetes and obesity as it had extracts and BA which strongly inhibited α-glucosidase and PL. *Acacia nilotica* is a Sudanese plant that is used by people in Sudan to manage diabetes (El-Kamali, 2009). Elbashir *et al.* investigated the anti-diabetic activity of ethanolic extract of *A. nilotica* and the plant was a potent α-glucosidase and PL inhibitor with an IC_{50} of 3.75 µg/ml and 1.65 µg/ml, respectively (Elbashir *et al.*, 2018). This suggests that LL could be a potential therapeutic plant for diabetes and obesity. Then, LL extracts and isolated compounds were assessed in HepG2 cells for their ability to increase glucose uptake in cells. Only LLL Hex showed a significant increase in glucose uptake which was comparable to that of insulin. Future work would consider more phytochemistry work on the extracts to isolate and purify compounds and retest them for anti-diabetic activities.

As a consequence of the potential anti-diabetic findings in Chapter 3, LL extracts and isolated compounds were further investigated for their anti-inflammatory and anti-oxidant activities using *in vitro* assays as per Chapter 4. Inflammation and oxidative stress have been linked to the development of diabetes and obesity. Samples were assessed for their ability to protect L929 cells from 10 µM of TNFα, which is the concentration that was found to be cytotoxic to 50% of the cells. Pre-incubation of cells with LL extracts and isolated compounds protected them ($P < 0.05$) from

cytotoxic effects of TNFα. Moreover, TNFα is known to be an activator of NF-ƙB, which is an inflammatory mediator. Hence, this was followed up by assessing the inhibition activity of LL extracts and compounds against NF-ƙB in NCTC cells, which are human skin cells that are transfected with NF-ƙB luciferase reporter vector. The active samples were BA, LLT EA, LLL Hex and LLL EA which gave a NF-ƙB % inhibition of 70, 40, 30 and 30, respectively. The BA concentration inhibition curve was performed and inhibited NF-ƙB expression with an IC_{50} of 22.8 µM. The inhibition of NF-ƙB is associated with enhanced insulin release and improved glucose homeostasis (Li *et al.*, 2018).

LLT extracts and isolated compounds showed no positive activity in the DPPH assay at the tested concentrations, whereas, LLL EA and LLL MeOH extracts of the leaves showed inhibitory activity against DPPH with IC_{50} of 6.5 µg/ml and 24.8 µg/ml, respectively. However, these two extracts of LLL require fractionation and isolation of intrinsic compounds to identify those responsible for the DPPH inhibition activity. Sylvie *et al.* (2014) investigated the types of compounds present in MeOH extracts of *Garcinia lucida*, *Hymenocardia lyrata* and *Acalypha racemosa* which are DPPH inhibitors (IC_{50} 1.74 µg/ml 2.61 µg/ml). The phytochemical screening of these extracts showed the presence of various classes of compounds. These are alkaloids, tannins, glycosides, terpenoids and flavonoids. Then, all LLT and LLL samples were investigated for ROS generation in an DCFDA assay in SH-SY5Y, Panc1 and HepG2 cells. None of the samples were ROS-generators in the tested cells, except for lupeol which increased ROS generation by threefold ($P<0.05$) in HepG2 cells only. Further to this, samples were retested in the same assay, but this time in the presence of tBuOOH, a ROS-generator. All LL samples showed at least 70% protection ($P<0.01$) to cells from ROS generated by tBuOOH, apart from lupeol which increased the generated ROS to over 280% in HepG2 cells. The finding obtained from lupeol was expected as it increased ROS when it was administered alone in HepG2 cells. This research showed that lupeol generates ROS in HepG2 cells and this is not concordant with the literature. Preetha *et al.* (2006) showed that *in vivo* lupeol possesses hepatoprotective activity against ROS generated by alfatoxins, which are known hepatotoxic and hepatocarcinogenic agents. Moreover, cadmium is hepatotoxic

and elicits its action by generating ROS and changing the hepatic redox state. Lupeol was administered at 150 mg/kg daily for three days prior to injecting rats with cadmium chloride; lupeol changed the hepatic redox state and scavenged ROS. However, the mismatch between the results obtained in this project and the literature can be due to two reasons; 1) *in vitro* studies do not always correlate with *in vivo* studies; 2) HepG2 are human hepatic cells, whereas the previous studies were on rats and therefore the difference in species can generate opposing results. These findings were followed up further by assessing the LL effects on HepG2 GSH levels. LLT EA, LLT Hex, LLL Hex and BA were found to increase GSH levels in HepG2 cells and results were statistically significant. LLT EA showed the highest increase in GSH levels in which it doubled GSH levels in comparison with the control ($P < 0.01$). This also contributes to the fact that LL can be a potential therapeutic agent for diabetes and obesity. Dinçer *et al.* (2002) investigated the relationship between reduced GSH levels and glycaemic control in diabetic patients where poorly controlled T2DM showed lower GSH levels in blood samples in comparison with the well-controlled T2DM patients. Minette *et al.* (2015) justified the decrease in the GSH levels in T2DM patients because this was as a result of compromised GSH synthesis and metabolising enzyme levels.

Following the evidence of anti-diabetic, anti-obesity, anti-inflammatory and anti-oxidant activity of LL, it was considered pertinent to carry out a retrospective investigation into any gene changes using RNA-Seq and RT-qPCR on RNA isolated from rat pancreatic tissues following treatment with LL tubers by Woods (2017) (Chapter 5). It was anticipated that this would provide information on the action of tubers on an organ which plays a vital role in the digestive process and BG regulation. Isolating high quality intact RNA is crucial when it comes to carrying out deep molecular analysis such as RNA sequencing and RT-qPCR. The isolated RNA samples showed low RIN values (5-6) and this was expected due to the presence of high endogenous levels of RNases, DNases and proteases in the pancreas which enhance autolysis immediately following death and dissection (Augereau *et al.*, 2016). Therefore, only two control and two treated samples were sent for RNA-Seq analysis. RNA-Seq showed that the cytokine-cytokine receptor interaction pathway was most

affected by the LLT treatment. Therefore, 7 selected genes from this pathway were chosen to be validated in RT-qPCR, these are *Adipoq, Il1β, Tnfrsf19, Cd40, Cd40ig, Lep* and *Ccl20*. RT-qPCR showed that *Adipoq* was increased by more than 15-fold ($P<0.01$) following LLT treatment. Adiponectin, a product of *Adipoq*, acts as an anti-inflammatory, anti-atherogenic and insulin-sensitising hormone. Reduced adiponectin levels are known to be prevalent in obese patients and T2DM, thus suggesting its role in obesity and diabetes. Yamauchi *et al.* (2003) administered globular adiponectin to transgenic *ob/ob* mice and tested animals showed higher insulin sensitivity and secreted more insulin when compared with non-transgenic mice. This suggests that LL tubers contain compounds that enhance adiponectin levels which may be beneficial for diabesity. All the other selected cytokines were down-regulated in RT-qPCR and this was statistically significant ($P < 0.05$) for *Il1β, Tnfrsf19* and *Lep*. The expression of such genes in the pancreas is known to suppress insulin and can result in apoptosis in pancreatic β-cells (Dogan *et al.*, 2006; Schön *et al.*, 2014; Marroquí *et al.*, 2012). These findings suggest that LL tubers may also act as anti-diabetics by protecting pancreatic β-cells from apoptosis and by enhancing insulin release which is stimulated by adiponectin.

OZR have a mutation in the leptin receptors that results in hyperphagia which causes obesity by the age of four weeks (Phillips *et al.*, 1996). They are also hyperinsulinaemic, hyperlipidaemic, hypertensive and have impaired glucose tolerance (Srinivasan and Ramarao, 2007). Hence, they were chosen in this study as their obesity and diabetic state does not require STZ or a HFD to be developed. This research was concluded by an *in vivo* study on OZR where their BW, FI, WI and BG were monitored following LL tuber treatment. Male and female rats were employed in the current study to find out any gender differences in response to LL tubers as in the Woods (2017) study only male SD rats were investigated. Woods study showed no biological effect on BW, FI and WI following LL treatment. Therefore, it was decided to improve on the Woods study by changing the route of administration by mixing the tubers with baby rusks and allowing rats to consume the mixture orally. Moreover, the dose of LL tubers in this study was increased up to 200 mg/kg instead of 42 mg/kg which was given by oral gavage in the study by Woods (2017). However, this study

found no clear differences between the control and treated groups in terms of BW, WI, FI and BG. This was similar to what had occurred with the normal rats in Woods' study. The lack of response could be as a result of the short duration of the study; LL tubers might need a longer duration to show positive effects however, this does not agree with the anecdotal evidence which indicates that the tubers begin to take action in less than 1.5h following their consumption.

7.1. Future work

Future work could include the following:

- Fractionation of the LL extracts from tubers and leaves and isolation of more compounds to assess their anti-diabetes, anti-obesity, anti-inflammatory and anti-oxidant activity using the same methods as in Chapters 3 and 4.
- Isolation of RNA samples from the hypothalamus, liver and pancreas tissues of LL treated OZR and investigate the gene expression by RNA-Seq and RT-qPCR experiments.
- Repeating the *in vivo* feeding study on OZR with some modifications. For example, LL tubers to be administered twice daily for at least 6 weeks. One dose to be given in the morning (9am) and the second dose to be administered just before the dark phase (6pm).
- Consider giving LL tubers to humans to assess the safety, efficacy and bioavailability of the tubers.

7.2. Conclusions

The main findings of the study were:

- There are four compounds which were isolated for the first time from tubers of LL. These are BA, lupeol, stigmasterol and sitosterol.
- LLT EA, BA, LLL MeOH and LLL EA were potent α-glucosidase inhibitors ($P < 0.05$) with IC_{50} of 9.5 µg/ml, 5.5 µM, 4.3 µg/ml, 0.58 µg/ml, respectively.

- In PL assay: LLL Hex, LLT EA and BA showed significant ($P < 0.05$) PL % inhibition of 30, 50, 50, respectively.

- LLL Hex increased glucose uptake in HepG2 cells by 50% ($P < 0.05$) and the results were comparable to that for insulin.
- All LLT and LLL extracts and isolated compounds protected L929 cells ($P < 0.05$) from cytotoxic effects of 10 µM TNFα, concentration that is cytotoxic to 50% of the cells.
- LLL EA, LLL Hex, LLT EA and BA showed NF-ƙB % inhibition of 30, 30, 40 and 70, respectively. The BA inhibition curve was performed and it inhibited NF-ƙB expression with an IC_{50} of 22.8 µM.
- Only two extracts were potent DPPH inhibitors, these are LLL EA and LLL MeOH with IC_{50} of 6.5 µg/ml and 24.8 µg/ml, respectively.
- Except for lupeol, all LLT and LLL extracts (30 µg/ml) and isolated compounds (30 µM) were potent ROS scavengers in a DCFDA assay with SH-SY5Y, Panc1 and HepG2 cells.
- In HepG2 cells, the GSH concentrations were significantly increased to 3.29 µM, 2.44 µM, 2.25 µM, 2.11 µM, 2.08 µM and 2.06 µM by LLT EA, LLT Hex, LLL Hex, LLL EA. BA and LLT MeOH, respectively.
- RNA-Seq of pancreatic tissues of SD rats showed that the cytokine-cytokine receptor interaction pathway was most affected by LL whole tuber treatment. RT-qPCR showed that the adiponectin gene (*Adipoq*) was highly up-regulated ($P < 0.05$), whereas genes that contribute to pancreatic β-cells damage such as *Il1β* and *Tnfrsf19* were down-regulated ($P < 0.05$).

In conclusion, based on these results, the following schematic diagram (Figure 7.1) shows the potential mechanisms of action of the LL tubers and leaves. This research produced findings that show how LL could potentially be used for managing diabesity because it possesses compounds that inhibit enzymes which are implicated in diabesity such as α-glucosidase and PL. Moreover, LL in this research showed potential anti-oxidant and anti-inflammatory activities by enhancing GSH synthesis and inhibiting ROS and inflammatory mediators such as TNFα and NF-ƙB which are implicated in

diabesity. Lastly, LL administration to male SD rats showed upregulation of *Adipoq* and downregulation of both *Il1β* and *Tnfrsf19* in pancreatic tissues. This result indicates the benefit of LL in protecting pancreatic β-cells from damage and apoptosis and in enhancing insulin release. Current licensed drugs used in the management of diabesity are associated with unpleasant side effects and hopefully LL has the potential of improving treatment for obesity and diabetes.

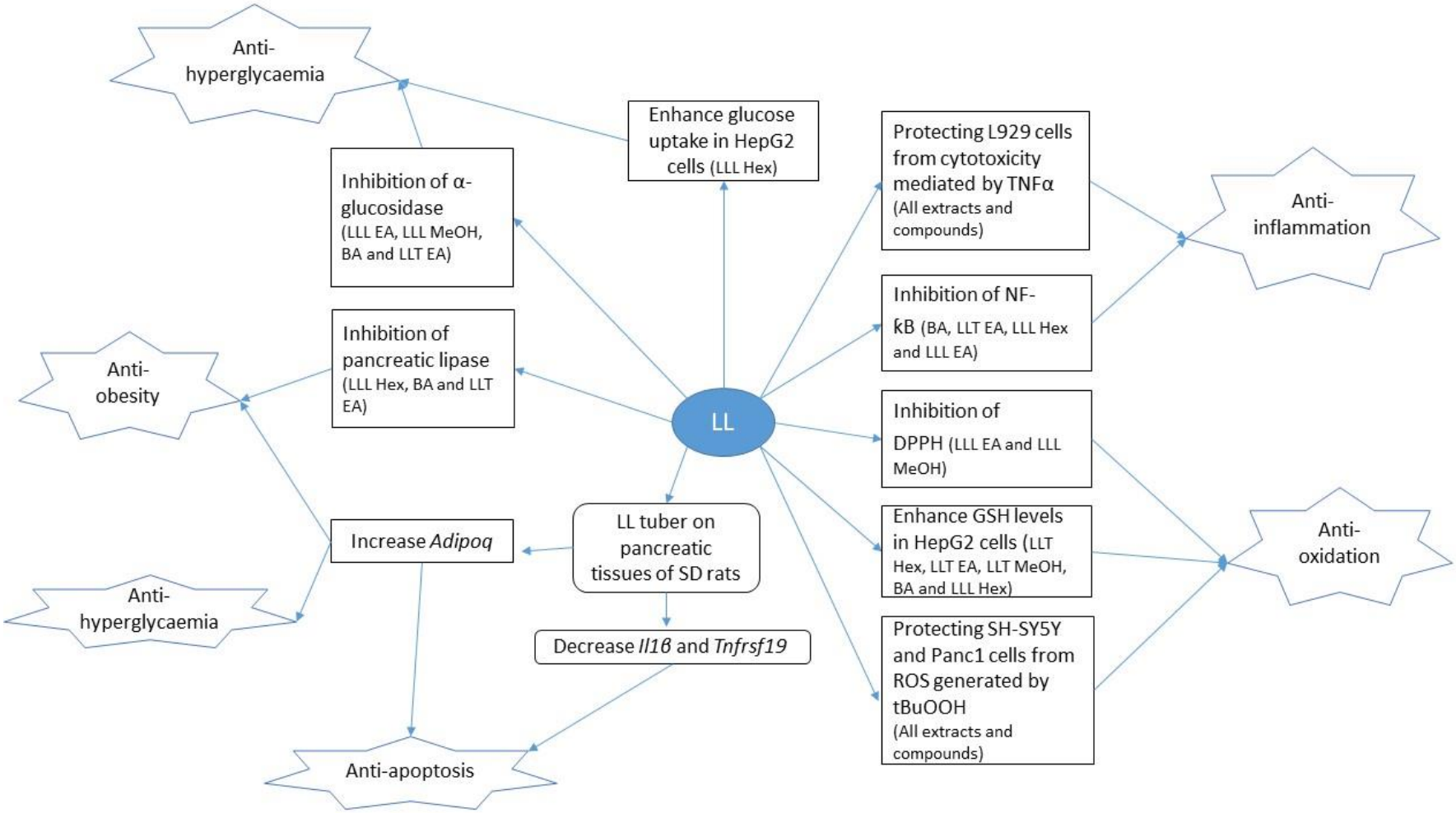

Figure 7. 1: Summary of the mechanism of actions by which LL can be used for diabesity management.

8. References

ADINORTEY, M. 2017. Biochemicophysiological Mechanisms Underlying Signs and Symptoms Associated with Diabetes mellitus. *Advances in Biological Research,* 11**,** 382-390.

ADOLF WIND FORM, A. H. 1907. Over Stigmasterin, a new Phytoserin from Calabar beans. *Reports of the German chemical society,* 39**,** 4378-4384.

AHANGARPOUR, A., SHABANI, R. & FARBOOD, Y. 2018. The effect of betulinic acid on leptin, adiponectin, hepatic enzyme levels and lipid profiles in streptozotocin–nicotinamide-induced diabetic mice. *Research in pharmaceutical sciences,* 13**,** 142-148.

AHMED, F. E., GOUDA, M. M., HUSSEIN, L. A., AHMED, N. C., VOS, P. W. & MOHAMMAD, M. A. 2017. Role of melt curve analysis in interpretation of nutrigenomics' MicroRNA expression data. *Cancer Genomics-Proteomics,* 14**,** 469-481.

AHMED, S., MAHMOOD, Z. & ZAHID, S. 2015. Linking insulin with Alzheimer's disease: emergence as type III diabetes. *Neurological Sciences,* 36**,** 1763-1769.

AKAR, Z., KÜÇÜK, M. & DOĞAN, H. 2017. A new colorimetric DPPH• scavenging activity method with no need for a spectrophotometer applied on synthetic and natural antioxidants and medicinal herbs. *Journal of enzyme inhibition and medicinal chemistry,* 32**,** 640-647.

AKEY, J., SOSNOSKI, D., PARRA, E., DIOS, S., HIESTER, K., SU, B., BONILLA, C., JIN, L. & SHRIVER, M. 2001. Melting curve analysis of SNPs (McSNP®): A gel-free and inexpensive approach for SNP genotyping. *Biotechniques,* 30**,** 358-367.

AL-TRAD, B., ALKHATEEB, H., ALSMADI, W. & AL-ZOUBI, M. 2019. Eugenol ameliorates insulin resistance, oxidative stress and inflammation in high fat-diet/streptozotocin-induced diabetic rat. *Life Sci,* 216**,** 183-188.

ALLABY, M. 2012. Lathyrus. 3 ed.: Oxford University Press.

ALLISON, K. C., CROW, S. J., REEVES, R. R., WEST, D. S., FOREYT, J. P., DILILLO, V. G., WADDEN, T. A., JEFFERY, R. W., VAN DORSTEN, B. & STUNKARD, A. J. 2007. Binge eating disorder and night eating syndrome in adults with type 2 diabetes. *Obesity (Silver Spring, Md.),* 15**,** 1287-1293.

ANISZEWSKI, T. 2007. *Alkaloids-Secrets of Life:: Aklaloid Chemistry, Biological Significance, Applications and Ecological Role,* Elsevier.

AQIL, F., MUNAGALA, R., JEYABALAN, J., JOSHI, T., GUPTA, R. C. & SINGH, I. P. 2014. The Indian Blackberry (Jamun), Antioxidant Capacity, and Cancer Protection. *Cancer*. Elsevier.

ARIMOCHI, H., SASAKI, Y., KITAMURA, A. & YASUTOMO, K. 2016. Differentiation of preadipocytes and mature adipocytes requires PSMB8. *Scientific reports,* 6**,** 1-8.

ASMUSSEN, C. & LISTON, A. 1998. Chloroplast DNA characters, phylogeny, and classification of Lathyrus (Fabaceae). *American Journal of Botany,* 85**,** 387-401.

IDF. 2017. International diabetes federation. *IDF Diabetes Atlas, 8th edn. Brussels, Belgium: International Diabetes Federation*.

AUGEREAU, C., LEMAIGRE, F. P. & JACQUEMIN, P. 2016. Extraction of high-quality RNA from pancreatic tissues for gene expression studies. *Analytical Biochemistry,* 500**,** 60-62.

AWAD, A., DOWNIE, A. C. & FINK, C. S. 2000. Inhibition of growth and stimulation of apoptosis by beta-sitosterol treatment of MDA-MB-231 human breast cancer cells in culture. *International journal of molecular medicine,* 5**,** 541-546.

AZMIR, J., ZAIDUL, I., RAHMAN, M., SHARIF, K., MOHAMED, A., SAHENA, F., JAHURUL, M., GHAFOOR, K., NORULAINI, N. & OMAR, A. 2013. Techniques for extraction of bioactive compounds from plant materials: A review. *Journal of Food Engineering,* 117**,** 426-436.

BABA, S. A. & MALIK, S. A. 2015. Determination of total phenolic and flavonoid content, antimicrobial and antioxidant activity of a root extract of Arisaema jacquemontii Blume. *Journal of Taibah University for Science,* 9**,** 449-454.

BABU, K. S., TIWARI, A. K., SRINIVAS, P. V., ALI, A. Z., RAJU, B. C. & RAO, J. M. 2004. Yeast and mammalian α-glucosidase inhibitory constituents from Himalayan rhubarb Rheum emodi Wall. ex Meisson. *Bioorganic & medicinal chemistry letters,* 14**,** 3841-3845.

BACHA, F., SAAD, R., GUNGOR, N. & ARSLANIAN, S. A. 2004. Adiponectin in youth: relationship to visceral adiposity, insulin sensitivity, and [beta]- cell function.(Metabolic Syndrome/ Insulin Resistance Syndrome/Pre-Diabetes). *Diabetes Care,* 27**,** 547-552.

BACHHAWAT, A. K. & YADAV, S. 2018. The glutathione cycle: Glutathione metabolism beyond the γ- glutamyl cycle. *IUBMB life,* 70**,** 585-592.

BAGUL, P. K., DEEPTHI, N., SULTANA, R. & BANERJEE, S. K. 2015. Resveratrol ameliorates cardiac oxidative stress in diabetes through deacetylation of NFkB-p65 and histone 3. *The Journal of Nutritional Biochemistry,* 26**,** 1298-1307.

BANERJEE, M. & SAXENA, M. 2012. Interleukin-1 (IL-1) family of cytokines: role in type 2 diabetes. *Clinica Chimica Acta,* 413**,** 1163-1170.

BANI, S., KAUL, A., KHAN, B., AHMAD, S. F., SURI, K., GUPTA, B., SATTI, N., QAZI, G. J. P. R. A. I. J. D. T. P. & DERIVATIVES, T. E. O. N. P. 2006. Suppression of T lymphocyte activity by lupeol isolated from Crataeva religiosa. *Phytotherapy Research,* 20**,** 279-287.

BARBÉ-TUANA, F. M., KLEIN, D., ICHII, H., BERMAN, D. M., COFFEY, L., KENYON, N. S., RICORDI, C. & PASTORI, R. L. 2006. CD40–CD40 ligand interaction activates proinflammatory pathways in pancreatic islets. *Diabetes,* 55**,** 2437-2445.

BARON, A. D. 1998. Postprandial hyperglycaemia and α-glucosidase inhibitors. *Diabetes Research and Clinical Practice,* 40**,** S51-S55.

BASKAR, A. A., AL NUMAIR, K. S., GABRIEL PAULRAJ, M., ALSAIF, M. A., MUAMAR, M. A. & IGNACIMUTHU, S. 2012. β-sitosterol prevents lipid peroxidation and improves antioxidant status and histoarchitecture in rats with 1, 2-dimethylhydrazine-induced colon cancer. *Journal of medicinal food,* 15**,** 335-343.

BASKAR, A. A., IGNACIMUTHU, S., PAULRAJ, G. M. & AL NUMAIR, K. S. 2010. Chemopreventive potential of β-sitosterol in experimental colon cancer

model-an in vitro and in vivo study. *BMC complementary and alternative medicine,* 10**,** 24-34.

BASTARD, J.-P., JARDEL, C., BRUCKERT, E., BLONDY, P., CAPEAU, J., LAVILLE, M., VIDAL, H., HAINQUE, B. 2000. Elevated levels of interleukin 6 are reduced in serum and subcutaneous adipose tissue of obese women after weight loss. *The Journal of Clinical Endocrinology & Metabolism,* 85**,** 3338-3342.

BATTA, A. K., XU, G., HONDA, A., MIYAZAKI, T. & SALEN, G. 2006. Stigmasterol reduces plasma cholesterol levels and inhibits hepatic synthesis and intestinal absorption in the rat. *Metabolism,* 55**,** 292-299.

BEGUM, S., SULTANA, I., SIDDIQUI, B. S., SHAHEEN, F. & GILANI, A. H. 2002. Structure and spasmolytic activity of eucalyptanoic acid from Eucalyptus camaldulensis var. obtusa and synthesis of its active derivative from oleanolic acid. *Journal of natural products,* 65**,** 1939-1941.

BELALCAZAR, L. M., HAFFNER, S. M., LANG, W., HOOGEVEEN, R. C., RUSHING, J., SCHWENKE, D. C., TRACY, R. P., PI- SUNYER, F. X., KRISKA, A. M., BALLANTYNE & THE LOOK AHEAD RESEARCH GROUP. 2013. Lifestyle intervention and/or statins for the reduction of C-reactive protein in type 2 diabetes: from the look AHEAD study. *Obesity,* 21**,** 944-950.

BENDING, D., ZACCONE, P. & COOKE, A. 2012. Inflammation and type one diabetes. *International Immunology,* 24**,** 339-346.

BERROUKECHE, F., MOKHTARI-SOULIMANE, N., IMESSAOUDENE, A., CHERRAK, A. S., RONOT, P., BOOS, A., BELHANDOUZ, A., MERZOUK, H. & ELHABIRI, M. 2019. Oral Supplementation Effect of Iron and its Complex Form With Quercetin on Oxidant Status and on Redistribution of Essential Metals in Organs of Streptozotocin Diabetic Rats. *Romanian Journal of Diabetes Nutrition and Metabolic Diseases,* 26**,** 39-53.

BESERRA, F. P., XUE, M., DE AZEVEDO MAIA, G. L., ROZZA, A. L., PELLIZZON, C. H. & JACKSON, C. J. 2018. Lupeol, a pentacyclic triterpene, promotes migration, wound closure, and contractile effect in vitro: Possible involvement of PI3K/Akt and p38/ERK/MAPK pathways. *Molecules,* 23**,** 2819-2836.

BHATHENA, S. J. & VELASQUEZ, M. T. 2002. Beneficial role of dietary phytoestrogens in obesity and diabetes. *The American Journal of Clinical Nutrition,* 76**,** 1191-1201.

BIMAKR, M., RAHMAN, R. A., TAIP, F. S., GANJLOO, A., SALLEH, L. M., SELAMAT, J., HAMID, A., ZAIDUL, I. J. F. & PROCESSING, B. 2011. Comparison of different extraction methods for the extraction of major bioactive flavonoid compounds from spearmint (Mentha spicata L.) leaves. *Food and Bioproducts Processing,* 89**,** 67-72.

BLAIKIE, T. P., EDGE, J. A., HANCOCK, G., LUNN, D., MEGSON, C., PEVERALL, R., RICHMOND, G., RITCHIE, G. A. & TAYLOR, D. 2014. Comparison of breath gases, including acetone, with blood glucose and blood ketones in children and adolescents with type 1 diabetes. *Journal of breath research,* 8**,** 046010.

BNF 2019. *BNF 77 (British National Formulary) March 2019*, Pharmaceutical Press.

BOLSHAKOVA, A., MAGNUSSON, K. E., PINAEV, G. & PETUKHOVA, O. 2013. Functional compartmentalisation of NF- κB- associated proteins in A431 cells. *Cell biology international,* 37**,** 387-396.

BONDAREVA, A. A., CAPECCHI, M. R., IVERSON, S. V., LI, Y., LOPEZ, N. I., LUCAS, O., MERRILL, G. F., PRIGGE, J. R., SIDERS, A. M. & WAKAMIYA, M. 2007. Effects of thioredoxin reductase-1 deletion on embryogenesis and transcriptome. *Free Radical Biology and Medicine,* 43**,** 911-923.

BOOTH, H. P., PREVOST, A. T. & GULLIFORD, M. C. 2015. Access to weight reduction interventions for overweight and obese patients in UK primary care: population-based cohort study. *BMJ open,* 5**,** e006642, 1-6.

BORI, I. D., HUNG, H.-Y., QIAN, K., CHEN, C.-H., MORRIS-NATSCHKE, S. L. & LEE, K.-H. 2012. Anti-AIDS agents 88. Anti-HIV conjugates of betulin and betulinic acid with AZT prepared via click chemistry. *Tetrahedron Letters,* 53**,** 1987-1989.

BOTHON, F. T., DEBITON, E., AVLESSI, F., FORESTIER, C., TEULADE, J.C. & SOHOUNHLOUE, D. K. 2013. In vitro biological effects of two anti-diabetic medicinal plants used in Benin as folk medicine. *BMC complementary and alternative medicine,* 13**,** 51-59.

BRADSHAW, P. C. 2019. Cytoplasmic and Mitochondrial NADPH-Coupled Redox Systems in the Regulation of Aging. *Nutrients,* 11**,** 504-538.

BRANDSMA, A. M., HOGARTH, P. M., NIMMERJAHN, F. & LEUSEN, J. H. J. I. 2016. Clarifying the confusion between cytokine and Fc receptor "common gamma chain". *Immunity,* 45**,** 225-226.

BRANDT, R. 1965. Synthesis of diacetyldichlorofluorescin: A stable reagent for fluorometric analysis. *Analytical biochemistry.,* 11**,** 6-9.

BRIANT, L., SALEHI, A., VERGARI, E., ZHANG, Q. & RORSMAN, P. 2016. Glucagon secretion from pancreatic α-cells. *Upsala journal of medical sciences,* 121**,** 113-119.

BRUUN, J. M., HELGE, J. W., RICHELSEN, B., STALLKNECHT, B. J. A. J. O. P.-E. & METABOLISM 2006. Diet and exercise reduce low-grade inflammation and macrophage infiltration in adipose tissue but not in skeletal muscle in severely obese subjects. *American Journal of Physiology-Endocrinology and Metabolism,* 290**,** E961-E967.

BURKE, S. & COLLIER, J. 2015. Transcriptional Regulation of Chemokine Genes: A Link to Pancreatic Islet Inflammation? *Biomolecules,* 5**,** 1020-1034.

BURKE, S., STADLER, K., LU, D., GLEASON, E., HAN, A., DONOHOE, D., ROGERS, R., HERMANN, G., KARLSTAD, M. & COLLIER, J. 2015a. IL-1[Beta] reciprocally regulates chemokine and insulin secretion in pancreatic [Beta]-cells via NF-[kappa]B. *American Journal of Physiology,* 309**,** E715-E726.

BURKE, S. J., KARLSTAD, M. D., REGAL, K. M., SPARER, T. E., LU, D., ELKS, C. M., GRANT, R. W., STEPHENS, J. M., BURK, D. H. & COLLIER, J. J. 2015b. CCL20 is elevated during obesity and differentially regulated by NF-κB subunits in pancreatic β-cells. *Biochimica et Biophysica Acta,* 1849**,** 637-652.

BUTLER, M. S. 2008. Natural products to drugs: natural product-derived compounds in clinical trials. *Natural Product Reports,* 25**,** 475-516.

BÖSENBERG, L. H. & VAN ZYL, D. G. 2008. The mechanism of action of oral anti-diabetic drugs: a review of recent literature. *Journal of Endocrinology, Metabolism and Diabetes of South Africa,* 13**,** 80-88.

CANDASAMY, M., MURTHY, T. E. G. K., GUBIYAPPA, K. S., CHELLAPPAN, D. K., GUPTA, G. 2014. Alteration of glucose lowering effect of glibenclamide on single and multiple treatments with fenofibrate in experimental rats and rabbit models. *Journal of Basic and Clinical Pharmacy,* 5**,** 62-67.

CESARI, I., HOERLÉ, M., SIMOES-PIRES, C., GRISOLI, P., QUEIROZ, E. F., DACARRO, C., MARCOURT, L., MOUNDIPA, P. F., CARRUPT, P. A., CUENDET, M., CACCIALANZA, G., WOLFENDER, J. L. & BRUSOTTI, G. 2013. Anti- inflammatory, antimicrobial and antioxidant activities of Diospyros bipindensis (Gurke) extracts and its main constituents.(Report). *Journal of Ethnopharmacology,* 146**,** 264-270.

CHANIAD, P., SUDSAI, T., SEPTAMA, A. W., CHUKAEW, A. & TEWTRAKUL, S. 2019. Evaluation of Anti-HIV-1 Integrase and Anti-Inflammatory Activities of Compounds from Betula alnoides Buch-Ham. *Advances in Pharmacological Sciences,* 2019, 1-11.

CHARAN, J. & KANTHARIA, N. D. 2013. How to calculate sample size in animal studies? *Journal of pharmacology & pharmacotherapeutics,* 4**,** 303-306.

CHARAUX, C. & RABATE, J. 1939. Constitution chimique de l'orobol. *Bull. Soc. Chim. Biol,* 21**,** 1330-1333.

CHATTERJEE, S., KHUNTI, K. & DAVIES, M. J. 2017. Type 2 diabetes. *The Lancet,* 389**,** 2239-2251.

CHATURVEDULA, V. S. P. & PRAKASH, I. 2012. Isolation of Stigmasterol and β-Sitosterol from the dichloromethane extract of Rubus suavissimus. *International Current Pharmaceutical Journal,* 1**,** 239-242.

CHAUDHURY, A., DUVOOR, C., REDDY DENDI, V. S., KRALETI, S., CHADA, A., RAVILLA, R., MARCO, A., SHEKHAWAT, N. S., MONTALES, M. T., KURIAKOSE, K., SASAPU, A., BEEBE, A., PATIL, N., MUSHAM, C. K., LOHANI, G. P. & MIRZA, W. 2017. Clinical Review of Anti-diabetic Drugs: Implications for Type 2 Diabetes Mellitus Management. *Frontiers in Endocrinology (Lausanne),* 8 (6) 1-12.

CHAUHAN, A., SHARMA, P., SRIVASTAVA, P., KUMAR, N. & DUDHE, R. 2010. Plants having potential anti-diabetic activity: a review. *Der Pharmacia Lettre,* 2**,** 369-387.

CHEN, J., WU, Y., ZOU, J. & GAO, K. 2016. alpha-Glucosidase inhibition and antihyperglycemic activity of flavonoids from Ampelopsis grossedentata and the flavonoid derivatives. *Bioorganic & Medicinal Chemistry,* 24**,** 1488-94.

CHEN, L., CHEN, R., WANG, H. & LIANG, F. 2015. Mechanisms linking inflammation to insulin resistance. *International Journal of Endocrinology,* 2015, 1-9.

CHEN, Y., DONG, H., THOMPSON, D., SHERTZER, H., NEBERT, D. & VASILIOU, V. 2013. Glutathione defense mechanism in liver injury: insights from animal models. *Food and Chemical Toxicology,* 60**,** 38-44.

CHEUKA, P., MAYOKA, G., MUTAI, P. & CHIBALE, K. 2017. The role of natural products in drug discovery and development against neglected tropical diseases. *Molecules,* 22**,** 58-99.

CHIEN, N. Q., HUNG, N. V., SANTARSIERO, B. D., MESECAR, A. D., CUONG, N. M., SOEJARTO, D. D., PEZZUTO, J. M., FONG, H. H. & TAN, G. T. 2004. New 3-O-acyl betulinic acids from Strychnos vanprukii Craib. *Journal of natural products,* 67**,** 994-998.

CHO, N., KIM, H. W., LEE, H. K., JEON, B. J. & SUNG, S. H. 2016. Ameliorative effect of betulin from Betula platyphylla bark on scopolamine-induced amnesic mice. *Bioscience, Biotechnology, and Biochemistry,* 80**,** 166-171.

CHOI, H. J., BAE, E. Y., SONG, J. H., BAEK, S. H. & KWON, D. H. 2010. Inhibitory effects of orobol 7- O - d - glucoside from banaba (Lagerstroemia speciosa L.) on human rhinoviruses replication. *Letters in Applied Microbiology,* 51**,** 1-5.

CHOI, J., KOBAYASHI, H., OKUDA, H., HARADA, K. H., TAKEDA, M., FUJIMOTO, H., YAMANE, S., TANAKA, D., YOUSSEFIAN, S., INAGAKI, N. & KOIZUMI, A. 2018. beta-cell-specific overexpression of adiponectin receptor 1 does not improve diabetes mellitus in Akita mice. *PLoS One,* 13**,** e0190863.

CHOROMANSKA, A., LUBINSKA, S., SZEWCZYK, A., SACZKO, J. & KULBACKA, J. 2018. Mechanisms of antimelanoma effect of oat β-glucan supported by electroporation. *Bioelectrochemistry,* 123**,** 255-259.

CHUNG, I.-M., RAJAKUMAR, G., LEE, J.-H., KIM, S.-H. & THIRUVENGADAM, M. 2017. Ethnopharmacological uses, phytochemistry, biological activities, and biotechnological applications of Eclipta prostrata. *Applied microbiology and biotechnology,* 101**,** 5247-5257.

CICERO, A. F. & BAGGIONI, A. 2016. Berberine and its role in chronic disease. *Anti-inflammatory Nutraceuticals and Chronic Diseases.* Springer.

CICHEWICZ, R. H. & KOUZI, S. A. 2004. Chemistry, biological activity, and chemotherapeutic potential of betulinic acid for the prevention and treatment of cancer and HIV infection. *Medicinal Research Reviews,* 24**,** 90-114.

CLARK, A. M. 1996. Natural products as a resource for new drugs. *Pharmaceutical Research,* 13**,** 1133-44.

CLARKSON, T. B. 2002. Soy, soy phytoestrogens and cardiovascular disease. *Journal of Nutrition,* 132**,** 566S-569S.

CLINICALTRIALS.GOV. 2019. *NCT00346502: Evaluation of 20% Betulinic Acid Ointment for Treatment of Dysplastic Nevi (Moderate to Severe Dysplasia)* [Online]. Bethesda (MD): National Library of Medicine (US). Available: https://clinicaltrials.gov/ct2/show/record/NCT00346502 [Accessed 19/04 2019].

CONARELLO, S. L., LI, Z., RONAN, J., ROY, R. S., ZHU, L., JIANG, G., LIU, F., WOODS, J., ZYCBAND, E. & MOLLER, D. E. 2003. Mice lacking dipeptidyl peptidase IV are protected against obesity and insulin resistance. *Proceedings of the National Academy of Sciences,* 100**,** 6825-6830.

CORDERO, C., GÓMEZ-GONZÁLEZ, S., LEÓN-ACOSTA, C., MORANTES-MEDINA, S. & ARISTIZABAL, F. 2004. Cytotoxic activity of five compounds isolated from Colombian plants. *Fitoterapia,*75**,** 225-227.

CORRÊA, R. S., COELHO, C. P., SANTOS, M. H. D., ELLENA, J. & DORIGUETTO, A. C. 2009. Lupeol. *Acta Crystallographica Section C,* 65**,** o97-o99.

COSTA, V., APRILE, M., ESPOSITO, R. & CICCODICOLA, A. 2013. RNA-Seq and human complex diseases: recent accomplishments and future perspectives. *European Journal of Human Genetics,* 21**,** 134-142.

CRAFT, S. 2012. Alzheimer disease: Insulin resistance and AD--extending the translational path. *Nature Reviews Neurology,* 8**,** 360-362.

CRONAN, J. J. & LAPORTE, D. 2005. Tricarboxylic acid cycle and glyoxylate bypass. *EcoSal Plus,* 1.

D'SOUZA, A. M., NEUMANN, U. H., GLAVAS, M. M. & KIEFFER, T. J. 2017. The glucoregulatory actions of leptin. *Molecular metabolism,* 6**,** 1052-1065.

DA COSTA MOUSINHO, N. M., VAN TONDER, J. J. & STEENKAMP, V. 2013. In vitro anti-diabetic activity of Sclerocarya birrea and Ziziphus mucronata. *Natural product communications,* 8**,** 1279-1284.

DA COSTA, R. M., NEVES, K. B., MESTRINER, F. L., LOUZADA-JUNIOR, P., BRUDER-NASCIMENTO, T. & TOSTES, R. C. 2016. TNFα induces vascular insulin resistance via positive modulation of PTEN and decreased Akt/eNOS/NO signaling in high fat diet-fed mice. *Cardiovascular Diabetology,* 15**,** 119-131.

DAMM, P., HOUSHMAND-OEREGAARD, A., KELSTRUP, L., LAUENBORG, J., MATHIESEN, E. R. & CLAUSEN, T. D. 2016. Gestational diabetes mellitus and long-term consequences for mother and offspring: a view from Denmark. *Diabetologia,* 59**,** 1396-1399.

DANDONA, P., ALJADA, A. & BANDYOPADHYAY, A. 2004. Inflammation: the link between insulin resistance, obesity and diabetes. *Trends in Immunology,* 25**,** 1-3.

DASH, S. K., CHATTOPADHYAY, S., GHOSH, T., DASH, S. S., TRIPATHY, S., DAS, B., BAG, B. G., DAS, D. & ROY, S. 2015. Self-assembled betulinic acid protects doxorubicin induced apoptosis followed by reduction of ROS-TNF- α-caspase-3 activity. *Biomedicine and Pharmacotherapy,* 72**,** 144-157.

DASTJERDI, Z. M., NAMJOYAN, F. & AZEMI, M. E. 2015. Alpha amylase inhibition activity of some plants extract of Teucrium species. *European Journal of Biological Sciences,* 7**,** 26-31.

DAVIES, M. J., D'ALESSIO, D. A., FRADKIN, J., KERNAN, W. N., MATHIEU, C., MINGRONE, G., ROSSING, P., TSAPAS, A., WEXLER, D. J. & BUSE, J. B. 2018. Management of hyperglycaemia in type 2 diabetes, 2018. A consensus report by the American Diabetes Association (ADA) and the European Association for the Study of Diabetes (EASD). *Diabetologia,* 61**,** 2461-2498.

DE FLORA, S., BENNICELLI, C., SERRA, D., IZZOTTI, A. & CESARONE, C. 2018. Role of glutathione and N-acetylcysteine as inhibitors of mutagenesis and carcinogenesis. *Absorption and utilization of amino acids.* CRC Press.

DE LA MONTE, S. M. & WANDS, J. R. 2005. Review of insulin and insulin-like growth factor expression, signaling, and malfunction in the central nervous system: relevance to Alzheimer's disease. *Journal of Alzheimer's Disease,* 7**,** 45-61.

DE LA MONTE, S. M. & WANDS, J. R. 2008. Alzheimer's disease is type 3 diabetes—evidence reviewed. *Journal of diabetes science and technology,* 2**,** 1101-1113.

DE MELO, C. L. L., QUEIROZ, M. G. R., ARRUDA FILHO, A. C. V., RODRIGUES, A. M., DE SOUSA, D. F., ALMEIDA, J. G. L., PESSOA, O. D. L., SILVEIRA, E. R., MENEZES, D. B., MELO, T. 2009. Betulinic acid, a natural pentacyclic triterpenoid, prevents abdominal fat accumulation in mice fed a high-fat diet. *Journal of Agricultural and Food Chemistry,* 57**,** 8776-8781.

DE MOURA, L. P., SOUZA PAULI, L. S., CINTRA, D. E., DE SOUZA, C. T., DA SILVA, A. S. R., MARINHO, R., DE MELO, M. A. R., ROPELLE, E. R. & PAULI, J. R. 2013. Acute exercise decreases PTP- 1B protein level and improves insulin signaling in the liver of old rats. *Immunity & Ageing,* 10, 1-9.

DE-EKNAMKUL, W. & POTDUANG, B. 2003. Biosynthesis of β-sitosterol and stigmasterol in Croton sublyratus proceeds via a mixed origin of isoprene units. *Phytochemistry,* 62**,** 389-398.

DEFRONZO, R. A., FERRANNINI, E., ALBERTI, K. G. M. M., ZIMMET, P. & ALBERTI, G. 2015a. *International Textbook of Diabetes Mellitus, 2 Volume Set*, John Wiley & Sons.

DEFRONZO, R. A., FERRANNINI, E., GROOP, L., HENRY, R. R., HERMAN, W. H., HOLST, J. J., HU, F. B., KAHN, C. R., RAZ, I. & SHULMAN, G. I. 2015b. Type 2 diabetes mellitus. *Nature reviews Disease primers,* 1**,** 15019.

DEL CARMEN RECIO, M. M., GINER, R. R., MÁÑEZ, S. L., GUEHO, J. L., JULIEN, H. L., HOSTETTMANN, K. L. & RÍOS, J. L. 1995. Investigations on the Steroidal Anti- Inflammatory Activity of Triterpenoids from Diospyros leucomelas. *Planta Medica,* 61**,** 9-12.

DENG, J., CHENG, W. & YANG, G. 2011. A novel antioxidant activity index (AAU) for natural products using the DPPH assay. *Food Chemistry,* 125**,** 1430-1435.

DENISOV, V., STRONG, W., WALDER, M., GINGRICH, J. & WINTZ, H. 2008. Development and validation of RQI: an RNA quality indicator for the Experion automated electrophoresis system. *Bio-Rad Bulletin,* 5761.

DENROCHE, H. C., HUYNH, F. K. & KIEFFER, T. J. 2012. The role of leptin in glucose homeostasis. *Journal of diabetes investigation,* 3**,** 115-129.

DEUTSCHLÄNDER, M., LALL, N., VAN DE VENTER, M. & HUSSEIN, A. A. 2011. Hypoglycemic evaluation of a new triterpene and other compounds isolated from Euclea undulata Thunb. var. myrtina (Ebenaceae) root bark. *Journal of Ethnopharmacology,* 133**,** 1091-1095.

DEXHEIMER, G. M., DE OLIVEIRA BECKER DELVING, L. K., DE OLIVEIRA, H. S., BIOLCHI, V., GOETTERT, M. I. & POZZOBON, A. 2017. Calyptranthes grandifolia O.Berg (Myrtaceae) ethanolic extract inhibits TNF-α gene expression and cytokine release in vitro. *Molecular Medicine Reports,* 15**,** 2873-2880.

DI PIETRO, C., RAGUSA, M., BARBAGALLO, D., DURO, L. R., GUGLIELMINO, M. R., MAJORANA, A., ANGELICA, R., SCALIA, M., STATELLO, L., SALITO, L., TOMASELLO, L., PERNAGALLO, S., VALENTI, S., D'AGOSTINO, V., TRIBERIO, P., TANDURELLA, I., PALUMBO, G. A., LA CAVA, P., CAFISO, V., BERTUCCIO, T., SANTAGATI, M., LI DESTRI, G., LANZAFAME, S., DI RAIMONDO, F., STEFANI, S., MISHRA, B. & PURRELLO, M. 2009. The apoptotic

machinery as a biological complex system: analysis of its omics and evolution, identification of candidate genes for fourteen major types of cancer, and experimental validation in CML and neuroblastoma.(Research article)(Report). *BMC Medical Genomics,* 2**,** 20-55.

DING, H., WU, X., PAN, J., HU, X., GONG, D. & ZHANG, G. 2018. New Insights into the Inhibition Mechanism of Betulinic Acid on alpha-Glucosidase. *Journal of Agricultural and Food Chemistry,* 66**,** 7065-7075.

DING, K. E. 2012. RAPID LARGE-SCALE PURIFICATION OF BETULINIC ACID. *Journal of Food Process Engineering,* 35**,** 881-887.

DINÇER, Y., AKÇAY, T., ALADEMIR, Z. & ILKOVA, H. 2002. Assessment of DNA base oxidation and glutathione level in patients with type 2 diabetes. *Mutation research,* 505**,** 75-81.

DOBRIAN, A. D., MA, Q., LINDSAY, J. W., LEONE, K. A., MA, K., COBEN, J., GALKINA, E. V. & NADLER, J. L. 2010. Dipeptidyl peptidase IV inhibitor sitagliptin reduces local inflammation in adipose tissue and in pancreatic islets of obese mice. *American Journal of Physiology-Endocrinology and Metabolism,* 300**,** E410-E421.

DOGAN, Y., AKARSU, S., USTUNDAG, B., YILMAZ, E. & GURGOZE, M. K. 2006. Serum IL1β, IL-2, and IL6 in insulin-dependent diabetic children. *Mediators of inflammation,* 2006, 1-6.

DONG, Y., CHEN, Y. T., YANG, Y. X., ZHOU, X. J., DAI, S. J., TONG, J. F., SHOU, D. & LI, C. 2016. Metabolomics Study of Type 2 Diabetes Mellitus and the Anti-diabetic Effect of Berberine in Zucker Diabetic Fatty Rats Using Uplc-ESI-Hdms. *Phytotherapy Research,* 30**,** 823-8.

DOWNEY, N. 2014. Interpreting melt curves: An indicator, not a diagnosis. *IDT Integrated DNA technologies*.

DUKE, J. A. 2017. *Handbook of Phytochemical Constituent Grass, Herbs and Other Economic Plants: Herbal Reference Library,* Routledge.

DUNCAN, B. B., SCHMIDT, M. I., PANKOW, J. S., BALLANTYNE, C. M., COUPER, D., VIGO, A., HOOGEVEEN, R., FOLSOM, A. R. & HEISS, G. 2003. Low-grade systemic inflammation and the development of type 2 diabetes: the atherosclerosis risk in communities study. *Journal of Diabetes,* 52**,** 1799-1805.

DĄBEK, J., KUŁACH, A. & GĄSIOR, Z. 2010. Nuclear factor kappa-light-chain-enhancer of activated B cells (NF-κB): a new potential therapeutic target in atherosclerosis? *Pharmacological reports,* 62**,** 778-783.

D'ADAMO, E. & CAPRIO, S. 2011. Type 2 diabetes in youth: epidemiology and pathophysiology. *Diabetes care,* 34**,** S161-S165.

EHSANIFARD, Z., MIR-MOHAMMADREZAEI, F., SAFARZADEH, A. & GHOBAD-NEJHAD, M. 2017. Aqueous extract of Inocutis levis improves insulin resistance and glucose tolerance in high sucrose-fed Wistar rats. *Journal of Herbmed Pharmacology,* 6**,** 160-164.

EILENBERGER, C., KRATZ, S. R. A., ROTHBAUER, M., EHMOSER, E.-K., ERTL, P. & KÜPCÜ, S. 2018. Optimized alamarBlue assay protocol for drug dose-response determination of 3D tumor spheroids. *MethodsX,* 5**,** 781-787.

EL-KAMALI, H. H. 2009. Ethnopharmacology of medicinal plants used in North Kordofan (Western Sudan). *Ethnobotanical Leaflets,* 13**,** 89-97.

ELBASHIR, S. M. I., DEVKOTA, H. P., WADA, M., KISHIMOTO, N., MORIUCHI, M., SHUTO, T., MISUMI, S., KAI, H., WATANABE, T. 2018. Free radical scavenging, α-glucosidase inhibitory and lipase inhibitory activities of eighteen Sudanese medicinal plants. *BMC Complementary and Alternative Medicine,* 18**,** 282-294.

ELINSON, N., AMICHAY, D. & BIRK, R. 2006. Leptin directly regulates exocrine pancreas lipase and two related proteins in the rat. *The British Journal of Nutrition,* 96**,** 691-696.

ELYA, B., BASAH, K., MUN'IM, A., YULIASTUTI, W., BANGUN, A. & SEPTIANA, E. K. 2011. Screening of α-glucosidase inhibitory activity from some plants of Apocynaceae, Clusiaceae, Euphorbiaceae, and Rubiaceae. *Journal of Biomedicine and Biotechnology,* 2012, 1-6.

ELYA, B., HANDAYANI, R., SAURIASARI, R., HASYYATI, U. S., PERMANA, I. T. & PERMATASARI, Y. I. 2015. Anti-diabetic activity and phytochemical screening of extracts from Indonesian plants by inhibition of alpha amylase, alpha glucosidase and dipeptidyl peptidase IV. *Pakistan Journal of Biological Sciences,* 18**,** 279-284.

ENOKI, T., OHNOGI, H., NAGAMINE, K., KUDO, Y., SUGIYAMA, K., TANABE, M., KOBAYASHI, E., SAGAWA, H. & KATO, I. 2007. Anti-diabetic activities of chalcones isolated from a Japanese herb, Angelica keiskei. *Journal of agricultural and food chemistry,* 55**,** 6013-6017.

ERNST, E. 2000. Herbal medicines: where is the evidence?: Growing evidence of effectiveness is counterbalanced by inadequate regulation. *British Medical Journal,* 2000, 321-395.

ERUSLANOV, E. & KUSMARTSEV, S. 2010. Identification of ROS using oxidized DCFDA and flow-cytometry. *Methods in Molecular Biology,* 594, 57-72.

ESPOSITO, K., NAPPO, F., GIUGLIANO, F., DI PALO, C., CIOTOLA, M., BARBIERI, M., PAOLISSO, G. & GIUGLIANO, D. 2003. Cytokine milieu tends toward inflammation in type 2 diabetes. *Diabetes care,* 26**,** 1647-1647.

ESSER, N., LEGRAND-POELS, S., PIETTE, J., SCHEEN, A. J. & PAQUOT, N. 2014. Inflammation as a link between obesity, metabolic syndrome and type 2 diabetes. *Journal Diabetes research clinical practice,* 105**,** 141-150.

EVERAERT, C., LUYPAERT, M., MAAG, J. L. V., CHENG, Q. X., DINGER, M. E., HELLEMANS, J. & MESTDAGH, P. 2017. Benchmarking of RNA-sequencing analysis workflows using whole-transcriptome RT-qPCR expression data. *Scientific Reports,* 7**,** 1559-1570.

EWALD, N., KAUFMANN, C., RASPE, A., KLOER, H., BRETZEL, R. & HARDT, P. 2012. Prevalence of diabetes mellitus secondary to pancreatic diseases (type 3c). *Diabetes/metabolism research and reviews,* 28**,** 338-342.

FAERCH, K., BORCH-JOHNSEN, K., HOLST, J. J. & VAAG, A. 2009. Pathophysiology and aetiology of impaired fasting glycaemia and impaired glucose tolerance: does it matter for prevention and treatment of type 2 diabetes? *Diabetologia,* 52**,** 1714-1723.

FANG, J.-Y., LIN, C.-H., HUANG, T.-H. & CHUANG, S.-Y. J. 2019. In Vivo Rodent Models of Type 2 Diabetes and Their Usefulness for Evaluating Flavonoid Bioactivity. *Nutrients,* 11**,** 530-553.

FANG, L., ITO, A., CHAI, H.-B., MI, Q., JONES, W. P., MADULID, D. R., OLIVEROS, M. B., GAO, Q., ORJALA, J. & FARNSWORTH, N. R. 2006. Cytotoxic Constituents from the Stem Bark of Dichapetalum g elonioides Collected in the Philippines, 1. *Journal of natural products,* 69**,** 332-337.

FARAG, Y. M. & GABALLA, M. R. 2010. Diabesity: an overview of a rising epidemic. *Nephrology Dialysis Transplantation,* 26**,** 28-35.

FATIMA, N., FAISAL, S. M., ZUBAIR, S., AJMAL, M., SIDDIQUI, S. S., MOIN, S. & OWAIS, M. 2016. Role of pro-inflammatory cytokines and biochemical markers in the pathogenesis of type 1 diabetes: correlation with age and glycemic condition in diabetic human subjects. *PLoS One,*11**,** 1-17.

FERNÁNDEZ, A., ÁLVAREZ, A., GARCÍA, M. D. & SÁENZ, M. T. 2001. Anti-inflammatory effect of Pimenta racemosa var. ozua and isolation of the triterpene lupeol. *Il Farmaco,* 56**,** 335-338.

FIGUEIREDO, A. C., BARROSO, J. G., PEDRO, L. G. & SCHEFFER, J. J. 2008. Factors affecting secondary metabolite production in plants: volatile components and essential oils. *Flavour and Fragrance journal,* 23**,** 213-226.

FIGUEIREDO-GONZÁLEZ, M., GROSSO, C., VALENTÃO, P. & ANDRADE, P. B. 2016. α-Glucosidase and α-amylase inhibitors from Myrcia spp.: a stronger alternative to acarbose? *Journal of pharmaceutical and biomedical analysis,* 118**,** 322-327.

FRUHBECK, G. 2006. Intracellular signalling pathways activated by leptin. *Biochemical Journal,* 393**,** 7-20.

FU, L., ZHANG, S., LI, N., WANG, J., ZHAO, M., SAKAI, J., HASEGAWA, T., MITSUI, T., KATAOKA, T. & OKA, S. 2005. Three New Triterpenes from Nerium o leander and Biological Activity of the Isolated Compounds. *Journal of natural products,* 68**,** 198-206.

FUJIOKA, T., KASHIWADA, Y., KILKUSKIE, R. E., COSENTINO, L. M., BALLAS, L. M., JIANG, J. B., JANZEN, W. P., CHEN, I. S. & LEE, K. H. 1994. Anti-AIDS agents, 11. Betulinic acid and platanic acid as anti-HIV principles from Syzigium claviflorum, and the anti-HIV activity of structurally related triterpenoids. *Journal of Natural Products,* 57**,** 243-7.

FUKAO, T., LOPASCHUK, G. D. & MITCHELL, G. A. 2004. Pathways and control of ketone body metabolism: on the fringe of lipid biochemistry. *Prostaglandins, leukotrienes and essential fatty acids,* 70**,** 243-251.

FUNKE, I. & MELZIG, M. 2005. Effect of different phenolic compounds on α-amylase activity: screening by microplate-reader based kinetic assay. *Die Pharmazie-An International Journal of Pharmaceutical Sciences,* 60**,** 796-797.

GABAY, O., SANCHEZ, C., SALVAT, C., CHEVY, F., BRETON, M., NOURISSAT, G., WOLF, C., JACQUES, C. & BERENBAUM, F. 2010. Stigmasterol: a phytosterol with potential anti-osteoarthritic properties. *Osteoarthritis and cartilage,* 18**,** 106-116.

GALLO, M. B. & SARACHINE, M. J. 2009. Biological activities of lupeol. *International Journal of Biomedical and Pharmaceutical Sciences,* 3**,** 46-66.

GANESAN, A. 2008. The impact of natural products upon modern drug discovery. *Current Opinion in Chemical Biology,* 12**,** 306-17.

GAO, J., CHENG, D. & LIU, X. 1993. Chemical constituents of Emilia sonchifolia L. DC. *journal of Chinese materia medica,* 18**,** 102-103.

GAO, Z., MALONEY, D. J., DEDKOVA, L. M. & HECHT, S. M. 2008. Inhibitors of DNA polymerase β: activity and mechanism. *Bioorganic & medicinal chemistry,* 16**,** 4331-4340.

GERBER, P. A. & RUTTER, G. A. 2017. The role of oxidative stress and hypoxia in pancreatic beta-cell dysfunction in diabetes mellitus. *Antioxidants & redox signaling,* 26**,** 501-518.

GHOSH, T., MAITY, T. K., SINGH, J. 2011. Evaluation of antitumor activity of stigmasterol, a constituent isolated from Bacopa monnieri Linn aerial parts against Ehrlich Ascites Carcinoma in mice. *Oriental Pharmacy and Experimental Medicine,* 11**,** 41-49.

GILLESPIE, K. 2001. Diabetes and gender. *Diabetologia,* 44**,** 3-15.

GINSBERG, H. N., ZHANG, Y.-L. & HERNANDEZ-ONO, A. 2005. Regulation of plasma triglycerides in insulin resistance and diabetes. *Archives of medical research,* 36**,** 232-240.

GIRIDHARAN, S. & SRINIVASAN, M. 2018. Mechanisms of NF-κB p65 and strategies for therapeutic manipulation. *Journal of inflammation research,* 11**,** 407-419.

GLISAN, S. L., GROVE, K. A., YENNAWAR, N. H. & LAMBERT, J. D. 2017. Inhibition of pancreatic lipase by black tea theaflavins: Comparative enzymology and in silico modeling studies. *Food Chemistry,* 216**,** 296-300.

GLOVER, B. J. & MARTIN, C. 2012. Anthocyanins. *Current biology : CB,* 22**,** R147-R150.

GLUCK, M. E., GELIEBTER, A. & SATOV, T. 2001. Night eating syndrome is associated with depression, low self- esteem, reduced daytime hunger, and less weight loss in obese outpatients. *Obesity research,* 9**,** 264-267.

GOMES, A., FERNANDES, E. & LIMA, J. L. F. C. 2005. Fluorescence probes used for detection of reactive oxygen species. *Journal of Biochemical and Biophysical Methods,* 65**,** 45-80.

GOUDA, W., MAGEED, L., EL DAYEM, S. M. A., ASHOUR, E. & AFIFY, M. 2018. Evaluation of pro-inflammatory and anti-inflammatory cytokines in type 1 diabetes mellitus. *Bulletin of the National Research Centre,* 42**,** 14-20.

GRAY, A. I., IGOLI, J. O. & EDRADA-EBEL, R. 2012. Natural products isolation in modern drug discovery programs. *Natural Products Isolation.* Springer.

GRIME, J. P., HODGSON, J. G. & HUNT, R. 2014. *Comparative plant ecology: a functional approach to common British species,* Springer.

GU, S., TANG, Z., SHI, L., SAWHNEY, M., HU, H. & DONG, H. 2015. Cost-Minimization Analysis of Metformin and Acarbose in Treatment of Type 2 Diabetes. *Value in health regional issues,* 6**,** 84-88.

GUEST, C. B., PARK, M. J., JOHNSON, D. R. & FREUND, G. G. 2008. The implication of proinflammatory cytokines in type 2 diabetes. *Frontiers in Bioscience,* 13**,** 5187-5194.

GUO, M. B., WANG, D. C., LIU, H. F., CHEN, L. W., WEI, J. W., LIN, Y. & XUE, H. 2018. Lupeol against high-glucose-induced apoptosis via enhancing the anti-oxidative stress in rabbit nucleus pulposus cells. *European Spine Journal,* 27**,** 2609-2620.

GUPTA, A. 2019. Digestion and Absorption of Lipids. *Comprehensive Biochemistry for Dentistry.* Springer.

GUPTA, R., SHARMA, A. K., DOBHAL, M., SHARMA, M. & GUPTA, R. 2011. Anti-diabetic and antioxidant potential of β- sitosterol in streptozotocin-induced experimental hyperglycemia. *Journal of diabetes,* 3**,** 29-37.

GURUNG, A. M. & PANG, E. C. K. 2011. *Lathyrus*: chapter 6. In: Chittaranjan Kole (Ed.) Wild crop relatives: Genomic and breeding resources, Legume crops and forages.

HABIB, M., NIKKON, F., RAHMAN, M., HAQUE, Z. & KARIM, M. 2007. Isolation of stigmasterol and ß-sitosterol from methanolic extract of root. *Pakistan Journal of Biological Sciences,* 10**,** 4174-4176.

HABTEMARIAM, S. 2011. α-Glucosidase inhibitory activity of kaempferol-3-O-rutinoside. *Natural product communications,* 6**,** 201-203.

HAFIZUR, R. M., HAMEED, A., SHUKRANA, M., RAZA, S. A., CHISHTI, S., KABIR, N. & SIDDIQUI, R. A. 2015. Cinnamic acid exerts anti-diabetic activity by improving glucose tolerance in vivo and by stimulating insulin secretion in vitro. *Phytomedicine,* 22**,** 297-300.

HAN, N. & BAKOVIC, M. 2015. Biologically active triterpenoids and their cardioprotective and anti-inflammatory effects. *Journal of Bioanalysis & Biomedicine,* 12**,** 1948-1955.

HAN, Y., XIA, C., CHENG, X., XIANG, R., LIU, H., YAN, Q. & XU, D. 1998. Preliminary studies on chemical constituents and pharmacological action of Eclipta prostrata L. *China journal of Chinese materia medica,* 23**,** 680-682.

HAO, L., SCHLUSSEL, Y., FIESELMANN, K., SCHNEIDER, S. & SHAPSES, S. 2017. Appetite and gut hormones response to a putative α-glucosidase inhibitor, Salacia chinensis, in overweight/obese adults: a double blind randomized controlled trial. *Nutrients,* 9**,** 869-882.

HARBORNE, A. 1998. *Phytochemical methods a guide to modern techniques of plant analysis*, springer science & business media.

HARDT, P. D., BRENDEL, M. D., KLOER, H. U. & BRETZEL, R. G. 2008. Is pancreatic diabetes (type 3c diabetes) underdiagnosed and misdiagnosed? *Diabetes care,* 31**,** S165-S169.

HART, P. A., BELLIN, M. D., ANDERSEN, D. K., BRADLEY, D., CRUZ-MONSERRATE, Z., FORSMARK, C. E., GOODARZI, M. O., HABTEZION, A., KORC, M. & KUDVA, Y. C. 2016. Type 3c (pancreatogenic) diabetes mellitus secondary to chronic pancreatitis and pancreatic cancer. *The Lancet Gastroenterology & Hepatology,* 1**,** 226-237.

HASSANPOUR, S., MAHERISIS, N. & ESHRATKHAH, B. 2011. Plants and secondary metabolites (Tannins): A Review. *International Journal of Forensic Software Engineering,* 1, 47-53.

HATTING, M., TAVARES, C. D., SHARABI, K., RINES, A. K. & PUIGSERVER, P. 2018. Insulin regulation of gluconeogenesis. *Annals of the New York Academy of Sciences,* 1411**,** 21-35.

HE, Q. Q., YANG, L., ZHANG, J. Y., MA, J. N. & MA, C. M. 2014. Chemical Constituents of Gold- red Apple and Their α- Glucosidase Inhibitory Activities. *Journal of food science,* 79**,** C1970-C1983.

HEKERMAN, P., ZEIDLER, J., KORFMACHER, S., BAMBERG-LEMPER, S., KNOBELSPIES, H., ZABEAU, L., TAVERNIER, J. & BECKER, W. 2007. Leptin induces inflammation- related genes in RINm5F insulinoma cells. *BMC Molecular Biology,* 8**,** 41-53.

HELLER, W. & FORKMANN, G. 2017. Biosynthesis of flavonoids. *The Flavonoids Advances in Research since 1986*. 499-535, Routledge.

HII, C. & HOWELL, S. 1985. Effects of flavonoids on insulin secretion and 45Ca2+ handling in rat islets of Langerhans. *Journal of Endocrinology,* 107**,** 1-8.

HONG, P., KOZA, S. & BOUVIER, E. S. 2012. A review size-exclusion chromatography for the analysis of protein biotherapeutics and their aggregates. *Journal of liquid chromatography & related technologies,* 35**,** 2923-2950.

HOSTETTMANN, K. & MARSTON, A. 2001. Countercurrent chromatography in the preparative separation of plant-derived natural products. *Journal of liquid chromatography & related technologies,* 24**,** 1711-1721.

HOTAMISLIGIL, G. S., SHARGILL, N. S. & SPIEGELMAN, B. M. 1993. Adipose expression of tumor necrosis factor-alpha: direct role in obesity- linked insulin resistance. *Science (New York, N.Y.),* 259**,** 87-91.

HSIEH, C.-T., HSIEH, T.-J., EL-SHAZLY, M., CHUANG, D.-W., TSAI, Y.-H., YEN, C.-T., WU, S.-F., WU, Y.-C. & CHANG, F.-R. 2012. Synthesis of chalcone derivatives as potential anti-diabetic agents. *Bioorganic & medicinal chemistry letters,* 22**,** 3912-3915.

HUANG, A. Similarity measures for text document clustering. *Proceedings of the sixth new zealand computer science research student conference (NZCSRSC2008)*, Christchurch, New Zealand, 2008. 9-56.

HUGUET, A.-I., DEL CARMEN RECIO, M. A., MÁÑEZ, S., GINER, R.-M. A. & RÍOS, J.-L. 2000. Effect of triterpenoids on the inflammation induced by protein kinase C activators, neuronally acting irritants and other agents. *European Journal of Pharmacology,* 410**,** 69-81.

HUNG, C. L. & CHEN, C. C. 2014. Computational Approaches for Drug Discovery. *Drug Development Research,* 75, 412-418.

HUNG, Y. J., CHU, N. F., WANG, S. C., HSIEH, C. H., HE, C. T., LEE, C. H. & FAN, S. C. 2006. Correlation of plasma leptin and adiponectin with insulin sensitivity and [beta]- cell function in children - the Taipei Children Heart Study. *International Journal of Clinical Practice,* 60**,** 1582-1587.

HUSSEIN-AL-ALI, S. 2014. The in vitro therapeutic activity of betulinic acid nanocomposite on breast cancer cells (MCF-7) and normal fibroblast cell (3T3). *Journal of Materials Science,* 49**,** 8171-8183.

HUYPENS, P., MOENS, K., HEIMBERG, H., LING, Z., PIPELEERS, D. & VAN DE CASTEELE, M. 2005. Adiponectin-mediated stimulation of AMP-activated protein kinase (AMPK) in pancreatic beta cells. *Life Sciences,* 77**,** 1273-1782.

IGOLI, O. J. & GRAY, I. 2008. Friedelanone and other triterpenoids from Hymenocardia acida. *International Journal of Physical Sciences,* 3**,** 156-158.

IKEDA, K., TAKAHASHI, M., NISHIDA, M., MIYAUCHI, M., KIZU, H., KAMEDA, Y., ARISAWA, M., WATSON, A. A., NASH, R. J. & FLEET, G. W. 1999. Homonojirimycin analogues and their glucosides from Lobelia sessilifolia and Adenophora spp.(Campanulaceae). *Carbohydrate research,* 323**,** 73-80.

IMAI, Y., DOBRIAN, A. D., WEAVER, J. R., BUTCHER, M. J., COLE, B. K., GALKINA, E. V., MORRIS, M. A., TAYLOR- FISHWICK, D. A. & NADLER, J. L. 2013. Interaction between cytokines and inflammatory cells

in islet dysfunction, insulin resistance and vascular disease. *Diabetes, Obesity and Metabolism,* 15**,** 117-129.
IMENSHAHIDI, M. & HOSSEINZADEH, H. 2016. Berberis vulgaris and berberine: an update review. *Phytotherapy research,* 30**,** 1745-1764.
ISONISHI, S., SAITOU, M., YASUDA, M., OCHIAI, K. & TANAKA, T. 2003. Enhancement of sensitivity to cisplatin by orobol is associatedwith increased mitochondrial cytochrome c releasein human ovarian carcinoma cells. *Gynecologic Oncology,* 90**,** 413-420.
IVEZAJ, V., WHITE, M. A. & GRILO, C. M. 2016. Examining binge- eating disorder and food addiction in adults with overweight and obesity. *Obesity,* 24**,** 2064-2069.
JACKMAN, L. M. & STERNHELL, S. 2013. *Application of Nuclear Magnetic Resonance Spectroscopy in Organic Chemistry: International Series in Organic Chemistry,* Elsevier.
JACOBSEN, L. M., LARSSON, H. E., TAMURA, R. N., VEHIK, K., CLASEN, J., SOSENKO, J., HAGOPIAN, W. A., SHE, J. X., STECK, A. K. & REWERS, M. 2019. Predicting progression to type 1 diabetes from ages 3 to 6 in islet autoantibody positive TEDDY children. *Pediatric Diabetes,* 20**,** 263-270.
JACOVO, E., VALENTINE, T. A., MALUK, M., TOOROP, P., LOPEZ DEL EGIDO, L., FRACHON, N., KENICER, G., PARK, L., GOFF, M., FERRO, V. A., BONOMI, C., JAMES, E. K. & IANNETTA, P. P. M. 2019. Towards a characterisation of the wild legume bitter vetch (Lathyrus linifolius L. (Reichard) Bässler): heteromorphic seed germination, root nodule structure and N- fixing rhizobial symbionts. *Plant Biology,* 21**,** 523-532.
JAMALUDDIN, F., MOHAMED, S. & LAJIS, M. N. 1994. Hypoglycaemic effect of Parkia speciosa seeds due to the synergistic action of β-sitosterol and stigmasterol. *Food Chemistry,* 49**,** 339-345.
JEONG, J. Y., JO, Y. H., LEE, K. Y., DO, S.-G., HWANG, B. Y. & LEE, M. K. 2014. Optimization of pancreatic lipase inhibition by Cudrania tricuspidatafruits using response surface methodology. *Bioorganic & Medicinal Chemistry Letters,* 24, 2329-2333.
JINGBO, W., AIMIN, C., QI, W., XIN, L. & HUAINING, L. 2015. Betulinic acid inhibits IL1β-induced inflammation by activating PPAR-γ in human osteoarthritis chondrocytes. *International Immunopharmacology,* 29**,** 687-692.
JO, Y. H., KIM, S. B., LIU, Q., DO, S.-G., HWANG, B. Y. & LEE, M. K. 2017. Comparison of pancreatic lipase inhibitory isoflavonoids from unripe and ripe fruits of Cudrania tricuspidata. *PloS one,* 12**,** 1-14.
JONES, W. P. & KINGHORN, A. D. 2006. Extraction of Plant Secondary Metabolites. In: Sarker S.D., Latif Z., Gray A.I. (eds) *Natural Products Isolation*. Methods in Biotechnology, 20, 323-351. Humana Press.
JOSHI, S. R., STANDL, E., TONG, N., SHAH, P., KALRA, S. & RATHOD, R. 2015. Therapeutic potential of alpha-glucosidase inhibitors in type 2 diabetes mellitus: an evidence-based review. *Expert Opinion on Pharmacotherapy,* 16**,** 1959-1981.
JULNARYN, I., ARAYA, H., BENJANUT, C., KITTANA, M. & SIRICHAI, A. 2012. Extracts of Edible Plants Inhibit Pancreatic Lipase, Cholesterol

Esterase and Cholesterol Micellization, and Bind Bile Acids. *Food Technology and Biotechnology,* 50**,** 11-16.

JUNG, E. H., RAN KIM, S., HWANG, I. K. & YOUL HA, T. 2007. Hypoglycemic effects of a phenolic acid fraction of rice bran and ferulic acid in C57BL/KsJ-db/db mice. *Journal of Agricultural and Food Chemistry,* 55**,** 9800-9804.

JYOTHI, S., CHAVAN, S. C. & SOMASHEKARAIAH, B. 2012. In vitro and in vivo antioxidant and anti-diabetic efficacy of Cassia auriculata L. flowers. *Global Journal of Pharmacology,* 6**,** 33-40.

SAHU, K.N., BALBHADRA, S.S., CHOUDHARY, J. & V KOHLI, D. 2012. Exploring pharmacological significance of chalcone scaffold: a review. *Current medicinal chemistry,* 19**,** 209-225.

KAHN, S. E., HULL, R. L. & UTZSCHNEIDER, K. M. 2006. Mechanisms linking obesity to insulin resistance and type 2 diabetes. *Nature,* 444**,** 840-846.

KAKU, H., TAJIRI, Y. & YAMADA, K. 2012. Anorexigenic effects of miglitol in concert with the alterations of gut hormone secretion and gastric emptying in healthy subjects. *Hormone and Metabolic Research,* 44**,** 312-318.

KAMBOJ, A. & SALUJA, A. K. 2011a. Isolation of stigmasterol and β-sitosterol from petroleum ether extract of aerial parts of Ageratum conyzoides (Asteraceae). *International Journal of Pharmacy and Pharmaceutical Sciences,* 3**,** 94-96.

KAMESWARARAO, B., KESAVULU, M. & APPARAO, C. 2003. Evaluation of anti-diabetic effect of Momordica cymbalaria fruit in alloxan-diabetic rats. *Fitoterapia,* 74**,** 7-13.

KANAUJIA, A., DUGGAR, R., PANNAKAL, S. T., YADAV, S. S., KATIYAR, C. K., BANSAL, V., ANAND, S., SUJATHA, S. & LAKSHMI, B. 2010. Insulinomimetic activity of two new gallotannins from the fruits of Capparis moonii. *Bioorganic & medicinal chemistry,* 18**,** 3940-3945.

KANDASAMY, A. D., SUNG, M. M., BOISVENUE, J. J., BARR, A. J. & DYCK, J. R. 2012. Adiponectin gene therapy ameliorates high-fat, high-sucrose diet-induced metabolic perturbations in mice. *Nutrition & Diabetes,* 2**,** 1-7.

KANETO, H., XU, G., FUJII, N., KIM, S., BONNER-WEIR, S. & WEIR, G. C. 2002. Involvement of c-Jun N-terminal kinase in oxidative stress-mediated suppression of insulin gene expression. *Journal of Biological Chemistry,* 277**,** 30010-30018.

KANG, W.-Y., SONG, Y.-L. & ZHANG, L. 2011. α-Glucosidase inhibitory and antioxidant properties and anti-diabetic activity of Hypericum ascyron L. *Medicinal Chemistry Research,* 20**,** 809-816.

KANGSAMAKSIN, T., CHAITHONGYOT, S., WOOTTHICHAIRANGSAN, C., HANCHAINA, R., TANGSHEWINSIRIKUL, C. & SVASTI, J. 2017. Lupeol and stigmasterol suppress tumor angiogenesis and inhibit cholangiocarcinoma growth in mice via downregulation of tumor necrosis factor-α. *PloS one,* 12**,** 1-16.

KAO, Y.-H., HIIPAKKA, R. A. & LIAO, S. 2000. Modulation of Endocrine Systems and Food Intake by Green Tea Epigallocatechin Gallate*. *Endocrinology,* 141**,** 980-987.

KARAN, S. K., MISHRA, S. K., PAL, D. & MONDAL, A. 2012. Isolation of β-sitosterol and evaluation of anti-diabetic activity of Aristolochia indica in

alloxan-induced diabetic mice with a reference to in-vitro antioxidant activity. *Journal of Medicinal Plants Research,* 6**,** 1219-1223.
KEDARE, S. B. & SINGH, R. 2011. Genesis and development of DPPH method of antioxidant assay. *Journal of food science and technology,* 48**,** 412-422.
KENICER, G. J., KAJITA, T., PENNINGTON, R. T. & MURATA, J. 2005. Systematics and biogeography of Lathyrus (Leguminosae) based on internal transcribed spacer and cpDNA sequence data. *American Journal of Botany,* 92**,** 1199-209.
KESSLER, R. C., BERGLUND, P. A., CHIU, W. T., DEITZ, A. C., HUDSON, J. I., SHAHLY, V., AGUILAR-GAXIOLA, S., ALONSO, J., ANGERMEYER, M. C. & BENJET, C. 2013. The prevalence and correlates of binge eating disorder in the World Health Organization World Mental Health Surveys. *Biological psychiatry,* 73**,** 904-914.
KHANAM, S. & SULTANA, R. 2012. Isolation of β-sitosterol & stigmasterol as active immunomodulatory constituents from fruits of Solanum xanthocarpum (Solanaceae). *International Journal of Pharmaceutical Sciences and Research,* 3**,** 1057-1060.
KIAGE- MOKUA, B. N., ROOS, N. & SCHREZENMEIR, J. 2012. Lapacho Tea (Tabebuia impetiginosa) Extract Inhibits Pancreatic Lipase and Delays Postprandial Triglyceride Increase in Rats. *Phytotherapy Research,* 26**,** 1878-1883.
KIM, G.-N., SHIN, J.-G. & JANG, H.-D. 2009. Antioxidant and anti-diabetic activity of Dangyuja (Citrus grandis Osbeck) extract treated with Aspergillus saitoi. *Food Chemistry,* 117**,** 35-41.
KIM, H.-J., JIN, B.-Y., OH, M.-J., SHIN, K.-H., CHOI, S.-H., KIM, D.-H. 2016. The effect of metformin on neuronal activity in the appetite-regulating brain regions of mice fed a high-fat diet during an anorectic period. *Physiology & Behavior,* 154**,** 184-190.
KIM, H. Y. & KIM, K. 2012. Regulation of signaling molecules associated with insulin action, insulin secretion and pancreatic β-cell mass in the hypoglycemic effects of Korean red ginseng in Goto-Kakizaki rats. *Journal of ethnopharmacology,* 142**,** 53-58.
KIM, J., LEE, Y. S., KIM, C. S. & KIM, J. S. 2012. Betulinic acid has an inhibitory effect on pancreatic lipase and induces adipocyte lipolysis. *Phytotherapy Research,* 26**,** 1103-6.
KIM, S.-S. Betulinic acid inhibits LPS-induced MMP-9 expression by suppressing NF-kB activation in BV2 microglial cells. *4th International Conference on Biomedical Engineering in Vietnam*, 2013. Springer, 238-243.
KING, A. J. 2012. The use of animal models in diabetes research. *British Journal of Pharmacology,* 166**,** 877-894.
KLEIN, D., BARBÉ-TUANA, F., PUGLIESE, A., ICHII, H., GARZA, D., GONZALEZ, M., MOLANO, R. D., RICORDI, C. & PASTORI, R. L. 2005. A functional CD40 receptor is expressed in pancreatic beta cells. *Diabetologia,* 48**,** 268-276.
KOHLGRUBER, A. & LYNCH, L. 2015. Adipose tissue inflammation in the pathogenesis of type 2 diabetes. *Current Diabetes Reports,* 15**,** 92-113.
KOIVUSALO, S. B., RÖNÖ, K., KLEMETTI, M. M., ROINE, R. P., LINDSTRÖM, J., ERKKOLA, M., KAAJA, R. J., PÖYHÖNEN-ALHO, M.,

TIITINEN, A. & HUVINEN, E. 2016. Gestational diabetes mellitus can be prevented by lifestyle intervention: the Finnish Gestational Diabetes Prevention Study (RADIEL): a randomized controlled trial. *Diabetes care,* 39**,** 24-30.

KONSTANTINOS, P., MACIEJ, B., ELENI, B., MANFREDI, R. & MICHAEL, E. 2018. Complications of Diabetes 2017. *Journal of Diabetes Research,* 2018, 1-4.

KRISHNAN, N., KONIDARIS, K. F., GASSER, G. & TONKS, N. K. 2018. A potent, selective, and orally bioavailable inhibitor of the protein-tyrosine phosphatase PTP1B improves insulin and leptin signaling in animal models. *Journal of Biological Chemistry,* 293**,** 1517-1525.

KROGH, R., KROTH, R., BERTI, C., MADEIRA, A. O., SOUZA, M. M., CECHINEL-FILHO, V., DELLE-MONACHE, F. & YUNES, R. A. 1999. Isolation and identification of compounds with antinociceptive action from Ipomoea pes-caprae (L.) R. Br. *Pharmazie,* 54**,** 464-466.

KUBOTA, N., TERAUCHI, Y., YAMAUCHI, T., KUBOTA, T., MOROI, M., MATSUI, J., ETO, K., YAMASHITA, T., KAMON, J., SATOH, H., YANO, W., FROGUEL, P., NAGAI, R., KIMURA, S., KADOWAKI, T. & NODA, T. 2002. Disruption of adiponectin causes insulin resistance and neointimal formation. *The Journal of biological chemistry,* 277**,** 25863-25866.

KULKARNI, R. N., WANG, Z. L., WANG, R. M., HURLEY, J. D., SMITH, D. M., GHATEI, M. A., WITHERS, D. J., GARDINER, J. V., BAILEY, C. J. & BLOOM, S. R. 1997. Leptin rapidly suppresses insulin release from insulinoma cells, rat and human islets and, in vivo, in mice. *Journal of Clinical Investigation,* 100**,** 2729-2736.

KUMAR, P. M., VENKATARANGANNA, M. V., MANJUNATH, K., VISWANATHA, G. L. & ASHOK, G. 2018. Momordica cymbalaria fruit extract attenuates high-fat diet-induced obesity and diabetes in C57BL/6 mice. *Iranian Journal of Basic Medical Sciences,* 21**,** 1083-1090.

KUPICHA, F. 1983. infrageneric structure of Lathyrus. *Notes-Royal Botanic Garden Edinburgh*. 41, 209-244.

KWON, Y.-I., APOSTOLIDIS, E. & SHETTY, K. 2008. In vitro studies of eggplant (Solanum melongena) phenolics as inhibitors of key enzymes relevant for type 2 diabetes and hypertension. *Bioresource Technology,* 99**,** 2981-2988.

LACROIX, I. M. E. & LI- CHAN, E. C. Y. 2014. Overview of food products and dietary constituents with anti-diabetic properties and their putative mechanisms of action: A natural approach to complement pharmacotherapy in the management of diabetes. *Molecular Nutrition & Food Research,* 58**,** 61-78.

LASZCZYK, M. N. 2009. Pentacyclic triterpenes of the lupane, oleanane and ursane group as tools in cancer therapy. *Planta medica,* 75**,** 1549-1560.

LAUBNER, K., KIEFFER, T. J., LAM, N. T., NIU, X., JAKOB, F. & SEUFERT, J. 2005. Inhibition of preproinsulin gene expression by leptin induction of suppressor of cytokine signaling 3 in pancreatic beta-cells. *Diabetes,* 54**,** 3410-3417.

LAWRENCE, T. 2009. The nuclear factor NF-κB pathway in inflammation. *Cold Spring Harbor perspectives in biology,* 1**,** 1-10.

LECUBE, A., MONEREO, S., RUBIO, M. Á., MARTINEZ-DE-ICAYA, P., MARTI, A., SALVADOR, J., MASMIQUEL, L., GODAY, A., BELLIDO, D. & LURBE, E. 2017. Prevention, diagnosis, and treatment of obesity. 2016 position statement of the Spanish Society for the Study of Obesity. *Endocrinologia, diabetes y nutricion,* 64**,** 15-22.

LEE, A., PATRICK, P., WISHART, J., HOROWITZ, M. & MORLEY, J. 2002. The effects of miglitol on glucagon- like peptide- 1 secretion and appetite sensations in obese type 2 diabetics. *Diabetes, Obesity and Metabolism,* 4**,** 329-335.

LEE, J. W., KANG, Y. J., CHOI, H. K. & YOON, Y. G. 2018. Fractionated Coptis chinensis extract and its bioactive component suppress Propionibacterium acnes-stimulated inflammation in human keratinocytes. *Journal of Microbiology and Biotechnology,* 28**,** 839-48.

LEE, S.-S., LIN, H.-C. & CHEN, C.-K. 2008. Acylated flavonol monorhamnosides, α-glucosidase inhibitors, from Machilus philippinensis. *Phytochemistry,* 69**,** 2347-2353.

LEE, S. M., YANG, H., TARTAR, D. M., GAO, B., LUO, X., YE, S. Q., ZAGHOUANI, H. & FANG, D. 2011a. Prevention and treatment of diabetes with resveratrol in a non-obese mouse model of type 1 diabetes.(Report). *Diabetologia,* 54**,** 1136.

LEE, T. K., POON, R. T., WO, J. Y., MA, S., GUAN, X. Y., MYERS, J. N., ALTEVOGT, P. & YUEN, A. P. 2007. Lupeol suppresses cisplatin-induced nuclear factor-kappaB activation in head and neck squamous cell carcinoma and inhibits local invasion and nodal metastasis in an orthotopic nude mouse model. *Cancer Research,* 67**,** 8800-9.

LEE, Y. H., MAGKOS, F., MANTZOROS, C. S. & KANG, E. S. 2011b. Effects of leptin and adiponectin on pancreatic beta-cell function. *Metabolism,* 60**,** 1664-1672.

LEMAURE, B., TOUCHÉ, A., ZBINDEN, I., MOULIN, J., COURTOIS, D., MACÉ, K. & DARIMONT, C. 2007. Administration of Cyperus rotundus tubers extract prevents weight gain in obese Zucker rats. *Phytotherapy Research,* 21**,** 724-730.

LI, F., SUN, S., WANG, J. & WANG, D. 1998. Chromatography of medicinal plants and Chinese traditional medicines. *Biomedical Chromatography,* 12**,** 78-85.

LI, J., FENG, J., WEI, H., LIU, Q., YANG, T., HOU, S., ZHAO, Y., ZHANG, B. & YANG, C. 2018. The Aqueous Extract of Gynura divaricata (L.) DC. Improves Glucose and Lipid Metabolism and Ameliorates Type 2 Diabetes Mellitus. *Evidence-based Complementary and Alternative Medicine,* 2018**,** 1-11.

LI, J., GONG, F. & LI, F. 2016. Hypoglycemic and hypolipidemic effects of flavonoids from tatary buckwheat in type 2 diabetic rats. *Biomedical Research,* 27.

LI, S., SHIN, H. J., DING, E. L. & VAN DAM, R. M. 2009. Adiponectin levels and risk of type 2 diabetes: a systematic review and meta-analysis. *Journal of the American Medical Association,* 302**,** 179-188.

LI, W. V. & LI, J. J. 2018. Modeling and analysis of RNA-seq data: a review from a statistical perspective. *Quantitative Biology,* 6**,** 195-209.

LI, X.-L., WANG, H., LIU, G., ZHANG, X.-Q., YE, W.-C. & ZHAO, S.-X. 2007. Study on chemical constituents from Desmodium styracifolium. *Journal of Chinese medicinal materials,* 30**,** 802-805.

LIANG, H., YIN, B., ZHANG, H., ZHANG, S., ZENG, Q., WANG, J., JIANG, X., YUAN, L., WANG, C.-Y. & LI, Z. 2008. Blockade of tumor necrosis factor (TNF) receptor type 1-mediated TNFα signaling protected Wistar rats from diet-induced obesity and insulin resistance. *Endocrinology,* 149**,** 2943-2951.

LIU, Y., BI, T., WANG, G., DAI, W., WU, G., QIAN, L., GAO, Q. & SHEN, G. 2015. Lupeol inhibits proliferation and induces apoptosis of human pancreatic cancer PCNA-1 cells through AKT/ERK pathways. *Naunyn-Schmiedeberg's archives of pharmacology,* 388**,** 295-304.

LOPEZ-CASTEJON, G., BROUGH, D. 2011. Understanding the mechanism of IL1β secretion. *Cytokine & Growth Factor Reviews,* 22**,** 189-195.

LOTIA, S., MONTOJO, J., DONG, Y., BADER, G. D. & PICO, A. R. 2013. Cytoscape app store. *Bioinformatics,* 29**,** 1350-1351.

LUO, J.-G., MA, L. & KONG, L.-Y. 2008. New triterpenoid saponins with strong α-glucosidase inhibitory activity from the roots of Gypsophila oldhamiana. *Bioorganic & medicinal chemistry,* 16**,** 2912-2920.

LUQMAN, S., KAUSHIK, S., SRIVASTAVA, S., KUMAR, R., BAWANKULE, D., PAL, A., DAROKAR, M. P. & KHANUJA, S. P. 2009. Protective effect of medicinal plant extracts on biomarkers of oxidative stress in erythrocytes. *Pharmaceutical Biology,* 47**,** 483-490.

LUQUE DE CASTRO, M. D. & PRIEGO-CAPOTE, F. 2010. Soxhlet extraction: Past and present panacea. *Journal of Chromatography A,* 1217**,** 2383-9.

LUTZ, S. Z., STAIGER, H., FRITSCHE, A. & HÄRING, H.-U. 2014. Antihyperglycaemic therapies and cancer risk. *Diabetes and Vascular Disease Research,* 11, 371-389.

LYTVYN, Y., ŠKRTIĆ, M., YANG, G. K., YIP, P. M., PERKINS, B. A. & CHERNEY, D. Z. 2014. Glycosuria-mediated urinary uric acid excretion in patients with uncomplicated type 1 diabetes mellitus. *American Journal of Physiology-Renal Physiology,* 308**,** F77-F83.

LÓPEZ-DÍEZ, R., SHEKHTMAN, A., RAMASAMY, R. & SCHMIDT, A. M. 2016. Cellular mechanisms and consequences of glycation in atherosclerosis and obesity. *Biochimica et Biophysica Acta (BBA)-Molecular Basis of Disease,* 1862**,** 2244-2252.

MACHADO- LIMA, A., IBORRA, R. T., PINTO, R. S., CASTILHO, G., SARTORI, C. H., OLIVEIRA, E. R., OKUDA, L. S., NAKANDAKARE, E. R., GIANNELLA- NETO, D. & MACHADO, U. F. 2015. In Type 2 Diabetes Mellitus Glycated Albumin Alters Macrophage Gene Expression Impairing ABCA1- Mediated Cholesterol Efflux. *Journal of cellular physiology,* 230**,** 1250-1257.

MAEDLER, K., SERGEEV, P., RIS, F., OBERHOLZER, J., JOLLER-JEMELKA, H. I., SPINAS, G. A., KAISER, N., HALBAN, P. A. & DONATH, M. Y. 2002. Glucose-induced β cell production of IL1β contributes to glucotoxicity in human pancreatic islets. *The Journal of clinical investigation,* 110**,** 851-860.

MAGISTRETTI, P. J. & ALLAMAN, I. 2013. Brain energy metabolism. *Neuroscience in the 21st century: From basic to clinical***,** 1591-1620.

MAHAYASIH, P. G. M. W., ELYA, B. & HANAFI, M. 2017. Alpha-glucosidase inhibitory activity of Garcinia lateriflora Blume Leaves. *Journal of Applied Pharmaceutical Science,* 7**,** 100-104.

MAJOR, C. D. & WOLF, B. A. 2001. Interleukin-1β stimulation of c-Jun NH2-terminal kinase activity in insulin-secreting cells: evidence for cytoplasmic restriction. *Diabetes,* 50**,** 2721-2728.

MARROQUÍ, L., GONZALEZ, A., ÑECO, P., CABALLERO-GARRIDO, E., VIEIRA, E., RIPOLL, C., NADAL, A. & QUESADA, I. 2012. Role of leptin in the pancreatic β- cell: effects and signaling pathways. *Journal of molecular endocrinology,* 49**,** R9-17.

MARSTON, A. 2011. Thin-layer chromatography with biological detection in phytochemistry. *Journal of Chromatography A,* 1218**,** 2676-2683.

MARTIGNONI, M., GROOTHUIS, G. M., DE KANTER, R. 2006. Species differences between mouse, rat, dog, monkey and human CYP-mediated drug metabolism, inhibition and induction. *Expert Opinion on Drug Metabolism & Toxicology,* 2**,** 875-894.

MBAZE, L. M. A., POUMALE, H. M. P., WANSI, J. D., LADO, J. A., KHAN, S. N., IQBAL, M. C., NGADJUI, B. T. & LAATSCH, H. 2007. α-Glucosidase inhibitory pentacyclic triterpenes from the stem bark of Fagara tessmannii (Rutaceae). *Phytochemistry,* 68**,** 591-595.

MCCUEN- WURST, C., RUGGIERI, M. & ALLISON, K. C. 2018. Disordered eating and obesity: associations between binge- eating disorder, night-eating syndrome, and weight- related comorbidities. *Annals of the New York Academy of Sciences,* 1411, 96-105.

MCDOUGALL, G. J., SHPIRO, F., DOBSON, P., SMITH, P., BLAKE, A. & STEWART, D. 2005. Different polyphenolic components of soft fruits inhibit α-amylase and α-glucosidase. *Journal of agricultural and food chemistry,* 53**,** 2760-2766.

MEEK, T. H. & MORTON, G. J. 2016. The role of leptin in diabetes: metabolic effects. *Diabetologia,* 59**,** 928-932.

MEZEI, O., BANZ, W. J., STEGER, R. W., PELUSO, M. R., WINTERS, T. A. & SHAY, N. 2003. Soy isoflavones exert anti-diabetic and hypolipidemic effects through the PPAR pathways in obese Zucker rats and murine RAW 264.7 cells. *Journal of Nutrition,* 133**,** 1238-1243.

MIDDLETON, E., KANDASWAMI, C. & THEOHARIDES, T. C. 2000. The effects of plant flavonoids on mammalian cells: implications for inflammation, heart disease, and cancer. *Pharmacological reviews,* 52**,** 673-751.

MINETTE, L., JUDY, L., TOMMY, S., MANPREET KAUR, S., ENRIQUE VERA, T., DEVIN, M., PO-TING, C., CESAR, O., AIRANI, S. & VISHWANATH, V. 2015. Investigating the causes for decreased levels of glutathione in individuals with type II diabetes. *PLoS ONE,* 10**,** 3-19.

MITCHELL, D. C., ABDELRAHIM, M., WENG, J., STAFFORD, L. J., SAFE, S., BAR-ELI, M. & LIU, M. 2006. Regulation of KiSS-1 metastasis suppressor gene expression in breast cancer cells by direct interaction of transcription factors activator protein-2α and specificity protein-1. *Journal of Biological Chemistry,* 281**,** 51-58.

MITTAL, J. & SHARMA, M. M. 2017. Enhanced production of berberine in In vitro regenerated cell of Tinospora cordifolia and its analysis through LCMS QToF. *3 Biotechnology,* 7**,** 25-37.

MITTAL, K., MANI, R. J. & KATARE, D. P. 2016. Type 3 diabetes: cross talk between differentially regulated proteins of type 2 diabetes mellitus and Alzheimer's disease. *Scientific reports,* 6**,** 1-8.

MIYAUCHI, K., TAKIYAMA, Y., HONJYO, J., TATENO, M. & HANEDA, M. 2009. Upregulated IL-18 expression in type 2 diabetic subjects with nephropathy: TGF-β1 enhanced IL-18 expression in human renal proximal tubular epithelial cells. *Diabetes research and clinical practice,* 83**,** 190-199.

MONTELEONE, M., STANLEY, A. C., CHEN, K. W., BROWN, D. L., BEZBRADICA, J. S., VON PEIN, J. B., HOLLEY, C. L., BOUCHER, D., SHAKESPEAR, M. R. & KAPETANOVIC, R. 2018. Interleukin-1β maturation triggers its relocation to the plasma membrane for gasdermin-D-dependent and-independent secretion. *Cell reports,* 24**,** 1425-1433.

MORIGNY, P., HOUSSIER, M., MOUISEL, E. & LANGIN, D. 2016. Adipocyte lipolysis and insulin resistance. *Biochimie,* 125**,** 259-266.

MORTON, G. J., KAIYALA, K. J., FISHER, J. D., OGIMOTO, K., SCHWARTZ, M. W. & WISSE, B. E. 2011. Identification of a physiological role for leptin in the regulation of ambulatory activity and wheel running in mice. *American Journal of Physiology-Endocrinology and Metabolism,* 300**,** 392-401.

MOUNA, A., DAVID, A., MAHMOOD AMEEN, A., KHALIJAH, A., MUSTAFA ALI, M. & MOHD RAIS, M. 2010. In vitro and in vivo anti-inflammatory activity of 17-O-acetylacuminolide through the inhibition of cytokines, NF-κB translocation and IKKβ activity. *PLoS ONE,* 5**,** 1-13.

MOVAHEDI, B., VAN DE CASTEELE, M., CALUWÉ, N., STANGÉ, G., BRECKPOT, K., THIELEMANS, K., VREUGDENHIL, G., MATHIEU, C. & PIPELEERS, D. 2004. Human pancreatic duct cells can produce tumour necrosis factor-α that damages neighbouring beta cells and activates dendritic cells. *Diabetologia,* 47**,** 998-1008.

NA, M., KIM, B. Y., OSADA, H., AHN, J. S. 2009. Inhibition of protein tyrosine phosphatase 1B by lupeol and lupenone isolated from Sorbus commixta. *Journal of Enzyme Inhibition and Medicinal Chemistry,* 24**,** 1056-1059.

NA, M. K., YANG, S., HE, L., OH, H., KIM, B. S., OH, W. K., KIM, B. Y. & AHN, J. S. 2006. Inhibition of protein tyrosine phosphatase 1B by ursane-type triterpenes isolated from Symplocos paniculata. *Planta medica,* 72**,** 261-263.

NARKHEDE, M., AJIMIRE, P., WAGH, A., MOHAN, M. & SHIVASHANMUGAM, A. 2011. In vitro anti-diabetic activity of Caesalpina digyna (R.) methanol root extract. *Asian Journal of Plant Science and Research,* 1**,** 101-106.

NBN-ATLAS. 2019. *Lathyrus linifolius (Reichard) Bässler (Bitter-Vetch)* [Online]. Available: https://species.nbnatlas.org/species/NHMSYS0000460181#overview [Accessed 11/01/2019].

NCUBE, N., AFOLAYAN, A. & OKOH, A. 2008. Assessment techniques of antimicrobial properties of natural compounds of plant origin: current methods and future trends. *African journal of biotechnology,* 7.

NEWMAN, D. J. & CRAGG, G. M. 2007. Natural products as sources of new drugs over the last 25 years. *Journal of Natural Products,* 70**,** 461-77.

NEYRET, A., GAY, B., CRANSAC, A., BRIANT, L., CORIC, P., TURCAUD, S., LAUGAA, P., BOUAZIZ, S. & CHAZAL, N. 2019. Insight into the mechanism of action of EP-39, a bevirimat derivative that inhibits HIV-1 maturation. *Antiviral Research,* 164**,** 162-175.

NGUEMFO, E., DIMO, T., DONGMO, A., AZEBAZE, A., ALAOUI, K., ASONGALEM, A., CHERRAH, Y. & KAMTCHOUING, P. 2009. Anti-oxidative and anti-inflammatory activities of some isolated constituents from the stem bark of Allanblackia monticola Staner LC (Guttiferae). *Inflammopharmacology,*17**,** 37-41.

NIEMETZ, R. & GROSS, G. G. 2005. Enzymology of gallotannin and ellagitannin biosynthesis. *Phytochemistry,* 66**,** 2001-2011.

NIKOULINA, S. E., CIARALDI, T. P., MUDALIAR, S., MOHIDEEN, P., CARTER, L. & HENRY, R. R. 2000. Potential role of glycogen synthase kinase-3 in skeletal muscle insulin resistance of type 2 diabetes. *Diabetes,* 49**,** 263-271.

NILSSON, S. G., FRANZEN, M. & JÖNSSON, E. 2008. Long- term land- use changes and extinction of specialised butterflies. *Insect Conservation and Diversity,* 1**,** 197-207.

NIRMAL, S. A., PAL, S. C., MANDAL, S. C. & PATIL, A. N. 2012. Analgesic and anti-inflammatory activity of β-sitosterol isolated from Nyctanthes arbortristis leaves. *Inflammopharmacology,* 20**,** 219-224.

OBANDA, D. N. & CEFALU, W. T. 2013. Modulation of cellular insulin signaling and PTP1B effects by lipid metabolites in skeletal muscle cells. *The Journal of nutritional biochemistry,* 24**,** 1529-1537.

OBI, F. O., USENU, I. A. & OSAYANDE, J. O. 1998. Prevention of carbon tetrachloride-induced hepatotoxicity in the rat by H. rosasinensis anthocyanin extract administered in ethanol. *Toxicology,* 131**,** 93-98.

ODEYEMI, S. & BRADLEY, G. 2018. Medicinal plants used for the traditional management of diabetes in the Eastern Cape, South Africa: Pharmacology and toxicology. *Molecules,* 23**,** 2759-2778.

OGURTSOVA, K., DA ROCHA FERNANDES, J., HUANG, Y., LINNENKAMP, U., GUARIGUATA, L., CHO, N., CAVAN, D., SHAW, J. & MAKAROFF, L. 2017. IDF Diabetes Atlas: Global estimates for the prevalence of diabetes for 2015 and 2040. *Diabetes research and clinical practice,* 128**,** 40-50.

OHTA, Y. & HAMADA, Y. 2004. In situ Expression of CD40 and CD40 Ligand in Psoriasis. *Dermatology,* 209**,** 21-28.

OJO, O. A., OJO, A. B., AJIBOYE, B. O., OLAIYA, O., AKAWA, A., OLAOYE, O., ANIFOWOSE, O. O., IDOWU, O., OLASEHINDE, O. & OBAFEMI, T. 2018. Inhibitory Effect of Bryophyllum pinnatum (Lam.) Oken leaf Extract and their Fractions on α-amylase, α-glucosidase and Cholinesterase Enzyme. *Pharmacognosy Journal,* 10, 497-506.

OKAMOTO, M., OHARA-IMAIZUMI, M., KUBOTA, N., HASHIMOTO, S., ETO, K., KANNO, T., KUBOTA, T., WAKUI, M., NAGAI, R., NODA, M., NAGAMATSU, S. & KADOWAKI, T. 2008. Adiponectin induces insulin secretion in vitro and in vivo at a low glucose concentration. *Diabetologia,* 51**,** 827-35.

OLIVARES, M., SCHÜPPEL, V., HASSAN, A. M., BEAUMONT, M., NEYRINCK, A. M., BENÍTEZ-PÁEZ, A., SANZ, Y., HALLER, D., HOLZER, P. & DELZENNE, N. 2018. The potential role of the dipeptidyl peptidase-4-like activity from the gut microbiota on the host health. *Frontiers in microbiology,* 9**,** 1-10.

ORTIZ-ANDRADE, R., GARCIA-JIMENEZ, S., CASTILLO-ESPANA, P., RAMIREZ-AVILA, G., VILLALOBOS-MOLINA, R. & ESTRADA-SOTO, S. 2007. α-Glucosidase inhibitory activity of the methanolic extract from Tournefortia hartwegiana: an anti-hyperglycemic agent. *Journal of ethnopharmacology,* 109**,** 48-53.

ORTIZ- LAZARENO, P. C., HERNANDEZ- FLORES, G., DOMINGUEZ-RODRIGUEZ, J. R., LERMA- DIAZ, J. M., JAVE- SUAREZ, L. F., AGUILAR- LEMARROY, A., GOMEZ- CONTRERAS, P. C., SCOTT-ALGARA, D. & BRAVO- CUELLAR, A. 2008. MG132 proteasome inhibitor modulates proinflammatory cytokines production and expression of their receptors in U937 cells: involvement of nuclear factor- κB and activator protein- 1. *Immunology,* 124**,** 534-541.

OUKARROUM, A., BARHOUMI, L., PIRASTRU, L. & DEWEZ, D. 2013. Silver nanoparticle toxicity effect on growth and cellular viability of the aquatic plant Lemna gibba. *Environmental toxicology and chemistry,* 32**,** 902-907.

OZOUGWU, J., OBIMBA, K., BELONWU, C. & UNAKALAMBA, C. 2013. The pathogenesis and pathophysiology of type 1 and type 2 diabetes mellitus. *Journal of Physiology and Pathophysiology,* 4**,** 46-57.

PAIS, R., GRIBBLE, F. M. & REIMANN, F. 2016. Stimulation of incretin secreting cells. *Therapeutic advances in endocrinology and metabolism,* 7**,** 24-42.

PAN, Q., SAIMAN, M. Z., MUSTAFA, N. R., VERPOORTE, R. & TANG, K. 2016. A simple and rapid HPLC-DAD method for simultaneously monitoring the accumulation of alkaloids and precursors in different parts and different developmental stages of Catharanthus roseus plants. *Journal of Chromatography B,* 1014**,** 10-16.

PANCHE, A., DIWAN, A. & CHANDRA, S. 2016. Flavonoids: an overview. *Journal of nutritional science,* 5, 1-15.

PANDEY, K. B. & RIZVI, S. I. 2009. Plant polyphenols as dietary antioxidants in human health and disease. *Oxidative medicine and cellular longevity,* 2**,** 270-278.

PAPPACHAN, J. M., FERNANDEZ, C. J. & CHACKO, E. C. 2018. Diabesity and anti-diabetic drugs. *Molecular Aspects of Medicine***,** 66, 3-12.

PATLOLLA, J. M. & RAO, C. V. 2012. Triterpenoids for cancer prevention and treatment: current status and future prospects. *Current Pharmaceutical Biotechnology,* 13**,** 147-155.

PECKET, R. 1960. The nature of the variation in flower colour in the genus Lathyrus. *New Phytologist,* 59**,** 138-144.

PENG, X., ZHANG, G., LIAO, Y. & GONG, D. 2016. Inhibitory kinetics and mechanism of kaempferol on alpha-glucosidase. *Food Chemistry,* 190**,** 207-215.

PHILLIPS, M. S., LIU, Q., HAMMOND, H. A., DUGAN, V., HEY, P. J., CASKEY, C. J. & HESS, J. F. 1996. Leptin receptor missense mutation in the fatty Zucker rat. *Nature Genetics,* 13**,** 18-19.

PIERRE, L. L. & MOSES, M. N. 2015. Isolation and characterisation of stigmasterol and β-sitosterol from Odontonema strictum (acanthaceae). *Journal of Innovations in Pharmaceutical and Biological Sciences,* 2**,** 88-96.

PRABHAKAR, P. K. & DOBLE, M. 2008. A target based therapeutic approach towards diabetes mellitus using medicinal plants. *Current Diabetes Reviews,* 4**,** 291-308.

PRABHAKAR, P. K. & DOBLE, M. 2011. Mechanism of action of natural products used in the treatment of diabetes mellitus. *Chinese journal of integrative medicine,* 17**,** 563-574.

PRAKASH CHATURVEDULA, V. S., SCHILLING, J. K., JOHNSON, R. K. & KINGSTON, D. G. 2003. New cytotoxic lupane triterpenoids from the twigs of Coussarea paniculata. *Journal Natural Products,* 66**,** 419-22.

PRAKASH, C. V. S. & PRAKASH, I. 2012. Isolation and structural characterization of Lupane triterpenes from Polypodium vulgare. *Research Journal of Pharmaceutical Sciences,* 1**,** 23-27.

PREETHA, S. P., KANNIAPPAN, M., SELVAKUMAR, E., NAGARAJ, M. & VARALAKSHMI, P. 2006. Lupeol ameliorates aflatoxin B1-induced peroxidative hepatic damage in rats. *Comparative Biochemistry and Physiology Part C: Toxicology & Pharmacology,* 143**,** 333-9.

PREUSS, H. G., RAO, C. V., GARIS, R., BRAMBLE, J. D., OHIA, S. E., BAGCHI, M. & BAGCHI, D. 2004. An overview of the safety and efficacy of a novel, natural(-)-hydroxycitric acid extract (HCA-SX) for weight management. *Journal of Medicinal Chemistry,* 35**,** 33-48.

PRIETO, J. M., RECIO, M. C. & GINER, R. M. 2006. Anti-inflammatory activity of β-sitosterol in a model of oxazoloneinduced contact-delayed-type hypersensitivity. *Boletín Latinoamericano y del Caribe de Plantas Medicinales y Aromáticas,* 5**,** 57-62.

PRÄBST, K., ENGELHARDT, H., RINGGELER, S. & HÜBNER, H. 2017. Basic colorimetric proliferation assays: MTT, WST, and resazurin. *Cell Viability Assays.* Methods in Molecular Biology, vol 1601. Humana Press, New York, NY.

PUNTHAKEE, Z., GOLDENBERG, R. & KATZ, P. 2018. Definition, classification and diagnosis of diabetes, prediabetes and metabolic syndrome. *Canadian Journal of Diabetes,* 42**,** S10-S15.

QIU, D., GUO, J., YU, H., YAN, J., YANG, S., LI, X., ZHANG, Y., SUN, J., CONG, J., HE, S., WEI, D. & QIN, J.-C. 2018. Antioxidant phenolic compounds isolated from wild Pyrus ussuriensis Maxim. fruit peels and leaves. *Food Chemistry,* 241**,** 182-187.

RAASMAJA, A., LECKLIN, A., LI, X. M., ZOU, J., ZHU, G.-G., LAAKSO, I. & HILTUNEN, R. 2013. A water-alcohol extract of Citrus grandis whole fruits has beneficial metabolic effects in the obese Zucker rats fed with high fat/high cholesterol diet. *Food Chemistry,* 138**,** 1392-1399.

RADIKA, M., VISWANATHAN, P. & ANURADHA, C. 2013. Nitric oxide mediates the insulin sensitizing effects of β-sitosterol in high fat diet-fed rats. *Nitric Oxide,* 32**,** 43-53.

RAKATZI, I., MUELLER, H., RITZELER, O., TENNAGELS, N. & ECKEL, J. 2004. Adiponectin counteracts cytokine- and fatty acid-induced apoptosis in the pancreatic beta-cell line INS-1. *Diabetologia,* 47**,** 249-58.

RAO, S. D., RAO, B. N., DEVI, P. U. & RAO, A. K. 2017. Isolation of lupeol, design and synthesis of lupeol derivatives and their biological activity. *Oriental Journal of Chemistry,* 33**,** 173-180.

RASOANAIVO, P., WRIGHT, C. W., WILLCOX, M. L. & GILBERT, B. 2011. Whole plant extracts versus single compounds for the treatment of malaria: synergy and positive interactions. *Malaria journal,* 10**,** 1-12.

RAUT, N. A., DHORE, P. W., SAOJI, S. D. & KOKARE, D. M. 2016. Selected bioactive natural products for diabetes mellitus. *In Studies in Natural Products Chemistry,* 48, 287-322. Elsevier.

RAVEENDRAN, A. V., CHACKO, E. C. & PAPPACHAN, J. M. 2018. Non-pharmacological treatment options in the management of diabetes mellitus. *European Endocrinology,* 14**,** 31-39.

RENGASAMY, K. R., ADEROGBA, M. A., AMOO, S. O., STIRK, W. A. & VAN STADEN, J. 2013. Potential antiradical and alpha-glucosidase inhibitors from Ecklonia maxima (Osbeck) Papenfuss. *Food Chemistry,* 141**,** 1412-1415.

RENTZSCH, M., WILKENS, A. & WINTERHALTER, P. 2009. Non-flavonoid phenolic compounds. *Wine chemistry and biochemistry,* 509-527. Springer.

RODBARD, H. W. 2016. Role of insulin therapy in diabetes.(An Evolutionary Perspective on Basal Insulin in Diabetes Treatment). *Journal of Family Practice,* 65**,** S3-S7.

ROMANIK, G., GILGENAST, E., PRZYJAZNY, A. & KAMIŃSKI, M. 2007. Techniques of preparing plant material for chromatographic separation and analysis. *Journal of biochemical and biophysical methods,* 70**,** 253-261.

ROTH, G. A., ABATE, D. & WYPER, G. M. A. 2018. Global, regional, and national age-sex-specific mortality for 282 causes of death in 195 countries and territories, 1980–2017 : a systematic analysis for the global burden of disease study 2017. *The Lancet,* 392, 1736-1788.

RYCKMAN, K., SPRACKLEN, C., SMITH, C., ROBINSON, J. & SAFTLAS, A. 2015. Maternal lipid levels during pregnancy and gestational diabetes: a systematic review and meta- analysis. *BJOG: An International Journal of Obstetrics & Gynaecology,* 122**,** 643-651.

SABU, M., SMITHA, K. & KUTTAN, R. 2002. Anti-diabetic activity of green tea polyphenols and their role in reducing oxidative stress in experimental diabetes. *Journal of Ethnopharmacology,* 83**,** 109-116.

SAEIDNIA, S., MANAYI, A., GOHARI, A. R. & ABDOLLAHI, M. 2014. The story of beta-sitosterol-a review. *European Journal of Medicinal Plants,* 4**,** 590-609.

SAITO, M., UENO, M., OGINO, S., KUBO, K., NAGATA, J., TAKEUCHI, M. 2005. High dose of Garcinia cambogia is effective in suppressing fat accumulation in developing male Zucker obese rats, but highly toxic to the testis. *Food and Chemical Toxicology,* 43**,** 411-419.

SALEEM, S., JAFRI, L., UL HAQ, I., CHANG, L. C., CALDERWOOD, D., GREEN, B. D. & MIRZA, B. 2014. Plants Fagonia cretica L. and Hedera nepalensis K. Koch contain natural compounds with potent dipeptidyl peptidase-4 (DPP-4) inhibitory activity. *Journal of ethnopharmacology,* 156**,** 26-32.

SALES, P. M., SOUZA, P.M., SIMEONI, L.A. & SILVEIRA, D. 2012. α-Amylase Inhibitors: A Review of Raw Material and Isolated Compounds from Plant Source. *Journal of Pharmacy & Pharmaceutical Sciences,* 15**,** 141-183.

SALTIEL, A. R. & OLEFSKY, J. M. 2017. Inflammatory mechanisms linking obesity and metabolic disease. *Journal of Clinical Investigation,* 127**,** 1-4.

SANNA, D., DELOGU, G., MULAS, M., SCHIRRA, M. & FADDA, A. 2012. Determination of Free Radical Scavenging Activity of Plant Extracts Through DPPH Assay: An EPR and UV-Vis Study. *Food Analytical Methods,* 5**,** 759-766.

SASIDHARAN, S., CHEN, Y., SARAVANAN, D., SUNDRAM, K. & LATHA, L. Y. 2011. Extraction, isolation and characterization of bioactive compounds from plants' extracts. *African Journal of Traditional, Complementary and Alternative Medicines,* 8, 1-10.

SCHAEFFLER, A. 2017. SP0160 Is diabetes an inflammatory disease and should be treated like that? *Annals of the Rheumatic Diseases,* 76**,** 39.

SCHAFFERT, L., MÄRZ, C., BURKHARDT, L., DROSTE, J., BRANDT, D., BUSCHE, T., ROSEN, W., SCHNEIKER-BEKEL, S., PERSICKE, M. & PÜHLER, A. 2019. Evaluation of vector systems and promoters for overexpression of the acarbose biosynthesis gene acbC in Actinoplanes sp. SE50/110. *Microbial cell factories,* 18**,** 114-130.

SCHAG, K., SCHONLEBER, J., TEUFEL, M., ZIPFEL, S. & GIEL, K. E. 2013. Food-related impulsivity in obesity and Binge Eating Disorder - a systematic review. *Obesity Reviews,* 14**,** 477-495.

SCHARPÉ, S., DE MEESTER, I., VANHOOF, G., HENDRIKS, D., VAN SANDE, M., VAN CAMP, K. & YARON, A. 1988. Assay of dipeptidyl peptidase IV in serum by fluorometry of 4-methoxy-2-naphthylamine. *Clinical chemistry,* 34**,** 2299-2301.

SCHUHLY, W., HEILMANN, J., CALIS, I. & STICHER, O. 1999. New triterpenoids with antibacterial activity from Zizyphus joazeiro. *Planta Medica,* 65**,** 740-3.

SCHWIENTEK, P., SZCZEPANOWSKI, R., RÜCKERT, C., KALINOWSKI, J., KLEIN, A., SELBER, K., WEHMEIER, U. F., STOYE, J. & PÜHLER, A. 2012. The complete genome sequence of the acarbose producer Actinoplanes sp. SE50/110. *BMC genomics,* 13**,** 112-130.

SCHÖN, S., FLIERMAN, I., OFNER, A., STAHRINGER, A., HOLDT, L. M., KOLLIGS, F. T. & HERBST, A. 2014. β- catenin regulates NF- κB activity via TNFRSF19 in colorectal cancer cells. *International journal of cancer,* 135**,** 1800-1811.

SELLAMI, M., LOUATI, H., KAMOUN, J., KCHAOU, A., DAMAK, M. & GARGOURI, Y. 2017. Inhibition of pancreatic lipase and amylase by extracts of different spices and plants. *International Journal of Food Sciences and Nutrition,* 68**,** 313-320.

SEMAAN, D. G., IGOLI, J. O., YOUNG, L., MARRERO, E., GRAY, A. I. & ROWAN, E. G. 2017. In vitro anti-diabetic activity of flavonoids and pheophytins from Allophylus cominia Sw . on PTP1B, DPPIV, alpha-glucosidase and alpha-amylase enzymes. *Journal of Ethnopharmacology,* 203**,** 39-46.

SEMWAL, R. B., SEMWAL, D. K., ASWAL, S. & KUMAR, A. 2018. Spectral studies and pharmacological relevance of berberine isolated from Berberis aristata roots. *Current Medical Drug Research,* 2, 1-8.

SEMWAL, R. B., SEMWAL, D. K., VERMAAK, I. & VILJOEN, A. 2015. A comprehensive scientific overview of Garcinia cambogia. *Fitoterapia,* 102**,** 134-148.

SEN, A., DHAVAN, P., SHUKLA, K. K., SINGH, S. & TEJOVATHI, G. 2012. Analysis of IR, NMR and antimicrobial activity of β-sitosterol isolated from Momordica charantia. *Science Secure Journal of Biotechnology,* 1**,** 9-13.

SERRANO, J., PUUPPONEN- PIMIÄ, R., DAUER, A., AURA, A. M. & SAURA- CALIXTO, F. 2009. Tannins: current knowledge of food sources, intake, bioavailability and biological effects. *Molecular nutrition & food research,* 53**,** S310-S329.

SEUFERT, J. 2004. Leptin Effects on Pancreatic β- Cell Gene Expression and Function. *Diabetes,* 53**,** S152-S158.

SEUFERT, J., KIEFFER, T. J. & HABENER, J. F. 1999. Leptin inhibits insulin gene transcription and reverses hyperinsulinemia in leptin-deficient ob/ob mice. *Proceedings of the National Academy of Sciences of the United States of America,* 96**,** 674-9.

SHANMUGAM, M., RANE, G., KANCHI, M., ARFUSO, F., CHINNATHAMBI, A., ZAYED, M., ALHARBI, S., TAN, B., KUMAR, A. & SETHI, G. 2015. The Multifaceted Role of Curcumin in Cancer Prevention and Treatment. *Molecules,* 20, 2728-2769

SHANNON, P., MARKIEL, A., OZIER, O., BALIGA, N. S., WANG, J. T., RAMAGE, D., AMIN, N., SCHWIKOWSKI, B. & IDEKER, T. 2003. Cytoscape: a software environment for integrated models of biomolecular interaction networks. *Genome research,* 13**,** 2498-2504.

SHARMA, D., VERMA, S., VAIDYA, S., KALIA, K. & TIWARI, V. 2018. Recent updates on GLP-1 agonists: Current advancements & challenges. *Biomedicine & Pharmacotherapy,* 108**,** 952-962.

SHIMOBAYASHI, M., ALBERT, V., WOELNERHANSSEN, B., FREI, I. C., WEISSENBERGER, D., MEYER-GERSPACH, A. C., CLEMENT, N., MOES, S., COLOMBI, M. & MEIER, J. A. 2018. Insulin resistance causes inflammation in adipose tissue. *Journal of Clinical Investigation,* 128**,** 1538-1550.

SHIRWAIKAR, A., SETTY, M. M., BOMMU, P. & KRISHNANAND, B. 2004. Effect of lupeol isolated from Crataeva nurvala Buch.-Ham. stem bark extract against free radical induced nephrotoxicity in rats. *Indian Journal of Experimental Biology,* 42(7), 686-690.

SIKARWAR, M. S. & PATIL, M. 2010. Anti-diabetic activity of Pongamia pinnata leaf extracts in alloxan-induced diabetic rats. *International Journal of Ayurveda Research,* 1**,** 199-204.

SINGH, A. 2011. *Herbalism, phytochemistry and ethnopharmacology*, CRC Press.

SJOHOLM, A. & NYSTROM, T. 2006. Inflammation and the etiology of type 2 diabetes. *Diabetes/Metabolism Research and Reviews*, 22**,** 4-10.

SONG, S.-H., KI, S., PARK, D.-H., MOON, H.-S., LEE, C.-D., YOON, I.-S. & CHO, S.-S. 2017. Quantitative analysis, extraction optimization, and

biological evaluation of Cudrania tricuspidata leaf and fruit extracts. *Molecules,* 22**,** 1489-1493.
SRINIVASAN, K. & RAMARAO, P. 2007. Animal models in type 2 diabetes research: an overview. *Indian Journal of Medical Research,* 125**,** 451-472.
SRIVASTAVA, S., SHREE, P., PANDEY, H. & TRIPATHI, Y. B. 2018. Incretin hormones receptor signaling plays the key role in anti-diabetic potential of PTY-2 against STZ-induced pancreatitis. *Biomedicine & pharmacotherapy = Biomedecine & pharmacotherapie,* 97**,** 330-338.
SROKA, Z. & CISOWSKI, W. 2003. Hydrogen peroxide scavenging, antioxidant and anti-radical activity of some phenolic acids. *Food and Chemical Toxicology,* 41**,** 753-758.
STAHL, E. & MANGOLD, H. 1975. Techniques of thin layer chromatography. *Chromatography-A laboratory handbook of chromatographic and electrophoretic methods. Springer-Verlag***,** 164-188.
STEEN, E., TERRY, B. M., J RIVERA, E., CANNON, J. L., NEELY, T. R., TAVARES, R., XU, X. J., WANDS, J. R. & DE LA MONTE, S. M. 2005. Impaired insulin and insulin-like growth factor expression and signaling mechanisms in Alzheimer's disease–is this type 3 diabetes? *Journal of Alzheimer's disease,* 7**,** 63-80.
SUMAN, R. K., MOHANTY, I. R., MAHESHWARI, U., BORDE, M. K. & DESHMUKH, Y. 2016. Natural dipeptidyl peptidase-IV inhibitor mangiferin mitigates diabetes-and metabolic syndrome-induced changes in experimental rats. *Diabetes, metabolic syndrome and obesity: targets and therapy,* 9**,** 261.
SUN, J., QU, C., WANG, Y., HUANG, H., ZHANG, M., LI, H., ZHANG, Y., WANG, Y. & ZOU, W. 2016. PTP1B, a potential target of type 2 diabetes mellitus. *Molecular Biology,* 5**,** 174-180.
SUNITHA, S., NAGARAJ, M. & VARALAKSHMI, P. 2001. Hepatoprotective effect of lupeol and lupeol linoleate on tissue antioxidant defence system in cadmium-induced hepatotoxicity in rats. *Fitoterapia,* 72**,** 516-523.
SYLVIE, D. D., ANATOLE, P. C., CABRAL, B. P. & VERONIQUE, P. B. 2014. Comparison of in vitro antioxidant properties of extracts from three plants used for medical purpose in Cameroon: Acalypha racemosa, Garcinia lucida and Hymenocardia lyrata. *Asian Pacific Journal of Tropical Biomedicine,* 4**,** S625-S632.
SÁINZ, N., BARRENETXE, J., MORENO-ALIAGA, M. J. & MARTÍNEZ, J. A. 2015. Leptin resistance and diet-induced obesity: central and peripheral actions of leptin. *Metabolism,* 64**,** 35-46.
SÁNCHEZ-BURGOS, J. A., RAMÍREZ-MARES, M. V., GALLEGOS-INFANTE, J. A., GONZÁLEZ-LAREDO, R. F., MORENO-JIMÉNEZ, M. R., CHÁIREZ-RAMÍREZ, M. H., MEDINA-TORRES, L. & ROCHA-GUZMÁN, N. E. 2015. Isolation of lupeol from white oak leaves and its anti-inflammatory activity. *Industrial Crops & Products,* 77**,** 827-832.
TATE, M., ROBINSON, E., GREEN, B. D., MCDERMOTT, B. J. & GRIEVE, D. J. 2016. Exendin-4 attenuates adverse cardiac remodelling in streptozocin-induced diabetes via specific actions on infiltrating macrophages. *Basic Research in Cardiology,* 111**,** 1-13.
TEMPEL, D. L., SHOR-POSNER, G., DWYER, D. & LEIBOWITZ, S. F. 1989. Nocturnal patterns of macronutrient intake in freely feeding and food-

deprived rats. *American Journal of Physiology-Regulatory, Integrative and Comparative Physiology,* 256**,** R541-R548.
TERRÓN, M., DELGADO-ADÁMEZ, J., PARIENTE, J., BARRIGA, C., PAREDES, S. & RODRÍGUEZ, A. 2013. Melatonin reduces body weight gain and increases nocturnal activity in male Wistar rats. *Physiology & behavior,* 118**,** 8-13.
TEWTRAKUL, S., SUBHADHIRASAKUL, S., TANSAKUL, P., CHEENPRACHA, S. & KARALAI, C. 2011. Antiinflammatory Constituents from Eclipta prostrata using RAW264.7 Macrophage Cells. *Phytotherapy Research,* 25**,** 1313-1316.
TILG, H. & WOLF, A. M. 2005. Adiponectin: a key fat-derived molecule regulating inflammation. *Expert opinion on therapeutic targets,* 9**,** 245-251.
TIONG, S., LOOI, C., HAZNI, H., ARYA, A., PAYDAR, M., WONG, W., CHEAH, S.-C., MUSTAFA, M. & AWANG, K. 2013. Anti-diabetic and Antioxidant Properties of Alkaloids from Catharanthus roseus (L.) G. Don. *Molecules,* 18**,** 9770-9784.
TOGASHI, N., URA, N., HIGASHIURA, K., MURAKAMI, H. & SHIMAMOTO, K. 2002. Effect of TNF-alpha--converting enzyme inhibitor on insulin resistance in fructose-fed rats. *Hypertension,* 39**,** 578-580.
TSALAMANDRIS, S., ANTONOPOULOS, A. S., OIKONOMOU, E., PAPAMIKROULIS, G.-A., VOGIATZI, G., PAPAIOANNOU, S., DEFTEREOS, S. & TOUSOULIS, D. 2019. The Role of Inflammation in Diabetes: Current Concepts and Future Perspectives. *European Cardiology Review,* 14**,** 50-59.
TSIOTRA, P. C., TSIGOS, C. & RAPTIS, S. A. 2001. TNFalpha and leptin inhibit basal and glucose-stimulated insulin secretion and gene transcription in the HIT-T15 pancreatic cells. *International Journal of obesity,* 25**,** 1018-1026.
TSOU, R. C., RAK, K. S., ZIMMER, D. J. & BENCE, K. K. 2014. Improved metabolic phenotype of hypothalamic PTP1B-deficiency is dependent upon the leptin receptor. *Molecular metabolism,* 3**,** 301-312.
UEHLING, D. E. & HARRIS, P. A. 2015. Recent progress on MAP kinase pathway inhibitors. *Bioorganic & Medicinal Chemistry Letters,* 25**,** 4047-4056.
VAN DE LAAR, F. A., LUCASSEN, P. L., AKKERMANS, R. P., VAN DE LISDONK, E. H., RUTTEN, G. E. & VAN WEEL, C. 2005. α-Glucosidase inhibitors for patients with type 2 diabetes: results from a Cochrane systematic review and meta-analysis. *Diabetes care,* 28**,** 154-163.
VELAZQUEZ, A. & APOVIAN, C. M. 2018. Updates on obesity pharmacotherapy.
VENIERATOS, P., DROSSOPOULOU, G., KAPODISTRIA, K., TSILIBARY, E. & KITSIOU, P. 2010. High glucose induces suppression of insulin signalling and apoptosis via upregulation of endogenous IL- 1b and suppressor of cytokine signalling-1 in mouse pancreatic beta cells. *Cellular Signalling,* 22**,** 791-800.
VIJAYLAKSHMI, P. & RADHA, R. 2015. An overview: Citrus maxima. *The Journal of Phytopharmacology,* 4**,** 263-267.
VINAYAGAM, R., JAYACHANDRAN, M. & XU, B. 2016. Anti-diabetic effects of simple phenolic acids: a comprehensive review. *Phytotherapy research,* 30**,** 184-199.

VINAYAGAM, R., XIAO, J. & XU, B. 2017. An insight into anti- diabetic properties of dietary phytochemicals.(Report). *Phytochemistry Reviews,* 16**,** 535-553.

VOSTERS, O., BEUNEU, C., NAGY, N., MOVAHEDI, B., AKSOY, E., SALMON, I., PIPELEERS, D., GOLDMAN, M. & VERHASSELT, V. 2004. CD40 expression on human pancreatic duct cells: role in nuclear factor- kappa B activation and production of pro-inflammatory cytokines. *Diabetologia,* 47**,** 660-668.

WAGNER, K.-H. & ELMADFA, I. 2003. Biological relevance of terpenoids. *Annals of Nutrition and metabolism,* 47**,** 95-106.

WANG, C., GUAN, Y. & YANG, J. 2010. Cytokines in the progression of pancreatic β-cell dysfunction. *International journal of endocrinology,* 2010, 1-10.

WANG, C.-J., WANG, J.-M., LIN, W.-L., CHU, C.-Y., CHOU, F.-P. & TSENG, T.-H. 2000. Protective effect of Hibiscus anthocyanins against tert-butyl hydroperoxide-induced hepatic toxicity in rats. *Food and chemical toxicology,* 38**,** 411-416.

WANG, J. & MAZZA, G. 2002. Inhibitory effects of anthocyanins and other phenolic compounds on nitric oxide production in LPS/IFN-γ-activated RAW 264.7 macrophages. *Journal of Agricultural and Food Chemistry,* 50**,** 850-857.

WANG, L., LEE, W., CUI, Y. R., AHN, G. & JEON, Y.-J. 2019. Protective effect of green tea catechin against urban fine dust particle-induced skin aging by regulation of NF-κB, AP-1, and MAPKs signaling pathways. *Environmental Pollution,* 552, 1318-1324

WANG, T., HE, C. 2018a. Pro-inflammatory cytokines: the link between obesity and osteoarthritis. *Cytokine & Growth Factor Reviews,* 44, 38-50.

WANG, X., HUANG, W., LEI, L., LIU, Y., MA, K. Y., LI, Y. M., WANG, L., HUANG, Y. & CHEN, Z.-Y. 2015. Blockage of hydroxyl group partially abolishes the cholesterol-lowering activity of β-sitosterol. *Journal of functional foods,* 12**,** 199-207.

WANG, Y., HONG, D., QIAN, Y., TU, X., WANG, K., YANG, X., SHAO, S., KONG, X., LOU, Z. & JIN, L. 2018b. Lupeol inhibits growth and migration in two human colorectal cancer cell lines by suppression of wnt–β-catenin pathway. *OncoTargets and Therapy,* 11**,** 7987-7999.

WAUMANS, Y., BAERTS, L., KEHOE, K., LAMBEIR, A.-M. & DE MEESTER, I. 2015. The dipeptidyl peptidase family, prolyl oligopeptidase and prolyl carboxypeptidase in the immune system and inflammatory disease, including atherosclerosis. *Frontiers in immunology,* 6**,** 387-405.

WEINSTOCK, R. S., XING, D., MAAHS, D. M., MICHELS, A., RICKELS, M. R., PETERS, A. L., BERGENSTAL, R. M., HARRIS, B., DUBOSE, S. N. & MILLER, K. M. 2013. Severe hypoglycemia and diabetic ketoacidosis in adults with type 1 diabetes: results from the T1D Exchange clinic registry. *The Journal of Clinical Endocrinology & Metabolism,* 98**,** 3411-3419.

WENG, J., SOEGONDO, S., SCHNELL, O., SHEU, W. H. H., GRZESZCZAK, W., WATADA, H., YAMAMOTO, N. & KALRA, S. 2015. Efficacy of acarbose in different geographical regions of the world: analysis of a real- life database. *Diabetes/metabolism research and reviews,* 31**,** 155-167.

WHO. 2018. Obesity and overweight. [ONLINE] Available at: https://www.who.int/news-room/fact-sheets/detail/obesity-and-overweight. [Accessed 18 January 2019].

WHO. 2019. *BMI classification* [Online]. Available: http://apps.who.int/bmi/index.jsp?introPage=intro_3.html [Accessed 22/03/2019].

WIJESEKARA, N., KRISHNAMURTHY, M., BHATTACHARJEE, A., SUHAIL, A., SWEENEY, G. & WHEELER, M. B. 2010. Adiponectin-induced ERK and Akt phosphorylation protects against pancreatic beta cell apoptosis and increases insulin gene expression and secretion. *Journal of Biological Chemistry,* 285**,** 33623-33631.

WINTERBOURN, C. C. 2019. Regulation of intracellular glutathione. *Redox biology,* 22, 1-2.

WOJTALA, A., BONORA, M., MALINSKA, D., PINTON, P., DUSZYNSKI, J. & WIECKOWSKI, M. R. 2014. Methods to monitor ROS production by fluorescence microscopy and fluorometry. *Methods in enzymology,* 542, 243-262. Academic Press.

WOLDEMICHAEL, G. M., SINGH, M. P., MAIESE, W. M. & TIMMERMANN, B. N. 2003. Constituents of antibacterial extract of Caesalpinia paraguariensis Burk. *Zeitschrift für Naturforschung C,* 58**,** 70-75.

WOODS, N. 2017. *GOING BACKWARDS TO GO FORWARDS: THE POTENTIAL USE OF MEDIAEVAL TUBERS AS FUTURE MEDICINE*. PhD, University of Strathclyde.

XIE, R., ZHANG, H., WANG, X. Z., YANG, X. Z., WU, S. N., WANG, H. G., SHEN, P. & MA, T. H. 2017. The protective effect of betulinic acid (BA) diabetic nephropathy on streptozotocin (STZ)-induced diabetic rats. *Food & function,* 8**,** 299-306.

XU, H. X., ZENG, F. Q., WAN, M. & SIM, K. Y. 1996. Anti-HIV triterpene acids from Geum japonicum. *Journal of Natural Products,* 59**,** 643-645.

YAMASHITA, K., LU, H., LU, J., CHEN, G., YOKOYAMA, T., SAGARA, Y., MANABE, M. & KODAMA, H. 2002. Effect of three triterpenoids, lupeol, betulin, and betulinic acid on the stimulus-induced superoxide generation and tyrosyl phosphorylation of proteins in human neutrophils. *Clinica Chimica Acta,* 325**,** 91-96.

YAMAUCHI, T., KAMON, J., WAKI, H., IMAI, Y., SHIMOZAWA, N., HIOKI, K., UCHIDA, S., ITO, Y., TAKAKUWA, K., MATSUI, J., TAKATA, M., ETO, K., TERAUCHI, Y., KOMEDA, K., TSUNODA, M., MURAKAMI, K., OHNISHI, Y., NAITOH, T., YAMAMURA, K., UEYAMA, Y., FROGUEL, P., KIMURA, S., NAGAI, R. & KADOWAKI, T. 2003. Globular adiponectin protected ob/ ob mice from diabetes and ApoE-deficient mice from atherosclerosis. *The Journal of biological chemistry,* 278**,** 2461-2468.

YANG, H., LEE, S. H., JI, H., KIM, J. E., YOO, R., KIM, J. H., SUK, S., HUH, C. S., PARK, J. H. Y., HEO, Y. S., SHIN, H. S., KIM, B. G. & LEE, K. W. 2019a. Orobol, an Enzyme- Convertible Product of Genistein, exerts Anti-Obesity Effects by Targeting Casein Kinase 1 Epsilon. *Scientific Reports,* 9**,** 8942-8953.

YANG, S., ZHONG, Y., LUO, H., DING, X. & ZUO, C. 1999. Studies on chemical constituents of the roots of Gypsophila oldhamiana Miq. *China journal of Chinese materia medica,* 24**,** 680-703.

YANG, Y., TIAN, Y., ZHANG, Q., LI, X., FU, Y., PEI, H. & LUI, D. 2019b. Comparative Effects of Flavonoids from Fructus Sophorae on Rat Osteoblasts in vitro. *Records of Natural Products,* 14, 65-76.

YILMAZER-MUSA, M., GRIFFITH, A. M., MICHELS, A. J., SCHNEIDER, E. & FREI, B. 2012. Inhibition of α-amylase and α-glucosidase activity by tea and grape seed extracts and their constituent catechins. *Journal of agricultural and food chemistry,* 60**,** 8924-8929.

YKI-JÄRVINEN, H. 2010. Liver fat in the pathogenesis of insulin resistance and type 2 diabetes. *Digestive diseases,* 28**,** 203-209.

YOGEESWARI, P. & SRIRAM, D. 2005. Betulinic acid and its derivatives: a review on their biological properties. *Current medicinal chemistry,* 12**,** 657-666.

YONEMOTO, R., SHIMADA, M., GUNAWAN-PUTERI, M. D., KATO, E. & KAWABATA, J. 2014. α-Amylase inhibitory triterpene from Abrus precatorius leaves. *Journal of agricultural and food chemistry,* 62**,** 8411-8414.

YOON, J. J., LEE, Y. J., KIM, J. S., KANG, D. G. & LEE, H. S. 2010. Protective role of betulinic acid on TNF-α-induced cell adhesion molecules in vascular endothelial cells. *Biochemical and Biophysical Research Communications,* 391**,** 96-101.

YOU, Y. J., NAM, N. H., KIM, Y., BAE, K. H. & AHN, B. Z. 2003. Antiangiogenic activity of lupeol from Bombax ceiba. *J Phytotherapy Research: An International Journal Devoted to Pharmacological Toxicological Evaluation of Natural Product Derivatives,* 17**,** 341-344.

ZABOLOTNY, J. M., KIM, Y.-B., WELSH, L. A., KERSHAW, E. E., NEEL, B. G. & KAHN, B. B. 2008. Protein-tyrosine phosphatase 1B expression is induced by inflammation in vivo. *Journal of Biological Chemistry,* 283**,** 14230-14241.

ZHANG, B., DENG, Z., RAMDATH, D. D., TANG, Y., CHEN, P. X., LIU, R., LIU, Q. & TSAO, R. 2015. Phenolic profiles of 20 Canadian lentil cultivars and their contribution to antioxidant activity and inhibitory effects on α-glucosidase and pancreatic lipase. *Food Chemistry,* 172**,** 862-872.

ZHANG, H., MATSUDA, H., YAMASHITA, C., NAKAMURA, S. & YOSHIKAWA, M. 2009. Hydrangeic acid from the processed leaves of Hydrangea macrophylla var. thunbergii as a new type of anti-diabetic compound. *European journal of pharmacology,* 606**,** 255-261.

ZHANG, J., CHEN, Q., ZHONG, J., LIU, C., ZHENG, B. & GONG, Q. 2019. DPP-4 Inhibitors as Potential Candidates for Anti-hypersensitive Therapy: Improving Vascular Inflammation and Assisting the Action of Traditional Antihypertensive Drugs. *Frontiers in immunology,* 10**,** 1050-1062.

ZHANG, W., HONG, D., ZHOU, Y., ZHANG, Y., SHEN, Q., LI, J.-Y., HU, L.-H. & LI, J. 2006. Ursolic acid and its derivative inhibit protein tyrosine phosphatase 1B, enhancing insulin receptor phosphorylation and stimulating glucose uptake. *Biochimica et Biophysica Acta (BBA)-General Subjects,* 1760**,** 1505-1512.

ZHANG, Y.-N., ZHANG, W., HONG, D., SHI, L., SHEN, Q., LI, J.-Y., LI, J. & HU, L.-H. 2008. Oleanolic acid and its derivatives: new inhibitor of protein tyrosine phosphatase 1B with cellular activities. *Bioorganic & medicinal chemistry,* 16**,** 8697-8705.

ZHANG, Z.-Y. & LEE, S.-Y. 2003. PTP1B inhibitors as potential therapeutics in the treatment of type 2 diabetes and obesity. *Expert opinion on investigational drugs,* 12**,** 223-233.

ZHAO, A. Z., BORNFELDT, K. E. & BEAVO, J. A. 1998. Leptin inhibits insulin secretion by activation of phosphodiesterase 3B. *Journal of Clinical Investigation,* 102**,** 869-873.

ZITKA, O., SKALICKOVA, S., GUMULEC, J., MASARIK, M., ADAM, V., HUBALEK, J., TRNKOVA, L., KRUSEOVA, J., ECKSCHLAGER, T. & KIZEK, R. 2012. Redox status expressed as GSH: GSSG ratio as a marker for oxidative stress in paediatric tumour patients. *Oncology letters,* 4**,** 1247-1253.

ZWENGER, S. & BASU, C. 2008. Plant terpenoids: applications and future potentials. *Biotechnology and Molecular Biology Reviews,* 3**,** 1-7.

Appendix 1, Anti-diabetic assays

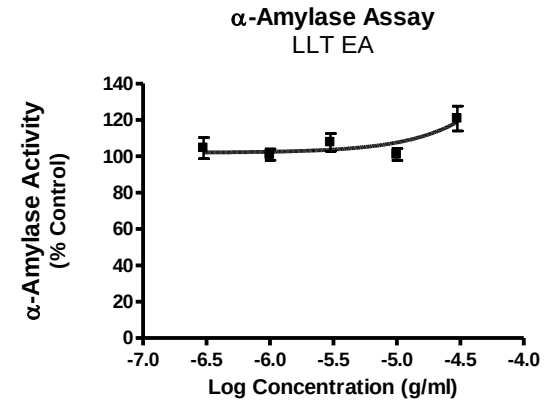

IC_{50} > 30μg/ml
n=3

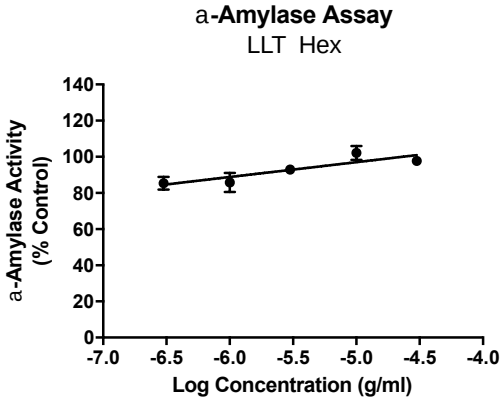

IC_{50} > 30mg/ml
n= 3

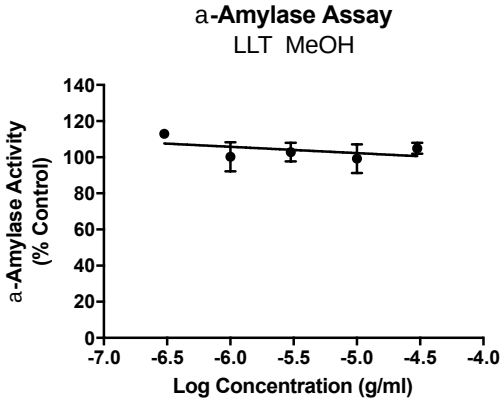

IC_{50} > 30mg/ml
n= 3

Figure A1. 1: The inhibitory effects of various concentrations of extracts of LLT on α-amylase activity. Data was analysed using One-Way ANOVA with a Dunnet Post-Test.

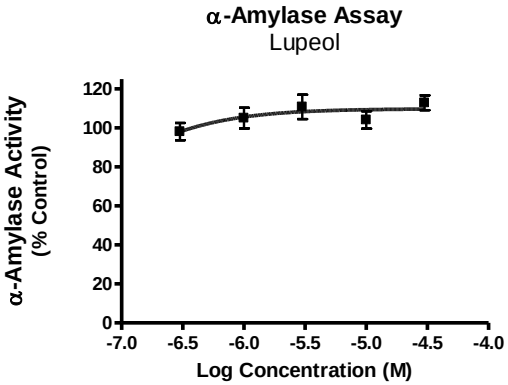

IC_{50} > 30μM
n=3

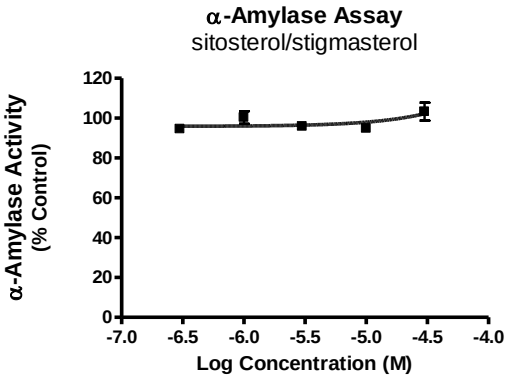

IC_{50} > 30μM
n=3

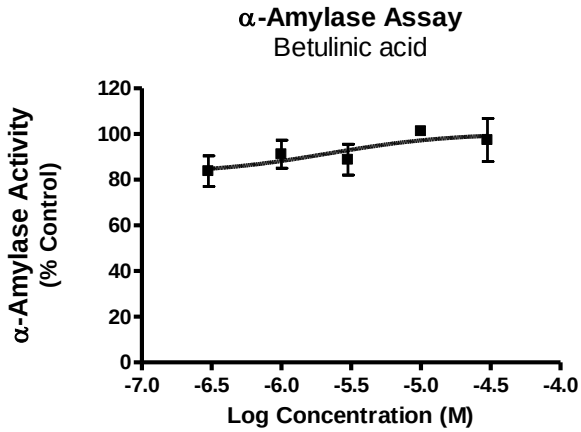

IC_{50} > 30μM
n=3

Figure A1. 2: The inhibitory effects of various concentrations of isolated compounds from LLT EA extract on α-amylase activity. Data was analysed using One-Way ANOVA with a Dunnet Post-Test.

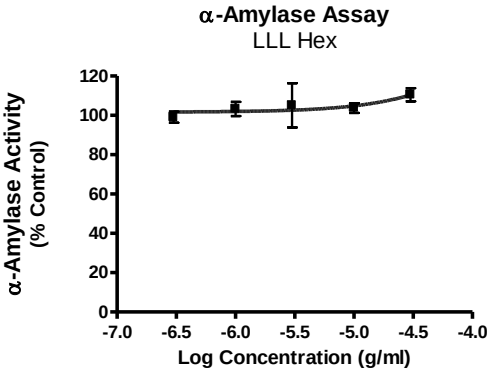

IC_{50} > 30μg/ml
n=3

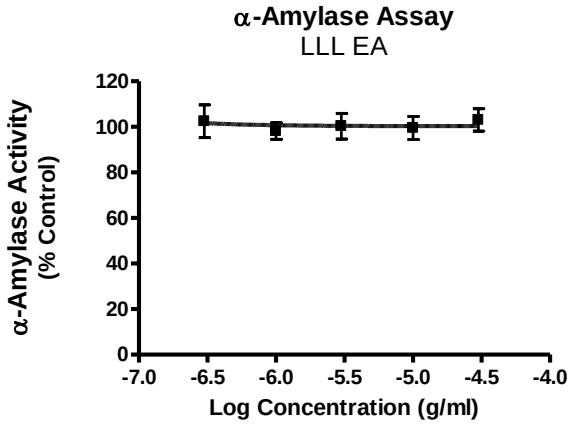

IC_{50} > 30μg/ml
n=3

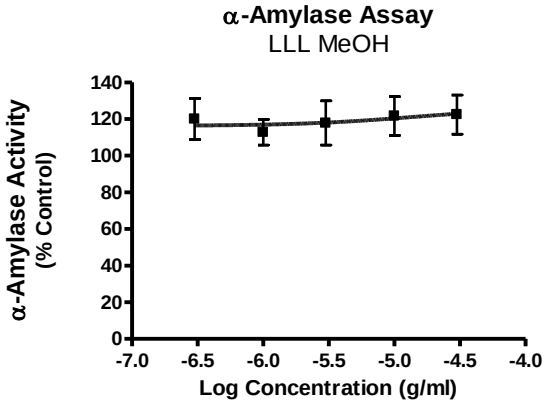

IC_{50} > 30μg/ml
n=3

Figure A1. 3: The inhibitory effects of various concentrations of extracts of LLL on α-amylase activity. Data was analysed using One-Way ANOVA with a Dunnet Post-Test. See previous

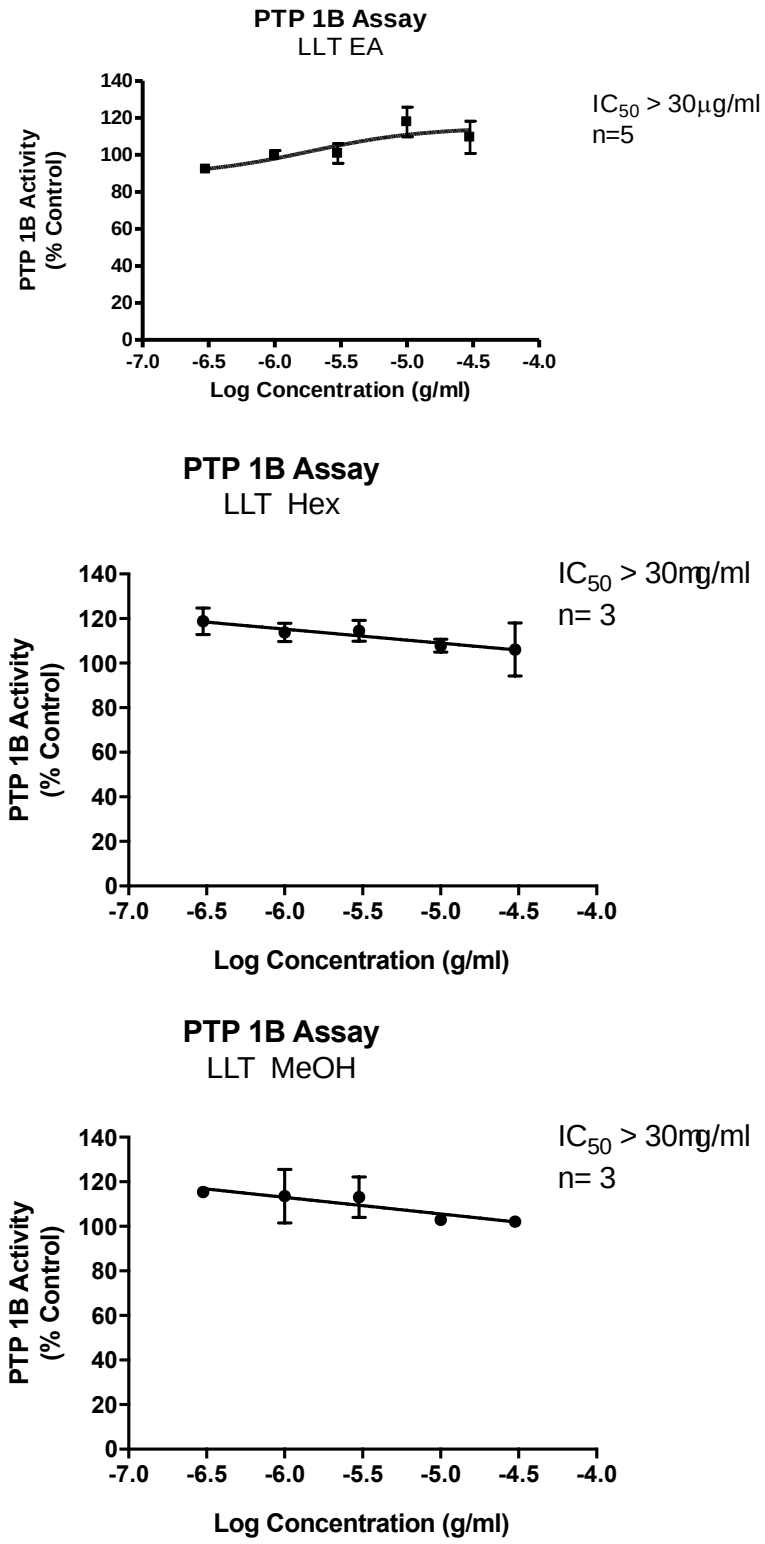

Figure A1. 4: The inhibitory effects of various concentrations of extracts of LLT on PTP 1B activity. Data was analysed using One-Way ANOVA with a Dunnet Post-Test.

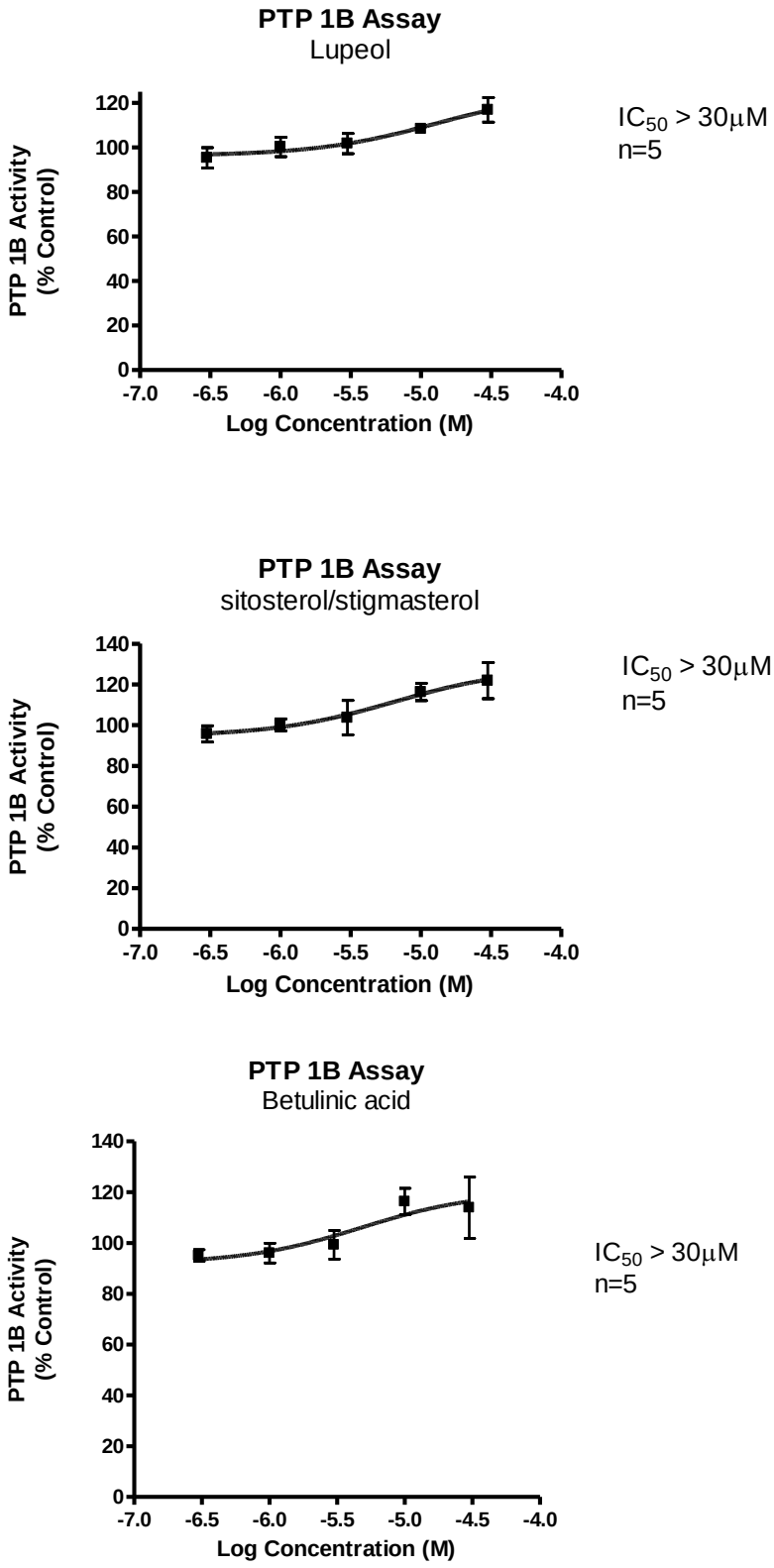

Figure A1. 5: The inhibitory effects of various concentrations of isolated compounds from LLT EA extract on PTP 1B activity. Data was analysed using One-Way ANOVA with a Dunnet Post-Test.

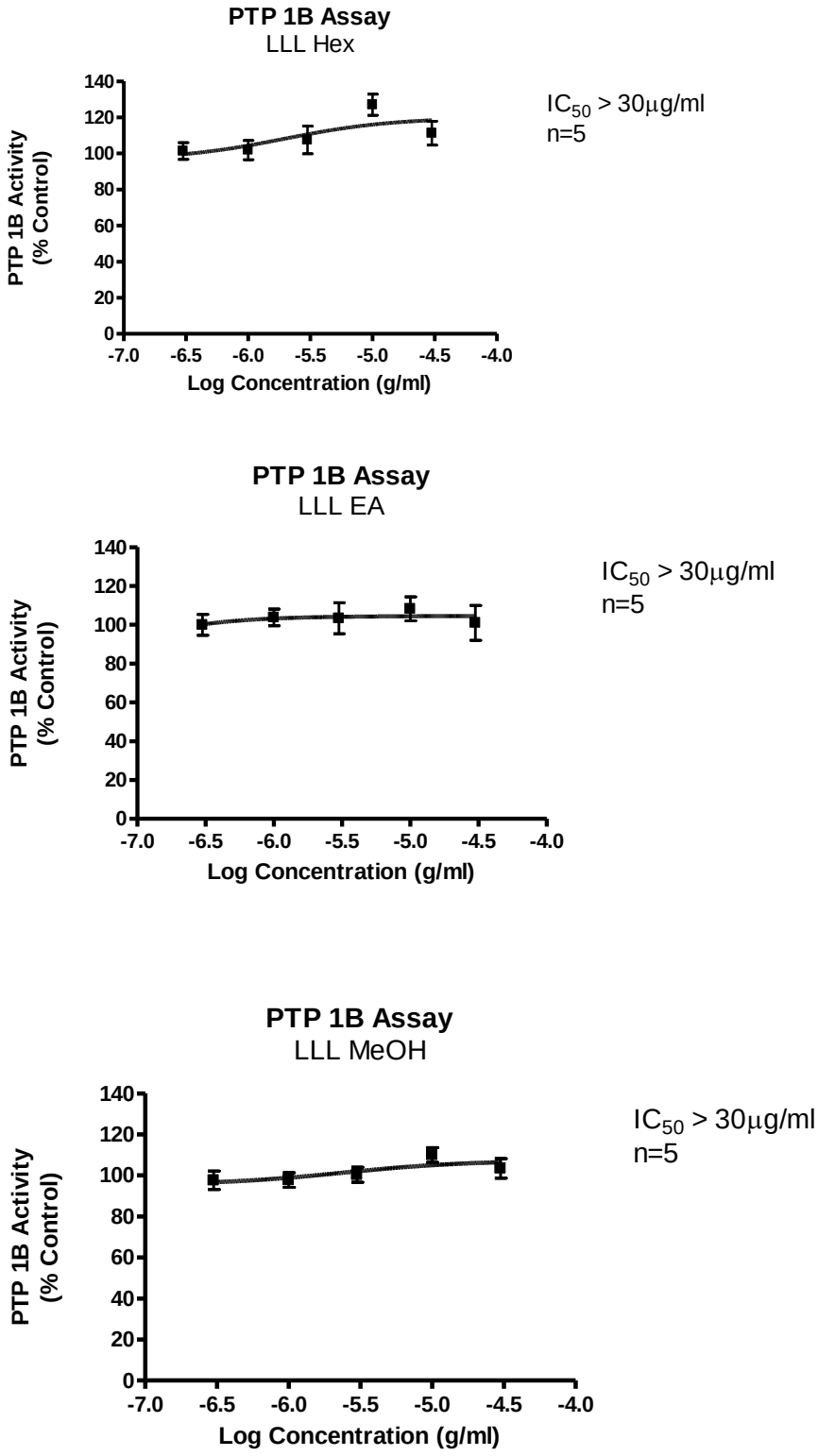

Figure A1. 6: The inhibitory effects of various concentrations of extracts of LLL on PTP 1B activity. Data was analysed using One-Way ANOVA with a Dunnet Post-Test.

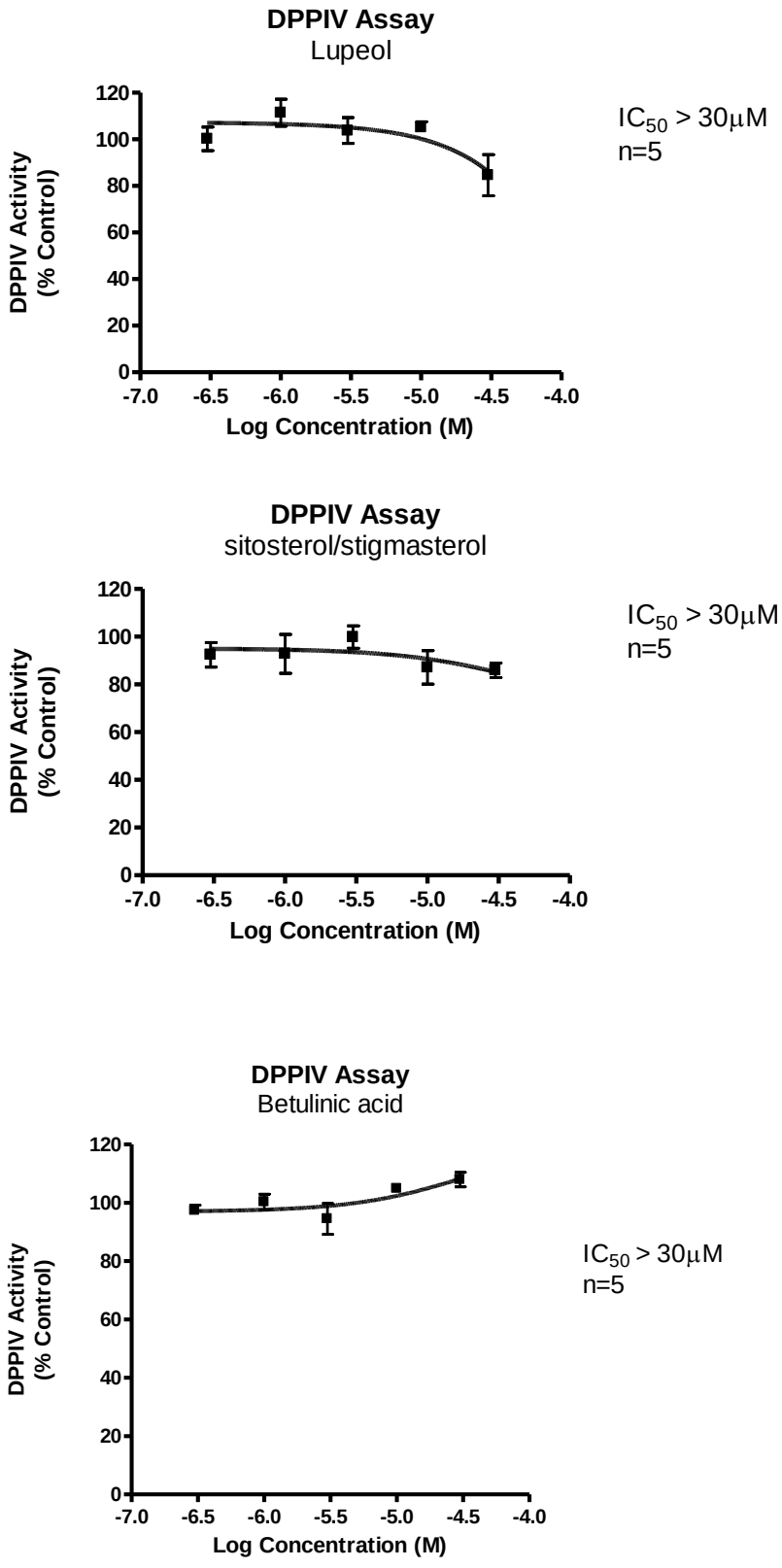

Figure A1. 7: The inhibitory effects of various concentrations of isolated compounds from LLT EA extract on DPPIV activity. Data was analysed using One-Way ANOVA with a Dunnet Post-Test.

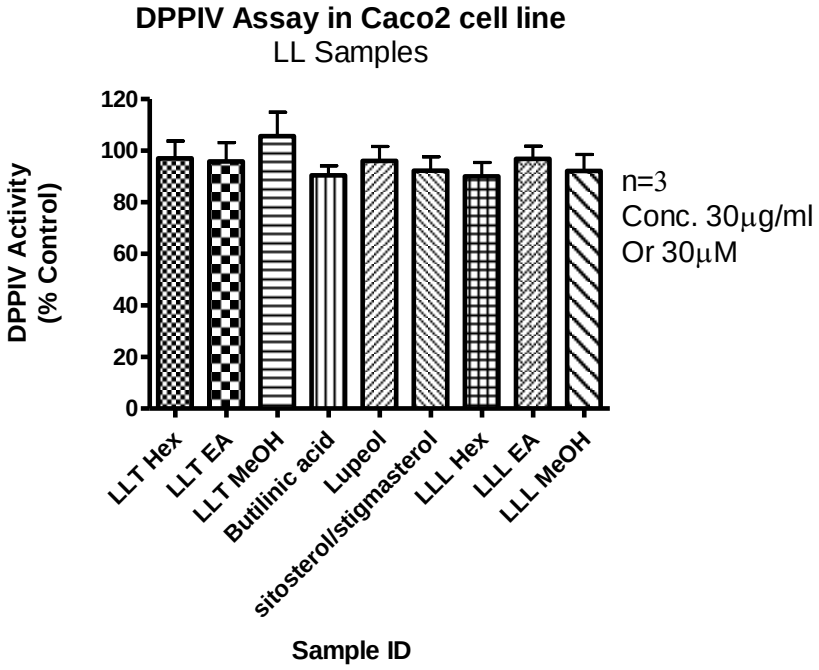

Figure A1. 8: The inhibitory effect of LLT and LLL extracts and isolated compounds on DPPIV released by Caco2 cell line. Data represents mean ± SEM, n=3.

Appendix 2, Anti-oxidant activity

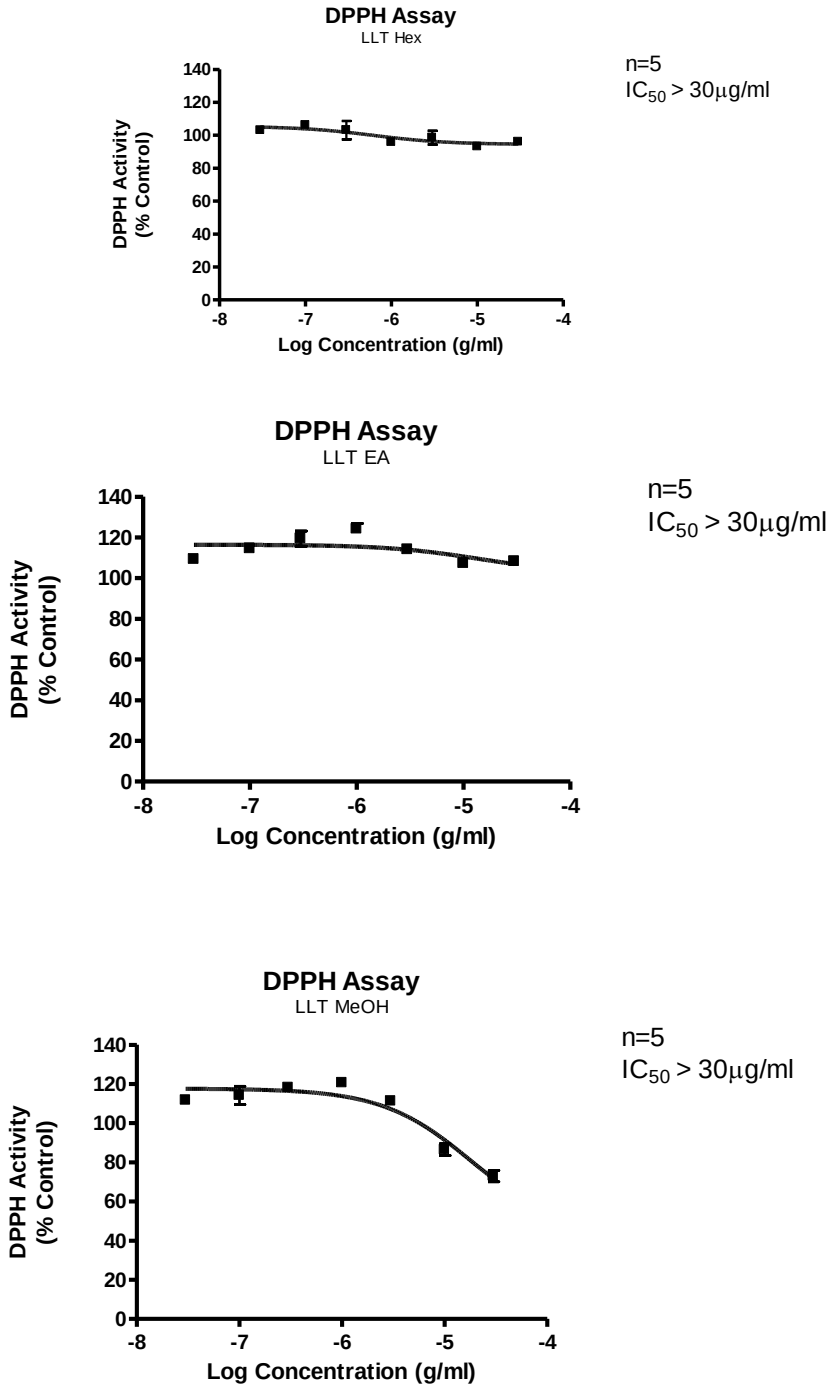

Figure A2. 1: The percentage inhibition of DPPH by extracts of LLT. Data represents mean ± SEM n=5.

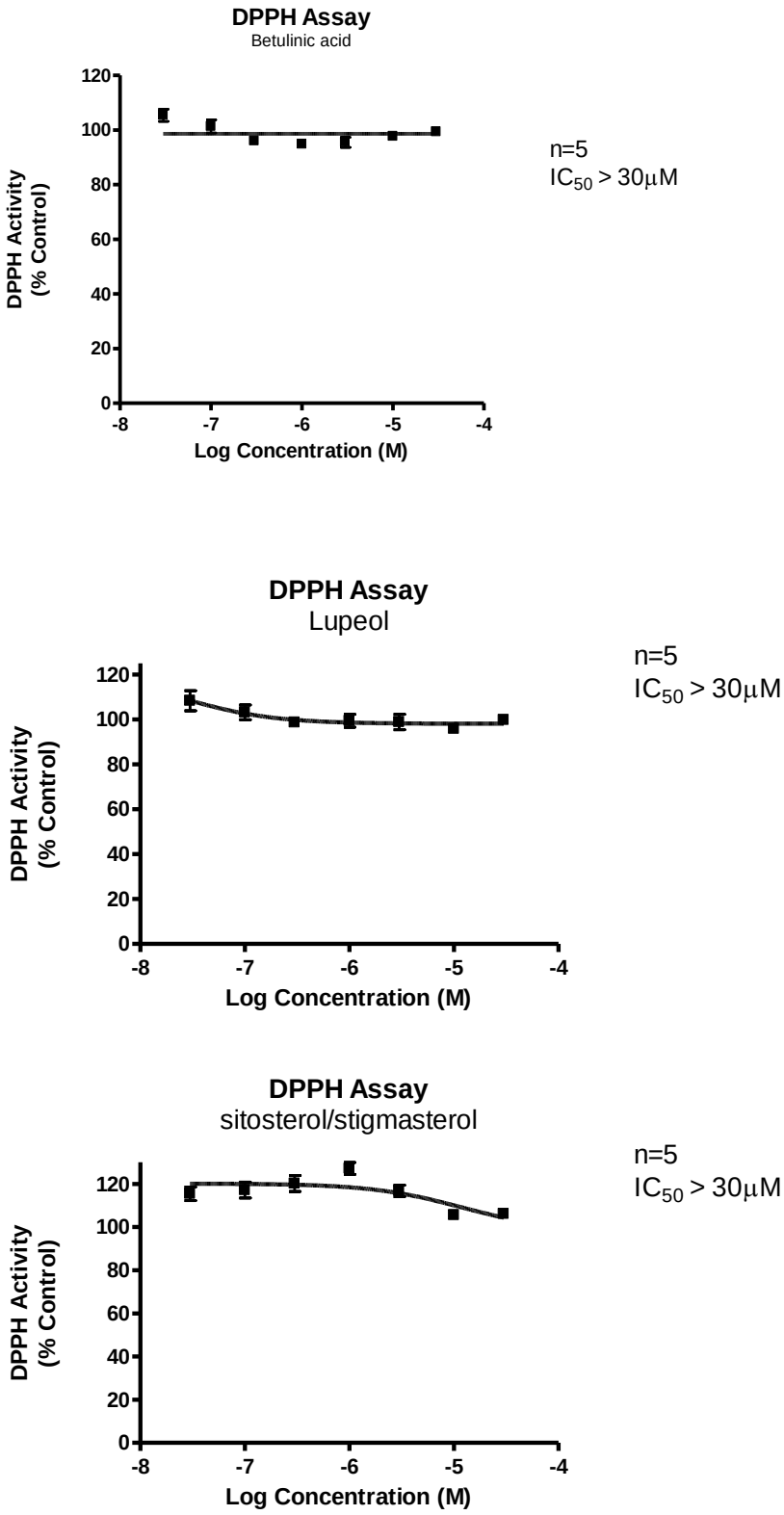

Figure A2. 2: The percentage inhibition of DPPH by isolated compounds from LLT EA extract. Data represents mean ± SEM, n=3.

Appendix 3, Nanodrop curves

A3.1. Nanodrop curves for isolated RNA samples from pancreatic tissues

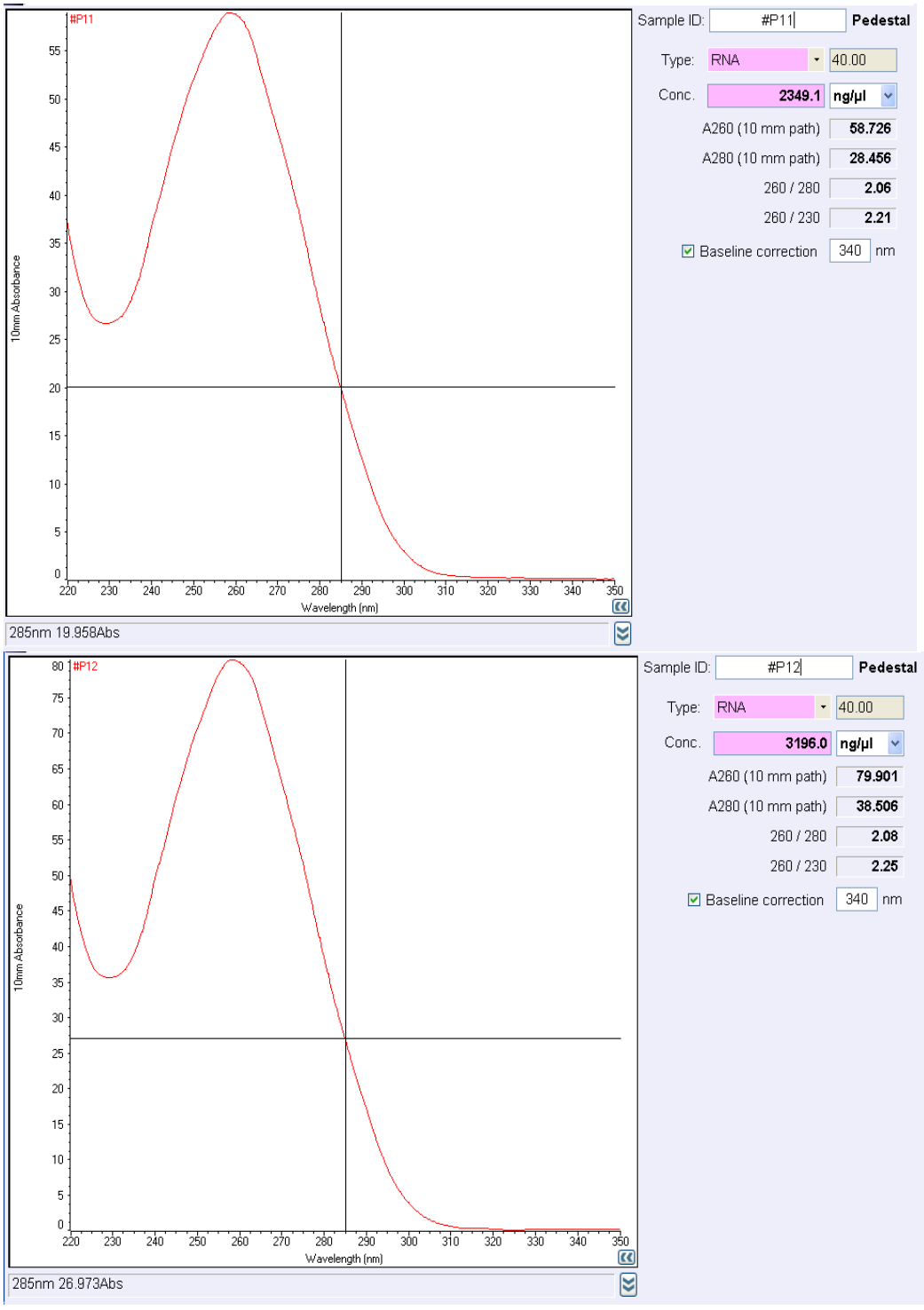

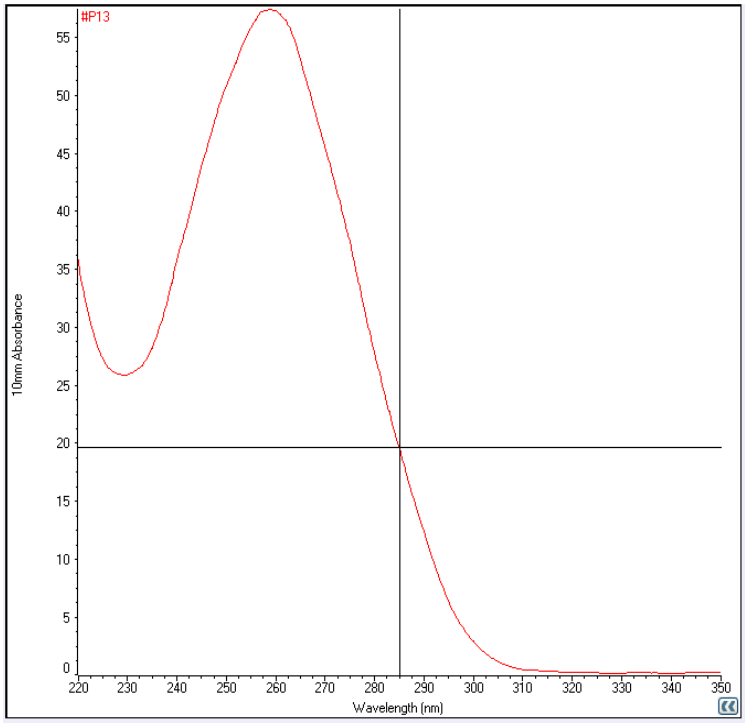

285nm 19.577Abs

Sample ID: #P13 **Pedestal**

Type: RNA 40.00

Conc. **2290.6** ng/µl

A260 (10 mm path) **57.264**

A280 (10 mm path) **27.833**

260 / 280 **2.06**

260 / 230 **2.22**

☑ Baseline correction 340 nm

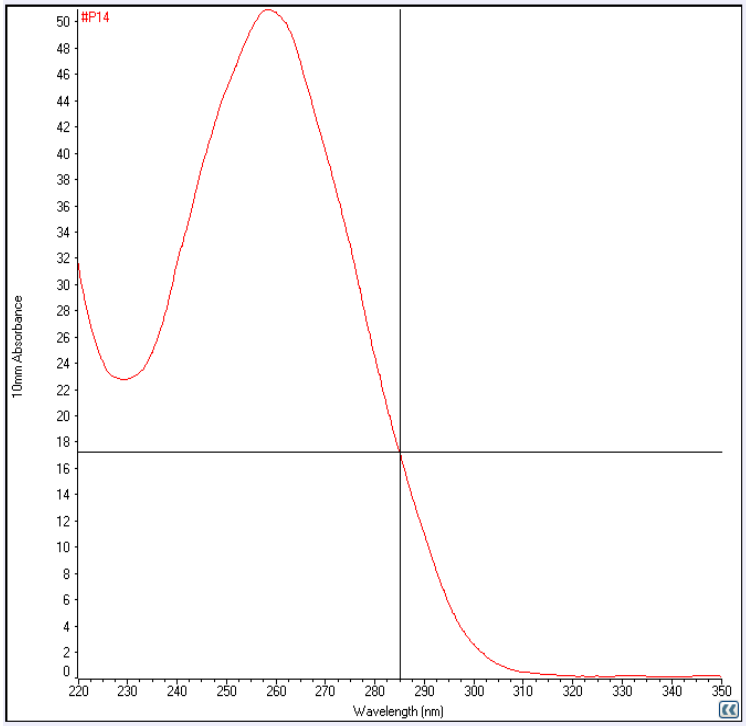

285nm 17.191Abs

Sample ID: #P14 **Pedestal**

Type: RNA 40.00

Conc. **2027.6** ng/µl

A260 (10 mm path) **50.690**

A280 (10 mm path) **24.535**

260 / 280 **2.07**

260 / 230 **2.23**

☑ Baseline correction 340 nm

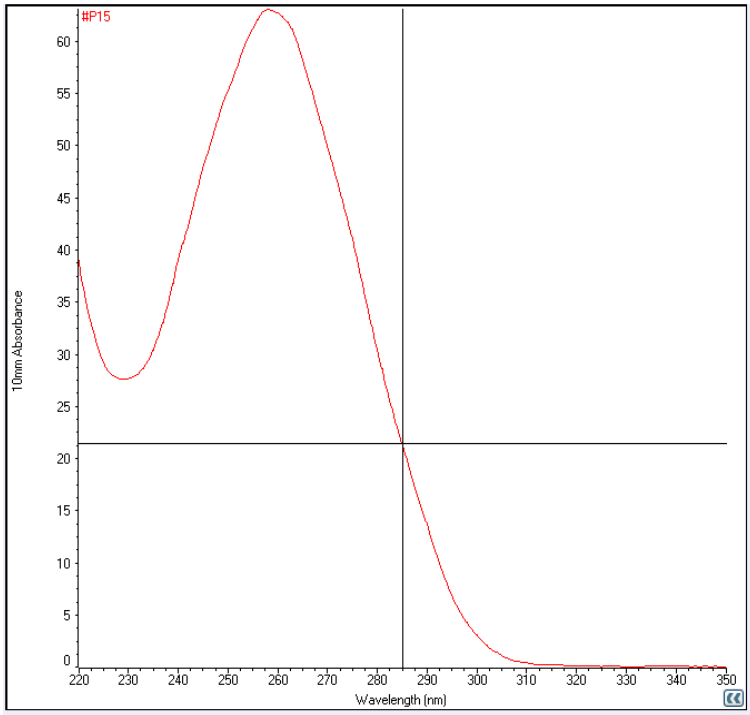

285nm 21.368Abs

Sample ID: #P15 **Pedestal**

Type: RNA 40.00

Conc. **2505.9** **ng/µl**

A260 (10 mm path) **62.648**

A280 (10 mm path) **30.448**

260 / 280 **2.06**

260 / 230 **2.28**

☑ Baseline correction 340 nm

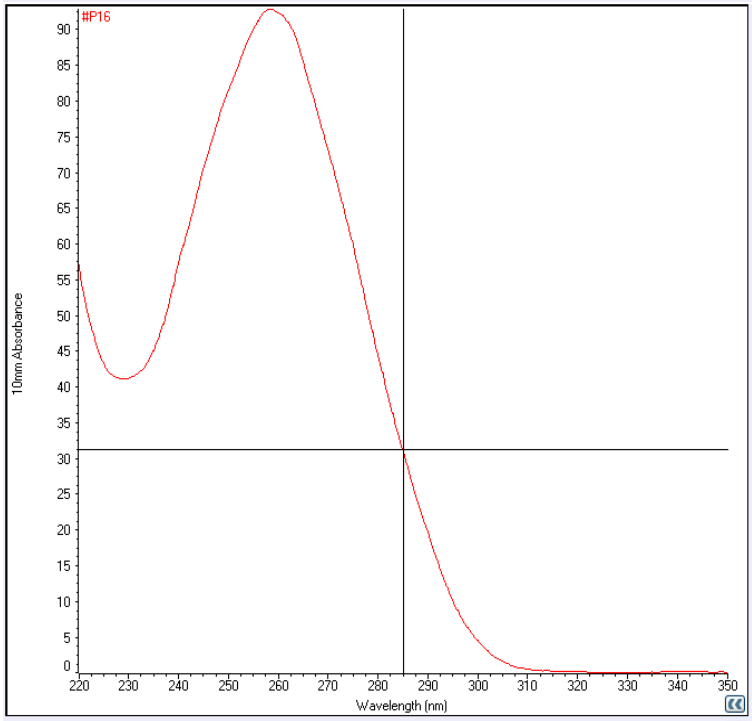

285nm 31.090Abs

Sample ID: #P16 **Pedestal**

Type: RNA 40.00

Conc. **3693.3** **ng/µl**

A260 (10 mm path) **92.333**

A280 (10 mm path) **44.537**

260 / 280 **2.07**

260 / 230 **2.25**

☑ Baseline correction 340 nm

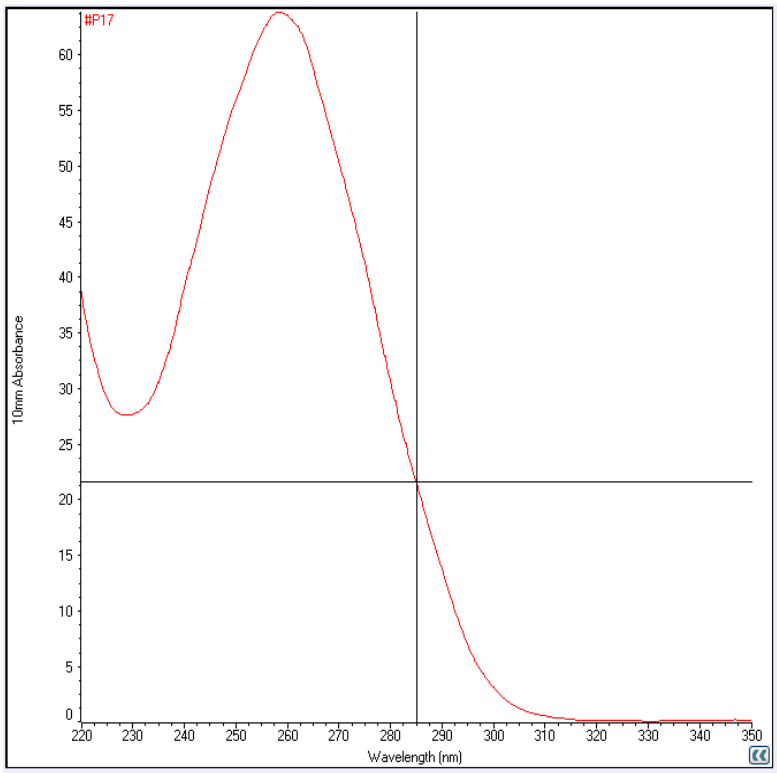

Sample ID: #P17 **Pedestal**

Type:	RNA 40.00
Conc.	**2540.7** ng/µl
A260 (10 mm path)	**63.517**
A280 (10 mm path)	**30.699**
260 / 280	**2.07**
260 / 230	**2.31**

☑ Baseline correction 340 nm

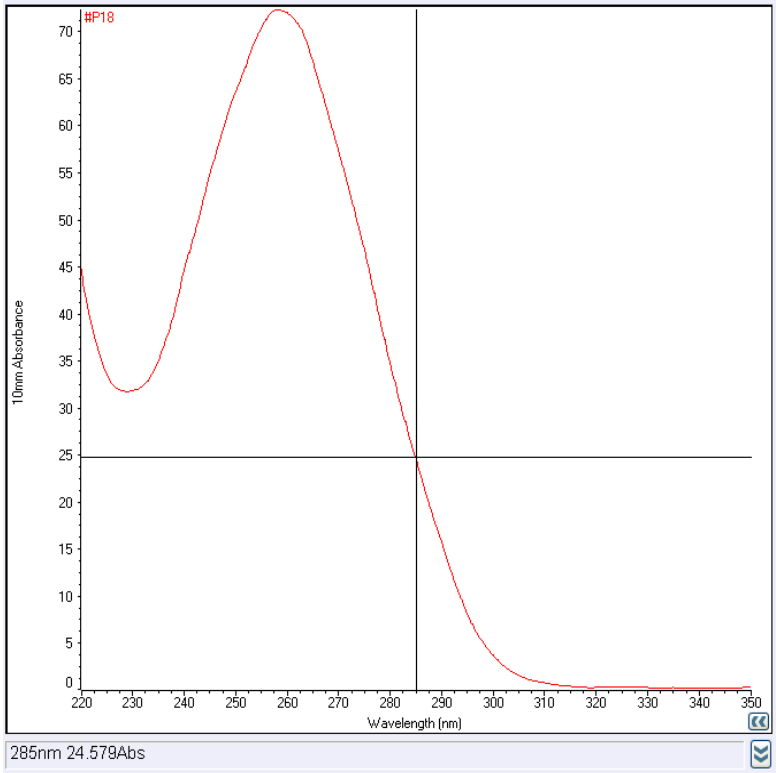

Sample ID: #P18 **Pedestal**

Type:	RNA 40.00
Conc.	**2879.8** ng/µl
A260 (10 mm path)	**71.995**
A280 (10 mm path)	**34.838**
260 / 280	**2.07**
260 / 230	**2.27**

☑ Baseline correction 340 nm

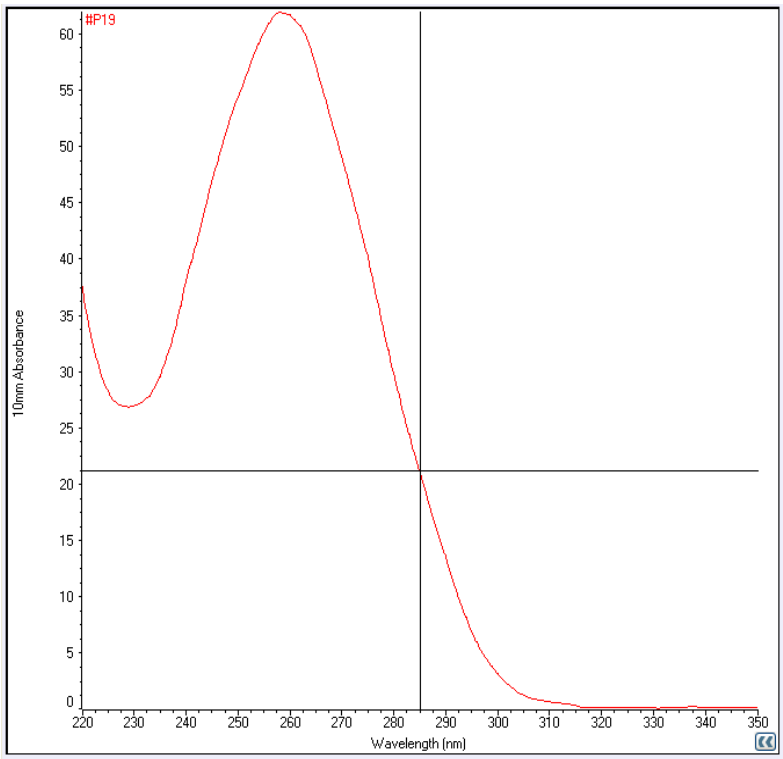

285nm 21.106Abs

Sample ID: #P19 **Pedestal**

Type: RNA 40.00

Conc. **2465.5** ng/µl

A260 (10 mm path) **61.638**

A280 (10 mm path) **29.869**

260 / 280 **2.06**

260 / 230 **2.30**

Baseline correction 340 nm

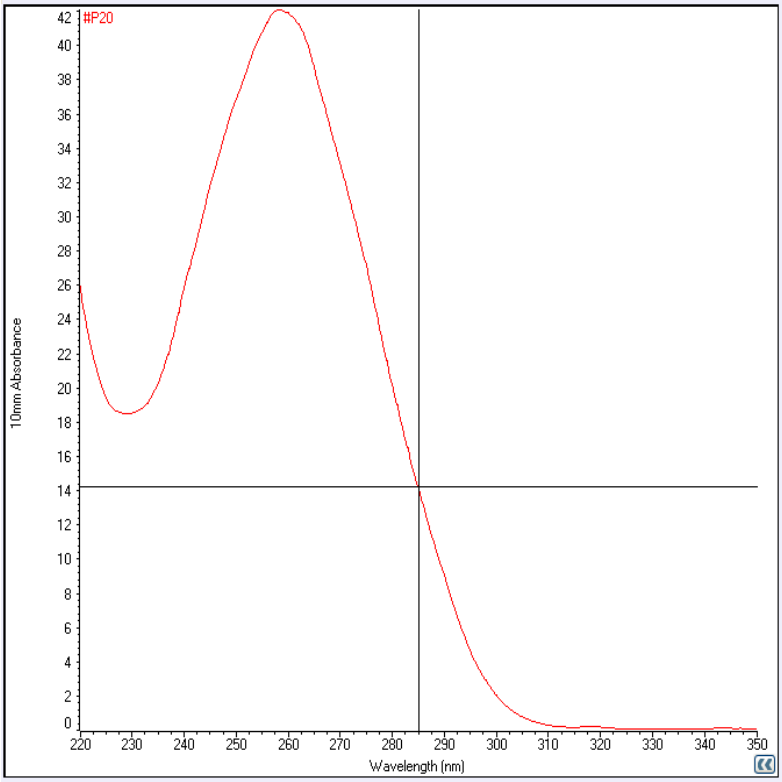

285nm 14.161Abs

Sample ID: #P20 **Pedestal**

Type: RNA 40.00

Conc. **1674.8** ng/µl

A260 (10 mm path) **41.869**

A280 (10 mm path) **20.196**

260 / 280 **2.07**

260 / 230 **2.27**

Baseline correction 340 nm

A3.2. Amplified products of RT-qPCR

Hprt1

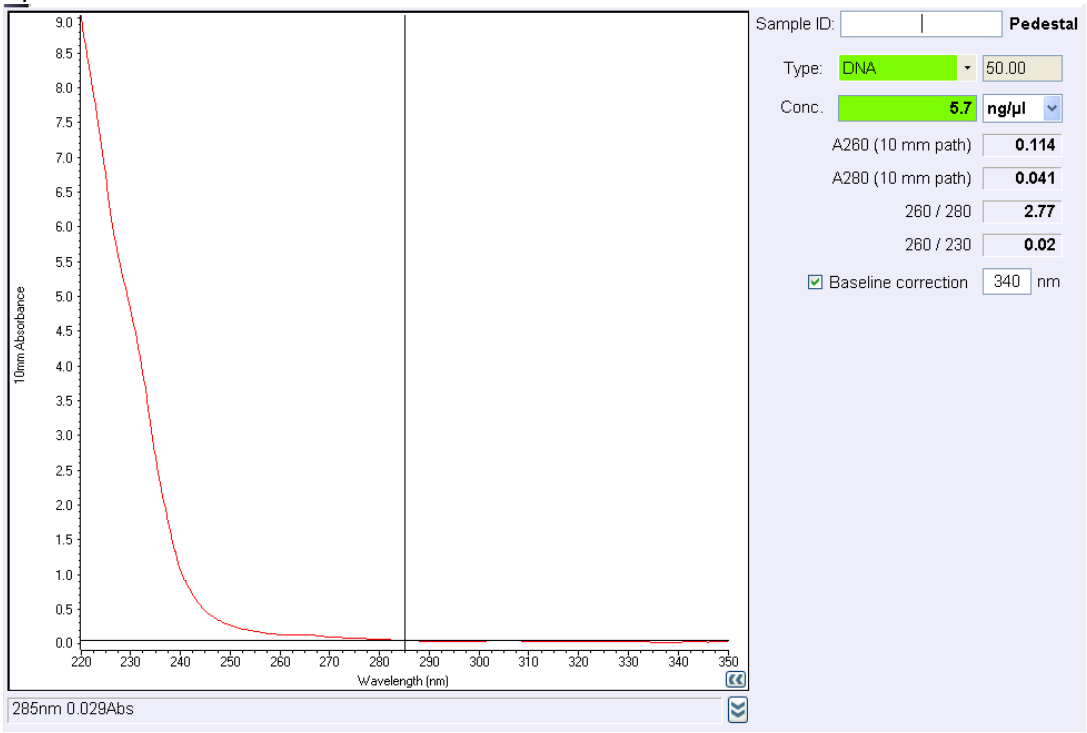

Adipoq

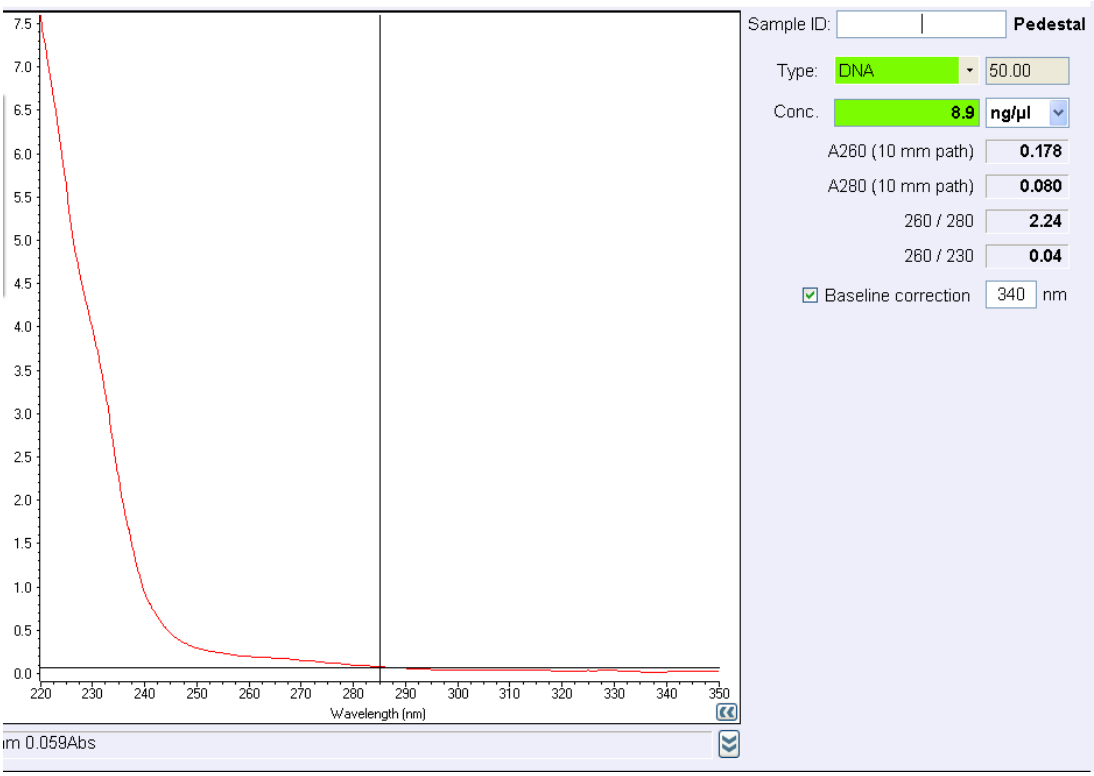

Il1b

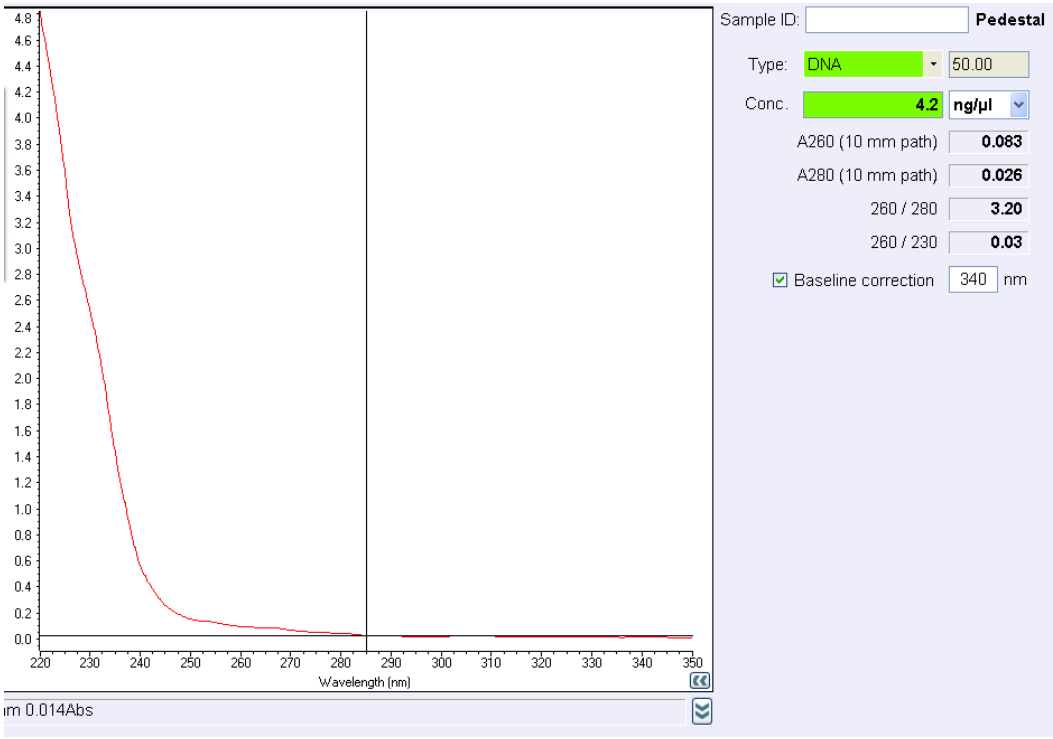

Tnfrsf19

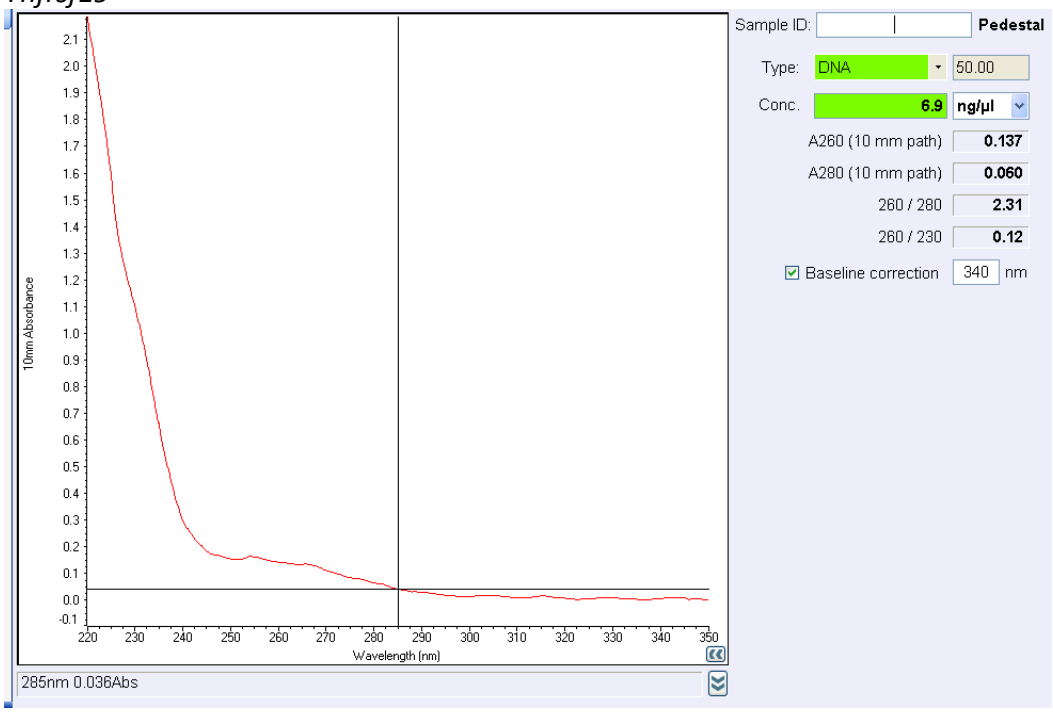

Cd40

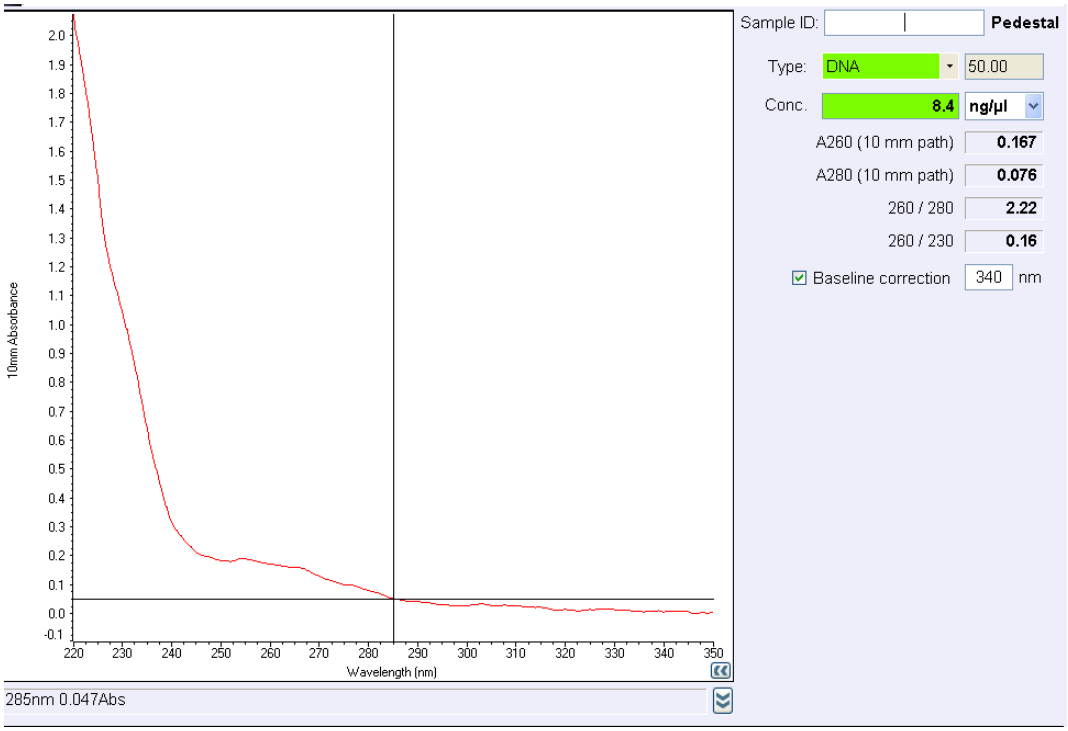
Sample ID:
Pedestal
Type: DNA 50.00
Conc. 8.4 ng/µl
A260 (10 mm path) 0.167
A280 (10 mm path) 0.076
260 / 280 2.22
260 / 230 0.16
Baseline correction 340 nm
10mm Absorbance
Wavelength (nm)
285nm 0.047Abs

Cd40ig

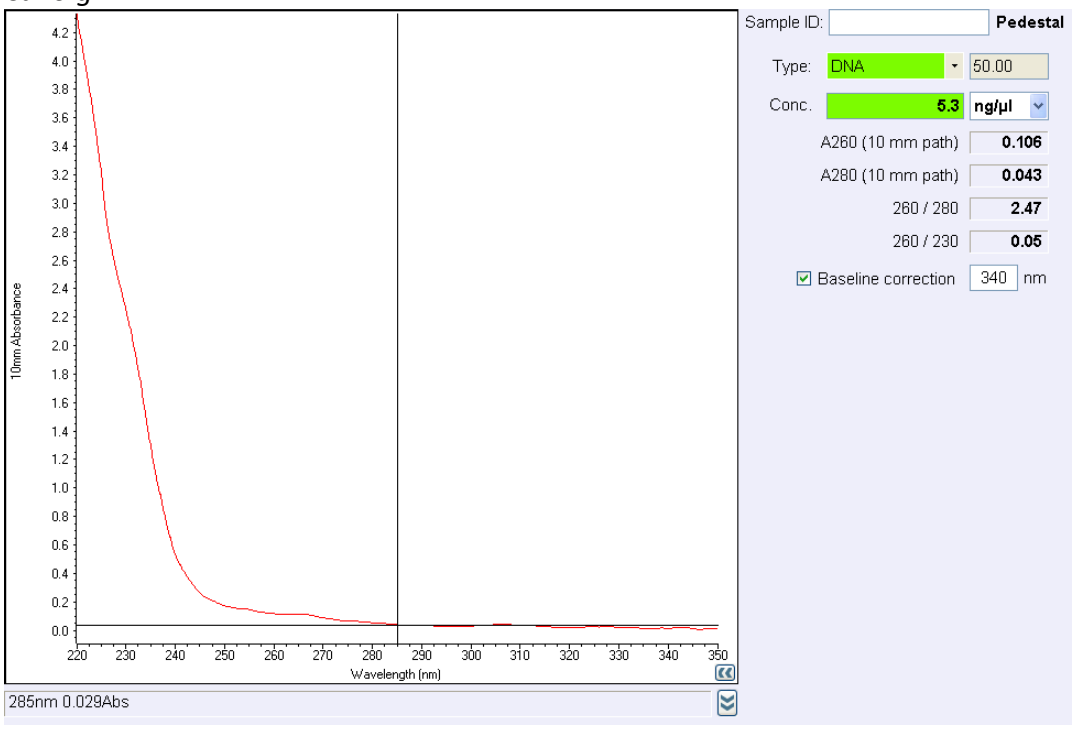
Sample ID:
Pedestal
Type: DNA 50.00
Conc. 5.3 ng/µl
A260 (10 mm path) 0.106
A280 (10 mm path) 0.043
260 / 280 2.47
260 / 230 0.05
Baseline correction 340 nm
10mm Absorbance
Wavelength (nm)
285nm 0.029Abs

Lep

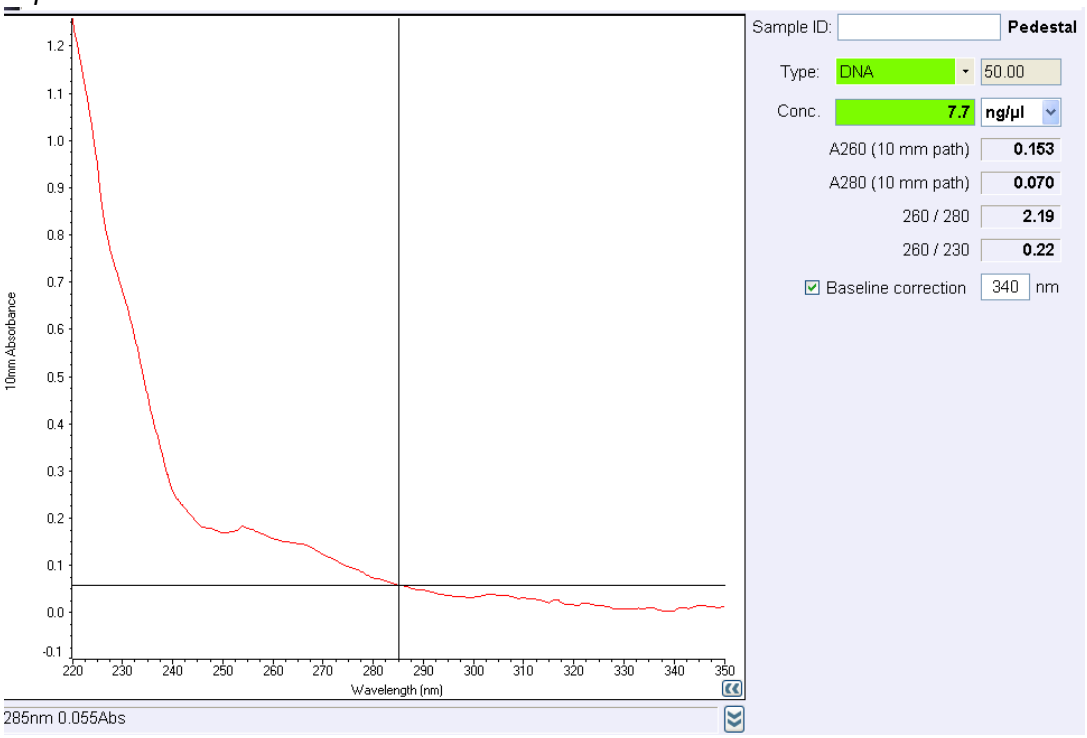
Sample ID:
Pedestal
Type: DNA 50.00
Conc. 7.7 ng/µl
A260 (10 mm path) 0.153
A280 (10 mm path) 0.070
260 / 280 2.19
260 / 230 0.22
Baseline correction 340 nm
10mm Absorbance
Wavelength (nm)
285nm 0.055Abs

Ccl20

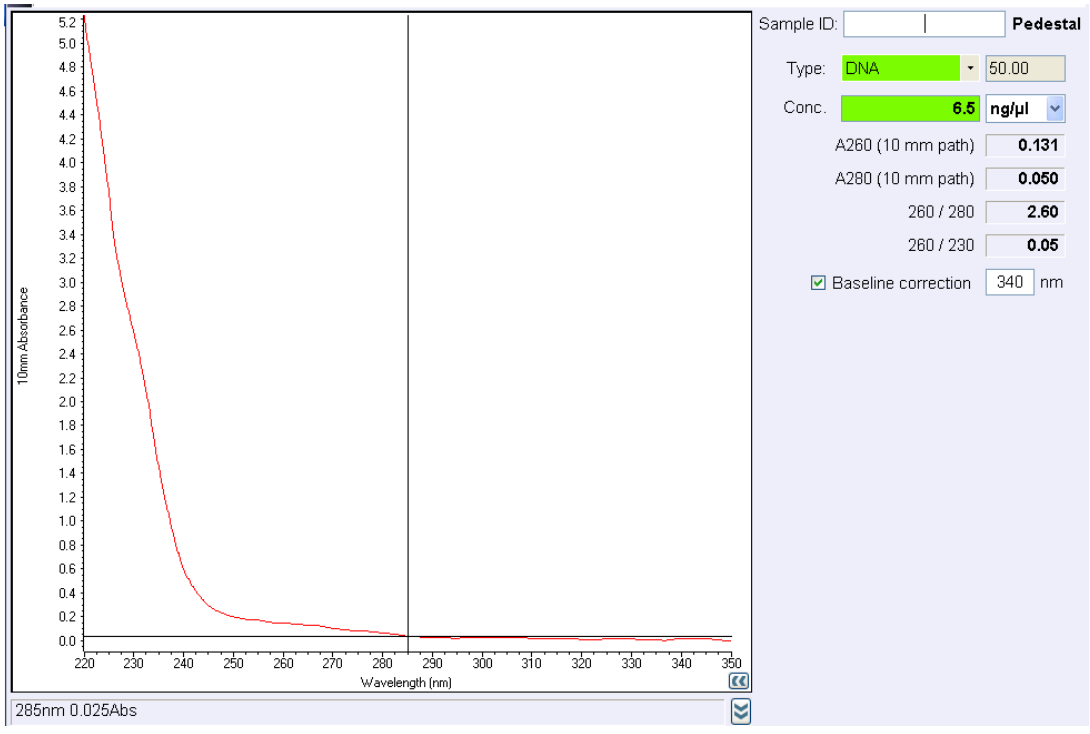
Sample ID:
Pedestal
Type: DNA 50.00
Conc. 6.5 ng/µl
A260 (10 mm path) 0.131
A280 (10 mm path) 0.050
260 / 280 2.60
260 / 230 0.05
Baseline correction 340 nm
10mm Absorbance
Wavelength (nm)
285nm 0.025Abs